Université de Strasbourg

École Doctorale des Sciences de la Vie et de la Santé

INCI-CNRS UPR3212

THÈSE présentée par :

Federica LARENO FACCINI

Soutenue le : **17 décembre 2021**

En vue d'obtenir le grade de **Docteur de l'université de Strasbourg**

Spécialité : Neurosciences

Implicit Time in the Cerebello-Prefrontal Network.
A Novel Approach in Mice

Membres du jury

Dr. Valérie DOYERE (CNRS, Université Paris-Saclay)	Rapportrice externe
Dr. Javier F. MEDINA (Baylor College of Medicine)	Rapporteur externe
Dr. Romain GOUTAGNY (CNRS, Université de Strasbourg)	Examinateur interne
Dr. Krystal PARKER (University of Iowa)	Examinatrice externe
Dr. Stéphane GASMANN (CNRS, Université de Strasbourg)	Président du jury
Dr. Anne GIERSCH (INSERM, Université de Strasbourg)	Membre invitée
Dr. Philippe ISOPE (CNRS, Université de Strasbourg)	Directeur de thèse

A nonna Luisa,

per aver acceso in me la scintilla di curiositá che
mi spinge sempre ad allargare i miei orizzonti.

p.s. avresti dovuto essere piú chiara quando
ti auguravi un dottore in famiglia

To nonna Luisa,

for starting in me that spark of curiosity that
pushes me to always expand my horizons.

p.s. you should have been clearer when
you were wishing for a doctor in the family

Acknowledgments

First of all I want to thank the jury members: **Dr. Valérie Doyère**, **Dr. Romain Goutagny**, **Dr. Javier F. Medina**, and **Dr. Krystal Parker** for taking the time to read my work and for participating in the discussion. You are also making this project (and myself) advance and improve, and for this I am grateful!

I am not good with words and even less with feelings so I'll try to be as eloquent as possible but you all guys know what you mean to me (and what complaining together about life meant to me), regardless of this (terribly awkward) attempt.

My first friend in this strange land on the wrong side of the Alps, **Charlotte,** you probably don't know how much our friendship helped me feel part of something here in Strasbourg but as typical in our relationship here I am explaining it to you. After you left us I really missed our ~~gossipin~~ discussions during breaks, although zoom is still better than nothing. Thank you for being the best person a Hufflepuff can be!

Ludo I owe you my newly discovered nature of trying to do stuff, break it and only then ask for a second opinion (usually yours) and for it I'll be eternally grateful! Jokes apart, you helped me to come out of my shell both in Strasbourg and in life. Thank you big potato! I hope the US won't break you dark sense of humor, can't wait to have you back on this side of the Atlantic.

My companion of memes and weekends in the lab, **Taddy**! I actually don't how to communicate with you without memes and sarcasms so I'll probably send you now a random funny picture to show you my love (and maybe you'll remember of it while reading these words).

Un grazie speciale alla mia isola italiana nel lab, **Theo[1]** (aka la portinaia piú informata del piano). Spero che qualcun altro ti ricorderá di lasciare il lab almeno per dormire e ti obbligherá a prendere vacanze! Grazie di tutte le risate e non mollare!

My rightful heir, **Pierre**! Although you are the latest addition to the lab, you were so helpful and supporting. I honestly couldn't have made it without you. Thank you! You have everything you need to conquer this project, you'll be amazing. Good luck!
P.S. I'm gonna be mailing you random donuts for the rest of your life.

I want to thank **Theo[2]**, **Gilles**, and **Adriana** for all the laughs and good moments passed together inside and out of the lab. I wish you all the best and I leave you in charge of teaching the old ways of lab pranks to Pierre!

A huge thank you to **Antoine**! I don't know if it is because you are about to become a PI or due to your new fatherhood or simply because you are genuinely a wonderful person, but you have been a second lab papa to me. And I can tell you, you will be an excellent father and supervisor. Thank you for everything and good luck!

Thank you to the rest of the team: **Bernard**, **Matilde**, **Fred**, **Didier**, and **Aline** for the help and support over the years!

A special thank goes to the best D&D group ever seen: the **Dungeon & Dendrites, Charlotte, Gilles, Ben, Shani, Louise** and our DM (**Dendrite Master**), **Clem**. We lived incredible and very serious adventures. Those evenings are greatly missed but I will forever sing of Albus and his cat lover, of Jillian the goth bard, Salazar the drunk, Chimichanga the birdspawn, Keya the 'shrooms lover, Gotchka the necromancer, and Clem the best DM!

The university wouldn't be the same without **Doctoneuro**. I want to thank **Clémence**, **Léa**, **Claire**, **Sarah**, **Lucas**, and all the others that have been part of this crazy group with me. I have a new found love for the color purple and it's all thanks to you (especially Clem for using it everywhere!).

I want to thank also all the friends from the INCI with whom I shared a laugh, a beer or any happy moment. Thank you **Lou**, **Lucien**, **Angel**, **Damien**, and all the others!
And a big thank you also to all the staff that handles the mice and makes sure they are healthy and (most of the times) were they should be: **Stéphane**, **Edouard**, **Denis**, **Christophe**, **Sophie**, **Dominique**, **Noemi**, and everybody else.

Greta, dobbiamo ringraziare lo zacca per almeno una cosa: averci fatto incontrare! Mentre pensavo a cosa scrivere ho realizzato che sono quasi 25 anni che ci conosciamo. E niente. Panico. Direi che questo é piú che sufficiente. Sei un punto fisso della mia vita e ne saró eternamente grata. Ti voglio bene.

Sin dalla triennale ci sopportiamo a vicenda, **Angy**. Di strada ne abbiamo fatta dalle lezioni di matematica sui rinoceronti. Spero ne faremo tanta altra assieme (anche se ormai lontane). Grazie di tutto il pesce, vecchia ciabatta.

Anche se il piú delle volte comunichiamo a rate, **Rifici** tu ci sei sempre stata per me. So che resto la tua Lareno preferita anche se non puoi ammeterlo pubblicamente! Grazie di essere sempre stata presente ed avere sempre avuto le parole giuste per me.

Grazie anche a tutti i miei amici di Trieste: **Clelia**, **Giorgia**, **Serena**, **Sara** e tutti gli altri. Siete stati la mia prima famiglia lontano da casa. Anche lontani ci siamo sempre supportati a vicenda, spero di riuscire a tornare in osmiza e a Barcola con tutti voi.

Un enorme grazie alla mia famiglia: **papá**, **mamma**, **Francy** (anche **Nymi** e **Lucy**). Grazie per avermi supportato e sopportato in questi anni passati lontano da casa. So che non sempre capite i miei problemi o la mia direzione nella vita ma non avete mai smesso di sostenermi e farmi sentire amata. Vi voglio bene (soprattutto a Nymi)!

A much needed thank you to **Dr. Romain Goutagny** (again) and **Dr. Sylvain Hugel** for providing both human and scientific support all throughout my PhD during my yearly progress reports.

I really want to thank **Dr. Anne Giersch** for having supported me throughout these years. You have always been a precious source of information and a very calming presence, especially in the -very

confusing- early days of the project. Thank you for everything, you are a wonderful person and scientist.

Of course the biggest thank you is for **Philippe**. For welcoming me in his lab and help me grow into a better person. You are a great supervisor and scientist. You have earned eternal supply of chocolate from me!

The last and most important thank you goes to **Louise**. Everything I have accomplished is also thanks to your love, support, and comprehension. You were so patient and nurturing over the last few months that I think you kept me alive (quite literally with the feeding part at least)! You already know everything I feel and that I'm unable to express in words (it's almost at the same level as the one for **Bandit**). Thank you.

Table of Contents

List of abbreviations

2KS	2 samples Kolmogorov-Smirnov test
ACC	Anterior Cingulate Cortex
BA	Brodmann Area
CF	Climbing Fiber
Cg1	Cingulate Cortex 1
CN	Cerebellar Nuclei
D1R	Dopamine D1 Receptor
dlPFC	Dorsolateral Prefrontal Cortex
DMN	Default Mode Network
FC	Fixed foreperiod Control (experimental condition)
FFT	Fast Fourier Transform
FP	Fixed foreperiod Photostimulation (experimental condition)
FS-PV	Fast-Spiking Parvalbumin positive (interneuron)
GABA	γ-aminobutyric acid
GC	Granule Cell
IL	Inferolimbic cortex
IntA	Anterior Interpositus Nucleus
IO	Inferior Olive
IPSCs	Inhibitory Post-Synaptic Currents
LTD	Long-Term Depression
LTP	Long-Term Potentiation
MD	Mediodorsal thalamic nucleus
MF	Mossy Fiber
MLI	Molecular Layer Interneuron
mPFC	medial Prefrontal Cortex
MSN	Medium Spiny Neurons
NB	No Behavior (experimental condition)
PC	Purkinje Cell
PCA	Principal Component Analysis
PF	Parallel Fiber
PFC	Prefrontal Cortex
PrL	Prelimbic Area
rCrusI	right CrusI
SBF	Striatal Beat-Frequency (model)
SMA	Supplementary Motor Area
VA	Ventral-anterior thalamic nucleus
VC	Variable foreperiod Control (experimental condition)
VL	Ventrolateral thalamic nucleus
VM	Ventromedial thalamic nucleus
VTA	Ventra Tegmental Area
VP	Variable foreperiod Photostimulation (experimental condition)

List of figures

Preamble

The traditional vision of the cerebellum relates to its role in motor control. However, since the last three decades, evidence has undeniably shown that the posterior cerebellum is involved in cognitive tasks (detailed in section 1.2) and its malfunction correlates with neuropsychiatric diseases (discussed in section 1.2 and 1.4.5) and several cognitive impairments.

One cannot discuss about higher cognitive functions without evoking the prefrontal cortex, the locus of such functions (discussed in section 1.1). Indeed, cerebellum and prefrontal cortex are anatomically and functionally connected and interestingly their evolution and growth in higher mammals seem to correlate (discussed in section 1.3).

One last player remains to be introduced: time. Of course, the more cerebellar-inclined reader will immediately think at the fine control the cerebellum has on the milliseconds synchronization of muscles and joints, but in this case, we are interested in the possible role the cerebellum has in influencing time integration needed to organize purely cognitive information and use this to structure events in time (discussed in section 1.4).

My project is an anomaly in a lab of people all working only on the cerebellum. So how did it come to be? This project is the brain child of a collaboration between Philippe Isope and Anne Giersch (Giersch et al., 2016).
Anne has an incredibly fascinating line of research on implicit time perception and action sequencing in schizophrenic patients. With her work she helped demonstrate that alterations in time processing in schizophrenic patients are due to a problem in autonomous sequencing of events in time. Involvement of the cerebellum in schizophrenia is becoming always more evident (thanks to the pioneering ideas of Dr. Andreasen, Andreasen, 1999).

My project was born. I was to implement in mice the experimental paradigm that Anne's lab uses on humans and we were to study the sequencing of events in a schizophrenia mouse model. The first part was easy, all it took was 2 years and a lot of troubleshooting and we reached the first objective: we had a working behavioral task to investigate implicit timing in mice and we could record the electrophysiological activity in the prefrontal cortex while stimulating the posterior cerebellum.

However, one thing had changed during these years: we realized that we became more interested in a parallel question: how is the cerebello-prefrontal network involved in the prediction of a reward when its delivery time is variable? This is how we settled on the variable foreperiod task.

Our new aim was thus to investigate implicit time prediction of a reward with variable delay in mice, especially in a schizophrenia model.

Unfortunately, during my PhD I haven't had the time to implement the schizophrenia model but nonetheless I have had an adventure developing the task that I will forever cherish. And I can't wait to see what Pierre (my successor), Philippe and Anne will discover in the future.

Behavioral task in brief

I will briefly expose the behavioral task (Fig.1) so to make clearer to the reader the stream of thoughts presented in the following introduction (for a more detailed description please see chapter 2.5).

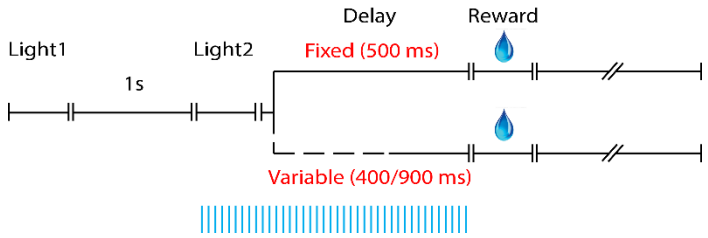

Fig. 1 Scheme of the behavioral task (explained in the text below).

The task consists of two visual cues (light 1, light 2) played in a sequence (separated by a constant duration of 1s), after the second cue there is a delay that can be either fixed (500ms) or variable (randomly chosen between two values: 400 and 900ms), followed by a water reward (available for 150ms). After the reward there is an eventless inter-trial duration (approximately 7s) before the task starts again. While the mouse performs the task, the electrophysiological activity in the left prefrontal cortex (prelimbic area, specifically) is recorded. The lateral cerebellum (right CrusI) is optogenetically stimulated with four different protocols of stimulation during the second preceding the delivery of the reward.

1 Introduction

1.1 Prefrontal Cortex

In this chapter I will discuss the definition of prefrontal cortex and (if and) how it can be applied to non-primate mammals.

1.1.1 A brief history of the Frontal Lobe

People have always been fascinated with the concepts of consciousness and soul. Since the early ages of scientific discovery, doctors and philosophers debated on their place of origin: heart or brain.

Ancient Egyptians thought the brain had a purely mechanical role and discarded it during the embalming process as it would have been useless in the afterlife. Aristotle (384 – 322 B.C.) shared similar views which unfortunately informed the official Catholic doctrine, and thus the university teachings, until the late XVIth century. In Aristotle's view, the heart was the source of the soul. Luckily many scientists and philosophers (which at the time were often the same figure) didn't agree with this view and the study of the brain progressed constantly although slowly.

The fathers of this counter-opinion were Herophilus (c335 - c280 B.C.) and Erasistratus (c310-c250 B.C.) from the medical school of Alexandria, Egypt. They performed numerous dissections and vivisections on animals and reached the conclusion that all the nerves were bringing information to the brain, where the consciousness resided (Wiltse & Pait, 1998).

One of reasons why people thought that the heart was the source of reason was because the voice came from that region of the body. Galen (129-c210), one of the most prominent physicians of the Roman Empire, demonstrated that the stimulus that generates the voice originates from the brain and must consequently be the source of reason (Freemon, 1994).

Inspired by the discoveries using the silver staining technique that allowed Golgi and Ramon y Cajal to study for the first time neurons (although with very different conclusions) (Glickstein, 2006) and from advancements in the field of neuropsychiatry, the XIXth-XXth centuries saw an explosion of scientific interest in the frontal cortex and mental disorders.

Empirical experience showed radical changes in people with damages to the frontal lobe. Probably the most notorious case being that of Phineas Gage, who, in 1848, survived an accident in which a steel pole perforated his left frontal lobe from side to side. He miraculously survived but his personality, which before was that of a high society gentleman, abruptly changed and he started swearing, drinking, and being prone to violence without showing any intellectual deficit (Filho, 2020). This evidence prompted a whole new series of experiments and medical developments in the early 1900. The general belief being that the frontal cortex was responsible for controlling emotions and social inhibitions.

In the second part of the XIXth century, Paul Broca, a French doctor, started studying the causes of speech disorders in adults. He identified a specific area in the left inferior frontal lobe (now known as Broca's area) as the locus of voluntary and coordinated speech (Finger, 2004).

The first person to scientifically apply learned behavior studies on animals and correlated these behaviors with a specific brain area, was probably Dr. Shepherd Ivory Franz. His studies on cats, dogs, and monkeys are pioneering in the field of neuropsychology, rehabilitation therapy, and plasticity. Around 1902-1907 he published works on partial and total ablation of the frontal cortex where he reported the loss of previously learned behaviors. Moreover, he demonstrated that in some cases, with rehabilitation, over time monkeys were able to relearn those behaviors (Colotla & Bach-Y-Rita, 2002).

In 1935, Dr. Fulton and Dr. Jacobsen, presented their research on frontal lobotomies in chimpanzees. From this study they concluded that the frontal lobe is not the source of intelligence, but it is indeed the controller of emotions and behavior. During the same years, Jacobsen performed his seminal experiments on delayed-response test in monkeys with uni- and bilateral ablation of the prefrontal cortex (Jacobsen & Nissen, 1937). They reported that a bilateral ablation was needed to prevent the learning process (later studies demonstrated that also unilateral ablation induce deficits albeit of smaller intensity, Fuster, 2008). These studies were the beginning of a very long history in the study of working memory.

It is thought that this experiment was the inspiration for the development of frontal leucotomies (lobotomies) as treatment for mental disorders, by Portuguese doctor Egas Moniz (Preul & Dagi, 2017), who went on to win the Nobel Prize for medicine in 1949 for it. He believed that psychiatric patients had a "*fixation of synapses*" which produced repetitive thoughts and behaviors. Thus, by severing these malfunctioning synapses he thought he could

improve or cure mental illnesses (Gross & Schäfer, 2011). His patients, he claimed, passed from being violent and stressed to being docile and calmer. No long-term follow-up of these patients was provided; hence the negative outcomes of the procedures went long unnoticed.

Fortunately, lobotomies quickly went out of fashion thanks to the introduction of the first drugs aimed at mental disorders.

1.1.2 We need to talk about the prefrontal cortex

There are questions that need answering early in the process of this manuscript: do rodents have a prefrontal cortex (PFC)? If so, is it meaningful to study PFC in rodents when the goal of biomedical research is the improvement of human condition?
As for many interesting questions in science, there is still no clear answer but there are indeed many strongly opinionated people.

To address the main question, we first need to answer a more basic one: what is the prefrontal cortex?

1.1.2.1 Is a clear definition of prefrontal cortex possible?

The initial interest on frontal and prefrontal regions sparked from accidental lesions in humans and primate studies. For this reason, the concept of prefrontal cortex originates in these higher mammals. There have been few attempts at producing a clear definition for what constitutes the prefrontal cortex.

The first was proposed by Brodmann himself. He famously classified areas of the human brain based on their cytoarchitecture (Brodmann, 1909). He called "*regio frontalis*" the areas in the frontal lobe with a granular layer IV (BA: 8–14, 46, and 47), what is now considered the PFC (Fuster, 2008). Since only primates have granular frontal areas, he considered the PFC to be an exclusive characteristic of primates.

To bridge the differences between species and prove that all mammals have a prefrontal cortex, Rose and Woosley in the late '40s proposed a hodological definition based on anatomical homology between species. They defined PFC as all the frontal areas contacted by the mediodorsal (MD) thalamic nucleus (Rose & Woosley, 1948). MD-PFC projections have been described in all major mammalian species: in humans (Klein et al., 2010; Rose &

Woosley, 1948), non-human primates (Giguere & Goldman-Rakic, 1988; Goldman-Rakic & Porrino, 1985; Middleton & Strick, 2001; Rose & Woosley, 1948), rats (Kuramoto et al., 2017), guinea pigs (Markowitsch & Pritzel, 1981), and mice (Collins et al., 2018; Fujita et al., 2020; Guldin et al., 1981) among others. This was an important step towards the contemporary understanding of what the prefrontal cortex is because they expanded the limits of it also in primates. Following this definition, an agranular region of the frontal lobe was finally considered prefrontal (Fig. 2A). This region is the Anterior Cingulate Cortex (ACC) which can be divided into three subregions: Infralimbic (IL), Prelimbic (PrL), and Cingulate (Cg). They correspond to Brodmann's area 25, 32, and 24, respectively (Fig. 2C).

Although MD remains to date the nucleus most involved with PFC, recent evidence shows projections to the PFC from multiple thalamic nuclei. Most notably, ventral-anterior (VA) (Goldman-Rakic & Porrino, 1985; Middleton & Strick, 2001), ventrolateral (VL) (Middleton & Strick, 2001) and ventromedial (VM) (Collins et al., 2018; Fujita et al., 2020).

It is thus important to acknowledge that the diversity of definitions and inter-species variability reduces our ability to have clear-cut limits to the PFC that can be directly transposed between species, and therefore requires us to be careful about the exact regions involved when comparing studies.

1.1.2.2 Can we compare the prefrontal cortex of primates and rodents?

The parcellation of prefrontal cortex in primates is source to confusion. There are various proposed parcellations, one of the most common divides it in dorsolateral, dorsomedial, medial, ventromedial and orbitofrontal (Carlén, 2017) (Fig. 2B). But equally common is to divide it in the 3 major areas: orbitofrontal, medial, and dorsolateral (Fuster, 2001; Preuss, 1995). I will be using the latter.

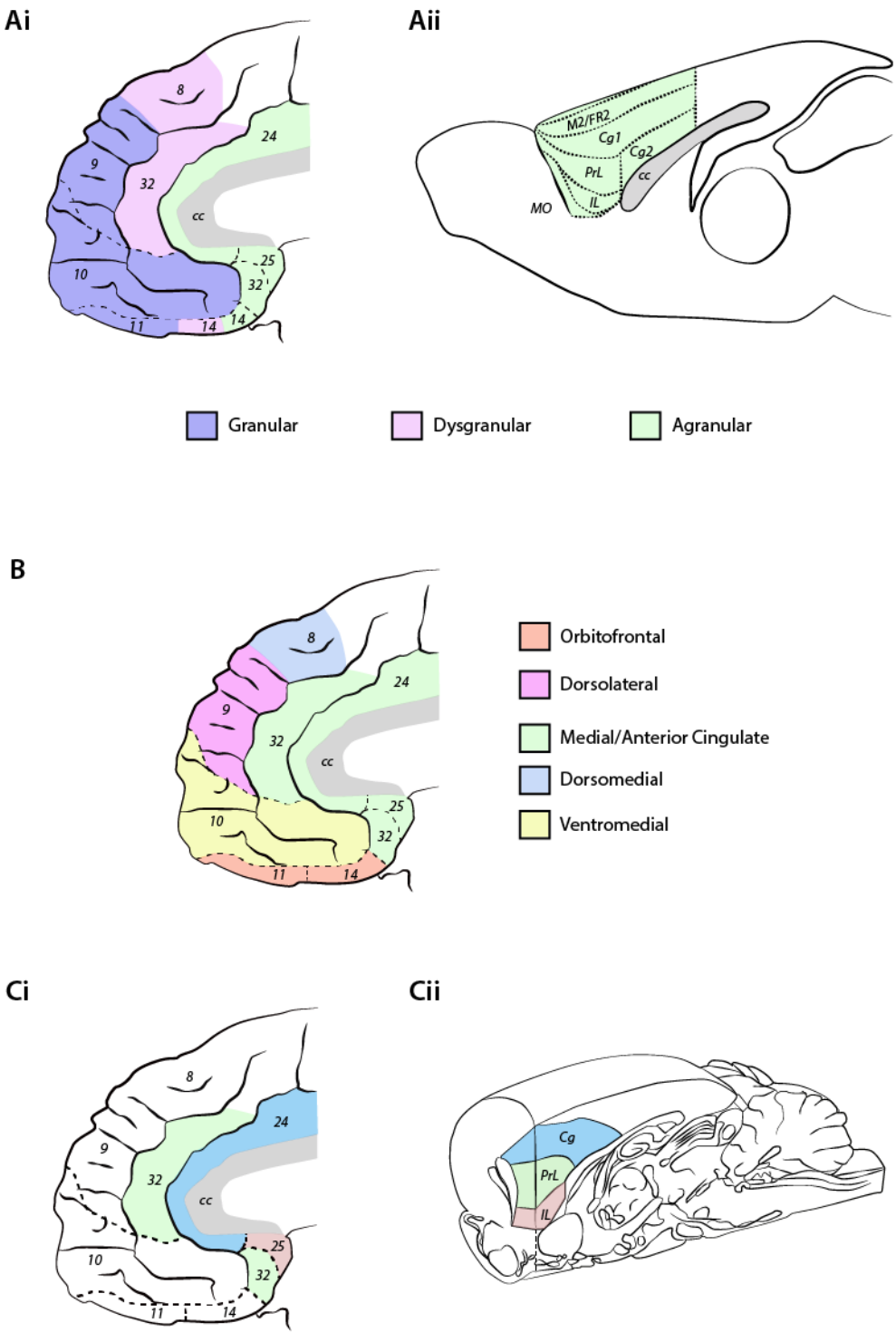

Fig. 2 Prefrontal cortex of humans and rodents

A. Cytological characterization of human (Ai) and rodent (Aii) PFC based on its lamination

B. Functional division of subregions of human PFC

C. Subregions composing ACC in humans (Ci) and mPFC in rodents (Cii, adapted from Tynan et al., 2013).

Orbitofrontal and dorsolateral are granular (further divided into granular and dysgranular depending on the thickness of layer IV) whereas medial is agranular (Fig. 2Ai). The dorsolateral part of the PFC is widely considered to be exclusive to primates. Firstly, the MD thalamic nucleus does not project to the dorsolateral area in the frontal lobe in rodents. Moreover, due to anatomical homologies between the medial PFC (mPFC) in primates and other mammals, it is thought that the dorsolateral PFC (dlPFC) is a recent addition appeared in the primate branch (Wise, 2008). Hence, rodents have only the primate equivalent of orbital and medial PFC.

A detailed cytoarchitectonic characterization of the mouse PFC and its subregions has been done by Van De Werd and coworkers (Van De Werd et al., 2010), and they attempted to clarify the nomenclature. Nonetheless they recognize that some of their results are in conflict with the widely used mouse atlas by Franklin and Paxinos (Franklin & Paxinos, 2007).

Laubach and coworkers wrote a much needed review analyzing the literature on PFC in primates and rodents (Laubach et al., 2018). They raised very interesting points on the confusion existing in this field. Mainly with the terms used, not only between the different animal models but also within the same animal model! The biggest example (that confused me a lot when I first approached the study of PFC) is the confusion around two terms in mouse research: mPFC and ACC. They are sometimes used as synonyms, other times they are two different areas but at other times ACC can be a subregion of mPFC. From their review they stand by the notion that mPFC and ACC are the same, at least in rodents.

Such confusion persists in primates. Vogt pushes for them to be considered different areas (Vogt, 2016) but regardless, many authors consider ACC to be part of mPFC, which then is composed of infralimbic (IL), prelimbic (PrL), and anterior cingulate (ACC/Cg, depending on the nomenclature used).

A comparative analysis performed by Laubach et al. on the geometry of the cortex and the relative position of ACC subregions, confirms the homology between rodents' mPFC/ACC with primate's ACC (Laubach et al., 2018) (Fig. 2C).

1.1.2.3 Specificities of the mouse PFC model

The general opinion for primates is that orbital and medial areas of the PFC are involved in the emotional aspect of cognition (Fuster, 2001) and in thinking about self, "mentalizing"

(Frith & Frith, 1999). The lateral part instead is involved with all the higher cognitive functions commonly attributed to PFC: working memory, decision-making, planning, and temporal processing of events and behaviors, among others (Fuster, 2001). However, there seems not to be a clear border of functions but more a rostrocaudal gradient of abstraction (hierarchical organization), with dlPFC being the highest order (Alexander & Brown, 2018; Badre & D'Esposito, 2009; Fuster, 2008).

Since rodents have no dlPFC, does it make them a less reproducible model for humans? In 1995 Preuss wrote a paper against the concept that rats have a PFC comparable to dlPFC of primates (Preuss, 1995), but he still supported the investigation of rodents' PFC as a view on the point in evolution before primates and rodents separated.

Granular dlPFC is indeed an exclusive characteristic of primates, and the incredible expansion that PFC has seen in primates must account at least in part for the higher cognitive abilities of this order. However, many of the functions attributed to dlPFC in primates can be considered common features of all mammals even if the brain structure controlling these behaviors could differ. Nonetheless, many of these functions have been related to rodents' orbital or medial PFC, such as: attentional set-shift (Birrell & Brown, 2000; Joel et al., 1997; Ragozzino et al., 1999), temporal processing (Mogensen & Holm, 1994; Parker et al., 2017), and categorization (Reinert et al., 2021).

In conclusion, it is clear that rodents and primates have different PFC and very different cognitive abilities. Nonetheless, with all due limitations, rodents can still serve as useful models for investigating some basic functions of primates' PFC, but caution should be used when tempted to compare results between species even more so than with other cortical areas.

1.1.2.4 Working memory resides in the PFC

Working memory is one of the main functions dependent on PFC. It is what allows us to hold, store and retrieve novel information, manipulate, and allocate them to long-term memory. One key factor of working memory is its limited duration in time and storing capacity. A long standing view proposed by Miller (Miller, 1956) is that the magic number of elements storable in the working memory is 7±2.

There are two widely popular models for working memory: Baddeley's and Cowan's models (of which I will do a very brief overview).

Baddeley first proposed his model in 1974 (Baddeley & Hitch, 1974). There are three main actors: 1) the Central Executive, which decides how to allocate resources and which input is to be ignored and which is to be kept, and controls the allocation of information towards long-term memory, 2) the Phonological Loop to handle spoken and written language, and 3) the Visuospatial Sketch which deals with visual and spatial information, mainly used for navigation.
He then updated the model in 2000 by adding an Episodic Buffer to allow for cross-modality integration of information (Baddeley, 2000).
In this model, to keep the elements in store, the information has to constantly enter a repetition loop (in the case of semantic information, this is called 'articulatory control process' and it corresponds to when we repeat a word in our head to not forget it).

Cowan's model (Cowan, 1988) has four components: 1) Central Executive which functions similarly to Baddeley's model, 2) Long-Term Memory, 3) Activated Memory which is a subset of the long-term memory, which is currently being activated and is needed to handle the novel input (also referred to as short-term memory), and 4) the Focus of Attention which is the limiting factor for the storage capacity of the working memory. His model focuses more on the cognitive aspect of working memory and in the bidirectional interaction between past information (long-term memory) and novel information (activated memory) which most probably takes place in the central executive. This explains the enhancement of working memory with familiar stimuli (contrary to Baddeley's model).
This model distinguishes autonomous and conscious working memory tasks as being both controlled by the central executive but by parallel systems.

Both these models seem to agree on identifying the *central executive* with PFC.

1.1.3 Structure and connectivity

The frontal lobe is separated from the parietal lobe by the central sulcus and from the temporal lobe by the sylvian fissure. Its cortex is composed by the motor, premotor, and prefrontal cortex. The last one is the associative cortex of the frontal lobe.

1.1.3.1 Cytoarchitecture

1.1.3.1.1 Layers and columns

The cortex has a laminar structure, with usually 6 layers (for granular; 5 for agranular cortices) (Fig.3A). This classification into layers derives from gradients of cell size and density (Narayanan et al., 2016). From more superficial to deeper (Kandel et al., 2013):

- Layer I: *molecular layer*. Very few cell bodies.
- Layer II: *external granular layer*. Small and sparse pyramidal cells.
- Layer III: *external pyramidal layer*. Small and dense pyramidal cells.
- Layer IV: *internal granular layer*. Mainly excitatory interneurons (Spiny Stellate Interneurons). Main input layer of the cortex. It's the layer that determines if an area is called "granular" (if present, e.g. primary visual cortex) or "agranular" (if absent, e.g. primary motor cortex) (Brodmann, 1909).
- Layer V: *internal pyramidal layer*. Big pyramidal cells.
- Layer VI: *multiform layer*. Sparse pyramidal cells.

In granular cortices, both layer I and IV receive sensory inputs from the thalamus. In agranular cortices instead, most of thalamic inputs enter in layer I (Mitchell & Cauller, 2001) where they synapse with apical dendrites of pyramidal cells of layers II/III and V (Cauller & Connors, 1994).

Layer II/III is the output layer for cortico-cortical communication; whereas layer V mainly projects to subcortical nuclei, spinal cord, distant cortical areas (Kandel et al., 2013; Opris & Casanova, 2014; Schüz & Braitenberg, 2001; Shipp, 2007), and thalamus (Collins et al., 2018; Thomson & Lamy, 2007).
Layer VI is probably the least studied. It produces most of cortico-thalamic projections and minor cortico-cortico projections (for a review see Thomson, 2010).

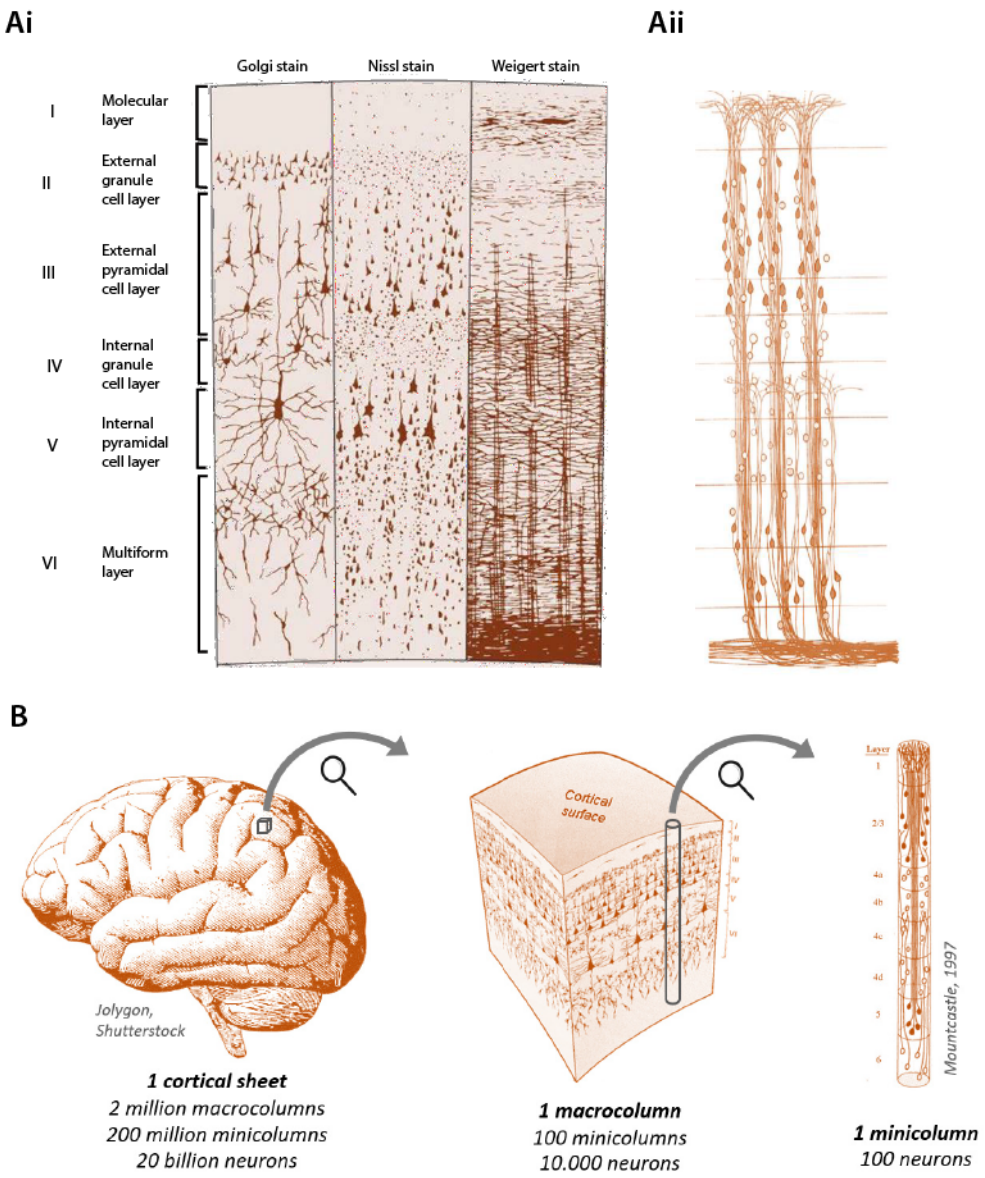

Fig. 3 Cytoarchitecture of human prefrontal cortex

Ai. Lamination of the human PFC shown with different stainings. Golgi stain highlights cell bodies and dendritic arborization. Nissl stain instead reveals cell bodies and proximal dendrites whereas the Weigert method highlights axonal processes.

Aii. Diagram of the distribution of neurons, dendrites and axon fibers.

B. Organization of the cortex in macro- and minicolumns.

Figures from: 'Insights from the brain: the road towards machine intelligence' by Matthieu Thiboust.

The cortex is the outermost part of the telencephalon. Its thickness varies among species: 2-4mm in humans (Narayanan, 2016; Schüz & Braitenberg, 2001), 2mm in rats (Narayanan, 2016; Schüz & Braitenberg, 2001) and 1mm in mice (Schüz & Braitenberg, 2001).

The cortex is generated inside-out. Progenitor cells proliferate in the ventricular zone and,

according to the Radial Unit Hypothesis (Rakic, 1988), the newly generate post-mitotic neurons migrate radially along the fibers of the radial glia. Thus, generating layers VI-II (Rakic, 1988). Layer I instead derives from the marginal zone of the cortical plate (Shipp, 2007). This migration gives rise to an ontogenetic column with cells deriving from the same progenitor, but early on during cortical development multiple ontogenetic columns merge creating heterogeneous columns (Rakic, 1988). Although, as Rakic states, it's unclear the relationship between ontogenetic columns and functional columns (what is usually called 'cortical column' as defined by Mountcastle, 1957) (Rakic, 2008). The Radial Unit Hypothesis further states that the 'tangential coordinates' of cells are determined by the position of progenitors inside the ventricular zone. Whereas the 'radial coordinate' is determined by the time at which each cell was generated, as early cells stabilize in more internal layers (Rakic, 1988, 1995).

To talk about the columnar cytoarchitecture, now the term 'macrocolumn' is used (Fig.3B), they are radial interlaminar columns of neurons that are highly interconnected and respond to the same modality of the same receptive field (Hubel et al., 1977; Mountcastle, 1957). Ranging in size between 300-600μm (Mountcastle, 1957), the size of a macrocolumn seems stable across species, the difference is in the number of columns not in their size (Mountcastle, 1997; Rakic, 1988). Later 'minicolumns' have been identified as the smallest computational unit of the cortex (Mountcastle, 1997; Opris & Casanova, 2014) and delimited lateral inhibition produced by bundles of interneuronal axons (Casanova et al., 2003). A macrocolumn is thus now defined by multiple minicolumns interconnected by short-range horizontal interconnections (Mountcastle, 1997) (Fig.3B).

There are thus multiple levels of elaboration of the input in the cortex of which minicolumns appear to be the smallest and macrocolumns are the largest level of local integration of the input. It has been proposed that minicolums might help selecting relevant features of the cognitive task and silence the irrelevant ones (Casanova et al., 2003; Opris, Hampson, et al., 2012).

1.1.3.1.2 Cellular categorization in the prefrontal cortex

Categorization of cell types in the cortex has proven extremely difficult and to date there is not a clear and accepted classification as various study used different criteria such as morphology, connectivity, function, electrophysiological properties or protein expression

patterns (Burkhalter, 2008; Narayanan et al., 2016). Moreover, different categorizations have been performed in different cortical areas and it is now becoming clear that different cortices display specificities (Radnikow & Feldmeyer, 2018; Tasic et al., 2018), especially in PFC (Bhattacherjee et al., 2019).

Identified by means of biophysical properties and morphology, inhibitory interneurons have short, local projections and mostly spineless dendrites. All excitatory neurons have typically spiny dendrites and represent the main cell type accounting for 85% of all cells (DeFelipe & Fariñas, 1992; Narayanan et al., 2016; Schüz & Braitenberg, 2001), but there are two main subclasses of excitatory neurons: 1) pyramidal excitatory neurons which have long axons projecting outside the cortex (in layer V) or to different minicolumns (layer II/III) and dendrites divided in basal (local) and apical (project to more superficial layers), and 2) non-pyramidal excitatory neurons (also called Spiny Stellate Interneurons) which have local excitatory projections (Schüz & Braitenberg, 2001) (Fig.4Ai).
In layer V two classes of pyramidal cells have been described based on their firing pattern: “intrinsically burst firing” and “regular spiking” cells (Thomson & Lamy, 2007).

Morphological characterization of interneurons classifies cells based on dendritic and axonal arborization into distinct groups, such as: chandelier cells, Martinotti cells, basket cells, double-bouquet cells, and others (Sultan & Shi, 2018) (Fig,4B). Classifications of interneurons based on their arborization patterns have been attempted, without clear and widely accepted results leading to a confusing situation with the same name used with different meanings. It is the case for the terms “fast spiking” and “regular spiking” cells which for some indicates subtypes of GABAergic interneurons (Kawaguchi & Kubota, 1997) while others used it for interneurons and pyramidal cells, respectively (McCormick et al., 1985; Narayanan et al., 2016; Rao et al., 1999).
A diffused classification method for inhibitory interneurons is based on molecular markers. Three markers appear to be able to classify the whole population: parvalbumin (a Ca^{2+} binding protein), somatostatin (neuropeptide), and 5HT3aR (ionotropic serotonin receptor) (Rudy et al., 2011). This last class is extremely heterogeneous with multiple subclasses identified (Lim et al., 2018), but a consensus is far from being reached (see Lim et al., 2018 for a review).

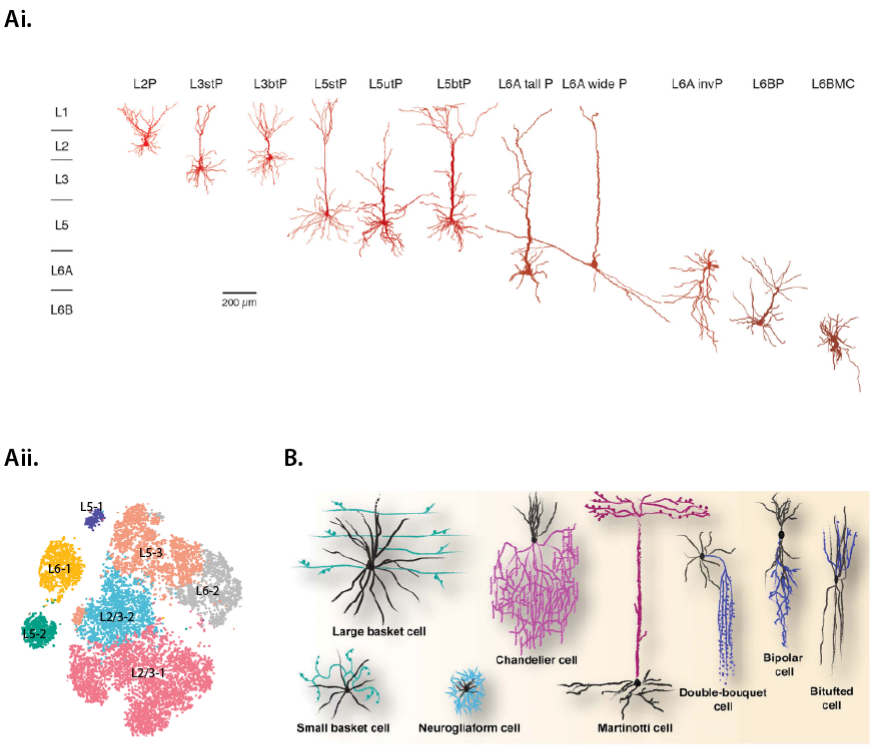

Fig. 4 Examples of classification of neocortical cell types
Ai. Morphological characterization of excitatory cells in rodent's mPFC (Radnikov & Feldmeyer, 2018).
Aii. Clustering (via t-SNE) of mPFC cell types by expression of layer-specific markers (Bhattacherjee et al., 2019).
B. Morphological characterization of interneurons in rodent's mPFC. Black lines: dendrites. Colored lines: axonal processes (Sultan and Shi, 2018).

A recent study from the lab of Marie Carlén performed a purely biophysical characterization of cells in the mPFC of mice. And they isolated fast-spiking parvalbumin-positive (FS-PV) interneurons in a group of identified interneurons with different spiking patterns (Kim et al., 2016).

Bhattacherjee and coworkers have recently performed a genetic classification of PFC's neurons in mouse by means of single-cell RNA sequencing (Bhattacherjee et al., 2019). They identified 13 excitatory and 12 inhibitory neuronal types. The excitatory cells showed clear differentiation between layers (and sublayers) (Fig.4Aii) whereas inhibitory cells did not show a prominent laminar organization (Bhattacherjee et al., 2019). Interestingly, a previous study outside the PFC (primary visual cortex and anterolateral motor cortex) showed homology of inhibitory neurons across distant areas of the cortex and high level of specialization of excitatory cells (Tasic et al., 2018), but both excitatory and inhibitory cells of the PFC appear

to express a combination of transcriptional markers specific only to PFC (Bhattacherjee et al., 2019).

These further show the high degree of specialization that PFC has reached in mammals. With specific neuronal types and thus, most probably, computational abilities unique to this area.

However, multiple institutions, such as the Allen Institute, have recently started an online database of cortical cell types in an attempt to promote a common nomenclature and classification.

1.1.3.2 Flow of information in PFC

Thalamic inputs arrive mainly in layer IV and I in primates (Kandel et al., 2013; Shipp, 2007; Thomson & Lamy, 2007). Whereas in rodents, it depends on the thalamic nucleus of origin. MD projects to layer I where it induces strong synaptic activation in layer II/III, VM instead projects diffusely on all layers producing subthreshold modulatory excitation (Collins et al., 2018).

Regardless of the input layer, the following step is usually the activation of pyramidal cells in layer II/III (Fig.5A) (and to a lesser degree, layer V) (Thomson et al., 2002). From here, they can either send cortico-cortical projections to nearby areas or contact infragranular layers (V and VI) in the same column from which the cortico-thalamic pathways originate (Collins et al., 2018).

Interestingly, Opris and coworkers were able to record from individual minicolums in behaving monkeys. They identified a microcircuit inside the minicolumn where neurons in layer II/III and layer V were paired and the specific activation of layer V neurons was relevant for correct performance in a decision-making task (Opris, Fuqua, et al., 2012; Opris, Hampson, et al., 2012). Similar flows of signal have been reported in other cortical areas in monkeys (Takeuchi et al., 2011).

This result is proposed to highlight the existence of an “Executive Microcircuit” within the PFC (Opris, Fuqua, et al., 2012; Opris, Hampson, et al., 2012) necessary for decision-making.

Thalamic projections mainly target pyramidal cells, which in turn can project to neighboring interneurons (Sanchez-Vives & McCormick, 2000) (Fig.5B) to produce feedforward inhibition on nearby pyramidal cells (Krimer & Goldman-Rakic, 2001).

A. Excitatory cells synapsing other excitatory cells

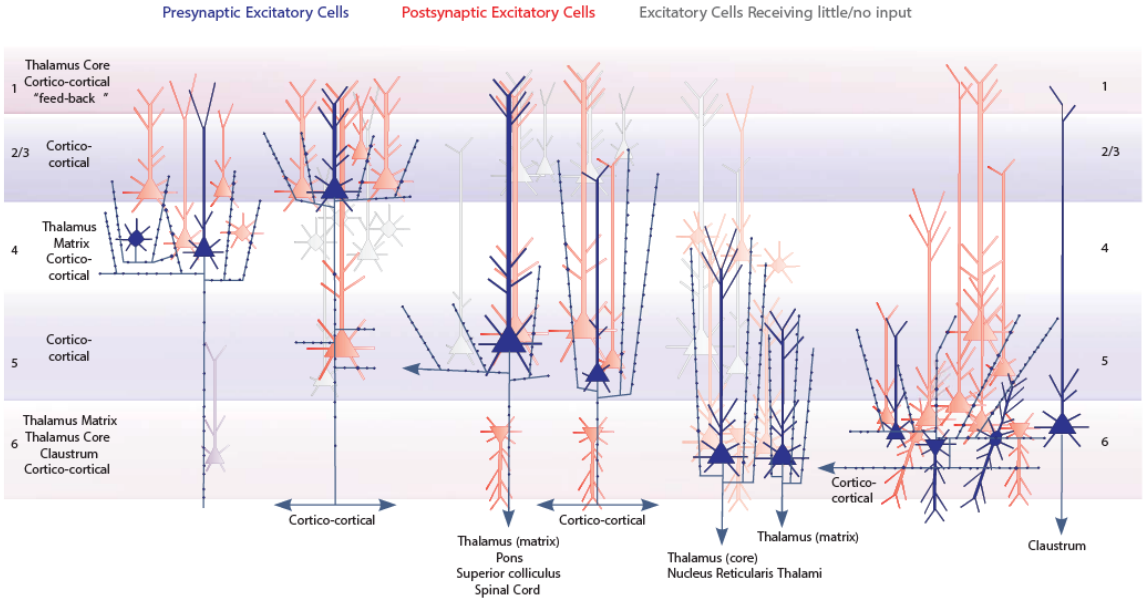

B. Excitatory cells synapsing interneurons

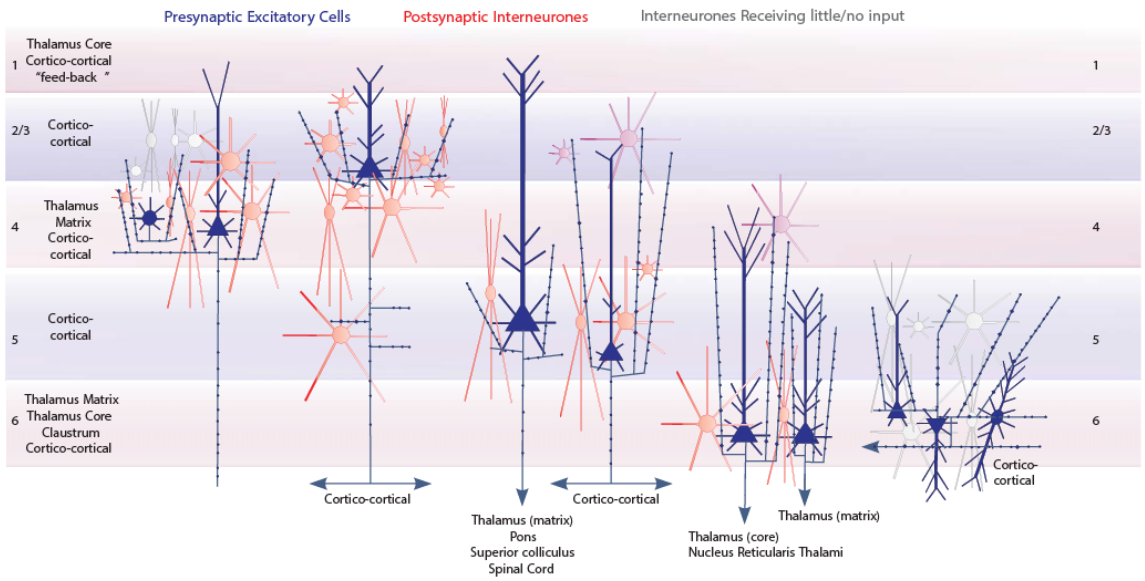

Fig. 5 Local microcicuitry of neocortex: projections of excitatory cells
Local connections of pyramidal cells onto other pyramidal cells (A.) and interneurons (B.). Blue cells are presynaptic. White cells are cells for which little to none functional connectivity has been recorded. Shades of red indicate cells that receive strong (darker red) to weak (lighter red) inputs. (Thomson & Lamy, 2007).

Interneurons receive also multiple contacts from other neighboring interneurons (Rao et al., 2000; Williams et al., 1992) and themselves (Konstantoudaki et al., 2014), generating recurrent networks aimed at controlling inhibition.

Inhibition plays a pivotal role in the prefrontal network, especially for controlling the temporal organization of actions. In monkeys, there is a constant level of basal inhibition in the dlPFC, and application of Bicuculine ($GABA_A$ antagonist) increases activity of both pyramidal cells and interneurons (Rao et al., 2000) and disrupts the performance in a working memory task (Sawaguchi et al., 1988). Moreover, paired recordings of neurons active at different times of the task (200-800ms apart) show inhibitory connections, indicating that inhibition is shaping the pattern of activity of the network while performing the task. For example, inhibitory interneurons can delay the activation of specific pyramidal cells (Constantinidis et al., 2002).

A similar situation is visible also in mice where FS-PV interneurons in the mPFC are tonically active during goal-directed behavior and their inhibition impairs performance and attention (Kim et al., 2016).

The interplay between excitation and inhibition gives rise to spontaneous slow (<10Hz) oscillations in all the cortex (and consequently also PFC) both *in vitro* and *in vivo* (Sanchez-Vives & McCormick, 2000). These oscillations are generated in layer V and propagated to more superficial layers. More recently it has been demonstrated how specific cell type can give rise to specific local neuronal oscillations.

The activation of FS-PV gives rise to local gamma (20-80Hz) oscillations, whereas specific activation of cortical pyramidal cells amplified only slow oscillations (Cardin et al., 2009).

The interactions between the PFC network and the cerebellum during cognitive tasks will be developed in chapter 1.3.

1.2 Cerebellum

1.2.1 History

1.2.1.1 First anatomical descriptions

Earlier on, I mentioned Galen as one of the promoters of the brain as source of reason. He also worked on the cerebellum, which he thought was the source of movement. But Roman law forbade human dissections, so he had only worked on animals, mainly the ox which led him to make wild assumptions on the human anatomy. Nonetheless, his work is the first reported description of the cerebellum and its division in a central region flanked by two hemispheres.

Centuries had to pass before somebody would dare criticize Galen's work. Vesalius (1514–1564), a Flemish physician, published the biggest work on human anatomy ever made until then "*De humani corporis fabrica*" (On the fabric of the human body). He worked with artists of Titian's school in Venice for the illustrations and produced the first meticulous description of the cerebellar surface (Catani & Sandrone, 2015). Raymond de Vieussens (1641–1716) and Félix Vicq dÁzyr (1746–1794), two French physicians, then described the cerebellar nuclei (Glickstein et al., 2009).

1.2.1.2 Functional studies on motricity

In 1776, Italian surgeon Vincenzo Malacarne (1744–1816) published the first ever monography on the cerebellum. This opus also determines the beginning of functional studies on the cerebellum. He notices that the number of folia is variable between individual and that it seems to be lower in mentally impaired people. Thus, he advances the idea that the cerebellum could be involved in learning (Glickstein et al., 2009).

One funny anecdote. For some years there was the theory, shared by many, that the cerebellum was a sexuality organ, and it was aberrant in sexual maniacs. This rather eccentric idea was put forward by phrenologist Franz Josef Gall (1758–1828) and his students (Eling & Finger, 2019). And it was definitively archived by Pierre Flourens (1794–1867). He removed the cerebellum from a rooster and noted that it indeed failed to copulate (although more likely due to its inability to move properly for the task than for lack of motivation).

This was part of Flourens studies on the role of cerebellum in movement of different animals. He concluded that it is essential for the coordination of movement (Fluorens, 1824), not for movement initiation as hypothesized by Luigi Rolando (1773–1831) in 1809 (Rolando, 1809).

In the meantime, research became more and more rigorous, allowing for finer dissection of cerebellar functions. Luigi Luciani (1840-1919) described the 3 cardinal symptoms of cerebellar pathologies: asthenia (muscle weakness), atonia (lack of muscle tone), and astasia (intentional tremor, tremor of muscles when performing a movement). He performed these experiments on dogs and macaques (Luciani, 1891). He later added the fourth classic symptom: dysmetria (error in gauging distance of the movement). He was the first one to perform experiments on hemicerebellectomized animals. But he removed not only one hemisphere but also half vermis which according to some physicians causes further degeneration of the tissue. It is possible to remove only one hemisphere leaving the vermis intact (called: 'functional hemicerebellectomy') but this method induces milder symptoms (Manni & Petrosini, 1997).
Moreover, Luciani disregarded the concept of functional localization in the cerebellum. He only considered the gross functional parcellation of the vermis controlling the trunk and the hemispheres controlling the limbs (Manni & Petrosini, 1997).

French-Polish neurologist Joseph Babinski (1857-1932), while working with cerebellar patients, noticed they presented two typical symptoms that supported Flourens' work on muscle coordination. They failed to properly coordinate muscle groups in order to perform complex movements (asynergia) and failed to perform rapid sequences of movements (dysdiadochokinesis) (Babinski, 1902).
Gordon Holmes (1876–1965), an Irish-British physician, worked with gunshot injured soldiers from World War I and was able to confirm all the symptoms described by Luciani. By building on these he developed the concept of ataxia (Holmes, 1917).
The two of them redefined the way cerebellum was seen and cemented the vision of the cerebellum as controller of fine motor coordination.

Not only was the clinical side advancing at high pace, basic research too made incredible progresses in the XXth century. Thanks to biochemical and optical improvements, it was finally possible to investigate the tissue at the cellular level.

At the end of the previous century, Santiago Ramon y Cajal had described the network in the cerebellar cortex and its two main inputs (Cajal, 1894). This network, so crystalline and apparently so simple was yet so complex and powerful that it would take almost 60 years before it was possible to properly investigate it, and it would need the development of electrophysiology.

In 1964 Masao Ito and coworkers would finally describe the inhibitory nature of Purkinje Cells (PC) projecting on the cerebellar nuclei (Ito et al., 1964). A discovery that challenged the popular belief that principal cells were exclusively excitatory (Glickstein et al., 2009). In the same years, the Inferior Olive (IO) is described to be a major input to contralateral cerebellar cortex (Szentágothai & Rajkovits, 1959) and that climbing fibers (CF) elicit strong excitatory inputs in PCs (Eccles et al., 1966), called "complex spikes" in contrast with the "simple spikes" induced by parallel fibers activity.

Soon after the whole cerebellar network is described (Eccles et al., 1967).

The attention also shifts on a bigger scale and the structure of the network itself is studied. Oscarson, Voogd, and Armstrong individually demonstrate the longitudinal parasagittal structure of cerebellar connectivity. Parasagittal bands of PCs receive inputs form segregated neurons in the IO and in turn project to specific areas of cerebellar nuclei (Armstrong et al., 1974; Oscarsson, 1979; Voogd, 1967), refining the notion of functional organization of the cerebellum.
Probably the climax of the century regarding cerebellar discovery was the formulation and development of the Marr-Albus-Ito theory of cerebellar learning (Albus, 1971; Masao Ito, 1984; Marr, 1969).

1.2.2 Anatomy

The cerebellum is located in the posterior cranial fossa together with the medulla and the pons. Positioned above the pons (with which it shares the vesicle of origin: the metencephalon), they delimit the fourth ventricle (Fig.6A).
It is connected to the brainstem through 3 bilateral peduncles: inferior cerebellar peduncle (*restiform body*), middle cerebellar peduncle (*brachium pontis*), and superior cerebellar peduncle (*brachium conjunctivum*). All the inputs and outputs of the cerebellum pass through

these peduncles. Inferior and superior peduncles contain mixed afferent and efferent tract, whereas the middle peduncle contains exclusively afferent fibers (Voogd & Ruigrok, 2012).

Based on gross anatomy, we can identify 3 lobes from the two principal fissures: anterior, posterior, and flocculonodular (Fig.6C). Anterior and posterior lobes are separated by the primary fissure. Whereas on the ventral side, the flocculonodular lobe is separated from the posterior lobe by the posterolateral fissure.

The cerebellar cortex is extremely convoluted into folia which gives rise to further possible divisions. Along the anteroposterior axis we can further subdivide the cortex into 10 lobules (Fig.6B), first identified in mice by Larsell in 1937 (Larsell, 1937).
Each lobule presents a central part (vermis), two lateral hemispheres and an intermediate part called paravermis (Fig.6C).

1.2.2.1 Phylogenetic division

Based on the phylogenetic evolution of the cerebellum, a different nomenclature has been proposed that divides the cerebellum in three regions: vestibulocerebellum, spinocerebellum and cerebrocerebellum (Fig.6C-D).
This system relates with the proposed functions of the different regions of the cerebellum.

The most primitive structure is the vestibulocerebellum, and it corresponds with the flocculonodular lobe. It is involved in balance and visual reflexes. It receives input from the primary vestibular afferents and projects directly to the vestibular nuclei and the brainstem.

The spinocerebellum appears later phylogenetically. It corresponds with the vermis and paravermis, which project to the fastigial and anterior interposed nuclei, respectively. Both nuclei project both upwards to the neocortex and downwards to brainstem and spinal cord.

Mostly involved with sensory and proprioceptive information, the main source of input for the spinocerebellum are the: spinocerebellar tracts, lateral reticular nucleus, cuneate nucleus, and oculomotor nucleus. It controls proximal (vermis), and distal (paravermis) muscles and it is involved with locomotion and voluntary movement. Coffman and coworkers have argued that this vision should be updated to highlight the major cortical inputs some part of the vermis receive from motor and premotor cortices and the projections that the

vermis itself has toward the neocortex (Coffman et al., 2011). Recently, the posterior part of the vermis has been involved with the limbic system, which granted it the name of 'limbic cerebellum' (Stoodley & Schmahmann, 2009).

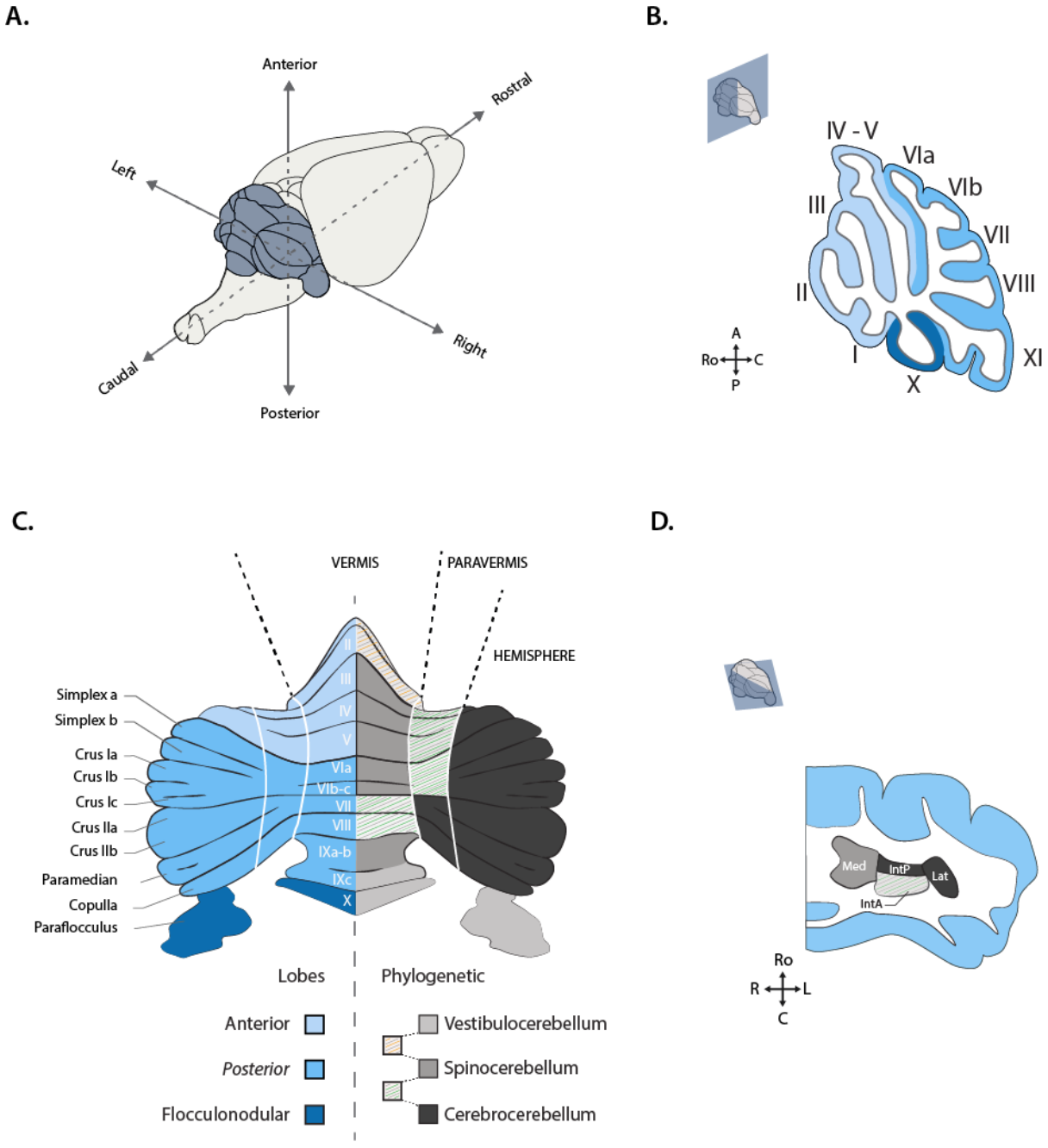

Fig. 6 Cerebellar anatomy

A. Localization of the cerebellum with regards to the rest of the central nervous system in rodent.

B. Sagittal section of the cerebellum, highlighting lobules (roman numbers) and lobes (color coded, legend in C).

C. Gross anatomical, lobes and phylogenetic divisions of the cerebellum. Lobule numbers in white roman numbers.

D. Transversal section (i.e. rostro-caudal, cf panel A) showing the phylogenetic division of the cerebellar nuclei (color coded, legend in C).

The evolutionarily more recent cerebrocerebellum corresponds to the lateral cerebellar hemispheres. This region projects only to the neocortex, after two relays through the dentate and posterior interposed nuclei, and the thalamus. The cerebrocerebellum is more developed in humans and apes than any other vertebrate (Kandel et al., 2013), mirroring the considerable development of the neocortex in these species. Historically the cerebrocerebellum has been associated with planning of motor actions, but a constantly growing body of literature is showing a role of this area in cognition and planning of abstract thoughts, as I will explain more in detail in chapter 1.3.

1.2.3 Description of the local network

One of the key features of the cerebellum, and the reason why it fascinates so many researchers is its "crystalline" microstructure. The cerebellar cortex is composed by repetitions of an almost constant microcircuit (but see Cerminara et al., 2015).

1.2.3.1 Inputs to the cerebellum

The cerebellum receives two main sources of glutamatergic input: mossy fibers (MFs) and climbing fibers (CFs) (Fig.7).

Monoaminergic inputs have also been observed, although their anatomy seems less precisely organized, and their role is poorly understood. Notably, there are noradrenergic fibers from the locus coeruleus, cholinergic fibers from the pedunculopontine nucleus and serotonergic afferents from the raphe nucleus. Their terminals are found within all three layers of the cortex and within all cerebellar nuclei.

1.2.3.1.1 Mossy fibers

They are the most numerous excitatory fibers, originating from various precerebellar nuclei, and carrying information from the neocortex (relayed through pontine nuclei), spinal cord, and brainstem. Of the inputs from the spinal cord, only the ventral and dorsal spinocerebellar tract are directly entering the cerebellum, while other sensory or proprioceptive information coming from the periphery is relayed through different pre-cerebellar brainstem nuclei (Sengul & Watson, 2015). The afferents can be either ipsilateral or bilateral, in which case they usually decussate after entering the cerebellar peduncles (Voogd & Ruigrok, 2012; Wu et al., 1999).

Through the MFs, different modalities are relayed to the cerebellum, such as: proprioceptive, tactile, somatosensory, vestibular, visual, and neocortical information.

Once these fibers enter the cerebellum, they contact and excite neurons (e.g., granule cells) in the granular layer, but they also send collaterals directly to the cerebellar nuclei, deep in the white matter (Fig.7). In the granular layer they form aggregates of multiple MFs terminals, dendrites of Granule cells, and Golgi cells' axons (Fig.7). Such aggregate is called glomerulus (Palay & Chan-Palay, 1974).

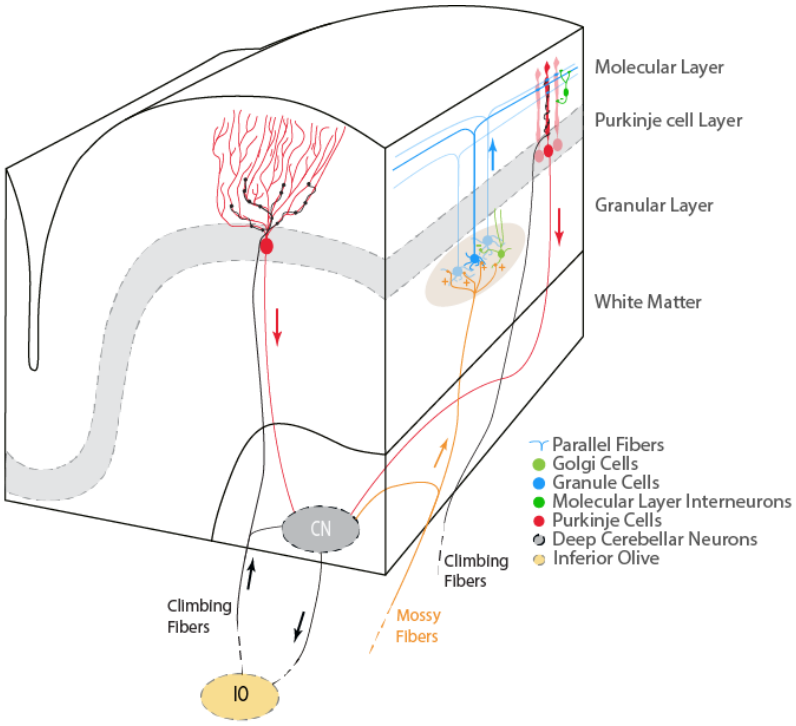

Fig. 7 Cerebellar network
Schematic section of the cerebellar network, representing selected cellular types and their connections.

1.2.3.1.2 Climbing fibers

The inferior olive (IO) is a nucleus tightly linked with the cerebellum. It is the only origin of the excitatory climbing fibers and it receives inhibitory feedback from the cerebellum, giving rise to a close recurrent loop (Bengtsson & Hesslow, 2006; Chaumont et al., 2013) (Fig.7). Almost all CFs project contralateral to the IO of origin and enter the cerebellum through the inferior cerebellar peduncle. Each CF contacts on average 6-10 Purkinje cells but each Purkinje cell is contacted by only one CF (Voogd & Ruigrok, 2012) which makes on average 300 synapses on the cell soma and proximal dendrites (Bloedel & Llinas, 1969). CFs spike at about 1Hz and

induce “complex spikes” in Purkinje cells. These are big sodium and calcium depolarizations on top of which there are usually 2-3 action potentials (the spikelets). These events play a major role in cerebellar learning and functioning, by shaping plasticities in the cerebellar cortex (notably at the PF-PC synapse) and controlling the firing patterns of the Purkinje Cells.

The IO receives inputs from most of the body (spinal cord, motor and premotor areas of the neocortex, and brainstem). The precise role of CFs is still unclear and most probably does not have a unique function , but its known function include a ‘teaching/error signal’ that drive learning (Marr, 1969) Recent evidence shows CFs encoding different aspects (correct prediction, unexpected omission, and anticipation) of prediction of events (Najafi & Medina, 2020; Ohmae & Medina, 2015) or rewards (Kostadinov et al., 2019).

1.2.3.2 Cerebellar cortex and Cortical Cell types

The cytoarchitecture of the cerebellar cortex has been described since the beginning of the century, thanks to the works of Golgi and Cajal.
The cerebellar cortex is highly convoluted and only a fraction of it is visible on the surface. Sultan and Braitenberg developed maps of flattened cerebella of different mammals (Sultan & Braitenberg, 1993). In humans it reaches a length of more than 2 meters but a width of only few centimeters. The general plan for the cortex seems to be conserved among species, with some minor variations.

The cortex is composed of only 3 layers: from external to more internal: molecular, Purkinje cell, and granular layers (Fig.7).

The molecular layer is very poor in cell somata, containing only Stellate and Basket cells inhibitory interneurons. The main elements of this layer are the vast dendrites of PCs (which we optogenetically stimulate during the experiments discussed in the manuscript) and the parallel fibers, which are the long axons of granule cells, running along the mediolateral axis and contacting many PCs on their way. Purkinje cells (first described by Purkinje in 1837, Glickstein et al., 2009) are the only output of the cerebellar cortex and thus the computational hub of the cerebellar cortex. They are voluminous GABAergic cells, with a spontaneous firing rate of 50Hz (Raman & Bean, 1999b). They project to cerebellar nuclei (Ito et al., 1964) and to vestibular nuclei outside of the cerebellum (Lisberger & Pavelko, 1988).

The Purkinje cell layer is the thinnest, consisting of a line of PCs somata and in between them Bergmann glia and Candelabrum cells (small interneurons which project to the molecular layer).

The granular layer is the deepest and contains the cell bodies of Granule cells, Golgi cells, Lugaro interneurons, and Unipolar Brush cells, and the termination of Mossy fibers.

1.2.3.2.1 Purkinje cells

PCs present the most developed dendritic tree among all neurons, it's fan-shaped and oriented on the sagittal plane (perpendicular to the long axis of the folium) (Fig. 8). The proximal dendrites are typically smooth with short stubby spines and have multiple excitatory synapses with a single CF and inhibitory ones with molecular layer interneurons (Palay & Chan-Palay, 1974). Whereas the distal dendrites present long spines on which multiple PFs synapse (Palay & Chan-Palay, 1974). Each PC receives an estimate of 175000 PFs boutons (Napper & Harvey, 1988) of which 85% are silent (Isope & Barbour, 2002), enabling them to sample a considerable amount of sensory, motor and non-motor inputs relayed by the granule cells.

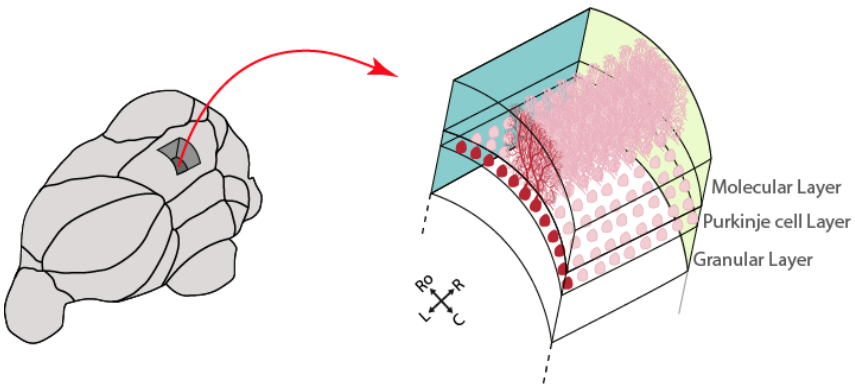

Fig. 8 Orientation of Purkinje cells
Purkinje cells lie in a thin middle layer (Purkinje cell layer) with the dendritic tree oriented along the sagittal plane

PCs axons contact multiple neurons in the cerebellar nuclei (Palay & Chan-Palay, 1974; Teune et al., 1998). Some of these cells are GABAergic nucleo-olivary neurons that project back to the IO to close the olivo-cortico-nucleo-olivary loop. Others are glutamatergic cells that will project outside of the cerebellum to the post-cerebellar nuclei.

Moreover, axon collaterals are to other PCs, and can be sent to the molecular layer, where

they synapse local interneurons (de Solages et al., 2008; Guo et al., 2021; Lainé & Axelrad, 2002; Witter et al., 2016).

PCs are spontaneously active at 40-50Hz (Raman & Bean, 1999a), generating action potentials called “simple spikes” (to differentiate them from the complex spikes induced by climbing fibers).

1.2.3.2.2 Granule cells

The granular layer is densely packed with granule cells (GCs), the smallest (5μm in rat) yet most abundant cells in the central nervous system (60% of total neurons, Harvey & Napper, 1991).

They are excitatory neurons with 3-5 small claw-shaped dendrites which form glomeruli (complex synapses) with excitatory MFs terminals (“rosettes”) and inhibitory Golgi cells’ axons (Sillitoe et al., 2018) (Fig.9). GCs can receive either unimodal inputs (Bengtsson & Jörntell, 2009) or multimodal ones by convergence of MFs from different pathways (Chabrol et al., 2015; Ishikawa et al., 2015).
GCs give rise to unmyelinated axons which move vertically up towards the molecular layer where they bifurcate to form the PFs. They run parallel to the long axis of the folium (in the medio-lateral axis) for up to 4.2-4.7mm in rat (Pichitpornchai et al., 1994) and thus cross perpendicularly the dendritic tree of multiple PCs, making only 1-2 contacts with each PC (Pichitpornchai et al., 1994).

Following stimulation, GCs can fire up to 800Hz in awake rats and rabbits (van Beugen et al., 2013). The PF-PC synapse controls the timing of simple spikes within the PC (Arancillo et al., 2015; Wise et al., 2010).

GCs are also excited by local excitatory interneurons, unipolar brush cells. These interneurons receive “intrinsic mossy fibers” (from nearby unipolar brush cells) and extrinsic mossy fibers, for example from vestibulocerebellar inputs. Thanks to this mechanism they may act as potent feed-forward amplifiers of vestibular sensory input (Mugnaini et al., 2011).

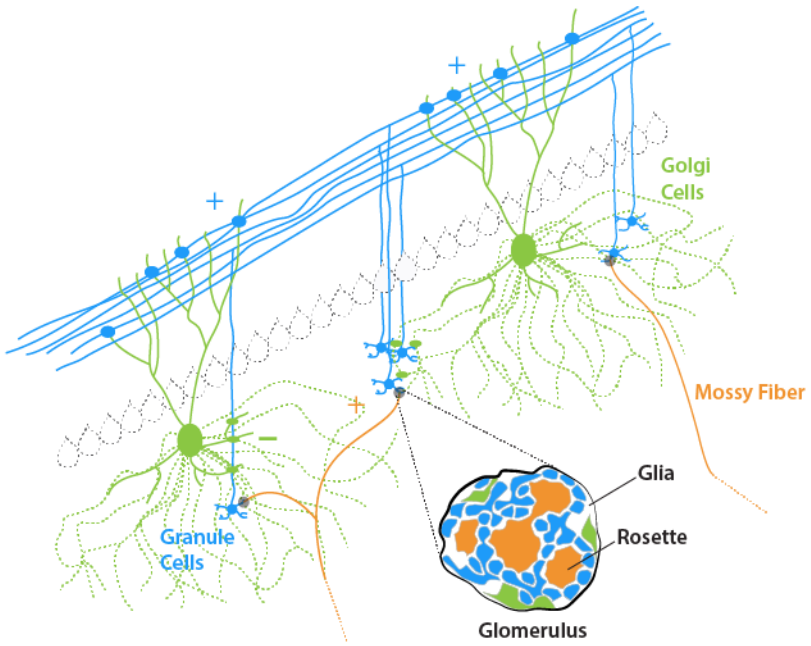

Fig. 9 Granule cell layer connectivity
Granule cells integrate signal from mossy fibers (excitatory, +) and Golgi cells (inhibitory, -) in a structure called 'glomerulus'.
Golgi cells also have apical dendrites in the molecular layer where they synapse PFs for feedforward inhibition.

1.2.3.2.3 Golgi cells

Golgi cells are a heterogeneous class of interneurons. They express and release mainly γ-aminobutyric acid (GABA), glycine or both (D'Angelo et al., 2013; Simat et al., 2007). Their axons take part in the glomeruli together with GCs and MFs, where the latter produces axo-axonic excitatory synapses on Golgi cells. Their soma is in the granular cell layer and presents a dendritic tree clearly divided in two: a basolateral branch that remains local and forms synapses *en passant* with MFs (Barmack & Yakhnitsa, 2008; D'Angelo et al., 2013), and an apical branch that is sent into the molecular layer where it synapses with PFs (Dieudonné, 1998). In this way, Golgi cells can perform either feedback or feedforward inhibition on GCs in the glomerulus (Fig.9).

Recent evidence shows a second mode of activity for Golgi cells, through a synchronized network within the electrically coupled Golgi cell's population (Gurnani & Silver, 2021) which allows them to control the gain of downstream GCs (Mitchell & Silver, 2003) and the (de)synchronization of the local network (Vervaeke et al., 2010).

1.2.3.2.4 Molecular Layer Interneurons, MLIs (Stellate and Basket cells)

MLIs are GABAergic interneurons, they are the only cells to have their somata in the molecular layer. They are divided in two groups based on the location of the soma inside the molecular layer but whether they are two separate cell types (Kozareva et al., 2020) or subgroups of the same family is still up for debate (Sultan & Bower, 1998).

Basket cells are located in the lower two thirds of the molecular layer and form a basket around the cell soma of PCs. They are excited by PFs and send axons to local PCs where they enwrap the axon hillock in a structure called "*pinceau*". This structure is able to shunt the generation of action potentials by depolarizing the extracellular milieu around the soma and the axon hillock, a process called ephaptic transmission (Blot & Barbour, 2014; Korn & Axelrad, 1980).

Stellate cells occupy the more superficial portion of the molecular layer. They are also excited by PFs and inhibit dendrites of local PCs.

MLIs are excited by CFs through glutamate spillover, by means of which they can influence PF-MLI synaptic transmission and terminate the complex spike induced by the same CF in PC (Szapiro & Barbour, 2007).

1.2.3.3 Cerebellar nuclei

The cerebellar nuclei (CN) (and the lateral vestibular nuclei outside the cerebellum, which is often considered as analog to a cerebellar nucleus) represent the final integration step of the cerebellum. Their axons are the only output of the cerebellum. They are present in all vertebrates (Nieuwenhuys et al., 1998) and are bilateral.

They reside deep in the white matter of the cerebellum and represent a heterogeneous group of cells which was first identified by Vieussens in 1685 and called it "rhomboid body" (Voogd & Ruigrok, 2012). Only in 1864 Stilling first described the four individual nuclei in the human cerebellum as, from medial to lateral: fastigial, emboliform, globose, and dentate. Followed by descriptions in other mammals by Weidenreich (Voogd & Ruigrok, 2012).
Today the nomenclature introduced by Stilling is still in use for humans. For other species, the nomenclature proposed by Ogawa (Ogawa, 1935) is more commonly used, from medial to lateral: medial, interposed (anterior and posterior), and lateral. The change in name regarding

the interposed nucleus is motivated by the less marked separation of globose and emboliform nuclei in rodents and insectivores (Voogd & Ruigrok, 2012).

1.2.3.3.1 Cell types and projections

The cellular composition of the CN is still being investigated. Classical categorizations identify 5 major cell types: 1) glutamatergic projection neurons, 2) inhibitory nucleo-cortical cells, 3) GABAergic nucleo-olivary projection neurons, 4) non-inhibitory interneurons, and 5) glycinergic premotor projection cells. Historically there were six accepted classes (Chan-Palay, 1977; Husson et al., 2014; Uusisaari et al., 2007; Uusisaari & de Schutter, 2011; Uusisaari & Knöpfel, 2012; Witter et al., 2013) and a recent study from Ankri and coworkers finally merged two classes of inhibitory neurons (nucleo-cortical neurons and local interneurons) (Ankri et al., 2015), but this is a rapidly changing landscape, and more subtypes are often reported.

The characterization was performed on the basis of biophysical properties (firing rate, waveform kinematics, and passive membrane properties), molecular markers (Kebschul et al., 2020), and cytoarchitecture (Fujita et al., 2020).

Most of these neurons are spontaneously active, with firing rates of 35-55Hz (Raman et al., 2000; Rowland & Jaeger, 2005; Thach, 1968). Only small glycinergic interneurons have been reported to be spontaneously inactive (Uusisaari & Knöpfel, 2011).

Recently a heterogeneous population of dopamine receptor D1 (D1R) has been identified in the ventral dentate nucleus in both humans and rodents (Locke et al., 2018). They are mainly local or nucleo-cortical GABAergic neurons, but a small number is glutamatergic. This result is highly interesting since dopamine is involved in higher cognitive functions and moreover, the ventral portion of the dentate relays cerello-prefrontal projections (Kelly & Strick, 2003). Indeed, inhibition of these neurons impairs such functions (Heskje et al., 2020; Locke et al., 2018)

Since a precise description of the CN network is beyond the scope the present manuscript, I will now further describe only the two most known cell classes.

1.2.3.3.1.1 Glutamatergic Projection Neurons

Main category of cells in the CN. They receive hundreds of synapses from PCs, MFs, CFs (Uusisaari & de Schutter, 2011) and local interneurons (Ankri et al., 2015). PCs show a particularly high degree of convergence (estimated to be 40:1 in rodents, Person & Raman, 2012). In turn they project outside of the cerebellum to all the non-olivary post-cerebellar nuclei (Sultan et al., 2012).

Spontaneously active, they maintain an elevated firing rate even with the incredibly high convergence of PCs input, and can be entrained to specific frequencies when the cerebellar cortex synchronizes during specific behaviors (Baumel et al., 2009; Özcan et al., 2020; Person & Raman, 2012), up to 160Hz for short bursts (Thach, 1968).

1.2.3.3.1.2 Inhibitory Nucleo-Cortical Cells

They co-release GABA and glycine (Husson et al., 2014) onto Golgi cells in the cerebellar cortex and locally in the CN through small collaterals (Ankri et al., 2015). Interestingly, these neurons are more restricted in terms of entrainment of firing rate compared to the large glutamatergic projection cells (Uusisaari & Knöpfel, 2011). This will, most probably, play a role in the excitation/inhibition balance in the CN and in the resulting signal integration.

1.2.3.3.2 Cortical control of CN neurons

Most of the knowledge regarding the connectivity in the CN is now limited to that of the glutamatergic projection cells as they are among the biggest and most numerous.

As mentioned above, nuclear neurons are mostly spontaneously active and receive PCs input with a high degree of convergence (40:1). At the same time PCs present a low degree of divergence. Each PC contacts on average 4-5 CN neurons (Sugihara et al., 2009). Which can be a different cell type (Sugihara et al., 2009).

One PC is not able to entrain or even inhibit a nuclear neuron (McDevitt et al., 1987). However, thanks to the high degree of convergence, multiple PCs synapse onto a single CN neuron and the general effect is a strong inhibition of the CN spontaneous activity (when the PCs' input is asynchronous, as discussed below). During voluntary and targeted movements activity of groups of PCs synchronizes (Chan-Palay, 1977; Heck et al., 2007; Thach, 1968). This synchronization entrains the CN network at the same frequency of PCs' discharge both *in vitro*

(Person & Raman, 2012) and *in vivo* (Özcan et al., 2020; Person & Raman, 2012). Person and Raman showed the evolution of this phenomenon by recording CN activity while modulating the degree of synchronicity of the cerebellar cortex from 0 to 50% (Person & Raman, 2012). The rationale behind this experiment was to study a more physiological situation where not all the inputs onto a single neuron are synchronized. When PC activity is desynchronized, they perform an inhibitory barrage, strongly reducing CN firing rate, but when synchronization of PC increases, the nuclear neurons show both an increase of firing rate and a synchronization to the rhythm imposed by the cerebellar cortex.

Two possible non-exclusive mechanisms have been proposed to account for this synchronization: 1) rebound activity following synchronized IPSCs (inhibitory post-synaptic currents), mediated by low-voltage-activated T-type calcium channels (Boehme et al., 2011) and 2) increased spiking probability due to synchronized pauses in IPSCs. The former mechanism disregards the information contained in the spike rate of PCs and introduces unexplainable delays in signal transduction that are not found in practice (Mauk & Buonomano, 2004).
The latter is a mechanism similar to that proposed by Fries to explain long-range oscillatory activity in the brain (Fries, 2005) (see 1.3.3.2.). This might suggest similar strategies at different scales of communication.

1.2.3.3.3 Role of CN in signal integration

A question remains, what is the role of CN in signal integration? Unfortunately, there is not an answer yet, but recent results are starting to shed a bit of light on the subject and interesting parallelisms with the neocortex are emerging.

During eyeblink conditioning both the cortex and anterior interposed nucleus (IntA) are involved in the task (rabbit: McCormick & Thompson, 1984; human: Thürling et al., 2015) but only inactivation of the cortex completely prevents the learning of the task (Koekkoek et al., 2003; Sakamoto & Endo, 2010). Whereas, once the task is learned, parts of the motor plan are stored in the IntA as inactivation of the cortex disrupts the timing but not the conditioned response itself (McCormick & Thompson, 1984; Perrett et al., 1993) but inactivation of the IntA abolishes conditioned response (Aksenov et al., 2004; Chapman et al., 1990).

Such a mechanism is reminiscent of what is seen in the motor cortex. Kawai et al. trained rats in complex and spatiotemporally precise motor sequences (that did not require dexterity) and reported that lesions to the motor cortex prevented rats from learning the tasks but if the lesion was done after the learning period, the behavior was not affected (Kawai et al., 2015). This implies, according to the authors, that the learned movement patterns are stored in subcortical structures, such as red nucleus, superior colliculus, and reticular formation, and that the motor cortex is needed to instruct these downstream structures, through plasticity phenomena.

Initial hypothesis posited of a possible similar mechanisms in PFC for cognitive tasks (Miller, 2000), but more recent studies argue that PFC maintains a basal level of activation during cognitive tasks, possibly for executive top-down control of the smooth sequencing of actions (Niki et al., 2019). It would be interesting to see if also purely cognitive cerebellar tasks have a transition similar to that seen for eyeblink conditioning or if they remain partly represented in the cortex similar to PFC. To the best of my knowledge, I'm not aware of any such study.

1.2.4 Cerebellar Modules

The three major areas of the cerebellum project specifically to different ipsilateral cerebellar nuclei: vermis projects to fastigial, paravermis to interposed, and hemispheres to dentate nucleus (Jansen & Brodal, 1940).

A cerebellar module is defined as the functional unit of the cerebellum.

A module is defined by three elements that form a recurrent somatotopic loop: 1) a subgroup of electrically coupled neurons in the inferior olive projects to 2) a parasagittal band of Purkinje cells in the cortex which contacts 3) a subgroup of CN neurons in a specific nucleus and that in turn send back collaterals to the original IO cells. These CN neurons also directly receive collaterals from the related IO neurons. This defines the olivo-cortico-nucleo-olivary recurrent loop (Chaumont et al., 2013; Uusisaari & de Schutter, 2011).

The cortical boundaries of a module are defined by the CFs, as they ramify along a parasagittal axis (modules are organized parasagittally, which is perpendicular to the spread of parallel fibers). Voogd initially identified four sagittal zones along the medio-lateral axis, A, B, C, and D in cat (Voogd, 1969). In the following years this broad division has been refined in smaller more precise modules (keeping Voogd's nomenclature). D1, D0, and D2 in the hemispheres;

C1, CX, C2, and C3 in the paravermis; A, AX, X, B, and A2 in the vermis (Apps & Hawkes, 2009; Voogd et al., 2003) (Fig.10).

Interestingly, the expression pattern of Zebrin II (later discovered to be Aldolase C) corresponds with the sagittal zones (Brochu et al., 1990; Hawkes & Leclerc, 1987).

Since a subset of IO neurons topographically contacts a stripe of PCs, these Purkinje cells, called microzone (Apps et al., 2018), share the same receptive field and receive synchronized activation from their CFs.

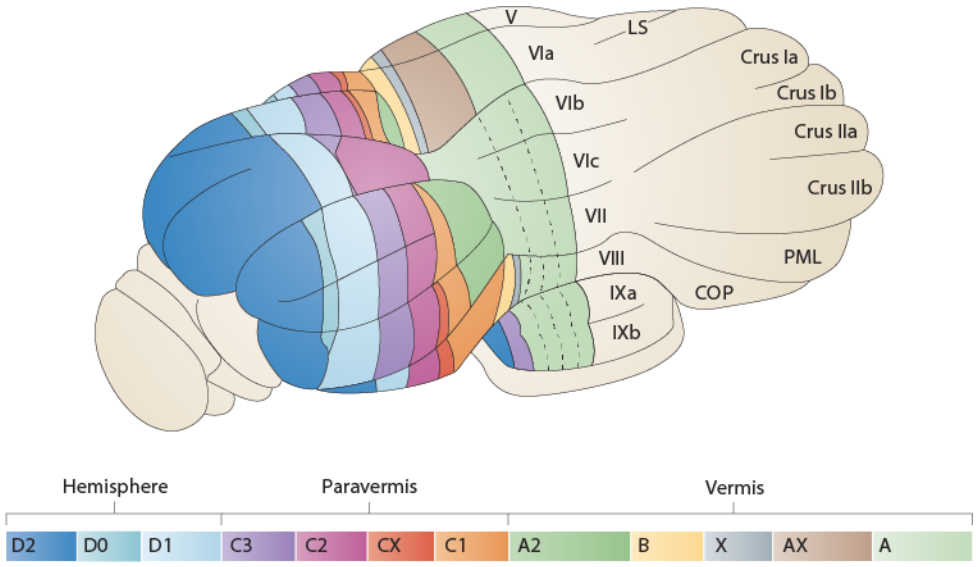

Fig. 10 Cerebellar modules
Modular organization of the cerebellar cortex. Each module is defined by a closed loop between: inferior olive, cerebellar cortex, and cerebellar nuclei. These modules have been linked with specific functional domains (adapted from Apps & Hawkes, 2009).

This modular division loosely represent somotatotopically muscle groups, in that sensory information (relayed through MFs and CFs) coming from neighboring body parts projects to similar areas in the cerebellar cortex (Apps & Hawkes, 2009; Voogd et al., 2003) although not in a precise and aligned manner as the parasagittal bands. Shambes and coworkers defined this somatotopy “patches” (Shambes et al., 1978). Moreover, the modules are task-related (Cerminara & Apps, 2011). Cerminara and Apps were able to relate specific behavioral task to definite modules (i.e., module A relates to balance and postural control of voluntary movements whereas module C2 is involved in limb control during voluntary movements).

1.2.5 Cerebellar functioning

What fascinates researchers about the cerebellum, is its ability to perform complex computations that apply to various domains (locomotor, emotional, and cognitive) with a microcircuit that is fairly conserved. Multiple models of cerebellar functioning have been proposed, in the following paragraphs I will discuss the main ones.

1.2.5.1 Cerebellar Supervised Learning (Marr-Albus-Ito model)

The perceptron (Fig.11) is an algorithm for supervised learning widely used in machine learning. It requires three elements (Raymond & Medina, 2018): 1) an adaptive processor able to modify the weights of individual connections (synaptic plasticity in the cerebellar cortex, and probably the CN), 2) a preprocessing stage of input (high signal divergence of MF in granule cell layer), and 3) an instructive signal (CF-PC synapse).

The incoming information (from MFs), from sensory cells (precerebellar nuclei), is processed in the granular layer. Where pattern separation, a process in which neural circuits convert similar input activity patterns into more distinct output patterns, can easily take place thanks to the high degree of divergence of MFs and to them being often multimodal (Chabrol et al., 2015; Ishikawa et al., 2015). The input stage (granular layer) act thus as a classification device. PF-PC synapses are created with individual weights, which differ between synapses. When the right pattern of PFs (linear sum of the weights) coincidentally arrives on the same PC (pattern selection), it is activated, and it produces an elaborated output. The individual weights (PF-PC synapse) can be depressed by CF coincidental activation (Ito & Kano, 1982) or potentiated (through high frequency PF stimulation and MLIs activation, Binda et al., 2016). The timing of the CF activation and the duration of the resulting complex spike are pivotal and can influence the nature of the computation/prediction (Herzfeld et al., 2018; Suvrathan et al., 2016). So, the weight of each PF-PC synapse is modified by the learning process to increase/decrease the role of this MF-GC-PC input onto the cerebellar output.

Before any actual biological proof of it, Marr proposed to apply the theory of the Perceptron to explain cerebellar learning (Marr, 1969), but Marr wrongly hypothesized a potentiating effect of CFs on PF-PC synapse. This theory would later be improved by Albus (1971) who proposed the depressing effect of CF's activation. Which finally Ito (Ito & Kano, 1982) confirmed with the discovery of CF's-induced LTD on PF-PC synapses.

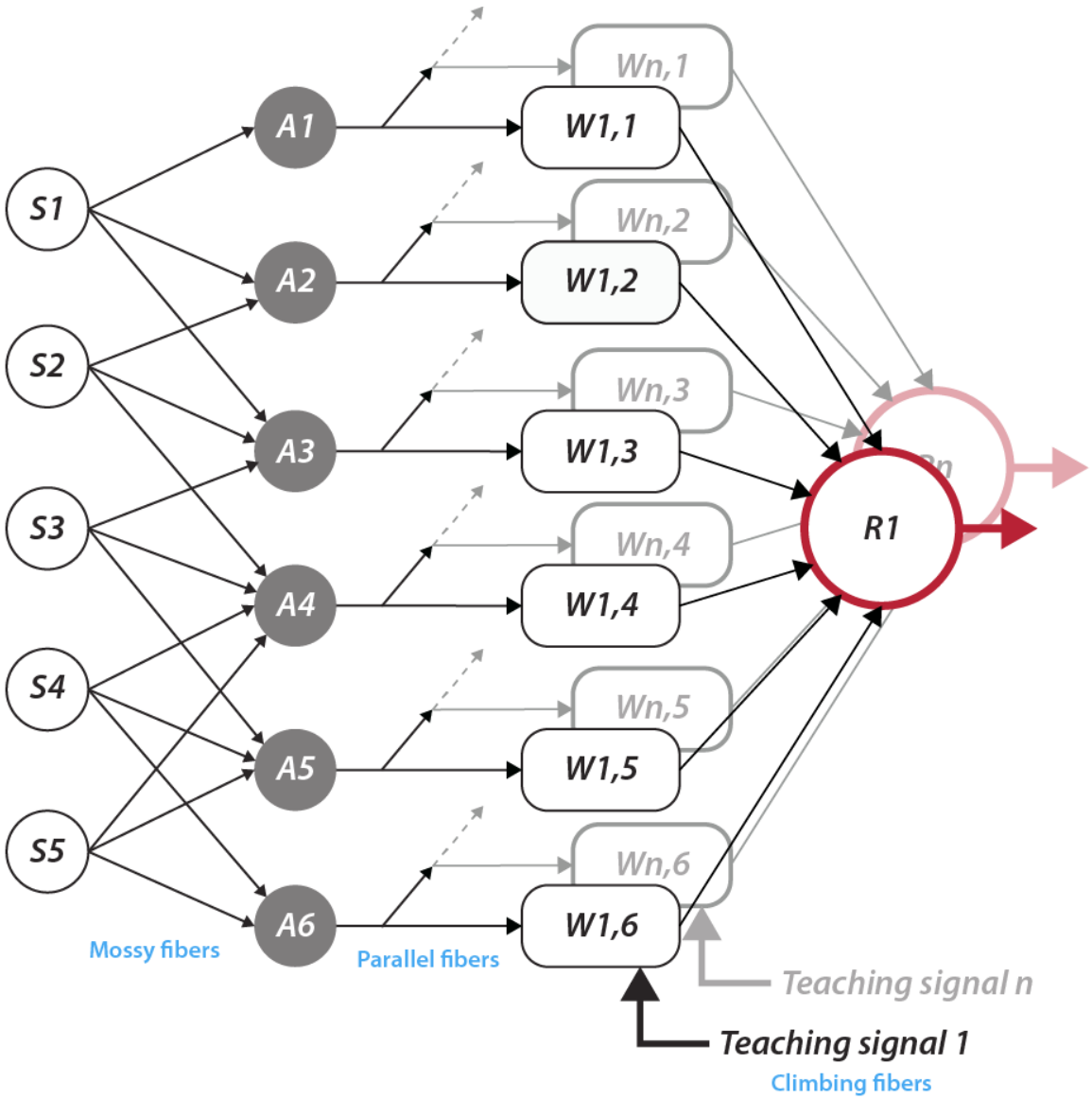

Fig. 11 Perceptron applied to cerebellar supervised learning
Sensory information incoming in the cerebellum (via mossy fibers) is delivered to multiple granule cells. Once the correct combination of inputs arrives onto them, they activate and transmit the signal to the output stage (Purkinje cells). Each PF-PC synapse has a specific weight which allows for the pattern selection to take place. These weights are adjusted by the teaching signal (climbing fibers). (adapted from Albus, 1971).

A recent review from Lisberger proposes improvements to this model, to better stress the diffused nature of cerebellar learning (Lisberger, 2021). He proposes that cortical learning is fast but short-lived. Through training, learning is moved and stored in the CN (Herzfeld et al., 2020; Lisberger, 2021).

1.2.5.2 Internal models

How can the cerebellum help with learning and online optimization of movements? It can't simply react to sensory information because such feedback systems are to slow (Wolpert et al., 1998). Instead, it predicts both the movements needed and the resulting sensory information through a series of internal models, which are neuronal algorithms providing an internal representation of the outside world (Bastian, 2006; Wolpert et al., 1998). Internal models require three inputs: 1) information from the cortex on its intentions, generally the motor plan (*efferent copy*), 2) somatosensory information from the periphery, and 3) a map of the kinematics of the body.

The *efferent copy* is provided by different cortices as a copy of the information sent to other subcortical structures. In this paradigm, PFC and premotor cortices provide a copy of the motor plan to be adjusted and then the motor cortex sends a final efferent copy to the cerebellum while sending the plan to the descending pathways of the spinal cord. Internal models could be used in different ways. For example, *inverse internal models* can determine the necessary movements to obtain the desired new position of the body, whereas *forward internal models* integrate the proprioceptive and sensory information with the motor plan to determine the future state of the body and the expected sensory input deriving from such movement (Wolpert et al., 1998; Wolpert & Kawato, 1998). In the latter, prediction is then subtracted from the actual sensory input (Blakemore et al., 1998). The resulting input is due to the unexpected (thus erroneous, since they were not planned) movements which will be corrected.

Evidences point towards the validity of *internal models* as basic computation mechanisms also for non-motor functions (Ito, 2008) such as semantic processing (Moberget et al., 2014; for a review see Argyropoulos, 2016; Moberget & Ivry, 2016).

1.2.5.3 Overview of cerebellar motor control

Sensory and motor information is conveyed to the cerebellum through CFs and MFs. The cerebellum then integrates this information and can control timing and coordination of both cognitive and motor tasks.

My project focuses on the cerebellar influence over cognitive tasks, and I will discuss them in the next two chapters. Because we know so more about cerebellar function in the context of motor control, I will present an overview of its role, keeping in mind that similar computations could use cognitive information instead of sensorimotor information to perform similar algorithms.

Regarding involuntary movements, there are few reflexes that have become indissolubly bound with the cerebellum. Examples are the eyeblink conditioning, which I presented above, and the vestibulo-ocular reflex (VOR).

This reflex allows gaze stabilization on a fixed target while the head is moving to keep the image steady on the retina. Vestibular information regarding the position of the head in space is used by the flocculus in the cerebellum to control the gain of eye movement (Miles & Eighmy, 1980; Miles & Lisberger, 1981). By preventing synaptic plasticity at PF-PC synapse, the gain of the reflex is perturbed (Boyden et al., 2006; Schonewille et al., 2010).

Impairments in the system can lead to a variety of motor and cognitive disorders depending on the area involved and the degree of the lesion or alteration.

The most common result of cerebellar malfunctions is ataxia (Holmes, 1917) which results in uncoordinated voluntary movements of different muscle groups (dysmetria), eyes, problems in swallowing (dysphagia) and speech delivery (dysarthria), and problems in balance (Ashizawa & Xia, 2016; Bodranghien et al., 2016; Schmahmann, 2004). Ataxia is a group of symptoms, not a single disease. It can result from genetic predispositions (family of spinocerebellar ataxias for example. For a review on hereditary ataxias, see Jayadev & Bird, 2013), infections (Ashizawa & Xia, 2016) or traumatic injuries (Chester & Reznick, 1987). All these disorders are grouped under the umbrella term of Cerebellar Motor Syndrome (Schmahmann, 2004).

1.3 Cerebello-Thalamo-Prefrontal Network in cognition

1.3.1 Clues from development

Working memory, rule-based learning, selective attention, temporal integration of language and thoughts, and cost/benefit evaluations are all features attributed to and thus composing higher cognitive functions. They are supposedly our most evolved social skills and appear the latest in both phylogeny and ontogenesis. These two aspects both related to the development of both PFC and cerebellar hemispheres (Tiemeier et al., 2010).

Regarding ontogenesis, some skills are not particularly developed until the early-to-mid 20s (everybody who has surpassed their teenage years perfectly knows that) (Paz-Alonso et al., 2014). This is when the PFC, the last cerebral area to mature (Fuster, 2002; Shaw et al., 2008), finishes its development and becomes fully myelinated,. Coincidentally, also the cerebellar hemispheres are the last area of the cerebellum to reach adult size, around the same age as PFC (Tiemeier et al., 2010).
Also phylogenetically, both PFC (Rilling, 2006; Schoenemann et al., 2005) and cerebellar hemispheres (Barton & Venditti, 2014; MacLeod et al., 2003) are the latest regions to appear and the most developed in the cerebrum and cerebellum, respectively, and they both are particularly developed in humans (PFC: Donahue et al., 2018; cerebellum: Sereno et al., 2020; both: Rilling, 2006).

Most interestingly, the area of the PFC that saw the most dramatic change in humans is the subcortical white matter (Balsters et al., 2010; Schoenemann et al., 2005). When comparing humans to macaques PFCs, the gray matter is 'only' 1.9 times greater while the white matter is 2.4 times more developed (Donahue et al., 2018).
This disproportion suggest a more prominent role of network connectivity in cognition than a single module and that areas functionally interconnected receive similar evolutionary pressures (Balsters et al., 2010), in accordance with the Executive Cognit Network proposed by Fuster (see 3.3.2.).

1.3.2 Anatomy of the loop

Cerebellum and neocortex engage in mostly reciprocal and topographical disynaptic connections (Kelly & Strick, 2003; Middleton & Strick, 2001) relayed through the thalamus

(cerebello-cortical direction) and pontine nuclei (cortico-cerebellar direction). In figure 12 a scheme of this recurrent loop is visible.

1.3.2.1 Cerebellar Hemispheres

CrusI and CrusII are the areas of the cerebellar cortex mostly projecting to the PFC in both primates (Kelly & Strick, 2003; Pisano et al., 2021; Ramnani, 2006; Stoodley & Schmahmann, 2009) and rodents (Badura et al., 2018; Kelly et al., 2020; Parker et al., 2017). CrusI is reportedly involved in social preference and novelty-seeking (Badura et al., 2018), language and working memory (Stoodley & Schmahmann, 2009), default mode network (DMN) (Buckner et al., 2011; Krienen & Buckner, 2009), and executive functions (Stoodley & Schmahmann, 2009).

One of the most important discoveries of the past 15 years in the cerebellar field is the involvement of the cerebellar hemispheres in major cognitive dysfunctions such as autism spectrum disorder (Kelly et al., 2020; Stoodley et al., 2017) and schizophrenia (Andreasen & Pierson, 2008; Parker et al., 2017).

These lateral projections are relayed by the ventral part of the dentate nucleus (Kelly & Strick, 2003; Middleton & Strick, 2001) (Fig.12). The dentate nucleus is segregated in functional zones, with the ventral area occupied mostly by prefrontal projections in monkeys (Kelly & Strick, 2003; Middleton & Strick, 2001) and more lateral and dorsal areas being dedicated to motor tasks. Interestingly, the ventral part of the dentate nucleus is the one that saw the major increase in volume in humans compared to the 'motor' dentate (Leiner et al., 1991; Matano, 2001), another element showing the evolutionary pressure to develop the more cognitive-related circuits.

A mention must be made to a recent paper of Guell et al. where they argue for a finer division of the pathways in the cerebellum (and in all the brain) (Guell et al., 2020). In this study they imaged human cerebella and identify three networks: default mode network (DMN), supervisory attentional system and visual. Where the DMN territory in the dentate occupies most of the ventral part. Limitations of this study (as proposed by the authors themselves) regard the inability to define a specifically motor area in the dentate nucleus. What they report is a cerebellar motor pathway that is merged with attention-driven cognitive tasks in the supervisory attentional system. Limitations aside, I feel it is important to stress their message that we need to resist the urge of merging all non-motor tasks into the 'cognitive

bucket'. DMN is more related to consciousness while supervisory attentional system to attention-based cognition and thus, it is possible that their underlining networks differ.

1.3.2.2 Vermis

The vermis has historically been tightly associated with muscular control of gait and balance. But recent literature is showing the involvement of some vermal lobules in cognitive processes (Badura et al., 2018; Stoodley & Schmahmann, 2009). Mainly in social and flexible behaviors, typically affected in autism spectrum disorder (Kelly et al., 2020; Pierce & Courchesne, 2001), schizophrenia (Andreasen & Pierson, 2008), and bipolar disorder (Strakowski et al., 2005).

Lobule VI has been linked with working memory and emotions (Guell et al., 2018; Stoodley & Schmahmann, 2009), flexible learning (Badura et al., 2018), language (Stoodley & Schmahmann, 2009) and executive functions (Stoodley & Schmahmann, 2009).

An electrophysiological mapping of cerebello-prefrontal connections in rats was performed by Watson and coworkers. They recorded field potential in the left PrL while stimulating the contralateral fastigial nucleus. They found an increase in the field potential with a mean latency of 13ms, compatible with the previously described disynaptic projection, relayed through the thalamus (Watson et al., 2014). They also performed a similar experiment in the opposite direction by stimulating PrL and recording in the cerebellum. The highest increase in field potential was evoked in lobule VII, with a mean latency of 35ms and single unit recordings of lobule VII showed complex spikes induced by PrL stimulation, indicating a possible relay through the IO (Watson et al., 2009).
Moreover, lobule VII seems mainly involved in language (Stoodley & Schmahmann, 2009). Its lateral parts (of VIIa) are CrusI/II which, as we have seen above, are the main actors of cerebellar cognitive functions.

Both lobule VI and VII show hypoplasia in autistic children (Pierce & Courchesne, 2001) and mouse model for ASD (Kelly et al., 2020).

Finally, the posterior vermis (VI-X) and medial parts of CrusI project to the fastigial nucleus with a high degree on convergence (due to the convergence of PC from the whole module). Small glutamatergic projection neurons from the caudal fastigial indirectly innervate also the

prefrontal cortex, ventral tegmental area and substantia nigra (Fujita et al., 2020), all areas involved with social behavior and emotion.

1.3.2.3 Thalamic relays

Fastigial inputs produced by small glutamatergic cells in mice, target few contralateral thalamic nuclei, but of these, only VM (Fujita et al., 2020) and MD (Fujita et al., 2020; Pisano et al., 2021) then project forward to the prefrontal cortex (Fig.12). VM is the relay of another cerebello-prefrontal projection: CrusI (passing through dentate nucleus) (Kelly et al., 2020).

In primates, MD is the main source of thalamic inputs to the whole PFC (Barbas et al., 1991). A small percentage of thalamic inputs originate also from VA and VL (Barbas et al., 1991).

Thalamic nuclei receive two types of inputs. *Driver inputs* which are the proper signal that needs to be relayed and *modulator inputs* which are weaker contacts aimed at modulating the gain of the integration of the driver signal (Bickford, 2015). These glutamatergic modulator input originate from layer VI of the neocortex and can contact every nucleus of the thalamus (Guillery, 1995; Sherman & Guillery, 2011). The origin of the driver input determines the nature of the thalamic nucleus. If the driver input originates only from the periphery, then the nucleus is called 'first order' (or class 2, Sherman & Guillery, 2011) (Mitchell, 2015). Whereas if the driver input originates in pyramidal cells from layer V of the neocortex, then the nucleus is called 'higher order' (or class 1, Sherman & Guillery, 2011) (Mitchell, 2015). The driver input is always feedforward, represent the minority of the cortico-thalamic tract (less than 20%, Xiao et al., 2009), and contacts thalamic neurons that project to neocortical layer I (Xiao et al., 2009). Thus, when it originates from the neocortex it is transmitting to another cortical area the signal already elaborated in the cortex of origin (cortico-thalamo-cortical projections).
MD is an example of higher order thalamic nucleus (Collins et al., 2018).

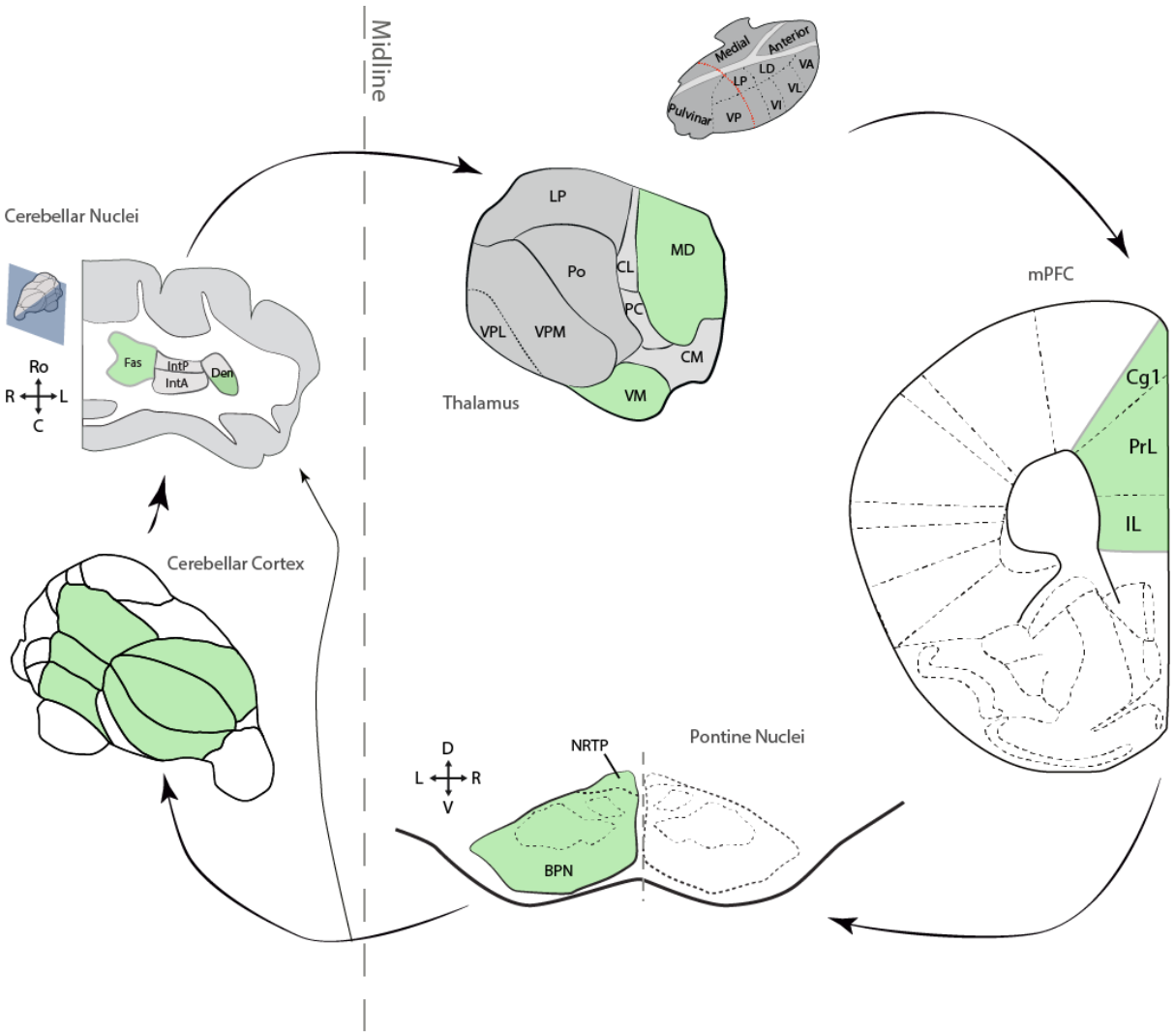

Fig. 12 Cerebello-Thalamo-Prefronto-Pontine-Cerebellar loop
Schematic representation of the relays in the loop (see text for details). The thalamus is shown in half (small insert on top) and from this, a transversal section is shown in big (cut at the level of the red line). Fas: fastigial nucleus. IntP/A: nucleus interpositus anterior/posterior. Den: dentate nucleus. LP:lateral posterior thalamic nucleus. Po: posterior thalamic nucleus. VPM/VPL: ventroposterior medial/lateral thalamic nucleus. CL: centrolateral thalamic nucelus. PC: posterocentral thalamic nucleus. CM: centro-medial thalamic nucleus. VM: ventromedial thalamic nucleus. MD: mediodorsal thalamic nucleus. NRTP: nucleus reticularis tegmentis pontis. BPN: basilar pontine nuclei.

1.3.2.4 PFC

In primates, majority of the projections originating from cerebellar hemispheres targets layer IV of dlPFC (BA 9 and dorsal 46) (Middleton & Strick, 2001; Strick et al., 2009), whereas in rodents, thalamic projections in the PFC arrive in layer I (Fujita et al., 2020; Kelly et al., 2020) where they synapse onto apical dendrites of pyramidal cells from layers II/III and V (Cauller & Connors, 1994).

Both the inputs from vermis and lateral cerebellum reportedly arrive to similar regions in the PFC (Kelly et al., 2020; Parker et al., 2017; Pisano et al., 2021). In rodents, mPFC is the main

target and it presents the highest density of cerebellar projections of all neocortex, with 400 neurons per mm^3 (Pisano et al., 2021).

1.3.2.5 Pontine nuclei

The cortico-ponto-cerebellar pathway is disynaptic (Schmahmann & Pandya, 1995) and composed of the ipsilateral corticoponto (Kamali et al., 2010; Wiesendanger & Wiesendanger, 1982) and the contralateral pontocerebellar tracts (Cicirata et al., 2005; Kamali et al., 2010) (Fig.12). Although recent evidence points at the existence of minor contralateral corticopontine tract (Morecraft et al., 2018).
The majority of pontine neurons are glutamatergic, and only 5% of total pontine neurons are inhibitory and local in primates, whereas there is no evidence of them in rats (Brodal, 2014).

Glutamatergic projection neurons of layer V of the neocortex form the corticopontine tract, which terminates in the pontine nuclei. The two main nuclei involved in the cortico-ponto-cerebellar pathway are the basilar pontine nuclei and the nucleus reticularis tegmenti pontis (Cicirata et al., 2005). Diffusion tensor magnetic resonance imaging studies in both humans and macaques showed a strong difference in proportions of fiber origin. In humans, the main provider of corticopontine fibers is the prefrontal cortex, whereas in macaques are the motor areas (Ramnani et al., 2006).

The pontocerebellar tract decussates and then enters the contralateral middle cerebellar peduncle (Brodal, 2014). From this point, the pontocerebellar fibers can go in the granular layer as MFs or contact nuclear neurons in the CN, or both.

The same regions of the cerebellum that project to a specific neocortical area, receive projections from that same neocortical area (Palesi et al., 2017), forming a recurrent cerebello-cortical loop.

The topographical somatotopy of the cortex is maintained in the pontine nuclei in rodents (Leergaard, 2003) and primates (Ramnani et al., 2006), although the exact organization of cortical projections is still not clear. The axonal terminals organize in curved cluster which then give rise to concentric topographic lamellae (Leergaard et al., 2006; Leergaard & Bjaalie, 2007), but together with the high segregation of the projections, also small clusters of

corticoponto axons that project to different regions of the pons have been reported. This seems to promote a small degree of integration and multimodality (Leergaard, 2003).

1.3.3 Functions

1.3.3.1 Universal Cerebellar Transform

The modular structure of the cerebellum is repeated almost identically across the whole cerebellum (Cerminara et al., 2015). For this and from clinical observations of various cerebellar damages, Schmahmann proposed the concept of Universal Cerebellar Transform (Schmahmann, 2000).

In this proposed model, the functions of the cerebellum are given by its structure and by the specific connections of each subregion. The general function is that of an "*oscillation dampener"* (Schmahmann, 2000) to rapidly optimize behavior to maintain equilibrium around a homeostatic point of the system of interest. To coordinate in time a network of networks. Thus, cerebellar dysfunctions will induce incoordination (dysmetria) of their network: ataxia (dysmetria of movements), disequilibrium (dysmetria of orientation), and "Cerebellar Cognitive Affective Syndrome" (dysmetria of thoughts).

Each microzone is a different transform which can perform different behaviors depending on the network in which it is actively involved. Thanks to association fibers between different networks, we obtain multi-modal integration and thus, complex behaviors (Guell et al., 2018). This shows how multiple transforms can operate in parallel to obtain more complex behaviors.

Some nuclei of the basal ganglia, such as the striatum, are another highly homogeneous structure and is hypothesized that they also operate a universal transform similarly to the cerebellum. I will discuss the interplay between these two structures in the following chapter.

It must be mentioned that this theory of the Universal Cerebellar Transform has been recently questioned by Diedrichsen and colleagues in favor of a multifunctional approach (Diedrichsen et al., 2019). In their review, they argue for a more functionally heterogeneous condition than what commonly accepted and thus it would be limiting to try and find an underlying common algorithm of the cerebellum.

1.3.3.2 Neuronal oscillations as a mechanism for information transmission

How is the information passed through different brain areas so far away and with such precision? And how is it possible that so many functions are apparently defined by the same neural substrates?

In recent years the concept of 'Dynome' has gained some attention (Kopell et al., 2014). Within this framework, the anatomical connectivity (Connectome) doesn't define the functions but the dynamic brain properties emerging from such connectivity do. Since the limited existing analyses and the computational power required to dissect a real Dynome are still out of range for many, the study of the functional connectome is still highly relied on. In this case the neuronal oscillations are used as a proxy to decipher the relationship between large-scale networks and cognitive states.

The generation and maintenance of oscillations shapes information transmission, as the excitability of the network is limited to specific windows of excitability (gating). Successful signal transmission between two areas requires coherent oscillations and synchronized excitability windows: they need to be phase-locked (Fries, 2005).

The idea of information gating at the network level has been long discussed in neuroscience (Gisiger & Boukadoum, 2011). The mechanism consists in blocking the inflow of information onto a cell or a network depending on the state of the network and is controlled by a third element (gating signal).

Different gating mechanisms have been proposed, both short- and long-range.
Bistable neurons are neurons that can be found oscillating between two states, a silent 'down' state and an active 'up' state. They can thus function as AND-gates and they can switch between the two states upon stimulation from a gating signal and thus switch to an excitable or non-excitable state (Gisiger & Boukadoum, 2011) (Fig.13A). This type of neurons have been found everywhere in the brain, such as cerebellum (Loewenstein et al., 2005), visual cortex (Cossart et al., 2003), and striatum (Wilson & Groves, 1981). In the PFC, dopamine seems to act as a stabilizer of the up-state, through D1R (Lewis & O'Donnell, 2000).

Another gating mechanism relies on inhibitory interneurons. In this case different possibilities have been advanced. The simplest being a scenario where the interneurons, when activated

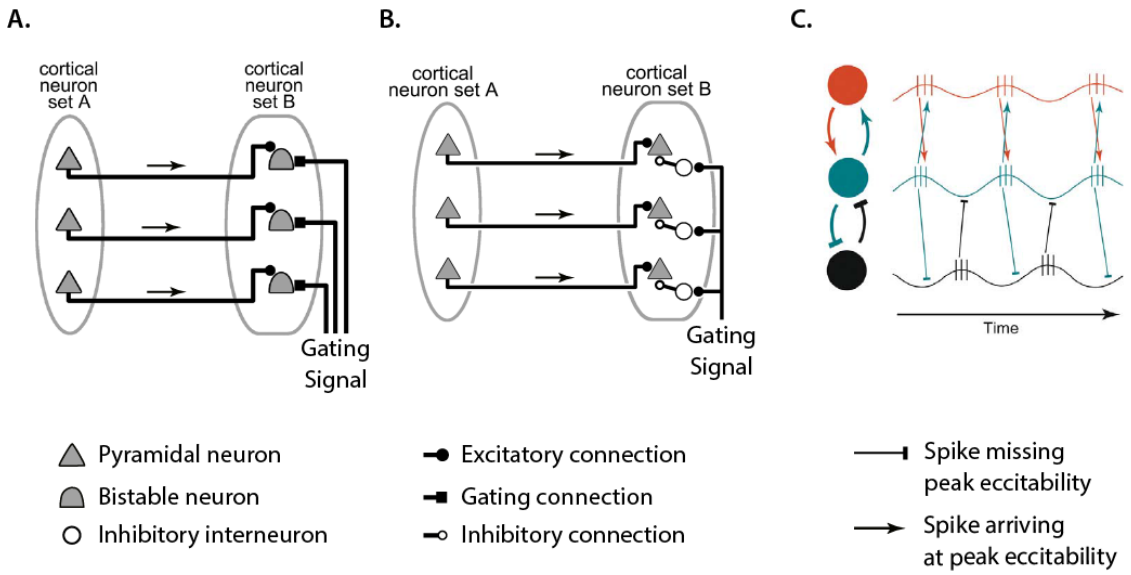

Fig. 13 Proposed gating mechanisms
A. **Bistable neurons** change state upon the gating signal which allows them to be receptive to excitation coming from pyramidal cells.
B. The gating signal activates **inhibitory interneurons** which then shunt the postsynaptic pyramidal neurons making it unable to respond to the excitation of other neurons. (A and B adapted from Gisiger & Boukadoum, 2011).
C. **Communication through coherence.** Neurons that fire with a similar phase (red and blue) have synchronous windows of excitability and thus can communicate more effectively than those that are out of phase (blue and black). Colored circles are neurons. Small vertical lines are action potentials (Figure adapted from Fries, 2005).

by the gating signal, shunt pyramidal cell's activity thus closing the gate (Gisiger & Boukadoum, 2011) (Fig.13B).

The most enticing hypothesis involving inhibition regards neuronal oscillations. In the cortex synchronous activation of FS-PV interneurons can induce and amplify gamma oscillations (20-80Hz) (Cardin et al., 2009), thanks to the interplay of the interconnected interneurons and pyramidal cells in the cortex, which can help synchronize areas for communication (Fries, 2005) (Fig.13C).
Such gating mechanisms have been proposed to control working memory in the PFC (Koene & Hasselmo, 2005; Lisman & Idiart, 1995. For a review: Badre, 2012)

Similarly, Fuster proposed the concept of the 'Executive Cognit Network' to address the dynamic nature of cognitive networks in the PFC (Fuster, 2006). For him, in the PFC the specific cognitive functions needed, arise from a transient connection of networks. This transient network arises from previous experience that binds together the neuronal assemblies that were synchronously active at the time.

1.3.3.3 Function of the loop

Morphologically heterogeneous structures such as the neocortex perform a very different transform from homogeneous structures, such as the cerebellum (Schmahmann et al., 2019). Their transform is determined by the interplay of cytoarchitecture of the column and its connections (Schmahmann et al., 2019). Through the pontine nuclei and the thalamus there is the interaction of these two transforms to give rise to a network of networks. The specific connections in this network of networks will determine the final complex output.

Sensorimotor tasks seem to activate prevalently the anterior lobe (I-V) of the cerebellum and partially vermal lobule VI, whereas the posterior lobe (VI, VII and CrusI/II) is activated by higher cognitive tasks (Buckner et al., 2011; Stoodley & Schmahmann, 2009). From their meta-analysis of the literature, Stoodley and Schmahmann supported this popular hypothesis. According to this study, the anterior lobe and lobule VI are motor related, CrusI and CrusII are for higher cognitive tasks and vermal lobule VII seems mainly involved with the limbic system and emotions (but it shows activation also for other cognitive tasks) (Stoodley & Schmahmann, 2009).

In 1998 Schmahmann and Sherman proposed the concept of the "Cerebellar Cognitive Affective Syndrome" (Schmahmann & Sherman, 1998). In this syndrome there are four recognized groups of symptoms. Impairments to executive functions, disturbed spatial cognition, personality changes, and linguistic impairments. It was the first step towards an official recognition of non-motor impairments resulting from cerebellar malfunctioning. But this is a broad grouping of a multitude of individual disorders and impairments.

In humans, impairments to the vermis more frequently produce changes of personality and behavior and instability of mood and social disinhibitions (Sacchetti et al., 2009; Snow et al., 2014) which are similar to what is seen with mPFC lesion (Buchanan et al., 2010; Maier et al., 2006). Whereas damages to the cerebellar hemispheres induce symptoms comparable to damages to dlPFC (Szczepanski & Knight, 2014) such as impairments to executive functions, working memory, and language (Buckner et al., 2011; Jacobi et al., 2021).
Similarly, in rodents' studies damages to vermis have been linked to the more emotive aspects of behavior (such as self-soothing behaviors) (Kelly et al., 2020; Limperopoulos et al., 2007)

whereas lateral cerebellar damages are related to more social and executive behaviors (Kelly et al., 2020).

The posterior lobe of the cerebellum is also related to the development of neuropsychiatric diseases such as ASD (Badura et al., 2018; Kelly et al., 2020), schizophrenia (Giersch et al., 2016; Parker et al., 2017), and bipolar disorder (Strakowski et al., 2005).

Both these two areas have projections to the prefrontal cortex, as we have seen above. Thus, it's possible that these two loops work in parallel to produce a complete behavior necessary for everyday life. On social, cognitive, and emotional aspects.

1.4 Implicit Time Processing

Time is ubiquitous in life. Every action we make needs time processing in some way: when we talk, we pronounce words with a specific rhythmicity, to move we coordinate our muscles with each other and with the environment surrounding us, and even when we think the activity of different brain areas needs to be organized in time.

How is the duration of an event perceived? Is there a dedicated structure for time processing or is it a diffused network? Is the mechanism the same for all time intervals? Can we make predictions on the future?
The knowledge in the field of time processing is progressing at high speed but we are still far from having clear answers.

1.4.1 Classification of time processing

Given the complexity of the subject, researchers have tried to segment it in precise and discrete classes using a multitude of categories. Some of which still stand today, others instead have recently been questioned by various evidence.

1.4.1.1 From multiple hours to milliseconds

We can perceive a vast array of orders of magnitude of time, from the passing of days to the quick movement of a fly. Different intervals of time require different mechanisms and rely on distinct brain structures. In general, time perception is divided into three categories: *circadian*, *interval*, and *millisecond* timings.

Circadian timing is the most clearly defined. With a duration of 24 hours, it regulates our metabolic and hormonal cycles. The suprachiasmic nuclei of the hypothalamus are considered the main clock for this system (Reppert & Weaver, 2002). This class will not be further discussed.

The other two groups are less clearly defined. Traditionally the *interval* timing is defined for periods of seconds to minutes, whereas the *millisecond* timing is related to infrasecond delays. There is not a single structure responsible for these two groups, and the PFC appears to be involved in both. Basal ganglia are reportedly involved in suprasecond timing and cerebellum in the millisecond intervals. The specific role of the last two structures is still being debated, in particular cerebellum's role in suprasecond timing (see 1.4.4.).

1.4.1.2 Implicit and explicit time

Time perception involves functionally (Zelaznik et al., 2002) and neuroanatomically (Coull & Nobre, 2008; Geiser et al., 2008) different substrates depending on whether the task requires an overt, conscious estimate of time. If it is the case, we talk about explicit timing (e.g., judging the length of an interval of time). If the task doesn't require conscious elaboration of time (i.e. time is associated to the dynamics of the non-temporal task, because the events composing the task occur in sequence), then we talk about implicit timing (Coull & Nobre, 2008). In this case, the temporal information is used to make predictions and anticipate events (either perceptual or motor), but without requiring any explicit judgement on time: it is not necessary to think about time. For example, determining the time of collision with a moving object. In this case the subject does not have to consciously calculate the object trajectory to avoid it, but the calculation still needs to be made unconsciously to move the body fast enough away from the moving object.

The distinction between implicit and explicit timing had not always been clear in the literature. It has been argued that if there are distinct elements in a task, then this can be used to tell time: even if the task does not require to think about time, the time between elements would nonetheless be explicitly used to do the task, in which case it is explicit timing (Zelaznik et al., 2002). For example, a task where the subject has to draw circles without stopping requires implicit timing processing as the timing in this case is unconsciously associated with the dynamics of the action, whereas, if the subject is instructed to stop at

every cycle for a period of time it uses explicit timing as this is a conscious use of time processing.
However Coull & Nobre (2008) showed that distinct neural networks subtended explicit from implicit timing, even when the implicit timing task involved distinct elements, and more recent publications refer to the Coull & Nobre definition (Breska & Ivry, 2016).

Both definitions agree on implicit timing being an emergent property of the action which is handled unconsciously by the neural substrate (the topic of what neural substrate is recruited by the task is discussed in the second part of this chapter).

In our study, we follow Coull and Nobre's definition and thus consider our task to rely on implicit timing even though the task itself presents discrete elements (as a reminder: two visual cues are played in a sequence and after either a fixed or variable delay a reward is delivered. See 2.5.1 for further details). By not reinforcing the timing component of the task (the reward is delivered in the same way and the cues are the same regardless of the delay in use in that specific trial) we expect time to be used implicitly for predictive computations.

1.4.2 How is time perceived?

The literature around time perception is vast and, although highly interesting, I will present only a brief overview of some of the most accepted theories on time perception. For a more in depth reading, an interesting review on the subject is that of Tallot and Doyère (Tallot & Doyère, 2020) describing both theory and experiments, and separating explicit and implicit time experimental paradigms.

1.4.2.1 Scalar property of time and pacemaker-accumulator model

The most widely accepted theory on time perception is without a doubt the "Scalar Expectancy Theory" (Gibbon, 1977). According to this theory, time accuracy is dependent on the length of the interval timed with increasing variability at longer intervals. For example, if the task is to compare two successive time intervals, a larger difference will be required for long rather than short durations. This represents the scalar property, which is similar to the description of human sensory perception by Weber-Fechner's laws (Buhusi & Meck, 2005; Dehaene, 2003).

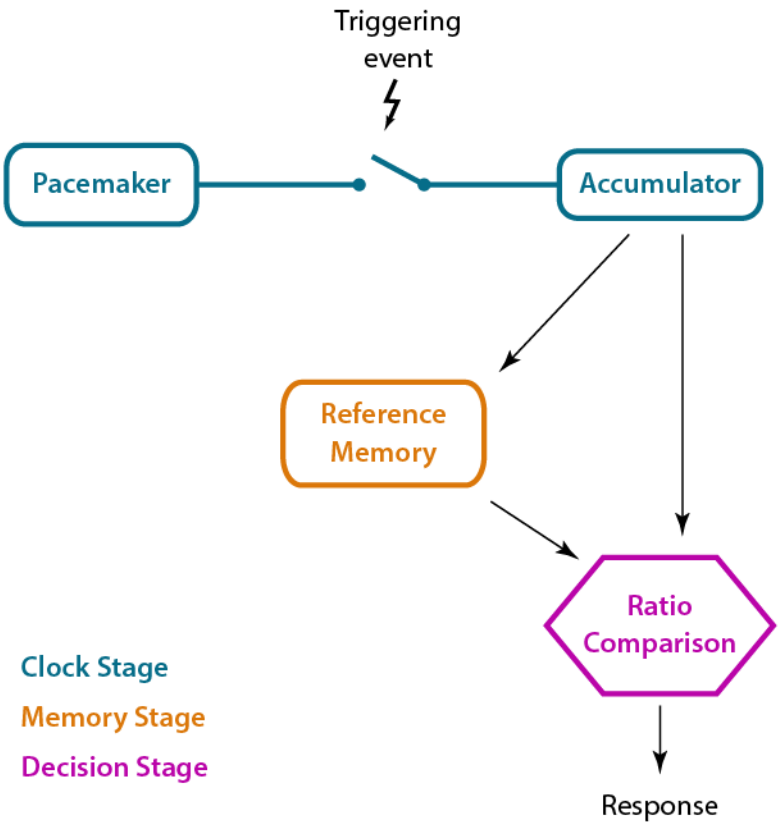

Fig. 14 Pacemaker-Accumulator model
When a triggering event happens, the switch between the pacemaker and the accumulator is closed. This allows for the counting, in the accumulator, of the number of pulses performed by the pacemaker during a behaviorally relevant epoch of time. This information, after the events, is stored in memory. During future repetitions of similar events, the new count in the accumulator is compared with the one stored in memory. If a threshold is passed then the elapsed time is sufficient and a decision is made.

In accordance with this theory, the pacemaker-accumulator model (Fig.14) has been proposed as a theoretical mechanism (Gibbon et al., 1984). The number of pulses produced by a pacemaker (internal clock) during a behaviorally relevant epoch of time is stored in an accumulator. The start of this epoch is marked by a triggering event which closes the switch between the pacemaker and the accumulator. After the epoch has passed, the information of the accumulator is moved to a reference memory. During successive repetitions or similar time intervals, the activity of the pacemaker (counted by the accumulator) is compared with the one stored in memory. The comparison is a ratio of these two values and if the result is above a certain threshold value the system responds otherwise it waits.

It is common knowledge that the more you think about time, the slower it seems to pass. Time perception is attention based (Buhusi & Meck, 2009). In the framework of the pacemaker-accumulator model, it means that by allocating more attention to the process the sampling rate of the accumulator increases and thus more beats will be used to fill the required interval. In contrast, if little attention is allocated to time, then fewer beats are used, and the interval will seem shorter.

This is just one of the many information-processing theoretical models proposed to explain time perception.

All the information-processing models seem to converge on one aspect, there are three components to time perception: 1) clock, 2) memory, and 3) decision-making stages. In the pacemaker-accumulator model, the scalar property of time is set by the memory stage, not the clock itself: the information from the accumulator is multiplied by a "memory translation constant" when moved to memory. The scalarity derives from this multiplication of the interval by a constant (see van Rijn et al., 2014 for a detailed review).

1.4.2.2 Coincidence detection as neural mechanism for time perception

The above-mentioned models are all theoretical and their application to biological systems is still to be fully agreed on. A few hypotheses relative to the physiology of time are summarized hereafter.

The most quoted group of hypotheses is that of the "coincidence detector" (Church & Broadbent, 1990). The idea is that there are multiple oscillators in the cortex (depending on the model, they are individual cells or populations of neurons) each with its own frequency and they all project to similar targets (the clock or detector). At the beginning of a timing task, the oscillators reset their phase and thus the pattern of phases is generated. This pattern will be detected by the clock during the timing interval, and once a specific pattern is reinforced enough (through repetition of the same interval), the interval of time is stored in memory through plasticity. Due to the small variability of each oscillator, there is going to be a summation of variability with the increase of the interval of time which accounts for the scalar property of time.

The difference with the previously mentioned models is that in this case there is not a

mechanism for the accumulation of ticks but are the patterns of the oscillators themselves that determine the interval of time being measured.

The Striatal Beat-Frequency (SBF) model (Matell & Meck, 2004) (Fig.15) is probably the most successful coincidence detector model. It is based on the striatal-thalamo-cortical network. The oscillators are cells in the neocortex and they all project to a subset of medium spiny neurons (MSN) in the striatum (the clock or detectors). In the striatum, there are groups of cells that are naturally tuned to specific intervals of time (Matell et al., 2003). The successful detection of a pattern in the striatum reinforces those synapses and thus strengthens the perception of that interval of time.

Interval timing and working memory have been proposed to rely on the same network of oscillators in the PFC (Lustig et al., 2005).

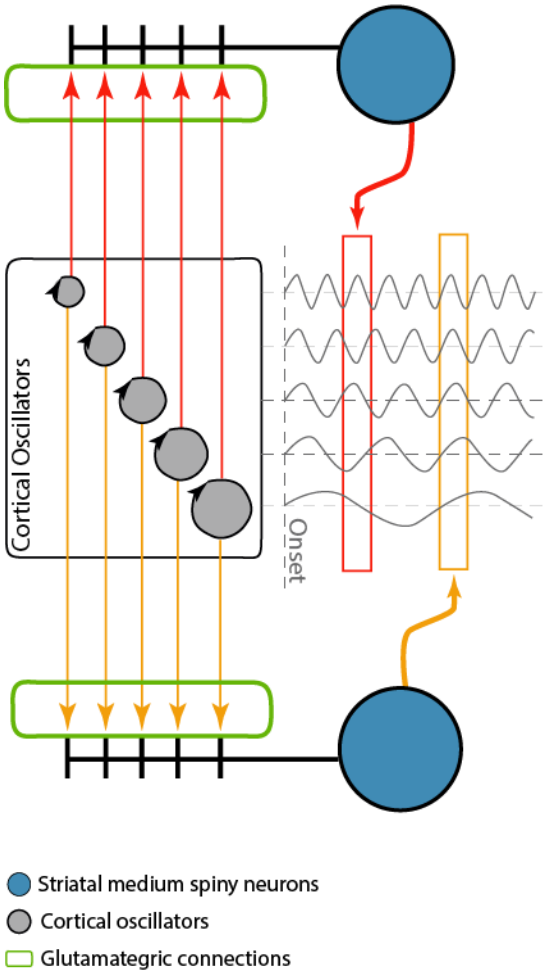

Fig. 15 Striatal Beat-Frequency model
Schematic representation of a coincedence detector model, the SBF model. At the start of an event, the phases of the various cortical oscillators are reset (dotted vertical line 'Onset'). On the right, it is depicted the oscillatory activity of the five cortical oscillators with different periods.
The same group of oscillators can thus produce multiple different patterns (in this example two of the possible patterns have been highlighted: two boxes, orange and red, on the right of the cortical oscillators). In this example two striatal neurons, in blue, are sensitive to two different patterns (color-coded boxes), generated by the same subset of cortical oscillators.
These oscillators project onto striatal medium spiny neurons through glutamatergic connections (green boxes).
These striatal neurons, through dopaminergic input (not shown) become receptive to a specific pattern of activation arriving from the cortical oscillators. (Adapted from van Rijn et al., 2014)

1.4.3 Temporal expectation and anticipation

In order to survive, animals have to constantly make predictions about the environment. Those that are better at making these predictions, can better react and adapt to the environment, thus increasing their fitness.

Prediction can take on different meanings, even meanings unrelated to actions or movement. It can predict the trajectory of a moving prey to catch it, or the next words in a sentence to properly time their vocalization or even to anticipate an abstract concept in order to organize a stream of thoughts.

1.4.3.1 Ramping activity

Neuronal ramping is commonly seen in interval timing tasks. It is limited to situationally relevant intervals of time (Fig.16); the ramping starts at the instructive cue and terminates at the imperative cue. The mathematical function used to describe this phenomenon is the Hazard Function (Luce, 2008). According to this function, an imperative event, that has not happened yet, becomes more probable with the passing of time and thus expectation/anticipation constantly increases until it is resolved with the imperative stimulus. Similar to event-related potentials, neuronal ramping has been proposed to be the accumulator (Janssen & Shadlen, 2005) and to drive working memory in the PFC (Bekolay et al., 2014; Lewis & Miall, 2006).

This ramping activity is correlated with the anticipation of some timed event. Neurons start to consistently increase or decrease their activity during a behaviorally relevant epoch of time

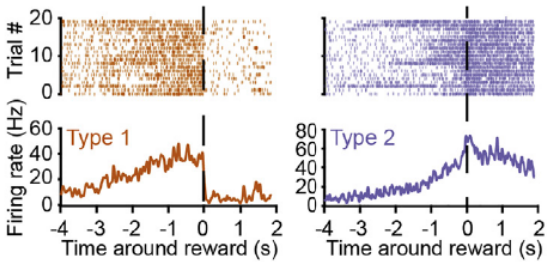

Fig. 16 Neuronal ramping
Examples of neuronal ramping of neurons differently locked to the same behavior. In this experiment mice were headrestrained on a cylinder and had to move inside a virtual maze to reach a reward. (adapted from Chabrol et al., 2019).

following the initial trigger. This activity has been seen at both single unit level (Chabrol et al., 2019; Donnelly et al., 2015; Gao et al., 2018; Parker et al., 2014, 2017) and population level (as event-related potentials) (van Rijn et al., 2011; vanVugt et al., 2012; Walter et al., 1964). Ramping activity can be observed in different brain areas, such as PFC (Donnelly et al., 2015; Parker et al., 2014, 2017), Cerebellum (Gao et al., 2018; Parker et al., 2017), anterolateral motor cortex (Chabrol et al., 2019; Gao et al., 2018), supplementary motor area (SMA) (Casini & Vidal, 2011), and somatomotor cortex (Nagai et al., 2004).

1.4.3.2 Predictive coding

Through predictive coding, the brain can make predictions about the expected sensory inputs. "*Predictive coding theories posit that the perceptual system is structured as a hierarchically organized set of generative models with increasingly general models at higher levels*" (from Winkler & Czigler, 2012). The predictive coding model is tightly linked with Bayesian inference (from which the terminology is often borrowed. For a comparison of the two, see Aitchison & Lengyel, 2017). Predictive coding requires a hierarchical model where predictions are passed in a top-down manner. In this way the hierarchically superior cortices pass their expectations to the cortices that are immediately below them in the hierarchy and receive from them a

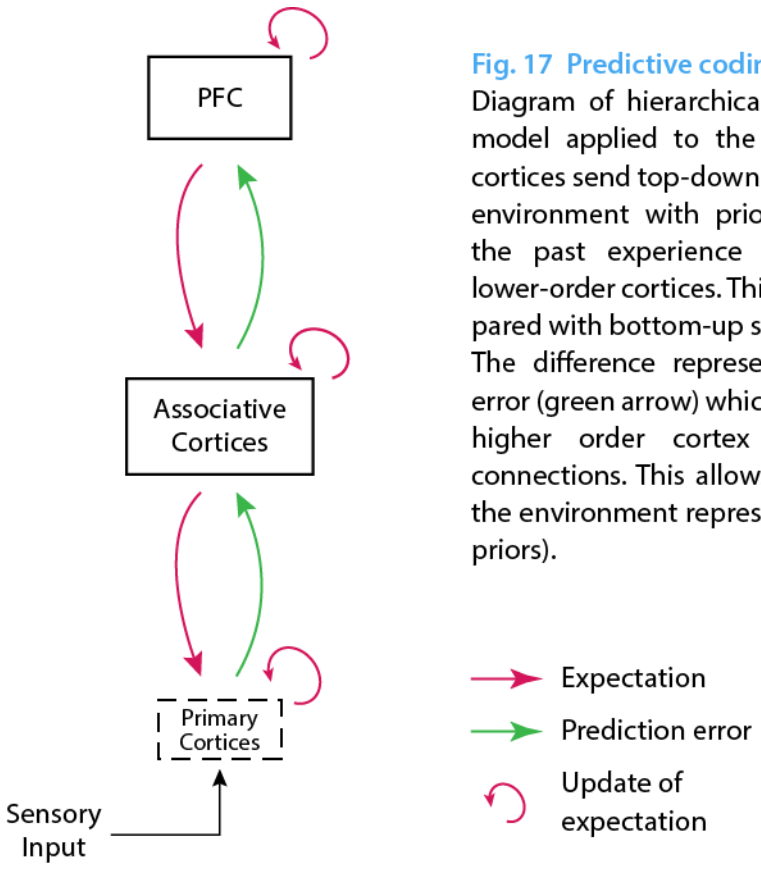

Fig. 17 Predictive coding
Diagram of hierarchical predictive coding model applied to the neocortex. Higher cortices send top-down expectations of the environment with prior knowledge from the past experience (purple arrow) to lower-order cortices. This prediction is compared with bottom-up sensory information. The difference represents the prediction error (green arrow) which is sent back to the higher order cortex through forward connections. This allows for the update of the environment representation (update of priors).

prediction error (obtained by comparing the prediction coming from the higher levels to sensory input coming from lower levels) that will be used to update future predictions.

In this model, a prediction is generated based on the prior knowledge of the environment, called expectation. As a 'hierarchical model', it operates in repetitive steps where the output of one level (the prediction) is sent to lower levels where it will be compared to the local expectation (Fig.17). The result of this comparison is the prediction error, and it is sent back through forward connections to higher level from which the original prediction came from. Here, this prediction error will be used to update the expectation and future predictions (Shipp et al., 2013).
In the PFC predictive coding has been proposed as one of the mechanisms for the maintenance of working memory. Elements are retained until they are useful for the updating of predictions. They are discarded once they no longer provide useful information to reduce the prediction error (Alexander & Brown, 2018).

This is a highly interconnected recursive network whose objective is to improve predictions to reduce prediction errors. The nature of the prediction depends on the connected structures.

1.4.3.3 Sampling frequency of reality

These theories clearly suggest that the brain is constantly generating and updating plans of both current and future environment. But at which frequency are these plans updated? The 'Subjective Present' is the time window in which we consciously perceive events as being synchronous, in humans this window is around 50-55ms, depending on the sensory modality and the complexity of the stimuli (Brecher, 1932; Elliott et al., 2006). This means that events that are separated by a delay higher than 50ms can be consciously perceived as separate in time in more than 50% of the cases (above chance level).

Evidence shows however, that there is unconscious time integration at shorter intervals, even for delays of few milliseconds which yield the same rate of asynchrony detection than perfect simultaneity (Elliott et al., 2007; Giersch et al., 2015). These results highlight the existence of an autonomous level of time sequencing that still informs our actions and decision making (Giersch et al., 2015).

1.4.3.4 Variable foreperiod and temporal prediction

Most of the studies on predictive coding and ramping are performed in controlled and rhythmic conditions, but reality is not predictable and often our brain has to produce expectations of unknown situations.

In this case it is hypothesized that the hazard function will be set to ramp on an interval decided from prior expectations deriving from experience (e.g., while waiting for the traffic light to change we expect it to be in the range of tens of seconds, not tens of minutes). Experimentally this situation is reproduced with 'variable foreperiod' tasks, where the time between a cue and a reward or action (foreperiod) is manipulated according to specific criteria.

It is common experience that rhythmic events are easier to predict. Indeed, increased implicit predictability of the foreperiod improves reaction time (Cravo et al., 2013; Herbst & Obleser, 2017), called 'foreperiod effect'. In accordance with the hazard function, reaction becomes faster and more accurate the longer the variable foreperiod is (Coull et al., 2016). This effect is not observed for fixed and predictable foreperiods (Coull et al., 2016). In the case of a variable foreperiod, the temporal expectation has to be routinely updated. If for example there are two possible intervals, the individual knows that the target will occur within a given interval. The probability that the target occurs at the earliest time is 50%. This probability has to be updated to 100% once this interval is over and the target has not occurred yet.

dlPFC (Coull et al., 2016; Triviño et al., 2011; Vallesi et al., 2007), left inferior parietal cortex (Coull et al., 2016), and cerebellum (Breska & Ivry, 2021) are among the areas implicated in the foreperiod effect, all contributing to the constant update of implicit temporal expectations. Interestingly, Coull and coworkers found that dlPFC is highly activated during variable highly unpredictable foreperiod tasks and only to a lesser extent during fixed foreperiod task (Coull et al., 2016). Indicating that probably dlPFC is fundamental for the dynamic update of temporal expectations.

Another source of debate around PFC is the laterality of implicit time. Most of the evidence in humans points to right dlPFC (Coull et al., 2016; Vallesi et al., 2007) but some studies involve mainly (Triviño et al., 2011) or partially (Coull et al., 2016) left dlPFC. In rodents however, the left mPFC is always involved in implicit prediction/expectation of reward (Totah et al., 2013a).

This confusion on the laterality could be explained by small differences in the task, which could recruit slightly different neural substrates.

As discussed above (see 1.3.3.2.) neuronal oscillations play a pivotal role in communication and information transmission between areas. It is widely accepted that low frequency oscillations (< 30Hz) convey long-range information whereas high frequency oscillations (gamma and above) are for local communication.
Different studies have investigated implicit temporal expectation both in the PFC (Totah et al., 2013a) and other cortical areas (mainly auditory cortex) (Cravo et al., 2013; Herbst & Obleser, 2019). Regardless of the area investigated, there is one oscillation that seems to be always involved in this task: delta (1.5 - 4Hz). Totah and coworkers showed an increase of delta power in correctly performed implicit timing tasks (Totah et al., 2013a). Although only ACC showed phase-locking to delta during the anticipation phase; the PrL instead was phase-locked to beta (10 – 30Hz). Cravo et al., proposed that slow frequency oscillations enable entrainment to sensory cues and enhance top-down control (Cravo et al., 2013).

1.4.4 Cerebellum in implicit time processing

The cerebellum is usually associated with extremely fast (infrasecond), precisely coordinated events. Such precision and speed are thought to be possible thanks to the internal models which implement predictive coding (Shadmehr, 2020; Wolpert & Kawato, 1998).

In this time frame, the lateral cerebellum is pivotal in the temporal prediction of events and in their organization in time (Wagner & Luo, 2020). GCs are thought to convey widespread predictive elements (from periphery and neocortex) which can be integrated in the cerebellar cortex by PCs (Wagner et al., 2017). On the other hand CFs convey prediction error signals in both rodents (Heffley et al., 2018; Heffley & Hull, 2019; Kostadinov et al., 2019) and primates (Larry et al., 2019), and through their control of short-term plasticity at the PF-PC synapse, they can help select the GCs that are signaling the right prediction and silence the wrong ones (see 1.2.5.1).

Interestingly, in all these reports CFs are active for both cued delivery of a reward (anticipation, positive prediction) and in response to un-cued reward (error of prediction) but not for error trials where the mouse makes a mistake and thus probably does not expect a

reward. Moreover, the CFs activity disappears once the task is fully learned and when the reward is fully predictable (Kostadinov et al., 2019).

Cerebellar nuclei seem to be able to keep track of the elapsed time across different trials and for durations longer than 1 second (Ohmae et al., 2013). Ohmae and coworkers presented a stimulus in a repetitive and isochronous manner to monkeys with an inter-stimulus interval between 100-600ms. By recording the activity in the dentate nucleus, they noted an increase in the basal firing rate correlated with the succession of stimuli (ramping across hundreds of milliseconds). This evidence could disprove the hypothesis for which the cerebellum is involved exclusively in duration-estimation timing (as opposed to basal ganglia that rely on beat timing) (Teki et al., 2011) or could hint at an influence of the basal ganglia on the cerebellum.
Moreover, it posits a role of cerebellum also in suprasecond timing.

In humans, cerebellar patients show impairments only on discontinuous movements (drawing circles in a sequence or rhythmic tapping) and not in continuous ones (continuous drawing of circles) (Spencer et al., 2003; Zelaznik et al., 2002). This result is explained by the authors as a sign of the specific role of the cerebellum in sequencing and timing discrete events. More evidence shows erroneous implicit perceptual (non-motor) timing in cerebellar patients (Bares et al., 2007; Beudel et al., 2008).

Multiple evidence is accumulating on the involvement of the cerebellum in suprasecond interval timing in both humans (Gooch et al., 2010; Onoda et al., 2003; Parker et al., 2017) primates (Ohmae et al., 2013), and rodents (Parker et al., 2017).

These data altogether show how the cerebellum, in particular lateral hemispheres (Ohmae et al., 2013; Parker et al., 2017; Wagner & Luo, 2020), codes for the prediction of events in both infra- and supra-second intervals, and could thus help coordinate responses by passing on this information to other structures such as basal ganglia and neocortex (Petter et al., 2016).

1.4.4.1 Cerebellum and basal ganglia interaction allows for a continuous perception of time

Cerebellum and basal ganglia can interact both ‘directly’ (through the thalamus) and indirectly (through the cerebral cortex). In this paragraph I will discuss the recently discovered direct

connections between cerebellum and different subnuclei of the basal ganglia (and dopaminergic pathways in general). In the next paragraph I will instead discuss some of the indirect connections and how these two areas may come together to influence time integration in the PFC.

Cerebellum and basal ganglia are reciprocally connected although not in a closed loop. The subthalamic nucleus in the basal ganglia projects disynaptically to the cerebellar cortex (Fig.18) in motor (HVIIB) and non-motor (CrusII) cerebellar cortices in primates (Bostan et al., 2010) and rodents (Sutton et al., 2015). The dentate nucleus, instead, projects to the striatum, through centrolateral thalamus, in both primates (Bostan et al., 2013; Hoshi et al., 2005) and rodents (Chen et al., 2014; Ichinohe et al., 2000). Interestingly the targeted cells in the striatum (MSN) are also both the target of the cortico-striatal motor projections (Zemanick et al., 1991) and are involved in time integration, according to the SBF model. The cerebellum could thus influence different aspects of timed movements through plasticity at these cortico-striatal synapses.

One of the main roles of the dopaminergic systems (which involves basal ganglia) is related to reward prediction errors (for a detailed review see Watabe-Uchida et al., 2017) and reward-based reinforcement learning. As we have seen above, rodents and primates show ramping of activity in anticipation and in response to a reward. Moreover, humans with cerebellar lesions fail to show reward-based reversal learning (Thoma et al., 2008). These evidences brought many researchers to hypothesize that cerebellum and basal ganglia collaborate to predict and associate events (Bostan & Strick, 2018).

Their collaboration could be framed in the context of 'degeneracy' (Mason, 2015) where two or more structures are able to perform similar functions through different cytoarchitectonics. Most probably the cerebellum and basal ganglia do have a millisecond and suprasecond specialization, respectively, but their functions overlap to ensure a smooth perception of reality and to partially compensate for minor local impairments (Petter et al., 2016).

1.4.4.2 Cerebello-PFC interaction for implicit timing

PFC is reportedly involved in explicit interval timing in both humans (Koch et al., 2003; Lewis & Miall, 2003b; Mangels et al., 1998) and rodents (Kim et al., 2009; Parker et al., 2017; Xu et

al., 2014). In humans, PFC is activated also during learning to properly time movement initiation (Lee et al., 2020).

The question of my project however, revolves around implicit timing. In the literature I have often found implicit and explicit non-motor timings mixed together as 'cognitively controlled task' (Lewis & Miall, 2006). In my understanding of the literature both of these timings are cognitively controlled but, as discussed in the dedicated paragraph, the key distinction is whether the timing aspect is an overt requirement for performing the task (explicit 'cognitive' time) or whether the timing is a by-product of the dynamics of the elements of the task (implicit 'cognitive' time) (Coull & Nobre, 2008). In the latter case PFC would still be involved, for these tasks rely on working memory and attention-shifting, but the timing aspect would be implicitly delivered to the PFC in order to organize the elements stored in memory.

Multiple studies of verbal working memory highlight the involvement of lateral cerebellum (especially CrusI) in verbal working memory (Stoodley & Schmahmann, 2009; Tomlinson et al., 2014), a task highly reliant on precise time prediction. Moreover, CrusI (that strongly projects to the PFC) shows activation related to learning and perfection of rule-based tasks (Balsters & Ramnani, 2011). Such activation is time-locked to the specific rule, not to the following movement, and once the rule is fully learned and the process becomes automatic, activity in the cerebellum decreases.

1.4.5 Is dopamine the puppet master of time processing?

Explicit interval timing relies on dopamine (Matell & Meck, 2004; Parker et al., 2014) and systemic block of dopamine strongly increases subjective temporal variability and thus alters interval timing (Tomassini et al., 2016). It is still being debated whether implicit timing is also reliant on dopamine (Piras & Coull, 2011).

PFC is part of the mesocorticolimbic dopamine system (Fig.18). One of the other main nodes in the reward system is the ventral tegmental area (VTA) in the midbrain. This region projects to both ventral striatum (Menegas et al., 2015) and PFC (Tzschentke, 2000). In the mesolimbic and mesocortical dopaminergic pathways, respectively. The VTA receives direct monosynaptic projections from the cerebellum (Watabe-Uchida et al., 2012) and stimulation

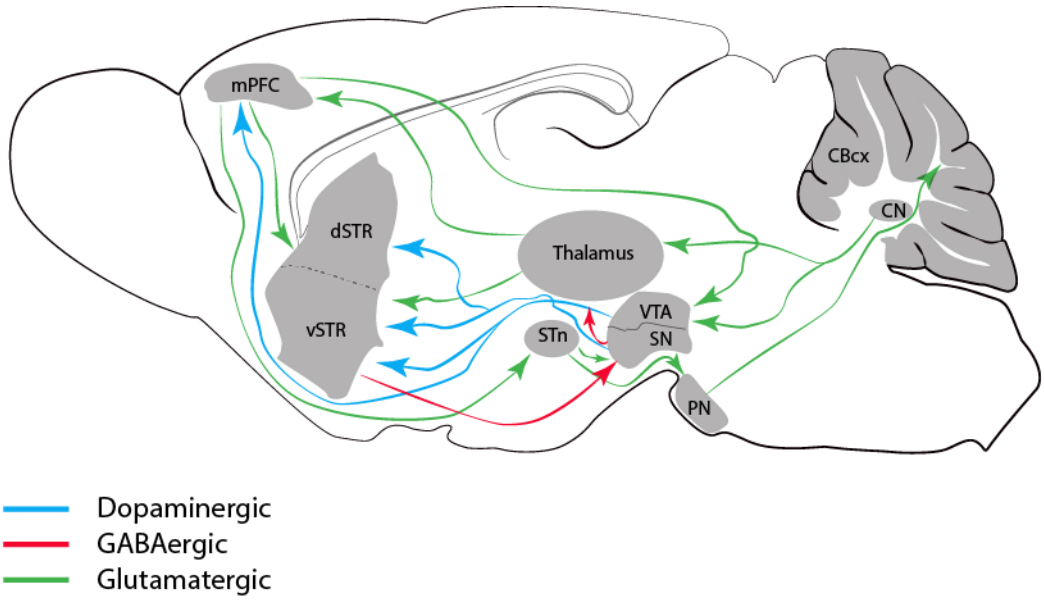

Fig. 18 Mesocorticolimbic pathway and cerebellar connections
Non-exhaustive diagram of the projections of the mesocorticolimbic pathway and its interactions with the cerebellum. Globus pallidus non included for clarity.
mPFC: medial prefrontal cortex. d/vSTR: dorsal/ventral striatum. STn: sub-thalamic nucleus. VTA: ventral tegmental area. SN: substantia nigra. PN: pontine nuclei. CBcx: cerebellar cortex. CN: cerebellar nuclei.

of the cerebellar nuclei activates the reward system passing through VTA neurons (Carta et al., 2019).

Moreover, blocking dopamine D1 receptors (D1R) in the mPFC in rodents alters explicit interval timing (Parker et al., 2014), and cerebellar stimulation is sufficient to rescue correct timing (Parker et al., 2017). Interestingly, similar impairments in interval timing (and in mPFC ramping activity) is obtained also by blocking D1R's expressing neurons in the dentate nucleus of rats (Heskje et al., 2020).

PrL is also involved with dorsomedial striatum and basolateral amygdala in timing the response to an aversive stimulus in a fear-conditioning task. During the such task, neuronal oscillations in these three areas have increased coherence in 3 - 6Hz frequency range (Tallot et al., 2020) time-locked between the conditioned and unconditioned stimuli, coherent with long-range communication of time expectation.

One final study I would like to mention on the subject is that of O'Reilly et al. (O'Reilly et al., 2008). Through fMRI, they imaged the brain while human participants were performing a

spatio-temporal perception task of predicting both direction and speed of a hidden target. The task had two variations, one where only the spatial information needed to be predicted and a second where both spatial and temporal information were variable. Interestingly the cerebellum was inactive in the first condition but when temporal aspect was to be predicted, CrusI activated in connection to both frontal areas (frontal eye field, pre-SMA, premotor cortex and PFC) and the putamen (O'Reilly et al., 2008). This again points towards the involvement of cerebellum, frontal cortex, and basal ganglia in the forward modelling of purely perceptual time events.

Lewis and Miall wrote a series of interesting reviews on the involvement of PFC in both time and working memory (Lewis & Miall, 2003a, 2006). Moreover, PFC is the highest association cortex of the brain and thus, it is in the perfect position to coordinate both perceptual and motor predictions. The cerebellum could control non-motor implicit interval timing through its projections to PFC and through its interaction with basal ganglia. Elements of the cognitive task are temporarily stored in the PFC as working memory (Baddeley, 1992). The cerebellum has been hypothesized to be responsible of organizing the timing and the sequencing of such elements (Breska & Ivry, 2021).

1.4.6 Cerebellar stimulation improves timing impairments in schizophrenia

Although my project doesn't directly involve schizophrenia and the related timing impairments, this subject has been one of its starting points and it is its future (with the next PhD student). Thus, I thought it would be a good idea to do a (very) brief overview of the literature on the topic.

Schizophrenic patients have impaired time perception (Ward et al., 2012) and a longer 'subjective present': 100ms instead of 50ms (Giersch et al., 2009). Interestingly also implicit time perception is altered (Giersch et al., 2013). A major hypothesis is that such impairments are due to altered predictive coding (Giersch et al., 2015; Lalanne et al., 2012) and cerebello-thalamo-cortical connections (Andreasen, 1999).

Predictive coding impairments seem to be due to an altered efferent copy which prevents the full cancellation of sensory inputs produced by self-generated actions (Shergill et al., 2005). It has been proposed that this alteration is due to a delayed efferent copy, not to a missing one

(Whitford et al., 2011).

A diverging hypothesis posits impairments in planning (predicting) and integrating sequences of events/actions due to abnormal communication between brain areas (Giersch et al., 2016). This hypothesis accounts also for the possible delay in the efferent copy since the following (predictable) events where not planned ahead and thus need a new processing.

As a further confirmation of cerebellar involvement, multiple evidence highlights improvements in time performance both in human patients (Demirtas-Tatlidede et al., 2010; Laidi et al., 2020; Parker et al., 2017) and rodent's model (Parker et al., 2017). To my knowledge, the effect of cerebellar stimulation on implicit time perception in rodents has not yet been investigated.

2 Materials and Methods

2.1 Ethical Assessment

Experiments were conducted in accordance with the guidelines of the Ministère de l'Education Supérieure et de la Recherche and the local ethical committee, the Comité Régional En Matière d'Expérimentation Animale de Strasbourg (CREMEAS) under the referral procedure n° A67-2018-38 (delivered on the 10th of December 2013 to the Chronobiotron UMS3415).

2.2 Mice

One strain of mice was used for the experiments: L7-ChR2-eYFP Mice (Chaumont et al., 2013). Mice were bred in the animal facility present in the building: Chronobiotron (UMS 3415, CNRS, Strasbourg). This line has a CD1 outbred background. Both male and female were used, aged 3 to 4 months. This strain expresses channelrhodopsin (ChR2) fused to yellow fluorescent protein (YFP) under the L7 (Pcp2) promoter, expressed only in the Purkinje cells in the cerebellar cortex (and in minor part in retinal bipolar neurons). Blue light (460nm) stimulation activates the cation permeable channels producing inward currents in the dendrites which reliably sum to generate action potentials (Chaumont et al., 2013).

Prior to implantation, mice were housed 3/5 per cage with littermates of the same sex, with food, water ad libitum and a 12/12 light/dark cycle. After surgery (see 2.3), mice were housed together with similarly implanted littermates, when possible. Mice were housed individually only if the implanted mouse was left without littermates due to accidental deaths or if the mice showed signs of fighting. In the latter case the dominant mouse was isolated from the rest of the littermates, and the health conditions of all mice involved was thoroughly followed in the following days.

2.3 Surgeries

During my PhD I have worked on setting up and constantly improving the experimental conditions. For this reason, the surgical procedures have evolved during the years. In the

following paragraph I will describe the surgery I have performed on analyzed mice. In Fig.19B is visible a scheme with all the implants in place.

Mice were anesthetized with Isoflurane (Vetflurane, Virbac, 3% for induction and 1.5-2.5% for maintenance) mixed with O_2, with a flux of 1 L/min. Once asleep, mice were placed on the stereotaxic frame (model 68526, RWD Life Science). Body temperature was monitored through a rectal probe connected to a heat-pad (TC-1000, Bioseb Lab) and kept at 37 °C. The eyes were kept moist by means of regular applications of Ocry-Gel (TVM).
Bupivacaïne (2 mg/kg) for pain control was injected topically prior to incision and Metacam (2 mg/kg) was injected intraperitoneally, to prevent pain and inflammation. The skin was cleaned with diaseptyl 0.5% and with ethanol 70%. Flat skull was confirmed with ± 0.1 mm of tolerance. Craniotomies were performed with a manual driller (OmniDrill35 Micro Drill, World Precision Instruments) with a ball mill tip of 0.019'' (Ball Mill, Carbide, #1/4, 0.019" Diameter, World Precision Instruments).
Respiration, temperature, and reflexes were checked regularly during the surgeries.

The skull was first cleaned with cotton embedded in a sterile saline solution (NaCl 0.9%) and then dried with a sterile cotton stick. Particular care was put in removing any possible residue of connective tissue or periosteum from the exposed skull.

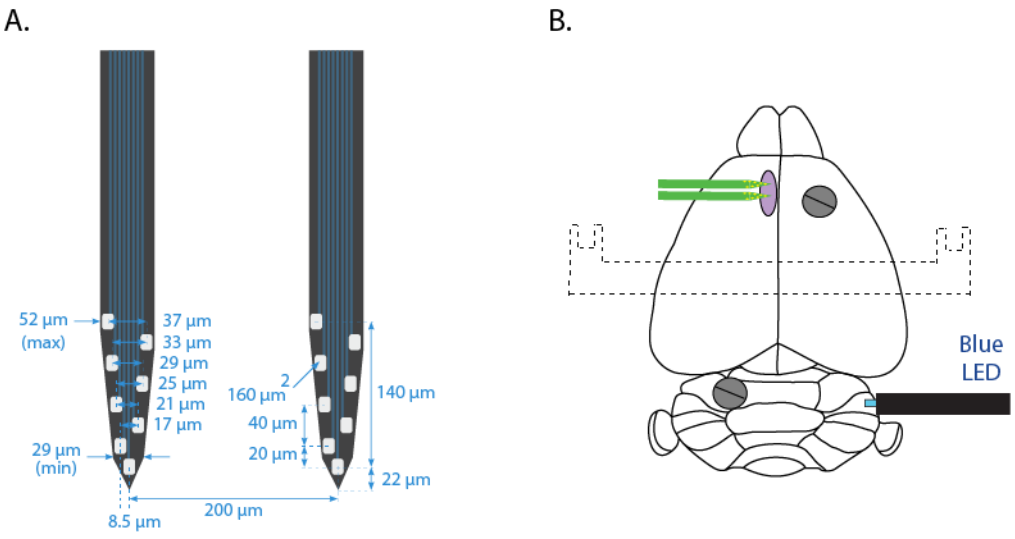

Fig.19 Probe and scheme of the implants
A. Diagram of the silicon probe with measurements (taken from Neuronexus' catalog).
B. Scheme of the implants. See text for details on the surgery.

The probe (Buzsaki16-CM16LP, Neuronexus, see section 2.4.2, Fig.19A) was implanted in layer V of the left PrL (AP: +1.9, ML: +0.3, DV: -1.6. The dorsoventral coordinate was calculated from the surface of the cortex, not from the skull), through a 0.5 mm craniotomy. The probe was painted with DiI (Vybrant DiI cell-labeling solution, Invitrogen, Thermo Fisher Scientific) for future histological confirmation of the recording coordinates. Biocompatible silicone (Kwik-Cast Silicone Sealant, World Precision Instruments) was used to close the craniotomy. Two stainless steel screws (DIN84 M1x2) were implanted as ground and reference to the probe, above left cerebellum, and right frontal area, respectively.

The cannula with optic fiber (zirconia cannula, Prizmatix. See section 2.4.3) was implanted on the surface of the cortex of right CrusI (AP: -6, ML: -3).

The head-bar (custom made, glass fiber) was sterilized and fixed to the skull, between Bregma and Lambda, using Super-Bond C&B (Sun Medical). After the first layer of cement cured, a final layer of dental cement (Paladur, Kulzer) was applied to secure the stability of the implants.

200 µL of sterile NaCl 0.9% was injected intraperitoneally for hydration. Mice were left to recover in an isolated cage under red light heat-lamp for a few hours and then placed back in the animal room once fully awake and in good health conditions. For the 48 hours following the surgery, mice had Oral Metacam (1 mg/kg) diluted in the water supply

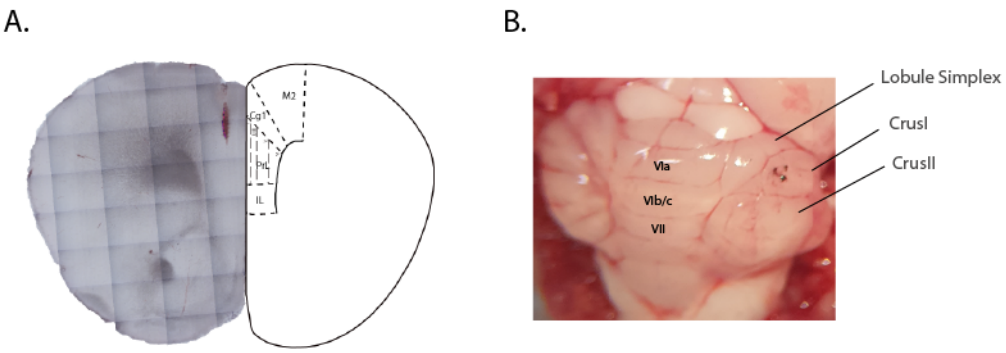

Fig.20 Location of the implants
A. Probe placement in the left PrL. Microscopy image of a fresh brain slice with probe location highlighted by fluorescence (left) and scheme of the area (right, from Paxinos & Franklin, 2013).
B. Picture of a fresh cerebellum with the marked spot of illumination on right CrusI.

for anti-inflammatory purposes. They were then allowed one full week of recovery before the beginning of the water restriction protocol.

At the end of the experiments, the mice were anesthetized with Isofluorane and euthanized with Euthasol (400 mg/kg). The implants were removed and to mark the position of the cannula, the surface of the cerebellum was cauterized through the craniotomy of the cannula (Fig. 20B). Then the brain was extracted and placed in paraformaldehyde 4% (PFA 4%) for 24 hours. Afterwards, the brain was inspected under microscope through fresh preparations to confirm the recording site. An example can be seen in Fig.20A, the lesion is fluorescent due to the DiI painted on the probe at the moment of the insertion.

2.4 Experimental setup

2.4.1 Behavioral setup

The behavioral setup is composed of a commercial part (the wheel and the head-restraining apparatus, Imetronic) and of a custom-made part (the cues, the reward delivery system and the software that controls it, LabView, National Instruments).

The wheel has 16 checkpoints along the perimeter that are recorded by the Imetronic system and logged in a specific file by the LabView interface. This allows to extract information on the instantaneous speed of the mice.
In front of the wheel there is a panel which contains green LEDs used to display the visual cues and a small speaker for the acoustic cues. It is possible to choose between four different shapes of light cue: line, circle, triangle and square.
For the mice in the preliminary tests' groups, sound was used as main cue. After discovering publications regarding a congenital cochlear degeneration which causes deafness in adult CD1 mice (Shone et al., 1991), the task was modified to include visual cues only.

The behavioral cues and the delivery of the reward are controlled by a custom-made software (LabView, National Instruments). The TTL for the reward triggers a solenoid valve (Series 3 – Miniature Inert Liquid Valve, part number: 003-0260-900, Parker) which allows the water to flow for a specific amount of time. The water then is delivered to the mouse through a spout. This spout is coaxial to a wider tube connected to a vacuum pump. Such a configuration allows

for the reward to be presented only for a limited amount of time, after which a vacuum pump removes it. This vacuum pump too is controlled by a similar solenoid valve, triggered by the same software.

The precise time of the lick is recorded by means of optic fibers. These fibers are mounted on the lick detector, placed between the mouth of the mouse and the waterspout (Fig 21A). They are placed facing each other creating an optic path. When the mouse licks, the tongue interrupts the optic path, and the time of this event is logged in the lick file.

In Fig.21 a frontal and lateral view of the setup are visible.

The interface between the software and the setup is an acquisition board (NI DAQ SCB-68A, National Instruments).

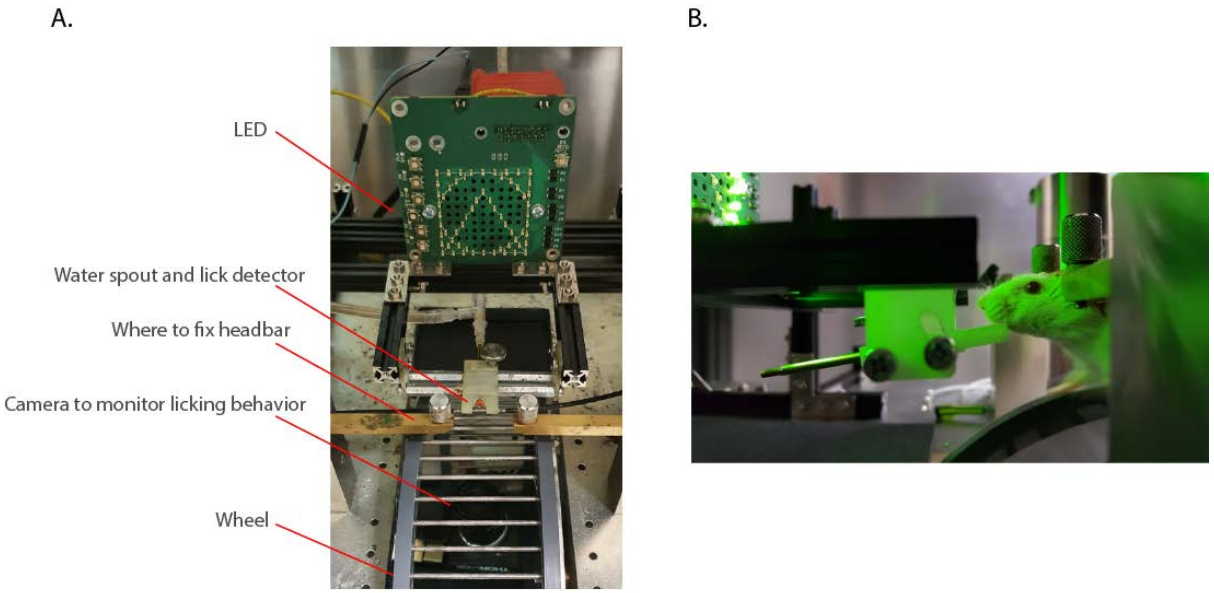

Fig.21 Behavioral setup
A. Frontal view of the setup with the main elements highlighted. The camera placed below the wheel is used to monitor the licking behavior and adjust the distance of the waterspout.
B. Lateral view of the setup with a headfixed mouse.

2.4.2 Electrophysiological setup

Chronically Implanted silicon probes with 16 channels (two shanks with 8 sites each) were used (Buzsaki16-CM16LP, Neuronexus). The probe was connected to headstage preamplifier (µPA16, Multichannel Systems) through an omnetics connector (A79039-001, NSD-18-DD-GS). As amplifier, a portable 32 channels acquisition amplifier (ME32-FAI-µPA, MultiChannel Systems) was used, with a 20 kHz sampling rate. No online filter was used. The amplifier was

controlled through the Multichannel Systems proprietary software (Multichannel Experimenter).

The TTL to start the recording is triggered by the behavioral software through the acquisition board (NI DAQ SCB-68A, National Instruments).

2.4.3 Optogenetics setup

During the recording session, the implanted cannula (zirconia cannula, Prizmatix. 1.25mm external diameter. 0.5mm diameter of the core optic fiber) is connected to an optic fiber (NA=0.63, 0.5mm core, Prizmatix). The light (16 mW/mm^2) is generated by a LED (Prizmatix; UHP-T-LED 460) and controlled by the acquisition board (NI DAQ SCB-68A, National Instruments). As mentioned above, strong synchronization of the cerebellar cortex can entrain the cerebellar nuclei to said frequency (Özcan et al., 2020). For this reason, four different protocols of stimulation were used: 125Hz, 40Hz, 6Hz, and Theta-Burst (bursts of 100Hz nested inside a 5Hz stimulation) (Fig.22B).

2.5 Behavior

2.5.1 Behavioral task

Two visual cues (0.5s each. Light1: a triangle, Light2: a square) were played 1s apart. After the second cue, there was a delay after which a water reward was presented for 0.15s. Depending

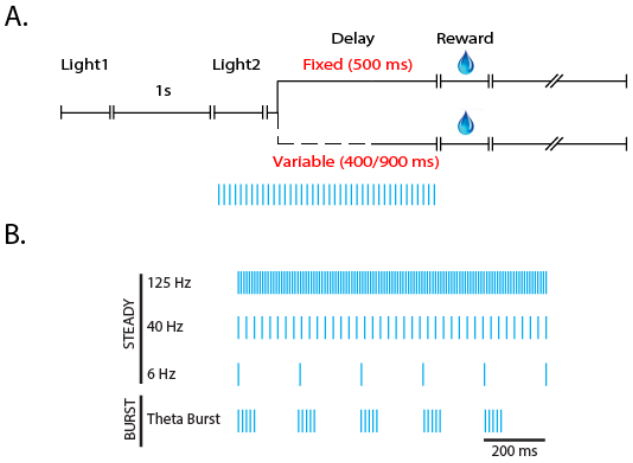

Fig.22 Behavioral task

A. Schematic representation of the behavioral task for both fixed (top branch) and variable (bottom branch) foreperiod. The photostimulation is limited to 1s from the beginning of the second visual cue to the release of the reward.

B. Structure of the four protocols of stimulation used. Each bar is a single pulse of light. The Theta-Burst protocol is composed of burst of 100Hz nested inside a 5Hz oscillation.

on the session, the delay could be either fixed at 0.5s (fixed foreperiod) or randomly chosen between 0.4s and 0.9s (variable foreperiod) (Fig22A).

During training and the first day of experiment the foreperiod was always variable. During the last day of experiment, the foreperiod was fixed.

2.5.1.1 Water restriction

Mice were water restricted to motivate them to perform the task. The water restriction started no sooner than one week after the surgeries. The mice had to have fully recovered from the surgical procedures and their body weight (BW) back to pre-surgical level.
During water restriction mice had a 30-minute daily window of time with water *ad libitum*. Since mice eat most of their food pellets with water, to prevent food restriction as well, during this window of time multiple pellets of food previously soaked in water were placed in the cage. The BW and general health status were checked daily and logged. If the mouse lost more than 20% of the original BW, the procedure was stopped, and the mouse removed from the experimental group.

The habituation to the water restriction lasted 7 days, after which their BW stabilizes, and mice were ready to start the training.
Once the training started, mice received the 30-minute ad libitum water only for the first day of training. After this they would receive the full daily water during the behavioral task (water-soaked food pellets were still provided in the cage after each training session).
The volume of water delivered during the training was more than 3mL which is the amount needed by a healthy mouse.

2.5.1.2 Training

Mice were trained for approximately 11 consecutive days (2 sessions a day of 30 minutes each). The duration of the training was variable as it depended on the performance of the individual mouse. The mouse was considered ready when it was able to lick reliably from the waterspout in the correct position for 3 consecutive training sessions.
At the beginning of the training the spout of the reward was very close to the mouse, since it had to learn where the water comes from, and it had to learn to lick instead of sucking from the spout. With the passing of the sessions and according to its improvements, the spout was

progressively manually distanced until it reached the right position (so that the drop of water coming out of the spout wouldn't cross the optic path of the lick detector but not too far for the mouse to reach).

2.5.1.3 Experimental sessions

The first day of experimental sessions was with variable foreperiod condition. Thus, no difference from the last sessions of training.
The following day instead the foreperiod was fixed. No further differences between the two conditions.

In both cases, multiple sessions were performed in one day: at first a session of 60 trials without the behavioral task (electrophysiological recordings ongoing and with same duration as normal). These recordings were used to establish a baseline of activity, followed by 60 trials of control condition with behavioral task ongoing but no photostimulation.
Afterwards, there were 4 sessions performed in randomized order between mice (to avoid possible artifacts due to the summation of smaller effects). These sessions correspond to the four possible protocols of stimulation explained above (2.4.3) and their corresponding internal control. Each session has 60 trials, of which: the first 30 are the internal control and the last 30 are with the specific photostimulation.

2.6 Mapping of the cerebello-prefrontal functional connections

A preliminary experiment performed was the stimulation of the right cerebellar cortex in different points while recording in the left PrL in order to determine the area most involved in cerebello-prefrontal connections. Six different areas of the cerebellar cortex were stimulated: lobule VI, lobule VII, CrusI and CrusII medial (paravermis) and CrusI and CrusII lateral (hemispheres).
Mice were anesthetized and prepared for surgery similarly as to 2.3. A frontal craniotomy was performed similarly to 2.3, whereas the craniotomy on the right cerebellum was performed as a rectangle of 3mm in width and 2mm in height so to expose the full right posterior lobe. Craniotomies were kept moist with NaCl 0.9% warmed at 37 °C.

An acute probe (16 channels, 4x4 tetrodes, Atlas Neuroengineering) was lowered in the left PrL (same coordinates as 2.3 and same recording system as in 2.4.2). For optogenetic stimulation, an optic fiber (0.5mm core diameter, 0.63 NA) was positioned directly on the cerebellar cortex and manually moved to the different stimulating areas.
Two protocols of stimulation were used: a steady (1s) and a pulse (4 pulses of 0.5s every 1s, 4s in total) protocol. 25 Recordings for each protocol were done on each mouse in each location.

After the end of the experiment, mice were euthanized with Euthasol (400 mg/kg) while still under anesthesia.

2.7 Data Analyses

Please note that for all analyses of electrophysiological recordings performed with a behavioral task, only the recordings of the trials where the mouse was actively engaged in the task were selected. A trial, to be considered a "good" trial, had to present at least more than 3 licks performed during the foreperiod (0s – reward delivery).

The placement of the probe was controlled post-mortem in histological analyses and only the mice where the probe was correctly placed in layer V or PrL were kept for electrophysiological analyses (Fig.20A). The behavioral data was independent of such misplacement and thus they were kept. For this reason, the number of mice differs between behavioral (n=11. Females=7, males=4) and electrophysiological (n=8. Females=5, males=3) data. Three mice were excluded from the electrophysiological analyses.

For most of the analyses, the data obtained from session with the various protocols of stimulation have been merged. This decision was taken due to the low sample size and the small size of the effects investigated. Some analyses are instead performed on separate protocols to investigate whether a specific frequency has a particular effect. This decision was taken conscious of the risks of missing some strong effects but limited to a specific protocol, but it has allowed us to investigate the broader question of whether a general stimulation of the cerebellum affects PrL in the task. Which, being this a work of development of the experimental setup, was of paramount importance.

2.7.1 Mapping of functional connections

For each recording, the 16 channels were averaged and bandpass filtered to 0.1 - 60Hz. All the recordings from the same mouse with the same condition were averaged together and the negative peak from the stimulation window and a baseline of same duration (1 s or 4s for steady and pulses protocol, respectively) were saved in a dataframe.
To investigate whether the stimulation increased the amplitude of the signal, a paired Wilcoxon signed rank test one-tailed was performed for the two protocols separately between baseline and stimulation values of the same mouse.

2.7.2 Local field potential

The local field potential (LFP) was extracted from the electrophysiological recordings and analyzed to investigate the dynamics of the local network in the layer V of left PrL.

Four bands of biologically relevant frequencies of oscillation were considered in our analyses: delta (1.5 – 4Hz), theta (4 – 10Hz), beta (10 – 30Hz), and gamma (30 – 80Hz). The specific frequency intervals were taken from Buzsáki and Draguhn (Buzsáki & Draguhn, 2004).

Two methods were used to extract different information about LFP's oscillatory activity. The continuous wavelet transform (CWT) was used to extract the time varying dynamics (2.7.2.1) whereas the Welch's method for spectral density estimation (2.7.2.2) was used to estimate the power intensity of the signal during the whole foreperiod.

2.7.2.1 Complex Morlet Wavelet Convolution

In order to investigate how the dynamics of the network changed over time in response to the behavioral task and the photostimulation, it was necessary to have a method which allows for time-resolved spectral decomposition of non-stationary signals. The CWT used here was described in Roux et al., 2007. In this method, a series of complex Morlet wavelets (Kronland-Martinet et al., 1987) is used to decompose the signal in its underlying frequencies components while maintaining a good time resolution.

For low frequencies (delta and theta) the raw signal was averaged across the 16 channels, then the amplitude for each frequency band was extracted by means of CWT and finally averaged across recordings of the same sessions for one mouse. The ridge of the resulting

average amplitude was computed for each mouse.
For higher frequencies (beta and gamma), the procedure is similar with the difference that the CWT is performed on the individual trace of each site. This was done to prevent possible phase aliasing due to the distance of the sites and the shorter period of such oscillations.

2.7.2.2 Welch's method

To investigate how the state of the network changes with the different experimental conditions, the power spectrum of the foreperiod was estimated using the Welch's method (Welch, 1967). Such a method computes the fast Fourier transform (FFT) of the signal divided into overlapping segments, computing the periodogram of each segment and then averaging them together. In this way the time information is still lost (typical problem with FFT) but it is somewhat taken into account by the segmentation of the signal.

The signal of each electrode was individually downsampled to 1kHz and the power spectrum computed: segment length of 1s with an overlap of 0.5s.
Only the frequency interval 1 – 80Hz of the resulting power spectrum was kept and normalized to the total power. Then the total power of each band of interest was averaged first between trials of the same mouse and then across all mice.
In this way the average percentage that each band contributes to the total power in the foreperiod is compared between conditions using a paired t-test.

2.7.3 Slope analyses and bootstrap

In most of the analyses the method of the bootstrap has been used. This technique allows to reduce the noise and identify the general trend of a small sample size by artificially increasing the sample size (n). Precautions have thus been taken in interpreting the results, as it is discussed few paragraphs below (2.7.6).
The bootstrapping is a method that resamples (with replacement) multiple times (permutations) from the same dataset creating multiple simulated samples.

A linear regression was computed on the foreperiod distribution and the slope values for each condition of all the mice were used as sample population for the bootstrap. 100 permutations were performed on each analysis. At each permutation 8 or 11 samples were taken for

electrophysiological or behavioral data, respectively. The mean of each permutation was stored as a new data point of the final bootstrapped distribution.

In case a shuffled distribution was used, the slope was computed on a foreperiod distribution whose points were shuffled in time so to destroy the proper time course but retaining the underlying values. The rest of the computations were the same as for the original data.

When comparing two bootstrapped distributions a 2 samples Kolmogorov-Smirnov test and Cohen's d effect size were computed.

2.7.4 Spike sorting

To isolate spikes and classify them into single units, Tridesclous (https://github.com/tridesclous/tridesclous), a Pyhton-based software, was used.

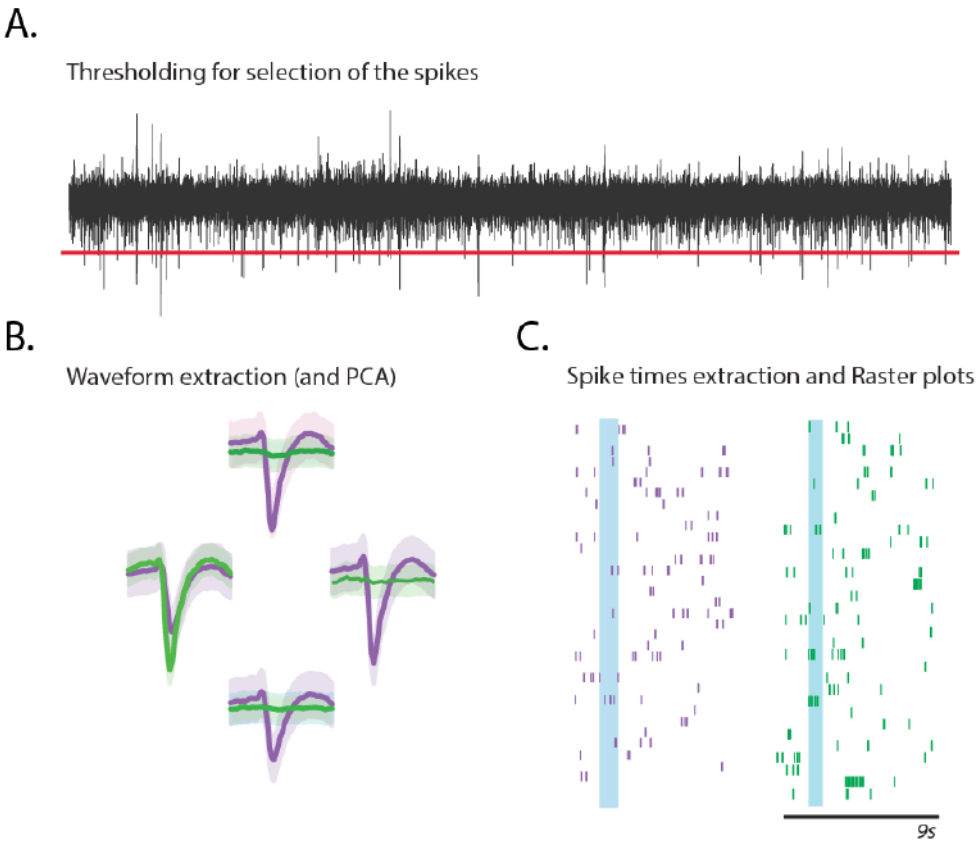

Fig.23 Spike sorting with Tridesclous
A. Bandpass filtered trace (black) with threshold (red line) for spike selection.
B. Average waveform of two example units compared across neighboring sites of the silicon probe (in this example is shown the geometry of a tetrode, not of the Buz16-CM probe).
C. Time aligned raster plot of the two example units. Each line is a trial. Light blue band: time and duration of photostimulation

This software has a threshold-based alghorithm for identifying spikes and then applies a principal component analysis (PCA) on these identified spikes to cluster them into specific units. The obtained units were successfully confirmed by plotting the autocorrelogram and confirming the presence of a trough at 0ms.

Fig.23 shows the workflow of Tridesclous. The signal of the whole session is uploaded and analyzed at once to improve the detection of units (the software automatically recognizes the different files as succession of similar trials, called segments). The signal is bandpass filtered (300Hz – 4kHz) (Fig.23A), the median signal is removed from each trace and a threshold for spike detection is manually selected (the signal is z-scored, thus the threshold used is a z-score value) (Fig.23A). Through the PCA and the average waveforms (Fig.23B), the clusters were manually refined and exported.

2.7.4.1 PCA and HC

The instantaneous firing rate of identified pyramidal cells (n=306) of selected trials was averaged across the session (Fig.24A). From this average distribution seven features were extracted: 1) slope of the foreperiod, 2) time of the highest instantaneous firing rate, 3) z-score value of the maximum absolute peak during the reward time, 4) mean firing rate of the whole trial, 5) area under the curve (AUC) during the first cue (0 – 0.5s), 6) AUC during second cue (1.5 – 2s), and 7) AUC during the reward (2.2 – 3.5s) (Fig.24B). Please note that before computing the AUCs, from the distribution of instantaneous firing rates, the probability density function (PDF) was computed and the AUCs were calculated on this PDF.

These 7 features were used to perform a PCA on the units, divided in the four experimental conditions (fixed/variable foreperiod and control/photostimulation). The number of principal components was chosen so that the sum of their explained variance would be ≥ 70%.
This process allows to reduce the dimensionality of the dataset from the original 7 dimensions (original number of variables). The data is not altered but simply new axes are identified that better highlight the variance in the data points. The first principal component will thus be a vector explaining the highest percentage of variance of the dataset. The second component will be orthogonal to it and explain the second highest variance and so forth until the variance explained by the components will be marginal and thus negligible.

On this new lower-dimensionality space, a hierarchical clustering (Ward's minimum variance method) was performed to identify clusters of similarly behaving units (Fig.24C). This unsupervised clustering method groups units based on Euclidian distances between them, creating a hierarchy of relative distances (visualized through a dendrogram).

Initially all the units are considered as individual clusters, the algorithm progressively merges clusters together in an order that minimizes the increase of variance inside the cluster until all units have been merged. When two clusters with a high variance between them are merged, the distance will be greater, and it will be mirrored in the dendrogram. There is thus a level of subjectivity in the choice of the number of clusters.

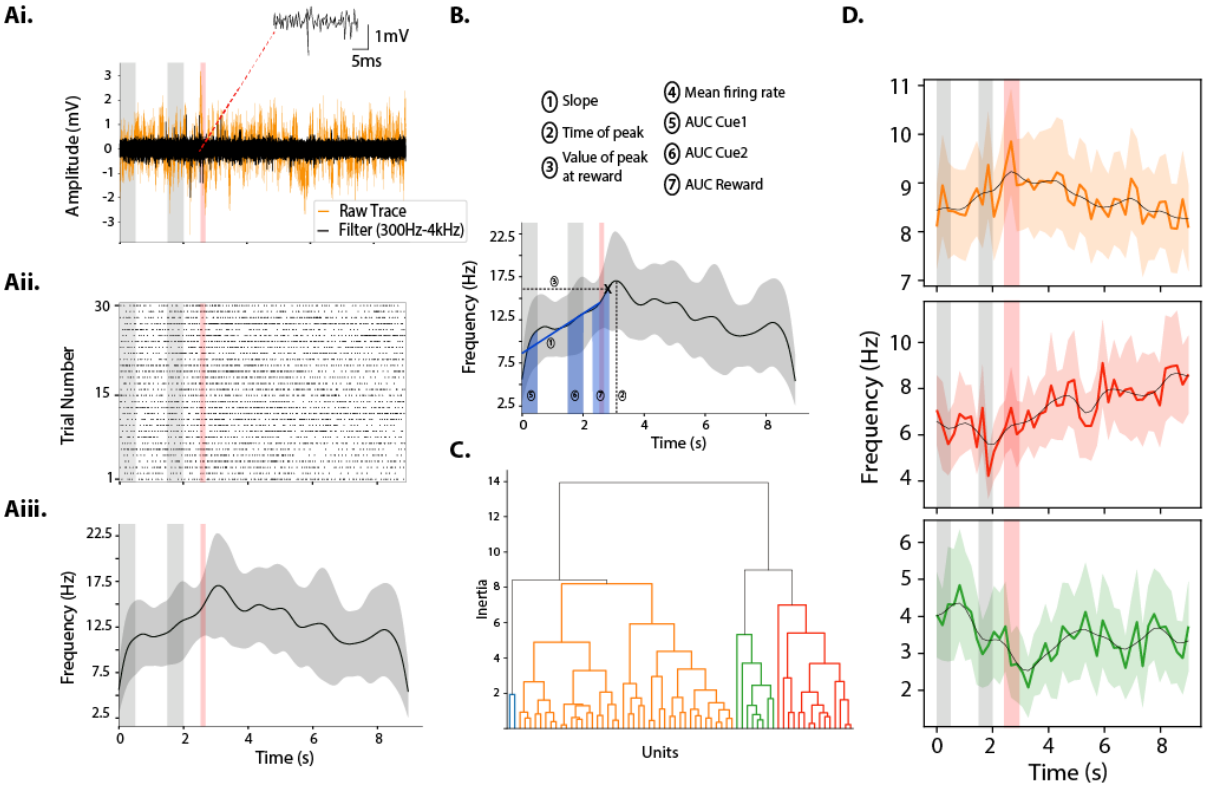

Fig.24 Clustering of units

A. Example of both raw (orange) and bandpass filtered (black) traces of an electrophysiological recording (Ai.). The inset is a magnification of a spike, the red dotted line indicate its original position in the trace (Top). Raster plot of a related unit (Aii.) and the mean istantaneous firing rate of such unit (Aii.). Grey vertical bars: time of the two visual cues. Red vertical band: time of the reward. Mean±SD.

B. Features choosen for PCA (top) and corresponding scheme on an example firing rate distribution (bottom).

C. Example of a dendrogram obtained from hierarchical clustering.

D. Average firing rate of units grouped through hierarchical clustering (C.). Used to identify units with similar behavior.

The clusters were confirmed by averaging the mean instantaneous firing rate of the selected units and confirming that the average behavior was differing from the other clusters (Fig.24D).

2.7.4.2 Z-score of units

The average instantaneous firing rate of each unit was z-scored and averaged within the cluster identified through hierarchical clustering.

The z-score was computed using the tail of the recordings (last 4 seconds) as baseline for the mean.

$$Z\ score = \frac{x - \mu_{bsln}}{\sigma_{bsln}}$$

Where x is each data point of the distribution, μ_{bsln} is the mean of the baseline (5-9s) and σ_{bsln} is the standard deviation of the baseline.

2.7.5 Analytical tools

All the analyses were performed with custom made scripts written in Python 3.8, available at: https://github.com/flareno/PhD_Scripts/tree/master/Final_Version_for_Thesis.

Various open-source packages were used:

- *Elephant* (and *viziphant*) for spike train analyses (and plotting) (Denker et al., 2018)
- *Neo* for electrophysiological data handling (Garcia et al., 2014)
- *Scipy* for statistical and FFT analyses (Virtanen et al., 2020)
- *Numpy* for data handling and basic vector functions (Harris et al., 2020)
- *Matplotlib* for generating plots (Hunter, 2007)
- *Pandas* for dataframe structures and related operations (McKinney, 2010)
- *Scikit-learn* for clustering and dimensionality reduction methods (Pedregosa et al., 2011)
- *Pingouin* for statistical analyses (Vallat, 2018)

2.7.6 Statistical analyses

Data was tested for normality (Shapiro test). When it was not possible to reject the null hypothesis, parametric tests were used. Otherwise, non-parametric tests were adopted.

For paired analyses it was either used paired t-test (parametric) or Wilcoxon signed-rank test (non-parametric).

For independent samples, first the homoscedasticity (equality of the variances) was tested by means of Lavene's test and if the null hypothesis was rejected, then Welch's t-test was used. Two-tailed test were always used unless stated otherwise.

To compute the effect size, Cohen's d effect size was used:

$$Cohen's\ d = \frac{|\mu_a - \mu_b|}{\frac{\sigma_a + \sigma_b}{2}}$$

Where μ_a and μ_b are the means of distribution a and b, respectively. And σ_a and σ_b are the standard deviation of distribution a and b, respectively.

Sawilowsky, following discussions with Cohen, produced a table with indications (rule of thumb) on how to interpret the effect size (Sawilowsky, 2009): very small (0.1), small (0.2), medium (0.5), large (0.8), very large (1.2), and huge (2) effect.

A value of 0.8 or greater is thus considered as threshold for significance.

3 Results

We had three main questions we tried to address with our analyses:

1) Were we successful in developing the task?/Can we study anticipation of a reward through it?
2) Does the variability on the timing of the reward affect the anticipation of it?
3) Does the photoactivation of the cerebellar cortex affect the prediction in the prefrontal network?

In this chapter I will discuss the results grouped by data type as it seems the clearer way to expose such complex dataset. In the following chapter of discussion, I will instead address the results in the form of the three questions mentioned above.

As a reminder I will quickly explain the behavioral task again: two visual cues are played in a sequence (constant timing), after the second cue there is a delay after which the reward is presented for a brief amount of time (150ms). This pre-reward delay can be either fixed (500ms) or variable (randomly chosen between 400 and 900ms) which then determines the condition: fixed and variable foreperiod, respectively. During photostimulation sessions, the rCrusI is stimulated for 1s starting with the presentation of the second cue. Four different protocols of stimulation where used: 125Hz, 40Hz, 6Hz, and Theta-Burst (see 2.4.3).

For most of the analyses, the data obtained from the four protocols of stimulation have been pulled together due to low sample size, but few analyses have been performed on the individual protocols. For a more detailed discussion on the subject please refer to 2.7 and 4.7.

On page 175 there is a table that summarizes the main results in the hope of helping the reader navigate this voluminous dataset and to not get lost in the various analyses.

3.1 Stimulation of CrusI elicits the strongest response in PrL

As described in the previous chapter (see 2.4), rCrusI was stimulated during the main experiments while recording the extracellular electrophysiological activity in the left PrL. Fig.25A shows the schematic description of the network. In order to confirm the optimal area

to stimulate in the cerebellar cortex, a preliminary set of experiment was performed (see 2.6 for details).

During this preliminary experiment, the right surface of the cerebellum was photostimulated in a grid in anesthetized mice (n=5) while recording in the contralateral layer V of PrL. The six stimulation spots were: vermal lobule VI and VII, CrusI and CrusII medial (paravermis), CrusI and CrusII lateral. Fig.25B represents the stimulation spots and the corresponding elicited activity in the PrL for one of the two stimulations used.

To quantify the changes, the amplitude of the signal during the stimulation was compared with that of baseline of similar duration taken at the beginning of each recording. Two protocols of stimulation were used during different trials: a steady illumination of 1s (steady protocol) and a series of 4 pulses of 0.5s each separated by 0.5s (pulses protocol). The trials of each mouse were averaged to obtain one single average trace for each mouse, for each protocol of stimulation. The mean±SEM for each condition can be found in the table 1 below.

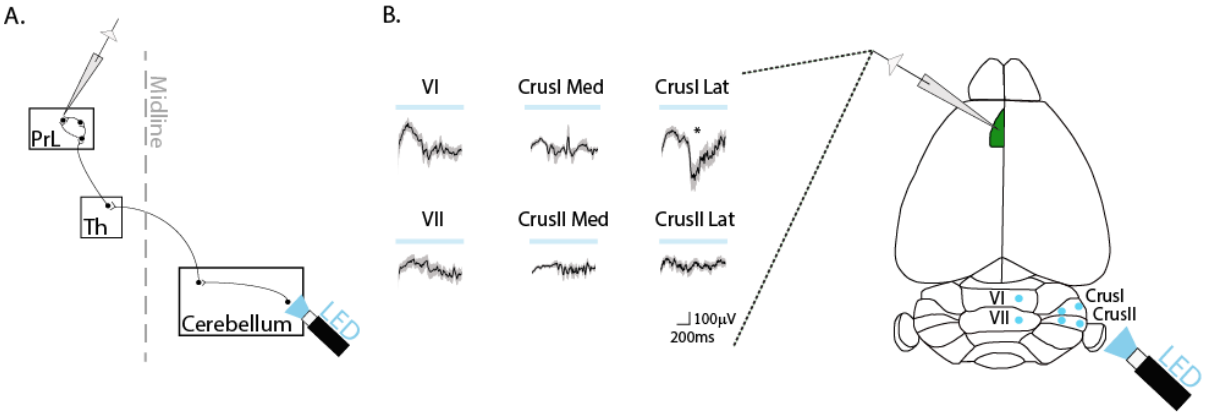

Fig.25 Mapping of cerebello-prefrontal functional connections

A. Scheme of the investigated network. The cerebellar cortex is stimulated with an LED. The signal is passed to the cerebellar nuclei which output to the contralateral thalamus. From here, thalamo-cortical projections contact pyramidal cells in the PrL. The signal is then integrated through recurrent networks and outputted to cortical and subcortical targets. The signal is recorded from layer V.

B. Average signal recorded in the PrL for every stimulated cerebellar area. Six areas were stimulated in the cerebellar cortex, for every area there is a correlated average signal recorded in the PrL (green area). Light blue band represents stimulation. Mean±SEM. * represents significance (see text). The traces showed correspond to the activity elicited by the steady protocol of stimulation. Mice used are L7-ChR2-eYFP which express ChR2 in the Purkinje cells (see 2.2).

In both conditions of stimulation, right CrusI lateral was the only spot of stimulation that elicited a significant reduction in amplitude of the signal (Wilcoxon signed-rank test, one-tail.

p-value = 0.03 for both conditions).

In supplementary figure 1 the complete traces for both protocols of stimulation are visible.

Area Stimulated	Steady Protocol (mean±SEM)		Pulses Protocol (mean±SEM)	
	Baseline (mV)	Stimulation (mV)	Baseline (mV)	Stimulation (mV)
CrusI Lateral	-0.09 ± 0.03	-0.39 ± 0.13*	-0.23 ± 0.05	-0.73 ± 0.12*
CrusI Medial	-0.07 ± 0.04	-0.43 ± 0.3	-0.13 ± 0.05	-0.53 ± 0.34
CrusII Lateral	-0.14 ± 0.05	-0.14 ± 0.04	-0.37 ± 0.13	-0.33 ± 0.08
CrusII Medial	-0.03 ± 0.008	-0.1 ± 0.03	-0.09 ± 0.02	0.2 ± 0.08
VI	-0.21 ± 0.039	-0.33 ± 0.11	-0.25 ± 0.06	-0.41 ± 0.02
VII	-0.23 ± 0.09	-0.22 ± 0.4	-0.32 ± 0.1	-0.33 ± 0.06

Table 1 Amplitude values recorded in the PrL during stimulation of different areas of the right cerebellar cortex.

3.2 Speed of the mouse

The first behavioral output is the speed of the mouse. This parameter was used as a proxy to investigate possible motor impairments due to photostimulation (3.2.1) and to study the behavioral changes in anticipation of the reward (3.2.2).

There are four main experimental conditions addressed all throughout this manuscript (Fig.22): 1) internal control of the fixed foreperiod condition, called Fixed Control (FC); 2) photostimulation during fixed foreperiod (regardless of the protocol of stimulation used), called Fixed Photostimulation (FP); 3) internal control of the variable foreperiod condition, called Variable Control (VC); 4) photostimulation during variable foreperiod (regardless of the protocol of stimulation used), called Variable Photostimulation (VP)

As mentioned in the previous chapter (2.7), and further discussed in the discussion (4.7), most of the analyses have been performed by merging the data obtained with all four protocols of stimulation. In Supp.Fig.2 it is possible to see the time course of the speed by protocol of stimulation.

3.2.1 Stimulation does not affect motor performance

To assess whether our results, especially behavioral ones, are due to a motor impairment induced by the stimulation of the cerebellum, the instantaneous speed (see 2.4.1) of each individual mouse during the whole trial was computed and averaged over the session by mouse (Fig. 26Ai, Bi). From this, the foreperiod (0 - 2.5s for fixed and 0 - 2.4s for variable) was

fitted through linear regression and the slope of this fit was computed. The distributions of slope values of all the mice (n=11) were compared between control and photostimulation sessions (regardless of the protocol used) segregated for foreperiod condition (Fig. 26Aii, Bii).

No difference was found between control and photostimulation nor in fixed or variable foreperiod condition (p-values= 0.83 and 0.83, respectively, 2 sample Kolmogorov-Smirnov test. Cohen's d effect size = 0.045 and 0.087, respectively).

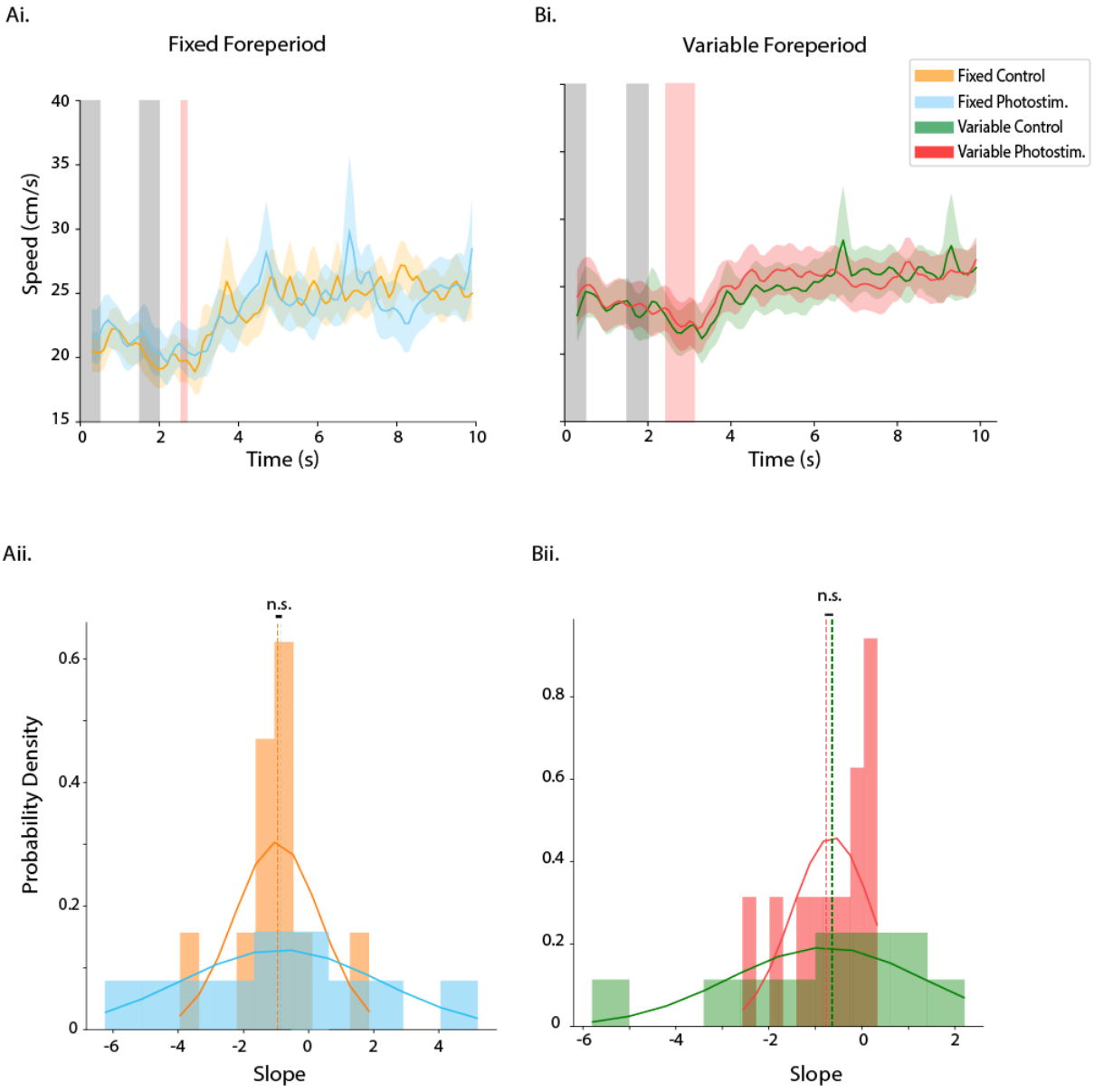

Fig.26 Stimulation does not affect movement

Ai.-Bi. Mean instantaneous speed in control and photostimulation conditions with fixed (Ai) and variable (Bi) foreperiod. Grey vertical bars: time and duration of the visual cues. Red vertical band: time and duration of the reward. (Colors in legend) Mean±SEM.

Aii. - Bii. Distribution of the slope values computed during the foreperiod for control and photostimulation with fixed (Aii) and variable (Bii) foreperiod. Continuous line: gaussian fit of the corresponding distribution. Dotten line: mean of the correspoding ddistribution.

3.2.2 Mice slowdown in anticipation of a reward

To determine whether the negative slopes seen in the previous analysis were indicative of a significant slowing down of the mice in anticipation of a reward (Fig.27Ci, Di. Supp.Fig.3), these values were compared with slope values obtained from a shuffled distribution. This shuffled distribution was obtained by randomly mixing the speed values in time during the foreperiod.

The slope values of the speed for each condition of foreperiod (fixed or variable) were bootstrapped 100 times (n=11 at every permutation, see 2.7.3). The resulting distribution was compared to an equally bootstrapped sample of slope values obtained from the shuffled distribution (Fig.27A). In the table below (Tab.2) the mean and SD values of the various distributions are listed. To compare the two distributions (bootstrapped original data and bootstrapped shuffled data) a 2 samples Kolmogorov-Smirnov test (2KS) was performed, and the Cohen's d effect size was also computed (see 2.7.6). Both conditions of foreperiod indicate a slope significantly different than the shuffled one: FC (p-value = $1.43 \cdot 10^{-19}$, 2KS. Effect size = 1.87) and VC (p-value = $1.42 \cdot 10^{-28}$, 2KS. Effect size = 2.09).

Due to bootstrapping, the sample size was artificially increased which can have an effect in reducing the observed p-value. Thus, for this and the following analyses using a similar method, the effect size will mostly be used to determine the outcome of the analyses. Indeed, in this case both conditions have an extremely high effect size which allows to conclude that mice significantly slow down, time-locked with the reward.

Experimental Condition	Data Type	Mean±SD	Effect Size
Fixed Control	Original	-0.90 ± 0.41	1.87 (Very large effect)
	Shuffled	-0.02 ± 0.53	
Fixed Photostimulation	Original	-0.88±0.89	1 (Large effect)
	Shuffled	-0.07±0.69	
Variable Control	Original	-0.64 ± 0.25	2.09 (Huge effect)
	Shuffled	0.05 ± 0.41	
Variable Photostimulation	Original	-0.89±0.68	1.5 (Very large effect)
	Shuffled	-0.05±0.43	

Table 2 Mean bootstrapped slope values of the instantaneous speed during the foreperiod (0s – reward time).

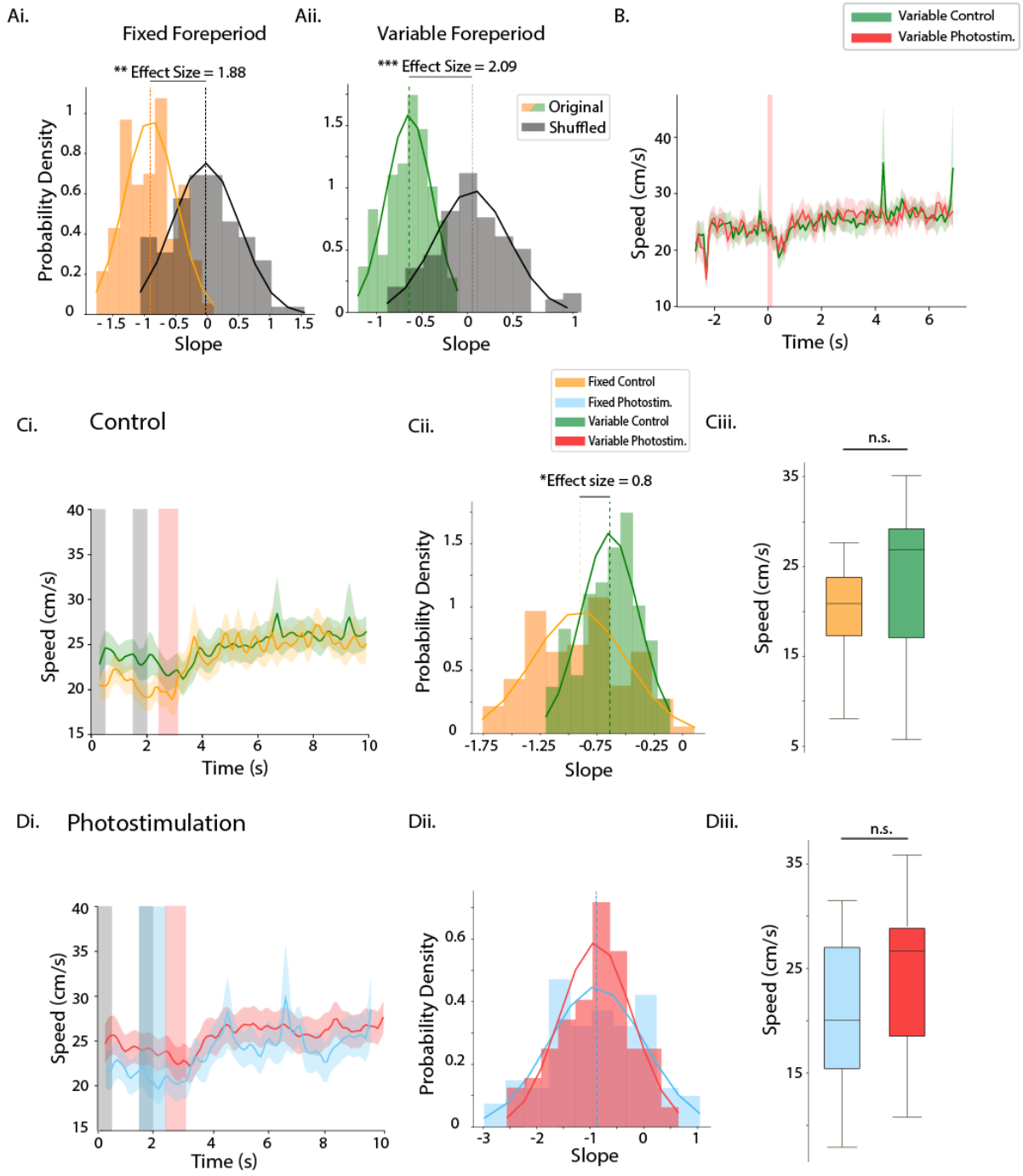

Fig.27 Reduction of speed in anticipation of the reward

A. Bootstrapped density distribution of original (orange/green) and shuffled (black) slope values for fixed (**Ai**) and variable (**Aii**) control trials. Continuous lines: gaussian fit of the underlying distribution. Dotted lines: respective means.

B. Mean instantaneous speed during control (green) and photostimulation (red) variable foreperiod condition. Same data as in Ci and Di but the various trials were aligned tot he time of the reward.

Ci-Di. Mean instantaneous speed during control (**Ci**) and photostimulation (**Di**) conditions. Grey bars: time and duration of visual cues. Red bars: possible time and duration of reward. Light blue bar: time and duration of photostimulation. Mean±SEM

Cii-Dii. Bootstrapped density distribution of the slopes of speed during the fixed and variable foreperiod during control (**Cii**) and photostimulation (**Dii**) conditions. Continuous line: gaussian fit of the corresponding distribution. Dotted line: mean of the corresponding distribution.

Ciii-Diii. Mean values of speed during foreperiod interval for fixed and variable foreperiod during control (**Ciii**) and photostimulation (**Diii**) trials.

3.2.2.1 With a fixed foreperiod mice have a stronger deceleration in anticipation of the reward

Similarly, to determine if the nature of the foreperiod affects the deceleration rate of the mice (Fig.27Ci, Di), the previously bootstrapped slope values (see 3.2.2) were compared between foreperiod condition for the control (p-value=$7.85 \cdot 10^{-6}$, 2KS test. Effect size=0.8. Fig. 27Cii) and photostimulation conditions (p-value=0.3, 2KS test. Effect size=0.009. Fig. 27Dii). Interestingly, in control condition there seems to be a significant change in the rate of deceleration, with FC having a more pronounced slope.

Looking at the time course of the instantaneous speed across the four conditions (Fig. 27Ci, Di) it seems that the most prominent difference between foreperiod conditions is the reduction of the average speed during FC (19.55±1.84 cm/s, mean±SEM) and FP (20.34±2.46 cm/s, mean±SEM) compared to VC (23.26±2.85 cm/s, mean±SEM) and VP (23.76±2.52 cm/s, mean±SEM), respectively.
When tested however, these reductions were not significant (p-values = 0.09 in both cases, paired t-test. Effect size = 0.5 and 0.43, respectively) (Fig. 27Ciii, Diii).

Another interesting result noticed during the analyses is shown in figure 27B. When the data of the speed during variable conditions is aligned in time to the delivery of the reward (instead of being aligned to the beginning of the trial as for all other analyses) the slowing down disappears (as it is averaged out by the two possible foreperiod values that are out of phase) but a bout of decreased speed immediately after the reward appears. Interestingly this phenomenon is not visible during fixed foreperiod (Fig.26Ai).

These results thus demonstrate that mice seem to anticipate the delivery of the reward in both foreperiods by decelerating up until the reward time. Moreover, with a fixed foreperiod they show a stronger deceleration.

3.3 Licking behavior

The second behavioral read-out is the distribution of licks during the task. This data was first used to determine if mice, in control condition, show an anticipatory licking (3.3.1). Then the effect of the foreperiod (3.3.1.2) and of the stimulation (3.3.1.1, 3.3.4) on such anticipatory behavior was investigated. Lastly, the attention/performance was investigated (3.3.2-3.3.4).

3.3.1 Increase of licking rate in anticipation of the reward

A time histogram was built from the lick events of each session of each mouse (Fig. 28A). From this time histogram, a probability density function (PDF) was drawn and a slope of the foreperiod was calculated (Fig.28A), similarly to what explained in 3.2.1. Thus, a distribution of slopes (n = 11) was obtained for each of the control conditions.

A slope in this case is representative of the rate of change in frequency of licks before the delivery of the reward and can thus be interpreted as the anticipation of such reward. In Fig. 28B the average time course of licking behavior for FC and VC is represented for clarity.

In the table below (Tab.3) the mean and SD values of the various distributions are listed. Similar to the analysis of the speed, the slope values were bootstrapped 100 times (n = 11 for each permutation) and compared to an equally bootstrapped distribution of slopes computed from a shuffled distribution of lick times (Fig.28C, Supp.Fig.4). The shuffled distribution is obtained by shuffling in time the count of licks (bins of the time histogram) for the foreperiod (similarly to the shuffling of the speed).

Both 2KS test and effect size were computed for each condition. Both conditions indicate a slope significantly different than the shuffled one: FC (p-value = $4.96 \cdot 10^{-43}$, 2KS test. Effect size = 3.02) and VC (p-value = $1 \cdot 10^{-11}$, 2KS test. Effect size = 1.11).

In both fixed and variable foreperiod conditions, mice show anticipatory licking behavior.

Experimental Condition	Data Type	Mean±SD ($\cdot 10^{-3}$)	Effect Size
Fixed Control	Original	12.8± 4.9	3.02*** (Huge effect)
	Shuffled	0.5 ± 3.2	
Fixed Photostimulation	Original	21.4±6.7	3.53*** (Huge effect)
	Shuffled	0.6±5.1	
Variable Control	Original	2.8 ± 2.8	1.11* (Large effect)
	Shuffled	-0.4 ± 2.9	
Variable Photostimulation	Original	2±5.6	0.46 (Small effect)
	Shuffled	-0.1±3.7	

Table 3. Mean bootstrapped slope of the licking behavior. In both foreperiod conditions, mice show anticipatory licking behaviour time-locked with the reward.

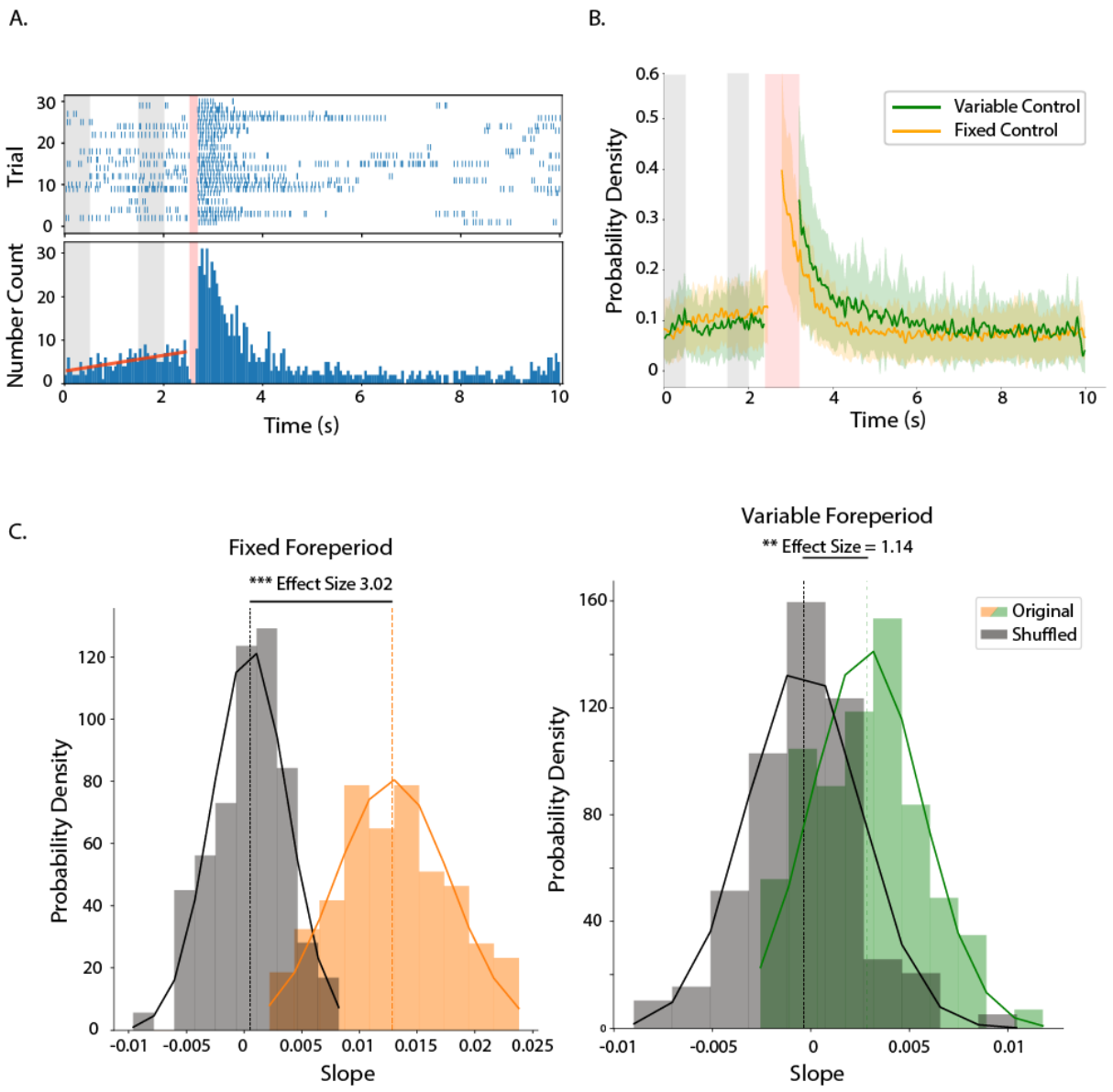

Fig.28 Licking rate shows the anticipation of the reward

A. Example of behavioral output. Top panel: raster plot of lick events across one session (repetition of 30 trials) for one mouse. Bottom panel: time histogram of the raster plot above. Red line: slope of the linear regression of the lick rate during the foreperiod. For simplicity, the slope is here represented on the raw time histogram, in reality it is computed on the PDF (which does not change the sape of the distribution). N.B. The lick events during the reward have been blanked in order to avoid contamination from possible false negatives due to the drop of water being read as lick event.

B. Probability density function of licks for fixed (orange) and variable (green) foreperiod control sessions. Grey bars: time and duration of visual cues. Red bars: possible time and duration of reward. Mean±SD

C. Bootstrapped density distribution of the slopes of lick rate during the foreperiod in control conditions. Original dataset (orange/green) and shuffled one (orange) for fixed (left) and variable (right) foreperiod. Continuous line: gaussian fit of the corresponding distribution. Dotted line: mean of the corresponding distribution.

The slopes of the licking behavior thus computed were bootstrapped 100 times (n=11 for each permutation) for the four experimental conditions. The effects of both the different foreperiods and of the photostimulation (without distinction of protocol) were then investigated.

3.3.1.1 Photostimulation during fixed foreperiod increases anticipatory licking

When comparing the previously computed distributions of slopes of the licks between control (Fig. 29Ai) and photostimulation conditions (Fig. 29Aii), only during fixed foreperiod condition, the photostimulation induces a significant increase in the slope of the licking distribution (p-value=$3.04 \cdot 10^{-14}$, 2KS test. Effect size=1.48, Fig.29Bi), whereas during variable foreperiod, the slope remains unchanged regardless of the stimulation (p-value=0.004, 2KS test. Effect size=0.19, Fig.29Bii).

3.3.1.2 A fixed foreperiod induces a stronger anticipatory licking behavior

The changes in the distribution of the slope values were further compared between foreperiod conditions: FC with VC (p-value=$4.1 \cdot 10^{-34}$, 2KS test. Effect size=2.59, Fig.29Ci) and FP with VP (p-value=$2.6 \cdot 10^{-44}$, 2KS test. Effect size=3.16, Fig.29Cii).
The mean and SD values for the distributions can be seen in Tab.3 above.

In both conditions (control and photostimulation) the slope is significantly higher with a fixed foreperiod. Indicative of a stronger anticipatory licking behavior of the mice (n=11).

We can thus conclude that a fixed foreperiod (FC) induces a stronger anticipatory behavior than a variable foreperiod (VC and VP) which is then further increased by a photostimulation of right CrusI (FP).

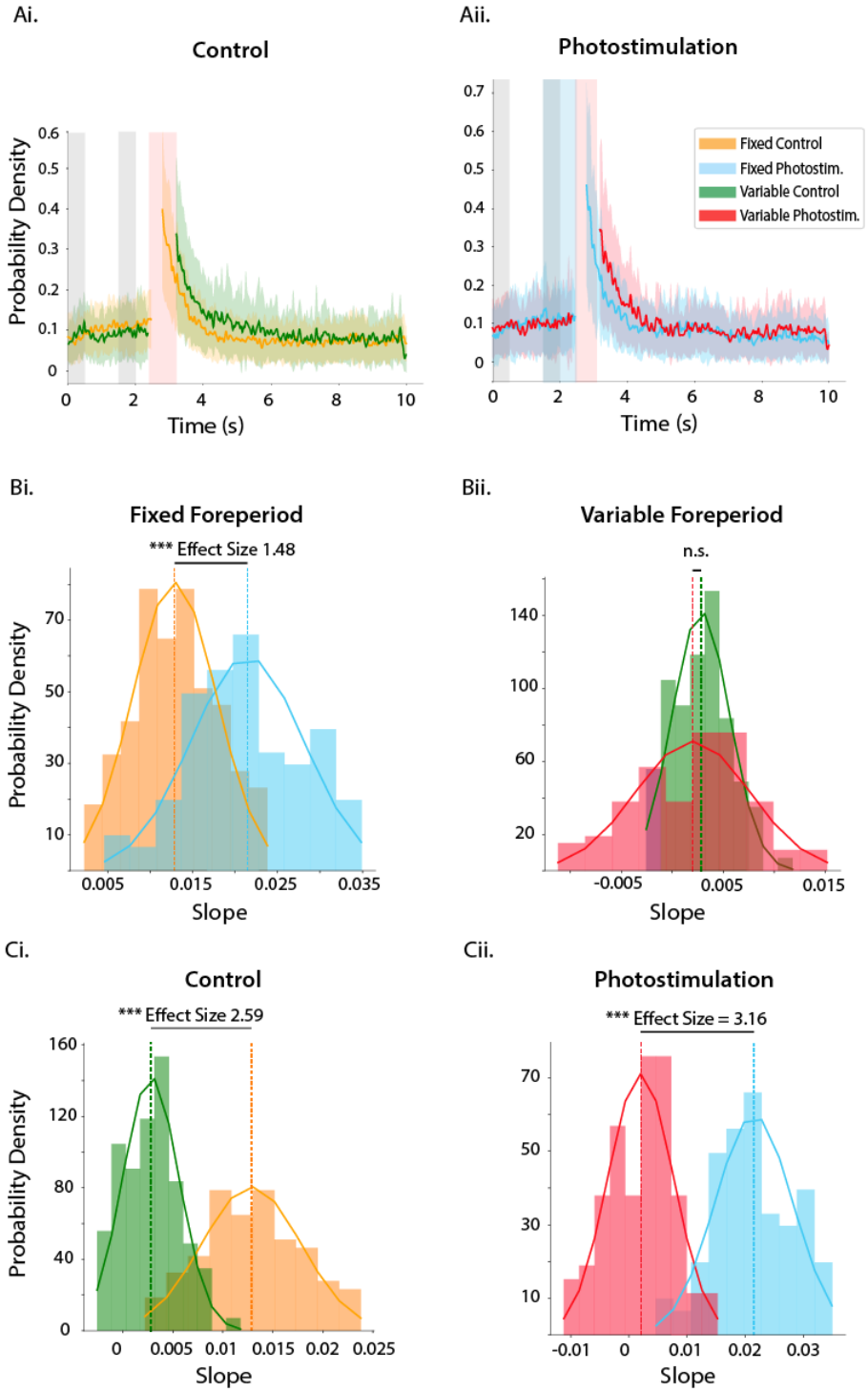

Fig.29 Licking behavior is affected by the foreperiod and by photostimulation

A. Probability density function of licks for fixed and variable foreperiod during control (Ai) and photostimulation (Aii) conditions. Grey bars: time and duration of visual cues. Red bars: possible time and duration of reward. Light blue bar: time and duration of photostimulation. Mean±SD

B. **Effect of stimulation.** Bootstrapped density distribution of fixed (Bi) and variable (Bii) foreperiods comparing session of control and photostimulation.

C. **Effect of foreperiod.** Bootstrapped density distribution of the slopes of lick rate during the fixed and variable foreperiod during control (Ci) and photostimulation (Cii) conditions.

Continuous line: gaussian fit of the corresponding distribution. Dotted line: mean of the corresponding distribution.

3.3.2 40 Hz photostimulation reduces the Success Ratio

To compute the success ratio of each session, the number of successful trials (trials where the mouse licks at least 3 times during the foreperiod) was divided by the total number of trials for a given session. The comparison was performed between each internal control and its related stimulation session. (As a reminder, the internal control is the session of 30 trials without stimulation performed before every session of 30 trials of stimulation, Fig.30Ai).

Both fixed and variable foreperiod were tested (separately) on all mice (n=11) (Fig.30AII-B, Supp.Fig.5). The two high frequencies stimulations (125Hz and 40Hz) during fixed foreperiod significantly reduced the success ratio (p-values = 0.048 and 0.006, respectively. Paired t test) of the mice (Fig.30B). But only 40Hz stimulation induces a large effect size (0.75) (Fig.30A-B), whereas 125Hz induces a small effect size (0.38). No significant difference was found in variable foreperiod condition.

Mean values of success ratio for the various experimental conditions are visible in the table below (Tab.4).

Protocol of Stimulation	Foreperiod	Success Ratio Control Trials (mean ± SD)	Success Ratio Photostimulation Trials (mean ± SD)
125Hz	Fixed	46.36 ± 35.07%	33.63 ± 35.79%
	Variable	63.94 ± 34.57%	51.1 ± 31.07%
40Hz	Fixed	48.79 ± 27.46%	29.09 ± 27.53%
	Variable	53.94 ± 29.92%	48.28 ± 38.27%
6Hz	Fixed	39.39 ± 34.41%	31.21 ± 32.16%
	Variable	48.18 ± 34.23%	48.28 ± 35.77%
Theta-Burst	Fixed	23.94 ± 18.9%	21.52 ± 19%
	Variable	41.21 ± 31.53%	44.51 ± 33.98%

Table 4. Mean success ratio in the behavioral task for the various experimental conditions.

Since the size of the effects is small and the sample size for each protocol of stimulation is also small, many of the analyses have been performed by merging all the protocols of stimulation (as seen in previous analyses).

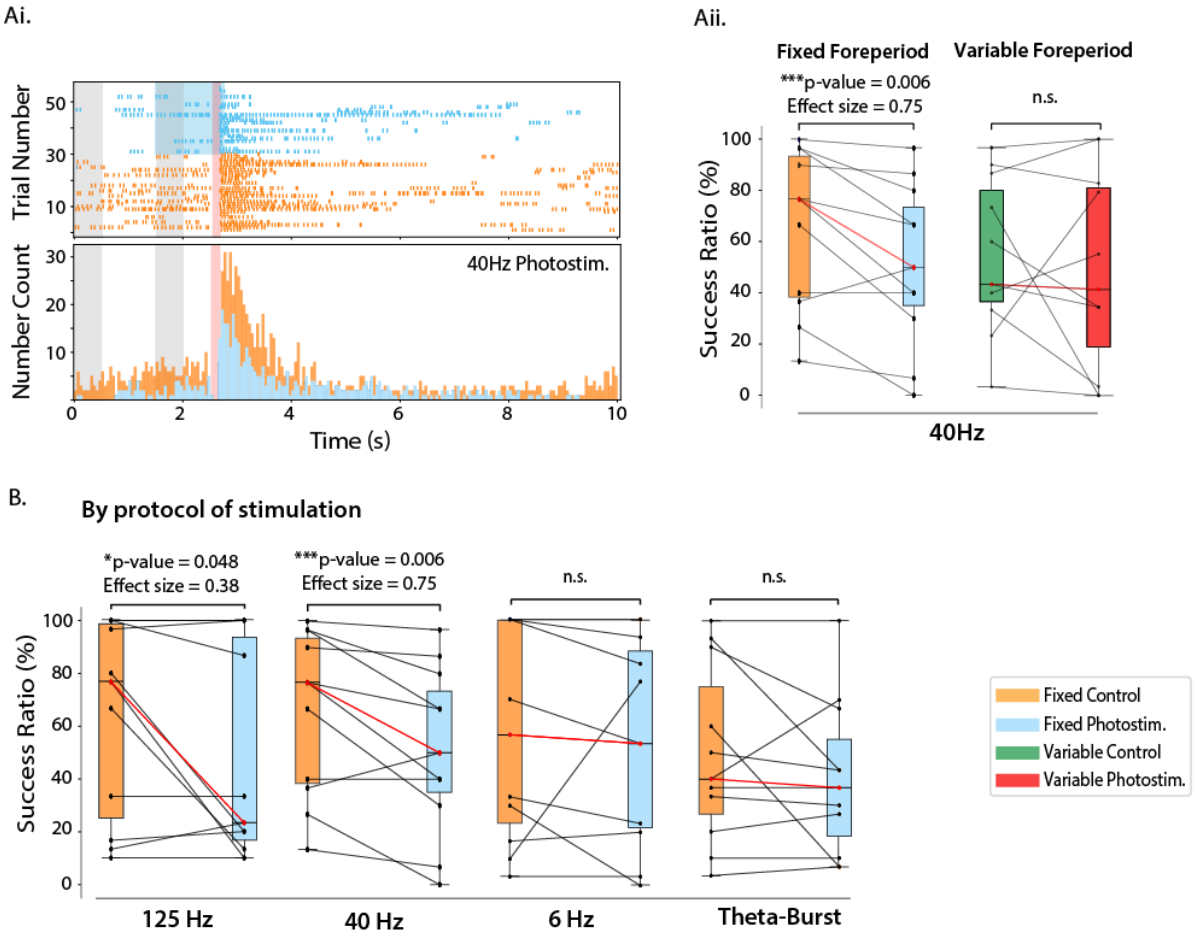

Fig.30 Success ratio reduced by 40Hz photostimulation of CrusI

Ai. Example of behavioral data from one session. Top panel: raster plot of lick times. Each row is a trial. The first 30 trials are control trials (orange), whereas the last 30 trials in the session have photostimulation (light blue). Blue band: time and duration of photostimulation. Bottom panel: time histograms built from the licks of the control and photostimulation sessions. The licks during the presence of the reward have been removed in order to prevent possible false positives from the reward itself. Grey band indicate time and duration of visual cues. Red band indicates time and duration of reward.

Aii. Comparison of success rate between control and 40Hz photostimulation conditions for both fixed (left) and variable (right) foreperiods.

B. Paired analyses of performance during the behavioural task, comparing control (orange) with photostimulation (light blue) sessions during fixed foreperiod condition. The various paired plots represent different photostimulation protocols. Black dots: individual mice. Black lines: pair belonging to the same mouse. Red dots: median values per condition and connection (n = 11).

C. Paired analysis of the success ratio for fixed and variable foreperiod of the whole control (left) and photostimulation (right) conditions (regardless of protocol used).

The success ratio of the four experimental conditions (no distinction of protocol) was computed and compared between experimental conditions (Fig.30C).
No difference was found between FC (52.05±10.33% mean±SD) and VC (59.29±18.51% mean±SD), but the photostimulation induces a reduction of the success ratio in both fixed (p-value = 0.0004, paired t test. Effect size = 1.82) and variable (p-value = 0.03, paired t test. Effect size = 0.55) foreperiod. Although the effect size in variable condition is considered to be only medium.

Interestingly the reduction induced in VP doesn't seem to be so strong (not only from the effect size) but also because the success ratio during FP (28.86±16.47% mean±SD) is significantly lower than VP's (48.04±24.69% mean±SD) (p-value = 0.0075, paired t test. Effect size = 0.98).

These results are coherent with the previous result of success ratio separated by protocol where half of the fixed foreperiod session (high frequency stimulations) saw a reduction induced by the photostimulation. The reduction between VC and VP seen when the data was pulled together was not identified in individual analyses of the sessions. This limitation of the different levels of investigation of the data is addressed in the last paragraph of the discussion (4.7).

3.3.3 Stimulation of rCrusI and variability of the reward differently affect the amount of licks performed

To investigate the effect of the various experimental conditions (photostimulation and variable foreperiod) on the behavior of the mice (n=11), the number of licks per trials was calculated and all the trials belonging to the same condition and the same mouse were averaged together. These averaged values were compared between corresponding conditions. For this analysis, two windows of time were selected and analyzed in parallel: interval during the photostimulation (1s) and interval of 1s after the reward (in Fig. 31A is visible a scheme of the behavioral task with highlighted the two windows of time used). The precise time in the task varies between trials for both windows due to the variability of the reward.

Regarding the interval of time during the photostimulation, the number of licks for FP and VC are significantly different from that of FC (p-values = 0.004 and 0.017, respectively. Paired t test. Effect size = 1.03 and 1.28, respectively) (Fig. 31Bi).

This result can be interpreted together with the increase of anticipatory licking during FP compared to FC with the hypothesis that the mice are licking less but in a more organized way and more locked with the release of the reward.

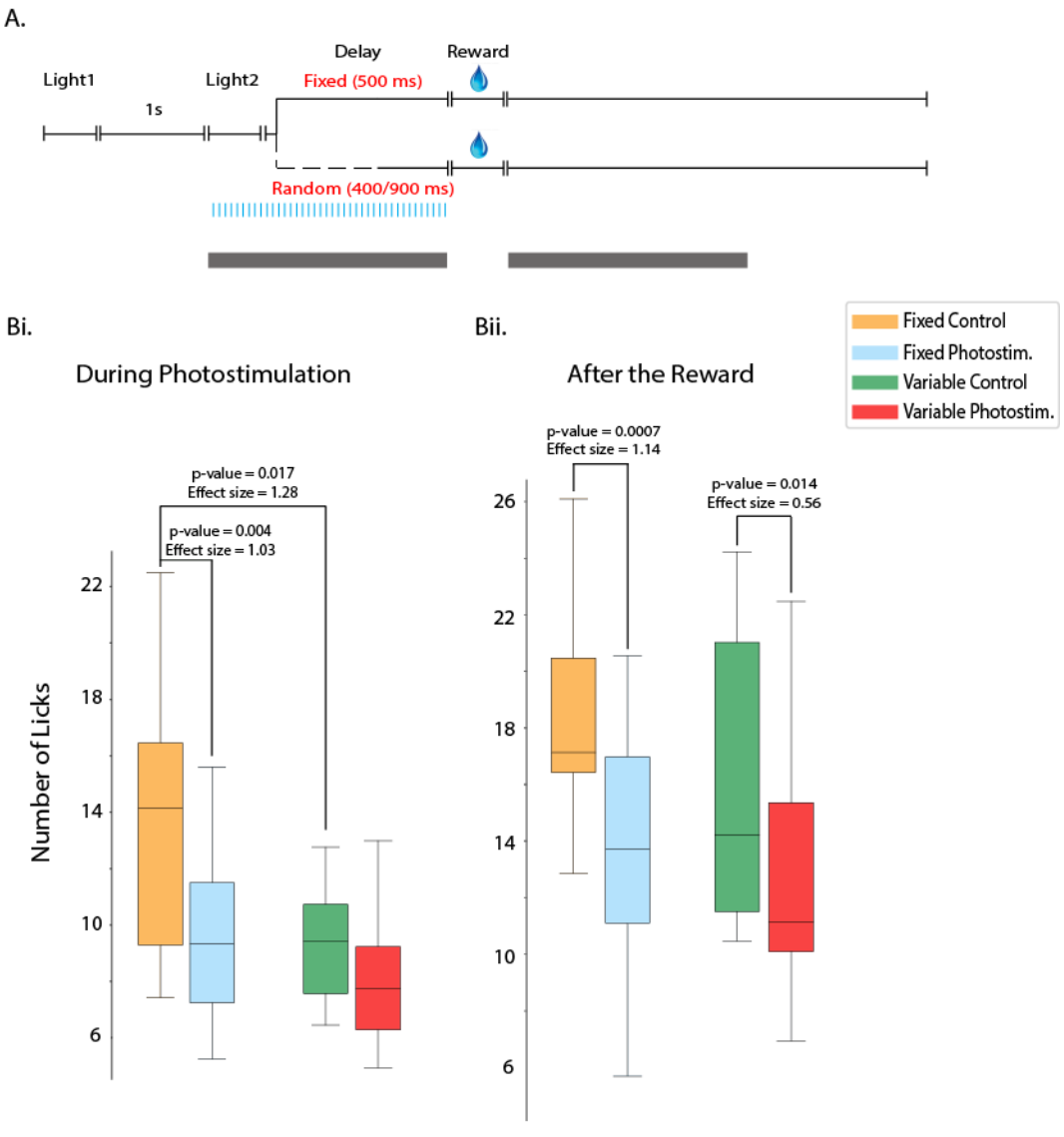

Fig.31 Photostimulation and foreperiod differently affect the number of licks

A. Scheme of the behavioral task (not in scale). See methods for a description of it. Two grey bands indicate the time interval for the computation of the number of licks for the two plots below: during stimulation (1.5 - 2.5) and after the reward (2.5 - 3.5 c.a.), respectively. The values are approximates because each trial has the variability of the fixed and variable foreperiod.

B. Changes in number of licks at specific time intervals during the four experimental conditions.

For the window of time after the reward instead, FP and VP were significantly different from FC and VC, respectively (p-values = 0.0007 and 0.014, respectively, paired t test. Effect size = 1.14 and 0.56, respectively) (Fig. 31Bii).

3.3.4 Theta-Burst stimulation affects the lick rate

In the literature, increase in lick frequency in anticipation of a reward is widely reported. Previously shown results in this manuscript (3.3.1) have discussed this same topic showing an increase locked with the reward time in control conditions.

To determine if such anticipatory licking is affected by optogenetic stimulation of rCrusI, a PDF of each lick distribution was computed for each session (as explained in 3.3.1). From this PDF distribution, three parameters were extracted from the foreperiod: 1) slope, 2) AUC, and 3) intercept of the slope on the y axis (Fig. 32A). For each parameter, paired analyses between internal control and respective stimulation session were performed (Supp.Fig.6).
These three parameters deliver different information about the lick distribution. The slope determines the rate of change, which is the main parameter related to anticipation. The intercept gives information on the amount of licks that determine the slope. Lastly, the AUC informs about the ratio of total licks performed in the foreperiod.

The effect size for the different conditions shows that the Theta-Burst stimulation induces a large change in the slope in both foreperiod conditions (0.83 for fixed and 0.95 for variable foreperiod) and only in variable foreperiod for the intercept (0.97).
Only with the variable foreperiod however, does the Theta-Burst stimulation significantly increase the slope (p-value=0.025, paired t test, one tail) and reduce the intercept (p-value=0.029, paired t test, one tail). No significant change was found for AUC (Fig. 32B) which is coherent with the result in 3.3.3 that doesn't highlight any difference in number of licks during the foreperiod between VC and VP.

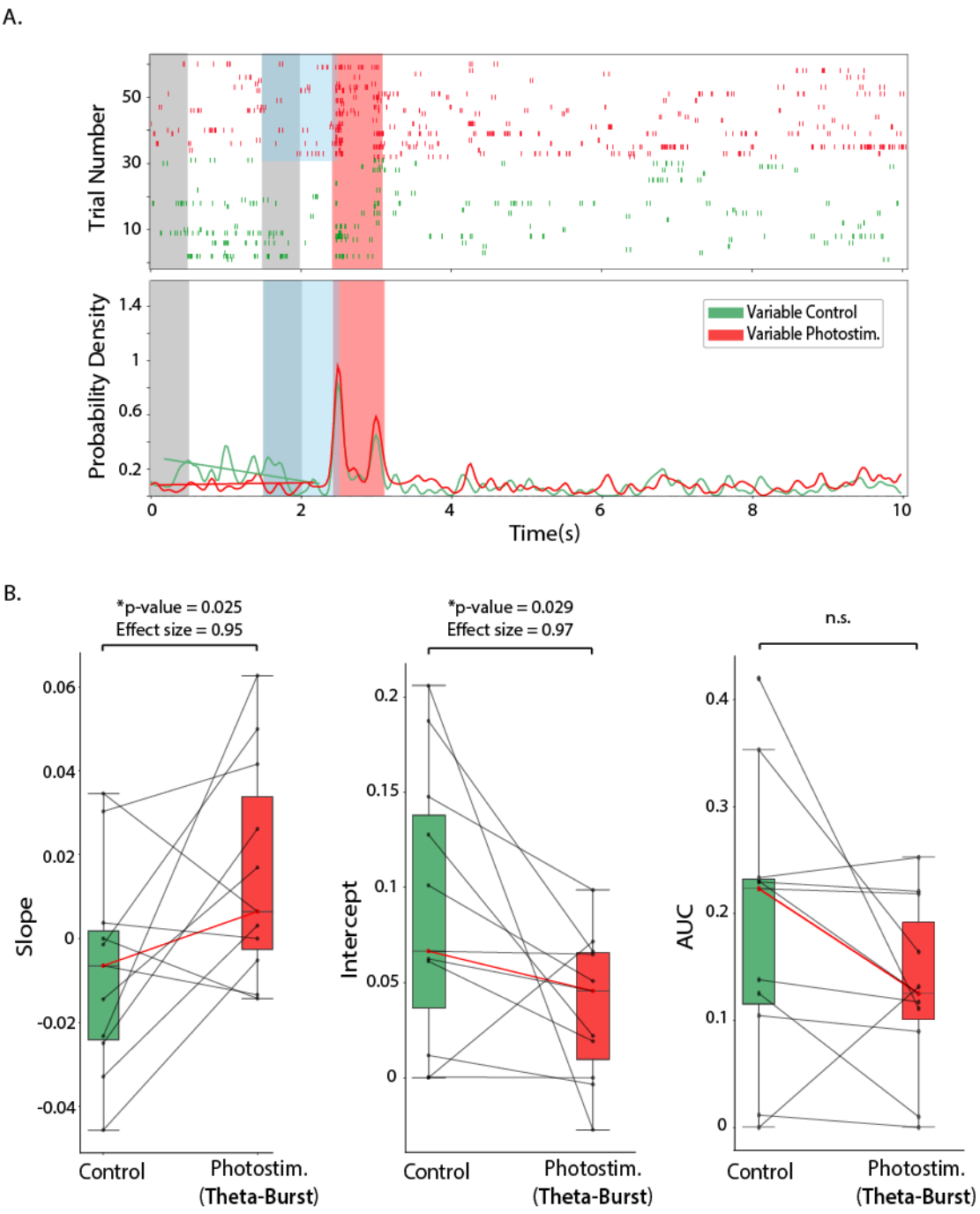

Fig. 32 Theta-Burst stimulation affects anticipatory licking with variable foreperiod

A. Example of a raster plot (top) and relative time histogram (bottom) of the licks of a session for one mouse with variable foreperiod. Control (green) and Theta-Burst photostimulation (red) session. Grey bands: time and duration of visual cues. Red band: possible time of the reward (the foreperiod is variable). Lightblue band: time and duration of theta-burst stimulation. Control (green) and photostimulation (red) sessions. In the bottom plot, the two continuous lines represent the slope of the corresponding lick distribution during foreperiod.

B. Paired plot of slope, intercept (of the slope on the Y axis) and AUC (during the period of the reward) values, respectively.

3.4 Oscillations in PrL

Through the silicon probe in the PrL, extracellular signals were recorded. In the present chapter I will discuss the analyses performed on the local field potential (LFP).

First, possible signs of anticipation of the reward were investigated in control conditions (3.4.1). Afterwards, the effects of the foreperiod on the equilibrium of the oscillations of the network were analyzed (3.4.2-3.4.3).

3.4.1 Ramping of oscillation before the reward

The amplitude of each oscillation was computed from time-frequency plots by means of complex Morlet wavelet convolution. From the resulting amplitude array of each frequency band (Fig. 33A, Supp.Fig.7), the ridge (the highest value for each time bin) was extracted for each trial as to have a time course of the variations of the peak amplitude. All the trials in which the mouse was correctly performing the task (see 2.7) were averaged together obtaining an average ridge per mouse per frequency band (Fig. 33B, Supp.Fig.8).

By using the same strategy of the previous analyses, the slope of the ridge of each mouse of each frequency band was computed. For both conditions and each band of oscillation, the distribution of the slopes (n = 8) was bootstrapped 100 times (n = 8 for each permutation) and compared with the slope distribution of a shuffled distribution (Fig.33C, Supp.Fig9). The shuffled distribution was obtained by mixing in time all the values from the foreperiod of each mouse's average ridge and computing the corresponding slope of the foreperiod.

The results, visible in the table below (Tab.5), show that the ridge of all frequency bands (except delta in FC and theta in VC) significantly increase their amplitude in anticipation of the reward.

Experimental Condition	Frequency Band	Data Type	Mean±SD ($\cdot 10^{-5}$)	p-value (2KS test, two tail)	Effect Size
Fixed Control	Delta	Original	-1.17±6.28	$4 \cdot 10^{-4}$	0.23
		Shuffled	-0.18±2.42		(Small effect)
	Theta	Original	3.2±0.83	$2.21 \cdot 10^{-59}$	5.14***
		Shuffled	-0.007±0.43		(Huge effect)
	Beta	Original	0.18±0.09	$8.57 \cdot 10^{-42}$	3.05***
		Shuffled	0.002±0.02		(Huge effect)
	Gamma	Original	0.024±0.012	$2.21 \cdot 10^{-59}$	3.56***
		Shuffled	-0.0001±0.0014		(Huge effect)
Variable Control	Delta	Original	8.66±7	$1.59 \cdot 10^{-24}$	1.66**
		Shuffled	-0.06±3.5		(Very large effect)
	Theta	Original	0.42±1.08	$3.57 \cdot 10^{-07}$	0.65
		Shuffled	-0.04±0.35		(Medium effect)
	Beta	Original	0.07±0.056	$2.68 \cdot 10^{-25}$	1.86**
		Shuffled	0.0035±0.02		(Very large effect)
	Gamma	Original	0.018±0.019	$2.62 \cdot 10^{-22}$	1.69**
		Shuffled	-0.0002±0.0023		(Very large effect)
Fixed Photostim.	Delta	Original	-5.53±12.5	/	/
	Theta	Original	2.03±3.21	/	/
	Beta	Original	0.21±0.14	/	/
	Gamma	Original	0.02±0.02	/	/
Variable Photostim.	Delta	Original	2.1±9	/	/
	Theta	Original	-00.8±1.49	/	/
	Beta	Original	0.14±0.14	/	/
	Gamma	Original	0.02±0.02	/	/

Table 5. Mean bootstrapped values os slope for the ridge of the amplitude of different frequency bands.

3.4.2 Delta is differently affected by the foreperiod

The power of delta oscillation is reportedly increased by the correct prediction of a variable event (Totah et al., 2013a), where is also visible a ramping of the power in anticipation of a stimulus.

To test whether the foreperiod had an effect on delta frequency, first the percentage of total power occupied by the delta band (1.5-4Hz) was investigated, then the ridge of the amplitude of this frequency band was computed and compared across experimental conditions.

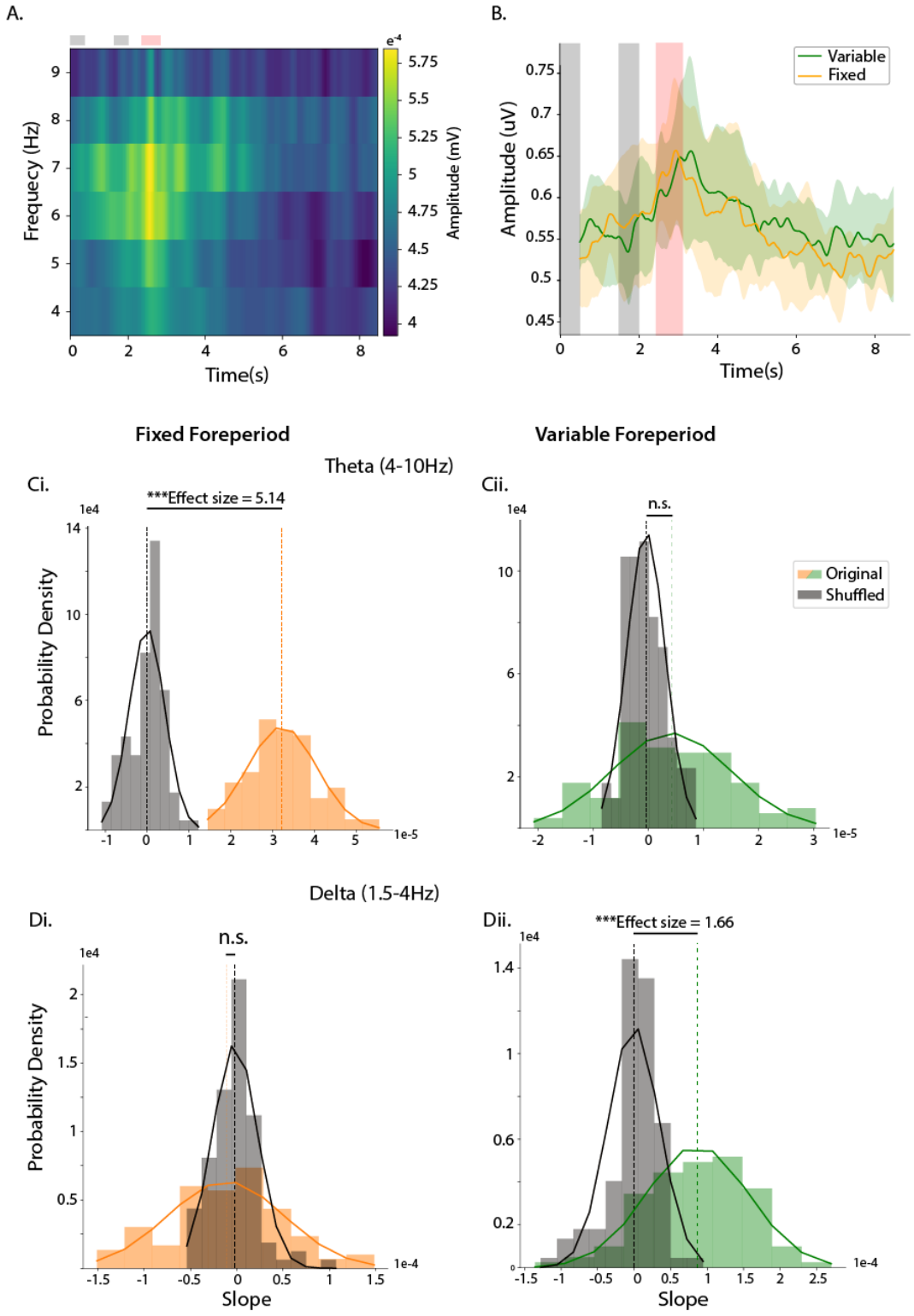

Fig.33 Behavior induces changes in the ridge

A. Example of scalogram. This example is the mean scalogramof all mice (n=8) for the theta band in variable foreperiod condition. Two grey bars on top indicate the time of the two visual cues and the red bar indicates the possible time of the reward.

B. Examples of ridge distribution. In this example mean ridge of theta band for fixed (orange) and variable (green) foreperiod in control condition. Vertical bands indicate behavioral events as in A. Mean±SEM.

C-D. Bootstrapped distributions of slopes from original dataset (orange/green) and shuffled dataset (black) for fixed (Ci-Di) and variable (Cii-Dii) foreperiod. The examples shown are for theta (C) and delta (D) bands. Continuous line: gaussian fit of the corresponding distribution. Dotted line: mean of the corresponding distribution.

3.4.2.1 Fixed foreperiod induces stronger delta power

The power of the foreperiod was computed with the Welch's method (see 2.7.2.2), only the power for frequencies in the range 1.5 – 80Hz was kept and normalized to the total sum of the power for each individual trial. The normalized power was then separated into the four frequency bands and averaged first by mouse and then all mice (n=8) were averaged together. In this way an estimate of the ratio of power for the four bands in each experimental condition was obtained (all protocols of stimulation were averaged together) (Fig.34A, Supp.Fig.10).

A significant reduction in the percentage of power of delta between fixed and variable foreperiod was seen in both control (p-value=0.04. paired t test, one tail. Effect size=0.89) and photostimulation (p-value=0.04. paired t test, one tail. Effect size=0.82) conditions (Fig. 34A).

In the table below can be found the mean values of the percentage of delta power for the four experimental conditions (Tab.6).

Foreperiod	Condition	Percentage of DELTA (mean±SEM)
Fixed	Control	33.91 ± 4.64%
	Photostimulation	35.48 ± 4%
Variable	Control	26.36 ± 1.79%
	Photostimulation	27.94 ±2.93%

Table 6. Mean percentage of total power taken by delta band.

No difference was found between control and photostimulation session for any of the foreperiod condition across all frequency bands.

3.4.2.2 Delta ramps only with variable foreperiod but photostimulation prevents it

A complementary analysis was performed on the slope of the ridge of the amplitude (see 3.4.1) for the delta band during control condition. The bootstrapped distribution of the ridge of VC was significantly higher than that of FC (p-value = $8.77 \cdot 10^{-15}$, 2KS test. Effect size = 1.48) (Fig. 34Bi). The analyses in 3.4.1 indicate that during FC the slope is almost flat whereas VC shows a positive slope.

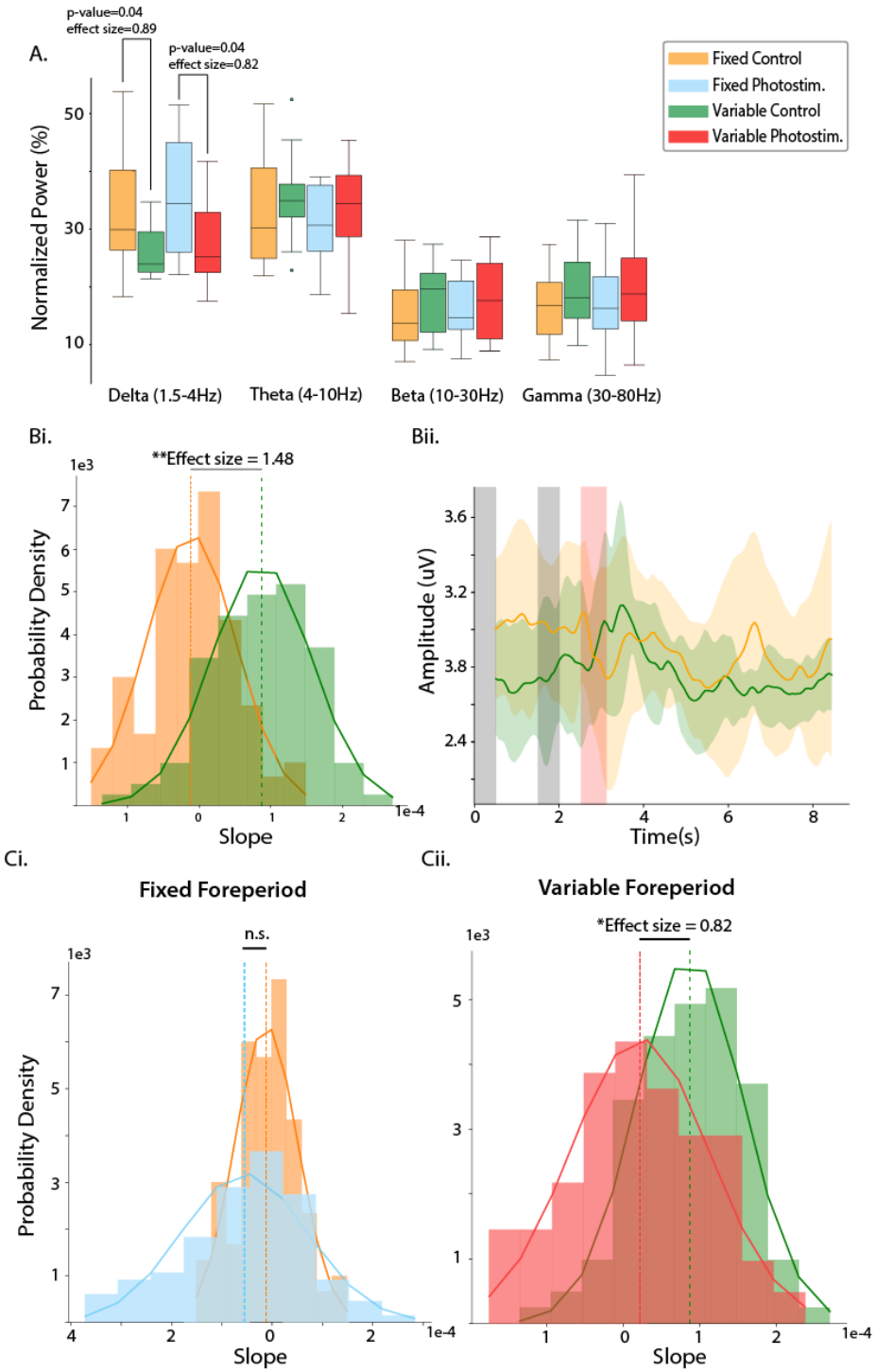

Fig.34 Delta oscillations are altered by the foreperiod

A. Ratio of total power occupied by the four bands of frequency during the four experimental conditions (FC, FP, VC, and VP. Colors in the legend).

Bi. Bootstrapped distributions of slopes of the ridge of delta frequency band for fixed (orange) and variable (green) foreperiod in control condition.

Bii. Mean ridge of delta band for fixed (orange) and variable (green) foreperiod in control conditions. Two grey bars indicate the time of the two visual cues and the red bar indicates the possible time of the reward. Mean±SEM.

C. Bootstrapped distributions of slopes of the ridge of delta frequency band for fixed (**Ci.**) and variable (**Cii.**) foreperiods comparing control and photostimulation conditions.

For **Bi** and **C**: Continuous line: gaussian fit of the corresponding distribution. Dotted line: mean of the corresponding distribution.

These two results together indicate that in FC condition, delta oscillation is strongly present but stable over time whereas during VC it is reduced in power, but its amplitude ramps up towards the reward (Fig. 34Bii).

Moreover, when comparing the bootstrapped slope between stimulation condition for the same foreperiod, with photostimulation there is a significant decrease in slope of the ridge of amplitude in delta band for the variable (p-value=$3.75 \cdot 10^{-6}$, 2ks test. Effect size = 0.82) but not fixed (p-value=$07.37 \cdot 10^{-4}$, 2ks test. Effect size = 0.46) foreperiod (Fig.34C).
The photostimulation of rCrusI during the variable foreperiod makes the slope flat and not distinguishable from an equally bootstrapped shuffled distribution (p-value=0.0004, 2ks test. Effect size=0.27, please compare it with the values of VC in Tab.5)

We can thus hypothesize that delta is engaged in time prediction when the moment of the reward is uncertain and a photostimulation (regardless of the protocol) of rCrusI prevents such ramping bringing the slope values to values comparable with fixed foreperiod condition.

3.4.3 Theta ramps only during the fixed foreperiod

By using the bootstrapped distributions of the slopes of the ridge of the amplitude (Tab.5) the effect of the foreperiod was investigated. Interestingly the situation is reversed from that of delta seen in the previous paragraph. The slope of the ridge of the amplitude is significantly higher in FC compared to VC (p-value=$1.95 \cdot 10^{-39}$, 2ks test. Effect size = 2.94. Fig.35A). As seen in 3.4.1, the slope of theta's ridge in VC is not significantly different from a shuffled distribution (Fig.33Ci), confirming that theta ramps only during fixed foreperiod and indicating that theta is probably engaged in time prediction only with a fixed foreperiod.

Interestingly, photostimulation affected theta only when there is ramping but differently from how delta was affected. Photostimulation significantly increased the variability of the slope value in FP compared to FC (p-value = 0.014, Lavene's test. Fig.35Bi) but not that of VP compared to VC (p-value = 0.69, Lavene's test, Fig.35Bii).
Please note that this last analysis of the variance was performed and the 'raw' slope values (n=8) without any bootstrapping as it would have affected the reliability of the resulting p-value (as already discussed).

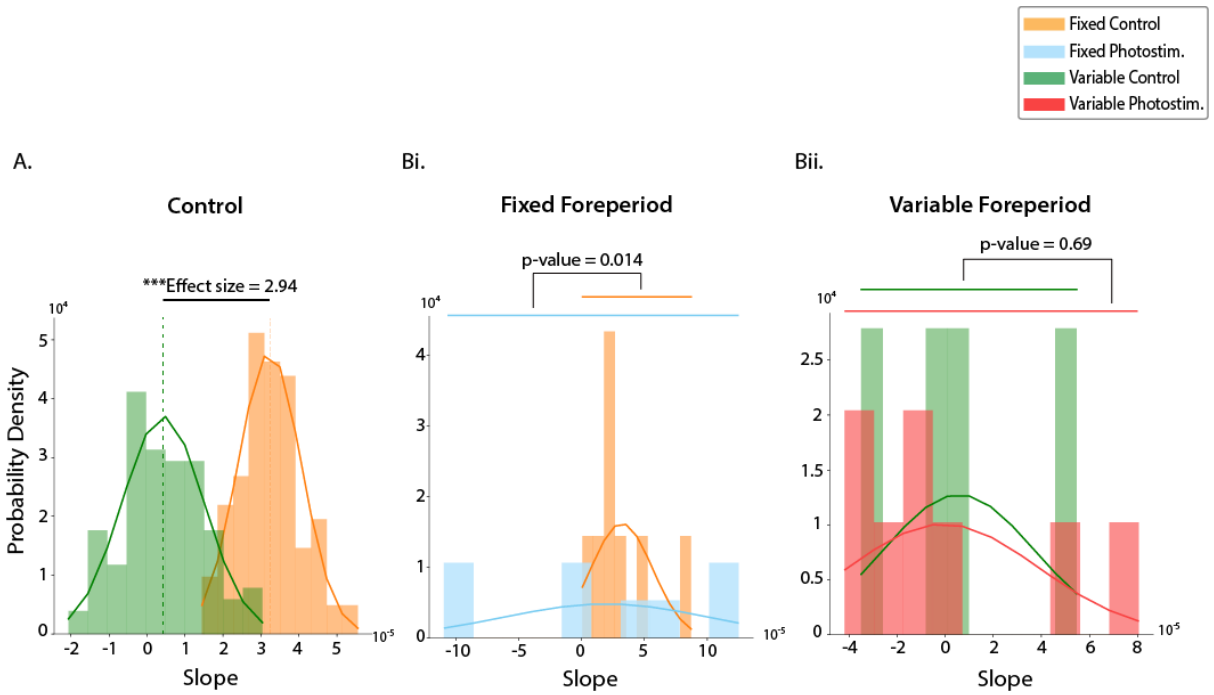

Fig.35 Theta ramps during fixed but not variable foreperiod

A. Bootstrapped distributions of slopes of the ridge of theta frequency band for fixed (orange) and variable (green) foreperiod in control condition.

B. Analysis of the variance between control and photostimulation conditions for fixed (Bi) and variable (Bii) forepriod. This analysis was performed on the raw slope data (no bootstrapping).

Continuous line: gaussian fit of the corresponding distribution. Dotted line: mean of the corresponding distribution.

In supplementary figures 11 and 12, it is visible the comparison of the bootstrapped slopes between foreperiods and photostimulation conditions, respectively.

3.5 Neuronal discharges in PrL

The last data type used is multi-unit recordings (see 2.4.2) acquired through silicon probes. As a reminder: multi-unit activity was recorded in layer V of left PrL through 2x8 silicon probes. The first analysis done was the characterization of the recorded units into putative cell types (3.5.1). Afterwards, units were analyzed time-locked with the behavior (3.5.2).

3.5.1 Characterization of cell types

As a first analysis the recorded units in the PrL were classified as putative pyramidal cells and interneurons, and their general electrophysiological properties were investigated.

The performance of the mice (n=8) was not taken into consideration during this analysis (contrary to previous and future analyses, in this case there was no previous selection of the traces depending on the behavioral performance).

3.5.1.1 Identifying Interneurons and Pyramidal Cells

From the electrophysiological recordings, 327 units were successfully isolated by means of spike sorting (see 2.7.4). These units were clustered into putative interneurons and putative pyramidal cells according to the literature (Barthó et al., 2004).

Two parameters from the average waveform of each unit were used for clustering: spike width at half-amplitude (half-width) and amplitude trough-to-peak (amplitude) (Fig. 36A). Please note that the average waveforms are z-scored, thus the values of the amplitude are all scaled and comparable.
All the units with half-width < 0.2ms and amplitude < 15 (arbitrary units) were considered as putative interneurons (n=21), the others as putative pyramidal cells (n=306) (Fig. 36B). The clustered units will now be referred to as interneurons and pyramidal cells, respectively.

Mean firing rate (Pyramidal cells = 9.08 ± 0.5Hz; Interneurons = 11.24 ± 1.15Hz. Mean±SEM) and mean inter-spike interval (ISI) (Pyramidal cells = 250 ± 20ms; Interneurons = 100 ± 10ms. Mean±SEM) was computed for the two clusters with the respective standard error of the mean (SEM) (Fig. 36C).

Interneuron's average ISI is compatible with their average firing rate, but it is not the case for pyramidal cells. With a mean firing rate of 9.08Hz the expected mean ISI is of 110ms, instead of the obtained one of 250ms. Such phenomenon was investigated by plotting the distribution of ISI of pyramidal cells (Fig. 36D). Indeed, the distribution is heavily positively skewed (Fisher-Pearson coefficient of skewness = 2.36).

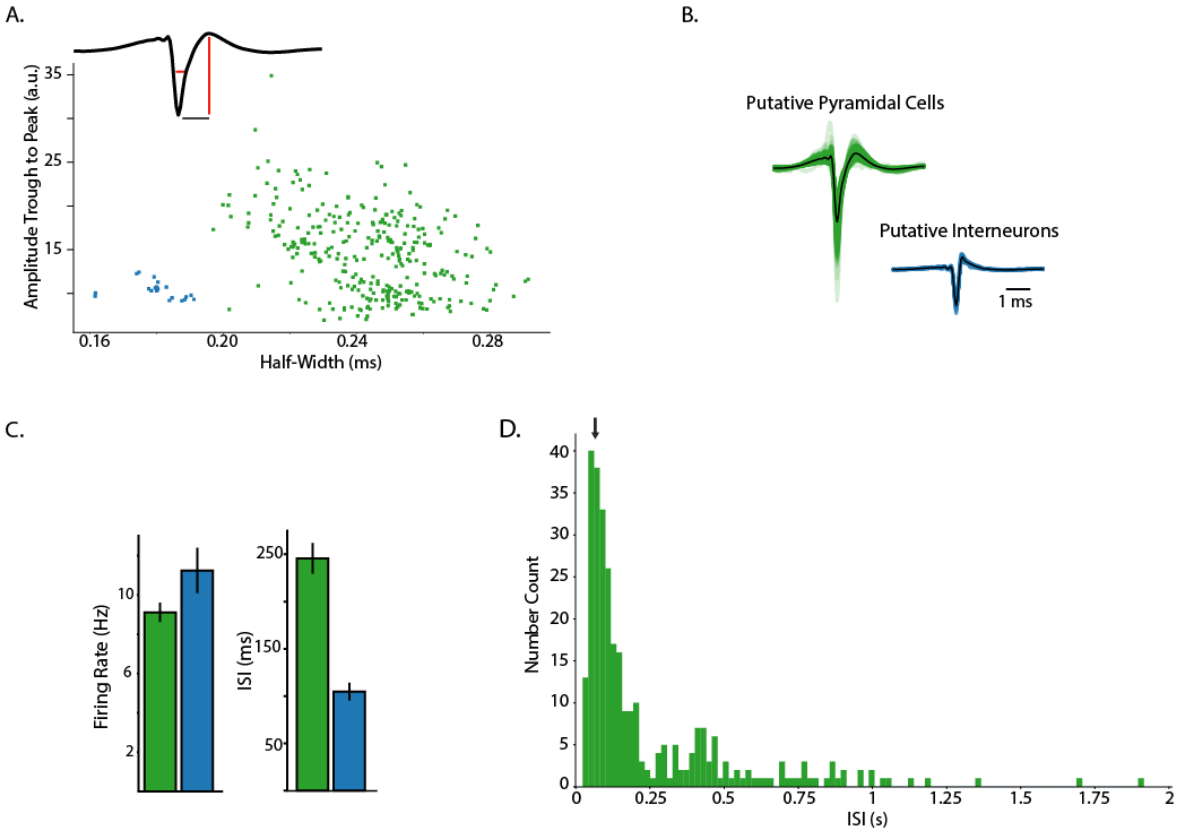

Fig.36 Identification of putative cellular types

A. Clustering of putative cellular types based on two parameters: spike width at half-amplitude (half-width, ms) and amplitude trough to peak (arbitrary units, zscore from baseline). Black trace used to represent the two time parameters selected (red traces). Blue dots: putative interneurons (n=21). Green dots : putative pyramidal cells (n=306).

B. Average waveforms of individual units (coloured lines) and average waveform of the cluster (black line).

C. Characterization of average firing rate and interspike interval for the two identified clusters. Units from all trials without distinction of experimental condition were used. Mean ± SEM.

D. Distribution of mean ISI values of all pyramidal cells. Black arrow indicates the ISI value (110ms) corresponding to the mean firing rate observed for the whole population.

3.5.1.2 Electrophysiological characterization of identified cell types

Identified cell types were further characterized by their electrophysiological properties while segregated based on the experimental conditions. Five conditions were considered: FC, FP, VC, VP, and an absolute control with cells recorded while the mouse was not performing any behavior, called No Behavior (NB). For representation purposes, the mean instantaneous firing right of all conditions was plotted in Fig. 37B-D for interneurons and pyramidal cells, respectively.

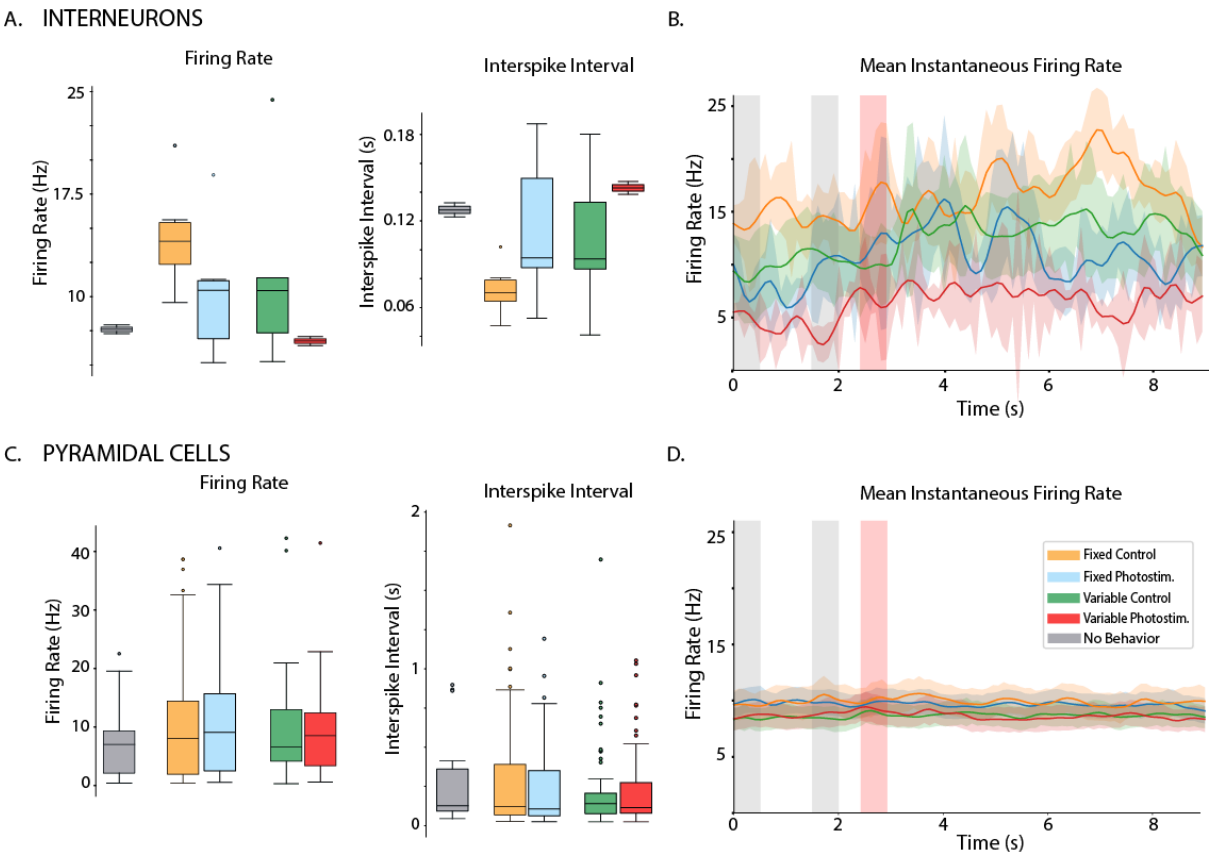

Fig.37 Characterization of putative Interneurons (Top) and Pyramidal Cells (bottom).
A. (Interneurons) and C. (Pyramidal Cells) Mean firing rate (left) and mean interspike interval, ISI (right) of the previously clustered cell types. Different conditions were investigated here: Control and Photostimulation in fixed and variable foreperiod conditions and NB condition (for the colors, please look at the legend in the figure).
B. (Interneurons) and D. (Pyramidal Cells) Temporal evolution of the mean instantaneous firing rate for the four conditions during the behavioural task. The plot shows relevant epochs of the task: the two light cues (grey bars) and the delivery of the reward (red bar). Given that both fixed and random foreperiod conditions have been plotted simultaneously, it's not shown the exact time of the reward but the interval of time where it can possibly have been present (possible time points: 2.43s/2.93s in variable foreperiod condition and 2.53s with a fidex foreperiod). Mean ± SEM.

For simplicity, the values of mean firing rate and mean ISI for both interneurons (Fig. 37A) and pyramidal cells (Fig. 37C), for all 5 conditions are listed in the table below (Tab.7).

Condition	Cell Type	Firing Rate (mean±SD)	ISI (mean±SD)	N
No Behavior	Interneuron	7.6±0.32Hz	127.7±4.87ms	2
	Pyramidal cell	7.07±5.53Hz	250.72±259.64ms	24
Fixed Control	Interneuron	14.4±3.56Hz	72.4±16.8ms	6
	Pyramidal cell	9.97±9.33Hz	269.18±325.11ms	93
Fixed Photostimulation	Interneuron	10.36±4.49Hz	113.7±47.4ms	6
	Pyramidal cell	10.21±8.74Hz	236.11±250.52ms	68
Variable Control	Interneuron	11.76±6.69	106.88±46.88ms	5
	Pyramidal cell	8.96±7.89Hz	221.92±264.19ms	67
Variable Photostimulation	Interneuron	6.75±0.32	142.91±4.49ms	2
	Pyramidal cell	8.73±7.19Hz	244.71±265.76ms	54

Table 7. Electrophysiological characterization of interneurons and pyramidal cells.

Due to the low number of the interneurons (n=21), no statistical analysis was performed on them, and they will not be further included in future analyses of this manuscript.

Regarding pyramidal cells, no significant difference was found between any of the groups for either firing rate or ISI.

3.5.2 Units ramp locked to the behavior

Previously identified pyramidal cells, from correctly performed trials, were used for further analyses. The instantaneous firing rate of selected trials was averaged across the session (Fig.38A). From this average distribution, seven features were extracted (see 2.7.4.1) and a PCA was performed on these units, divided in the four experimental conditions (FC, FP, VC, and VP). Four principal components were extracted from each analysis.

On this new space, a hierarchical clustering was performed to identify clusters of similar units. For FP, VC, and VP 3 clusters were identified, whereas for FC 4 clusters were found.

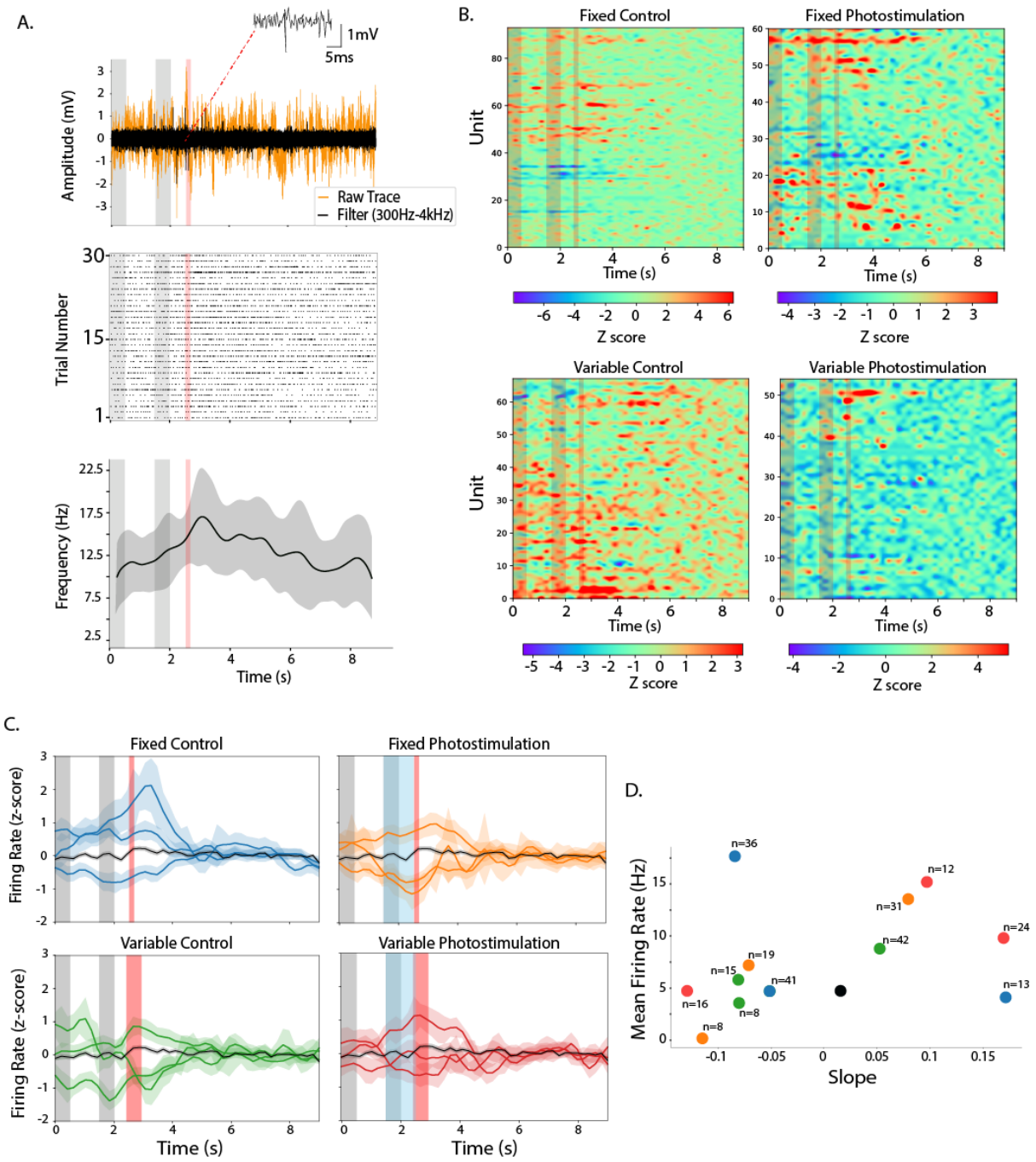

Fig.38 Firing rate in the PrL is modulated by the behavior

A. Example of raw (orange) and filtered (black) trace from a recording. The inset is a magnification of a spike, the red dotted line indicate its original position in the trace (Top). Raster plot of a unit obtained from the above trace (Middle) and mean istantaneous firing rate of said unit (Bottom). Red vertical band: time of reward. Mean±SD

B. Color maps of the z-scored firing rate of each unit for the four experimental conditions. Units are sorted by identified clusters. Please note the varying color scales.

C. Z-score of mean firing rate for the clusters previously identified for fixed (top) and variable (bottom) foreperiod. Colors unrelated. Black distribution: 'control' distribution obtained by averaging all units from all experimental conditions. Mean±SEM

D. Values of slope for each identified cluster plotted against the respective mean firing rate. Color matching conditions in E. Black dot: control distribution.

The activity of the clustered units was z-scored (Fig. 38B) and averaged by cluster (Fig.38C). The clusters with less than 3 units were excluded (one cluster from FC was thus excluded). In Fig.38C the z-scored time course of the selected units is visible and as a control, the distribution obtained by averaging all recorded units was used. From each of these clusters, the slope and mean firing rate during the foreperiod was computed and plotted against each other. As visible in Fig.38D, there are clusters of units above the control one (up-regulated units) and others well below it (down-regulated units).

We can indeed confirm that there are clusters that are up-regulated and others that are down-regulated (Fig.38D, Tab.8), which shows that the network is entrained by the behavioral task also at the single cell level.

Condition / State	FC	FP	VC	VP	Tot
Up	13	31	42	36	122
Down	77	27	23	16	143
Tot	90	58	65	52	265

Table 8 Sample size for up- and down-regulated units for the four experimental conditions. Please note that the difference between total pyramidal cells identified (n=306) and the total in this table (n=265) is due to the exclusion of the No-Behavior recordings from these analyses.

In Fig.38C the z-scored clusters of units for each of the four experimental conditions are visible. In all four conditions there are clusters showing ramping activity entrained with the behavior, although VC and VP seem to be the least entrained conditions.
FC seems to present the cluster with the strongest ramping activity which is completely lost in FP. Since control and photostimulation conditions (of the same foreperiod) were recorded during the same session (within few seconds from each other), we feel we can advance bolder statements on the evolution of the situation even if it is not possible (with the current state of the analyses) to confirm the identity of the individual units between different recordings.

4 Discussion

To survive is to anticipate foreseeable events so to better react to the environment. Those that are able to better predict and time events, have a higher fitness. In chapter 1.4 of the introduction, we have seen the main hypotheses on how time can be perceived and processed. Moreover, we have seen that there are mathematical models (predictive coding and hazard function) to explain how the brain can apply Bayesian inference (Aitchison & Lengyel, 2017) to constantly generate and update predictions about the environment.

The aim of my project was to develop a behavioral task that would allow us to investigate the processing of implicit timings and how these are used to predict a reward with varying degrees of predictability.

I will thus now proceed at addressing the three questions I posed at the beginning of the previous chapter, highlighting interesting results and limitations of our approach.
Lastly, I will discuss possible future perspectives of the project.
During this discussion behavioral and electrophysiological results will be kept separate as they probably reflect different branches of a more diffused network and thus to compare them would be comparing probably different stages of a network integrating information coming from multiple areas. The system we set up to investigate is fairly complex and my work represent only the first piece of a wider puzzle that I'm sure the lab will continue to unveil after me.

First however, I will discuss how the optimal area for cerebellar stimulation was chosen and how putative neuronal cell types were identified from multiunit recordings. Then I will need to address the main possible limitation of my project: possible motor impairments produced by cerebellar stimulation.

4.1 Cerebello-prefrontal functional connections

Multiple areas of the cerebellar cortex are reportedly connected with PFC (see chapter 1.3). To determine the optimal area of stimulation, a preliminary experiment was performed (see 3.1). Surprisingly, only one region (CrusI) among those stimulated (lobule VI and VII, CrusI and

CrusII medial, and CrusI and CrusII lateral) induced a significant perturbation of the LFP in the contralateral PrL.

Such result on one side confirms CrusI to be functionally connected with PFC (E. Kelly et al., 2020) but it also rises question as to why a connection with vermal lobules was not highlighted, contrary to previous studies (Watson et al., 2009).

This experiment was performed in mice anesthetized with Isofluorane, which is known to alter neuronal activity in PFC (Zhang et al., 2020; Zhang et al., 2019). It is thus possible that such configuration masked some, maybe weaker, connections that in awake animals are normally functional. It is also to be noted that our photostimulation of the vermis in lobule VI might have been too anterior to elicit a response in the mPFC, as its anterior part is still widely involved in more motor tasks.

4.2 Cell type identification

Spike sorting was performed on multiunit recordings and the individual units obtained were clustered into putative pyramidal cells and putative interneurons and their electrophysiological properties were analyzed (see 3.5.1).
Unfortunately, due to a conservative approach, very few interneurons were isolated (n=21) which prevented any further analysis of this class.

This electrophysiological characterization did not highlight any difference between conditions. Although, this is not surprising given that no segregation was done on the specific conditions depending on the performance of the mouse in the task. It could be thus interesting to repeat this analysis selecting the trials where the mice were actively engaged in the task.
As mentioned in the previous chapter, the distribution of ISI values for the pyramidal cells results highly skewed (Fig.36D) with the highest peak around 110ms (coherent with the population mean firing rate of 9Hz) and a second, smaller, peak around 420ms.
Further analyses are ongoing to investigate this phenomenon and whether two subpopulations of pyramidal cells exist in our dataset.

4.3 Might motor related impairments explain the behavioral data?

Cerebellum is undeniably involved in motor coordination and there are two motor aspects that need to be addressed: locomotion and licking behavior.

The cerebellar area more involved with the coordination of the limbs for locomotion is anterior vermis (core muscles) and anterior paravermis (limbs) (Armstrong et al., 1988; Darmohray et al., 2019), which is considerably distant from rCrusI where the optic fiber was implanted but possible volume conduction of the light cannot be excluded.
The speed of the mice was thus investigated (3.2.1) and comparison between control and photostimulation conditions of the two foreperiods didn't reveal any difference in locomotor behavior (Fig.26).

Regarding licking behavior, the literature reveals a complex situation on the involvement of the cerebellum. rCrusI is reportedly involved in the control of licking rhythmicity and mostly in the coordination of licking and breathing movements together (Bryant et al., 2010).
To address this point, the number of licks performed during photostimulation was computed and compared with the number of licks performed during the same time window during control trials (3.3.3).
There is indeed a significant reduction in the number of licks between FC and FP but such reduction is not visible during the variable foreperiod, between VC and VP. And looking at the distribution of values (Fig.31), it is visible that VC, VP, and FP are comparable whereas FC is the only condition significantly different. This indicates a possible general increase in licking and in the anticipation of the reward induced by the fixed foreperiod which is reduced by photostimulation of rCrusI (this point will be discusses in more detail in the following paragraphs).

It is to be noted that the success ratio (a measure of the degree of engagement with the task) (3.3.2) shows a reduction in performance with photostimulation in both foreperiod conditions. Although, the reduction in VP is so limited that FP is significantly lower than it, whereas the two control conditions (FC and VC) are comparable.
This result is coherent with the reduction in the number of licks performed after the reward

during photostimulation (3.3.3), and also in this case (as with the success ratio), the reduction with variable foreperiod has an effect size that is considered to be medium (0.56).

We thus currently exclude any possible major motor alterations induced by photostimulation. Nonetheless, this remain correlative evidence and a more targeted investigation will be needed in the future to exclude any possible effect of our stimulation of the licking behavior. A possible approach would be to use a high-speed camera to record facial movements while the mouse is performing the task and then analyze the footage possibly using machine learning algorithms such as DeepLabCut (Mathis et al., 2018) to investigate any possible micro-expression induced by the photostimulation.

4.4 Does the task allow us to investigate anticipation of an event?

To investigate whether we were successful in designing and developing the task, various parameters were taken into consideration. Three data types were analyzed to have indication of time-varying activity locked with the behavior: running speed, licking behavior, and amplitude of the LFP by frequency band.
In this paragraph I will address only data from control conditions since the target is to determine whether mice can show anticipation of the reward. Moreover, no attention will be placed on differences between foreperiods as it is the subject of the next paragraph.

In both foreperiod conditions mice significantly slowed down on the wheel in anticipation of the reward (3.2.2), which has already been reported in the literature (Chabrol et al., 2019).

It is interesting to mention Fig.27B and Fig.26Bi, where it is possible to see the average time course of the speed during variable foreperiod when the traces are aligned to the reward and to the beginning of the trial, respectively. In the former case, the response to the reward is highlighted whereas in the latter, the anticipation of it is the one to be highlighted. And when looking at the response to the reward (with traces aligned to the reward, Fig.27B) a clear temporary deceleration is visible, but such behavior is lacking with a fixed foreperiod (Fig.26Ai).
A possible interpretation is that with a fixed foreperiod, mice can better anticipate (the slope is indeed steeper) and thus better prepare to the action of licking the reward, whereas, with

a variable foreperiod, mice still know that a reward is to be had (there is still a significant deceleration) but they are unable to properly time the movement and thus they need to slow down after the reward to focus on the action of licking.

Also, both licking behavior (3.3.1) and oscillatory activity (3.4.1) have been shown to ramp, with various degrees, time-locked with the behavioral task.

I will discuss possible interpretations of such ramping activity for all this data in the following paragraphs, but regarding the question of this present paragraph, we can conclude that the task we developed is indeed successful in allowing us to investigate anticipatory behavior both in behavioral and electrophysiological domains.

4.5 Does the nature of the foreperiod affect the results?

4.5.1 The foreperiod effect induces stronger anticipatory licking with fixed foreperiod

When looking at behavioral data, both speed (3.2.2.1) and licking behavior (3.3.1.2) show a steeper slope (in negative and positive direction, respectively) during fixed foreperiod conditions compared to variable conditions. These results are not surprising per se as the 'foreperiod effect', the phenomenon for which increased implicit predictability improves reaction time and performance, is well known in the literature (Coull et al., 2016).
It is important however, to remind that mice are trained over approximately two weeks with the variable foreperiod and that they are exposed to the fixed foreperiod for only one day, which means that the rhythmicity of the fixed condition is able to implicitly improve the behavioral performance of a well-rehearsed behavior within only few tens of trials.

Moreover, it is to be noted that both success ratio (3.3.2) and number of licks after the reward (3.3.3) are unchanged by the difference in foreperiod (FC and VC). Only the number of licks immediately before the reward is reduced with a variable foreperiod, which indicates that the differences in behavior previously seen are not due to less attention or less engagement in the task but instead they are due to different strategies applied by the animals, possibly due to differences in prediction of the moment of the reward.

4.5.2 Theta and Delta oscillations ramping underlie different functions

Two frequency bands were of particular interest. Delta (1.5-4Hz) has been shown to have a very high percentage of total power but constant max amplitude during fixed foreperiod conditions whereas with a variable foreperiod it has lower power, but its amplitude ramps locked with the reward (3.4.2). On the other hand, Theta (4-10Hz) seems to behave opposite to it showing a ramping amplitude locked with the reward only during a fixed foreperiod and flat during a variable one (3.4.3).

Slow-wave oscillations have been widely linked with top-down control of attention (Cravo et al., 2013; Totah et al., 2013b) and timing (Parker, 2016), and they have been shown to entrain subcortical structures, among which the cerebellum, into coherent slow oscillations (Roš et al., 2009). Such differences revealed by our results may indicate slightly different roles for these two frequencies.
We obviously are not yet in a position to understand what these roles are, further experiments will be needed to clarify the specific functions of the network, but I can put forward some hypotheses on possible explanations of our data.

Theta oscillations in the PFC are involved in memory consolidation within the hippocampal-prefrontal network (Backus et al., 2016), and ramping of such frequencies in the mPFC of rats has been proposed to help this memory consolidation by selecting relevant information over the noise of stimuli (Jarovi et al., 2018). We can thus speculate that the ramping of theta exclusively during the fixed foreperiod might be indicative of consolidating into memory the new constant timing.

Delta frequency band has instead been involved with prediction of a stimulus, top-down attention (Totah et al., 2013b), interval timing (Parker et al., 2017), and cortico-cortical communication for decision making (Nácher et al., 2013).
Since our recordings were performed in the output layer of mPFC (layer V) it is possible to hypothesize that the ramping shown is an activity to synchronize different areas over an interval of time (whose length is probably determined by the hazard function) and to update predictions of the possible time of the reward.

4.6 Photostimulation of rCrusI

The last question left to address is whether the cerebello-prefrontal network is involved in such timing functions.

4.6.1 Behavior

In the previous paragraph, the foreperiod effect, represented by the stronger anticipatory licking behavior during FC compared to VC, was discussed. Interestingly photoactivation of rCrusI during fixed foreperiod induced a further increase of such anticipatory behavior. Whereas no effect of the photostimulation was reported during a variable foreperiod (3.3.1.1).

It is worth reminding the result exposed in 3.3.4, where an analysis of the slope of the licking behavior found a significant difference between control and photostimulation session only during variable foreperiod with a Theta-Burst stimulation (Fig.32).
Such contradiction may be explained by the effect of merging together data from various sessions: this may indeed bring to light small but ubiquitous effects but at the same time it can hide stronger effects that are induced by a specific frequency of stimulation. We made this decision of pulling data together for most of the analysis conscious of the side effects (this topic is further discussed in the last paragraph of the discussion, 4.7).

In what may seem contrary to the previous behavioral result, photostimulation with the fixed foreperiod reduces both success ratio and the number of licks (during both windows of time). Although difficult to interpret, we hypothesize that photostimulation might be reducing top-down attention thus the mouse requires more effort to perform (hence the reduction in successful trials) but this higher effort means also that when the mouse is actually performing correctly, it shows a stronger anticipatory lick.

The cerebellum has been linked in various ways with top-down attention and attention shift (Sokolov et al., 2017; Stoodley, 2016). Thus, alternatively it is also possible that through volume conduction of the light, our photostimulation is actually affecting two different networks (one for attention and one for forward predictions) and the results are summed in our behavioral data.

4.6.2 LFP

As seen in 4.5.2, there are two frequency bands that behave opposite to each other: theta and delta. Ramping only during fixed and variable foreperiod, respectively.

Very interestingly, photostimulation seems to affect both bands but only if they are ramping and it affects them differently.
Delta, which ramps only during variable foreperiod, is affected by photostimulation only during this condition (VP). The result of such photostimulation is the complete prevention of the ramping of the amplitude (3.4.2).
On the other hand, theta is also affected by photostimulation (during fixed foreperiod) but the effect of cerebellar stimulation is different in that the slope is not affected per se thus the average behavior of the mice is unchanged, but the variability in the sample is significantly increased (3.4.3, Fig.35Bi).

In both cases it seems that by perturbing physiological cerebellar activity also prefrontal activity is altered: by either reducing the ramping or making this ramping less reliable (increase of the variability among mice). These results are coherent with the hypothesis of the cerebello-prefrontal network being involved in fine tuning implicit time processing.

These analyses have their limitations in that they are unable to capture finer changes in the dynamics. The analysis of the slope of the ridge indeed allowed us to investigate the ramping locked with the behavior but it is insensitive to possible changes in the time of onset of the ramping, which seems to be the case for the ridge of theta band during fixed foreperiod (FC and FP, Sup.Fig.8). In this case the linear regression doesn't detect a change in slope (as we discussed in the results and above in the paragraph) but there seems to be indeed a change in the onset time, with the photostimulation inducing a later onset. This will have to be addressed with more sophisticated analyses.

4.6.3 Clusters of units are entrained by the behavioral task

The identified pyramidal cells were clustered to identify similarly behaving units (3.5.2). We can speculate on the effect of photostimulation since the recordings come from the same day, few seconds apart. Indeed, the cluster of FC with the highest rate of positive ramping

seems to have disappeared in FP condition, and VP seems to have a reduced ramping activity compared to VC.

This section of the analyses was the most superficial one and indeed we will need to perform further analyses on this data. We currently are unable to discuss properly the evolution of the network in the various experimental conditions beyond stating an entrainment of the firing rate of the individual units to the behavioral task.

4.7 Final thoughts and future perspectives

This work represents the beginning of a new branch of research in the team. Through it we have successfully developed and implemented a behavioral task for studying implicit time processing and predictive coding in the cerebello-prefrontal network.
This was confirmed by various data types all showing a degree of entrainment to the timing of the behavioral task. Moreover, we were able to reproduce the foreperiod effect.

We have highlighted differences in two low-frequency oscillations and speculated on their different underlying functions.

Initially we had set out to investigate the frequency-dependent role of the cerebellum through different protocols of stimulation. Unfortunately, we had to merge the data obtained from the various protocols since the effects recorded were so small that we needed a much greater sample size than what we would have had in the individual groups of recordings. We thus were able only to study the effects of a general cerebellar stimulation. Since this work will be the basis of future more targeted projects, we felt it was safer to look for strong results, emerging from the group data instead of trying to dissect the effect of individual protocols.

This approach has indeed allowed us to analyze properly our dataset but at the cost of possibly masking smaller effects produced only by one of the protocols (3.3.4, for example).

We feel this model holds a great potential to further dissect the cerebello-prefrontal network and its complex cognitive functions. In the present work only healthy mice were used, for the future the plan is to finally include a schizophrenia mouse model to investigate time processing alterations that have been widely reported in the literature (1.4.6). This new step

will allow to test if the photostimulation of the cerebellar cortex can actually recover some of the timing impairments previously discussed in the manuscript.

5 Bibliography

Aitchison, L., & Lengyel, M. (2017). With or without you: predictive coding and Bayesian inference in the brain. In *Current Opinion in Neurobiology* (Vol. 46, pp. 219–227). Europe PMC Funders. https://doi.org/10.1016/j.conb.2017.08.010

Aksenov, D., Serdyukova, N., Irwin, K., & Bracha, V. (2004). GABA Neurotransmission in the Cerebellar Interposed Nuclei: Involvement in Classically Conditioned Eyeblinks and Neuronal Activity. *Journal of Neurophysiology*, *91*(2), 719–727. https://doi.org/10.1152/jn.00859.2003

Albus, J. S. (1971). A theory of cerebellar function. *Mathematical Biosciences*, *10*(1–2), 25–61. https://doi.org/10.1016/0025-5564(71)90051-4

Alexander, W. H., & Brown, J. W. (2018). Frontal cortex function as derived from hierarchical predictive coding. *Scientific Reports*, *8*(1), 1–11. https://doi.org/10.1038/s41598-018-21407-9

Andreasen, N. C. (1999). A unitary model of schizophrenia. Bleuler's "fragmented phrene" as schizencephaly. In *Archives of General Psychiatry* (Vol. 56, Issue 9, pp. 781–787). https://doi.org/10.1001/archpsyc.56.9.781

Andreasen, N. C., & Pierson, R. (2008). The Role of the Cerebellum in Schizophrenia. In *Biological Psychiatry* (Vol. 64, Issue 2, pp. 81–88). NIH Public Access. https://doi.org/10.1016/j.biopsych.2008.01.003

Ankri, L., Husson, Z., Pietrajtis, K., Proville, R., Léna, C., Yarom, Y., Dieudonné, S., & Uusisaari, M. Y. (2015). A novel inhibitory nucleo-cortical circuit controls cerebellar Golgi cell activity. *ELife*, *4*(MAY). https://doi.org/10.7554/eLife.06262

Apps, R., & Hawkes, R. (2009). Cerebellar cortical organization: A one-map hypothesis. In *Nature Reviews Neuroscience* (Vol. 10, Issue 9, pp. 670–681). https://doi.org/10.1038/nrn2698

Apps, R., Hawkes, R., Aoki, S., Bengtsson, F., Brown, A. M., Chen, G., Ebner, T. J., Isope, P., Jörntell, H., Lackey, E. P., Lawrenson, C., Lumb, B., Schonewille, M., Sillitoe, R. V, Spaeth, L., Sugihara, I., Valera, A., Voogd, J., Wylie, D. R., & Ruigrok, T. J. H. (2018). Cerebellar Modules and Their Role as Operational Cerebellar Processing Units. In *Cerebellum* (Vol. 17, Issue 5, pp. 654–682). https://doi.org/10.1007/s12311-018-0952-3

Arancillo, M., White, J. J., Lin, T., Stay, T. L., & Sillitoe, R. V. (2015). In vivo analysis of purkinje cell firing properties during postnatal mouse development. *Journal of Neurophysiology*, *113*(2), 578–591. https://doi.org/10.1152/jn.00586.2014

Argyropoulos, G. P. D. (2016). The cerebellum, internal models and prediction in 'non-motor' aspects of language: A critical review. *Brain and Language*, *161*, 4–17. https://doi.org/10.1016/j.bandl.2015.08.003

Armstrong, D., Harvey, R., & Schild, R. (1974). Topographical localization in the olivo-cerebellar projection: an electrophysiological study in the cat. *J Comp Neurol*, *154*, 287–302.

Armstrong, D. M., Edgley, S. A., & Lidierth, M. (1988). Complex spikes in Purkinje cells of the paravermal part of

the anterior lobe of the cat cerebellum during locomotion. *The Journal of Physiology*, *400*(1), 405–414. https://doi.org/10.1113/jphysiol.1988.sp017128

Ashizawa, T., & Xia, G. (2016). Ataxia. In *CONTINUUM Lifelong Learning in Neurology* (Vol. 22, Issue 4,MovementDisorders, pp. 1208–1226). American Academy of Neurology. https://doi.org/10.1212/CON.0000000000000362

Babinski, J. (1902). Sur le rôle du cervelet dans les actes volitionnels necessitant une succession rapide de mouvements (diadoco- cinésie). *Rev Neurol*, *10*, 1013–1015.

Backus, A. R., Schoffelen, J. M., Szebényi, S., Hanslmayr, S., & Doeller, C. F. (2016). Hippocampal-prefrontal theta oscillations support memory integration. *Current Biology*, *26*(4), 450–457. https://doi.org/10.1016/j.cub.2015.12.048

Baddeley, A. (1992). Working memory. *Science*, *255*(5044), 556–559. https://doi.org/10.1126/science.1736359

Baddeley, A. (2000). The episodic buffer: A new component of working memory? In *Trends in Cognitive Sciences* (Vol. 4, Issue 11, pp. 417–423). Trends Cogn Sci. https://doi.org/10.1016/S1364-6613(00)01538-2

Baddeley, A., & Hitch, G. (1974). Working Memory. *Psychology of Learning and Motivation*, *8*, 47–89. https://www.sciencedirect.com/science/article/pii/S0079742108604521

Badre, D. (2012). Opening the gate to working memory. In *Proceedings of the National Academy of Sciences of the United States of America* (Vol. 109, Issue 49, pp. 19878–19879). National Academy of Sciences. https://doi.org/10.1073/pnas.1216902109

Badre, D., & D'Esposito, M. (2009). Is the rostro-caudal axis of the frontal lobe hierarchical? In *Nature Reviews Neuroscience* (Vol. 10, Issue 9, pp. 659–669). Nat Rev Neurosci. https://doi.org/10.1038/nrn2667

Badura, A., Verpeut, J. L., Metzger, J. W., Pereira, T. D., Pisano, T. J., Deverett, B., Bakshinskaya, D. E., & Wang, S. S. H. (2018). Normal cognitive and social development require posterior cerebellar activity. *ELife*, *7*. https://doi.org/10.7554/eLife.36401

Balsters, J. H., Cussans, E., Diedrichsen, J., Phillips, K. A., Preuss, T. M., Rilling, J. K., & Ramnani, N. (2010). Evolution of the cerebellar cortex: The selective expansion of prefrontal-projecting cerebellar lobules. *NeuroImage*, *49*(3), 2045–2052. https://doi.org/10.1016/j.neuroimage.2009.10.045

Balsters, Joshua H., & Ramnani, N. (2011). Cerebellar plasticity and the automation of first-order rules. *Journal of Neuroscience*, *31*(6), 2305–2312. https://doi.org/10.1523/JNEUROSCI.4358-10.2011

Barbas, H., Henion, T. H. H., & Dermon, C. R. (1991). Diverse thalamic projections to the prefrontal cortex in the rhesus monkey. *Journal of Comparative Neurology*, *313*(1), 65–94. https://doi.org/10.1002/cne.903130106

Bares, M., Lungu, O., Liu, T., Waechter, T., Gomez, C. M., & Ashe, J. (2007). Impaired predictive motor timing in patients with cerebellar disorders. *Experimental Brain Research*, *180*(2), 355–365. https://doi.org/10.1007/s00221-007-0857-8

Barmack, N. H., & Yakhnitsa, V. (2008). Functions of interneurons in mouse cerebellum. *Journal of Neuroscience*, *28*(5), 1140–1152. https://doi.org/10.1523/JNEUROSCI.3942-07.2008

Barthó, P., Hirase, H., Monconduit, L., Zugaro, M., Harris, K. D., & Buzsáki, G. (2004). Characterization of neocortical principal cells and interneurons by network interactions and extracellular features. *Journal of Neurophysiology*, *92*(1), 600–608. https://doi.org/10.1152/jn.01170.2003

Barton, R. A., & Harvey, P. H. (2000). Mosaic evolution of brain structure in mammals. *Nature*, *405*(6790), 1055–1058. https://doi.org/10.1038/35016580

Barton, R. A., & Venditti, C. (2014). Rapid evolution of the cerebellum in humans and other great apes. *Current Biology*, *24*(20), 2440–2444. https://doi.org/10.1016/j.cub.2014.08.056

Bastian, A. J. (2006). Learning to predict the future: the cerebellum adapts feedforward movement control. In *Current Opinion in Neurobiology* (Vol. 16, Issue 6, pp. 645–649). Curr Opin Neurobiol. https://doi.org/10.1016/j.conb.2006.08.016

Baumel, Y., Jacobson, G. A., & Cohen, D. (2009). Implications of functional anatomy on information processing in the deep cerebellar nuclei. In *Frontiers in Cellular Neuroscience* (Vol. 3, Issue NOV, p. 14). Kelly and Strick. https://doi.org/10.3389/neuro.03.014.2009

Bekolay, T., Laubach, M., & Eliasmith, C. (2014). A spiking neural integrator model of the adaptive control of action by the medial prefrontal cortex. *Journal of Neuroscience*, *34*(5), 1892–1902. https://doi.org/10.1523/JNEUROSCI.2421-13.2014

Bengtsson, F., & Hesslow, G. (2006). Cerebellar control of the inferior olive. *Cerebellum*, *5*(1), 7–14. https://doi.org/10.1080/14734220500462757

Bengtsson, F., & Jörntell, H. (2009). Sensory transmission in cerebellar granule cells relies on similarly coded mossy fiber inputs. *Proceedings of the National Academy of Sciences of the United States of America*, *106*(7), 2389–2394. https://doi.org/10.1073/pnas.0808428106

Beudel, M., Galama, S., Leenders, K. L., & De Jong, B. M. (2008). Time estimation in Parkinson's disease and degenerative cerebellar disease. *NeuroReport*, *19*(10), 1055–1059. https://doi.org/10.1097/WNR.0b013e328303b7b9

Bhattacherjee, A., Djekidel, M. N., Chen, R., Chen, W., Tuesta, L. M., & Zhang, Y. (2019). Cell type-specific transcriptional programs in mouse prefrontal cortex during adolescence and addiction. *Nature Communications*, *10*(1). https://doi.org/10.1038/s41467-019-12054-3

Bickford, M. E. (2015). Thalamic circuit diversity: Modulation of the driver/modulator framework. *Frontiers in Neural Circuits*, *9*(JAN2016). https://doi.org/10.3389/fncir.2015.00086

Binda, F., Dorgans, K., Reibel, S., Sakimura, K., Kano, M., Poulain, B., & Isope, P. (2016). Inhibition promotes long-Term potentiation at cerebellar excitatory synapses. *Scientific Reports*, *6*(1), 1–12. https://doi.org/10.1038/srep33561

Birrell, J. M., & Brown, V. J. (2000). Medial frontal cortex mediates perceptual attentional set shifting in the rat.

Journal of Neuroscience, *20*(11), 4320–4324. https://doi.org/10.1523/jneurosci.20-11-04320.2000

Blakemore, S. J., Wolpert, D. M., & Frith, C. D. (1998). Central cancellation of self-produced tickle sensation. *Nature Neuroscience*, *1*(7), 635–640. https://doi.org/10.1038/2870

Bloedel, J. R., & Llinas, R. (1969). Neuronal interactions in frog cerebellum. *Journal of Neurophysiology*, *32*(6), 871–880. https://doi.org/10.1152/jn.1969.32.6.871

Blot, A., & Barbour, B. (2014). Ultra-rapid axon-axon ephaptic inhibition of cerebellar Purkinje cells by the pinceau. *Nature Neuroscience*, *17*(2), 289–295. https://doi.org/10.1038/nn.3624

Bodranghien, F., Bastian, A., Casali, C., Hallett, M., Louis, E. D., Manto, M., Mariën, P., Nowak, D. A., Schmahmann, J. D., Serrao, M., Steiner, K. M., Strupp, M., Tilikete, C., Timmann, D., & van Dun, K. (2016). Consensus Paper: Revisiting the Symptoms and Signs of Cerebellar Syndrome. In *Cerebellum* (Vol. 15, Issue 3, pp. 369–391). NIH Public Access. https://doi.org/10.1007/s12311-015-0687-3

Boehme, R., Uebele, V. N., Renger, J. J., & Pedroarena, C. (2011). Rebound excitation triggered by synaptic inhibition in cerebellar nuclear neurons is suppressed by selective T-type calcium channel block. *Journal of Neurophysiology*, *106*(5), 2653–2661. https://doi.org/10.1152/jn.00612.2011

Bostan, A. C., Dum, R. P., & Strick, P. L. (2010). The basal ganglia communicate with the cerebellum. *Proceedings of the National Academy of Sciences of the United States of America*, *107*(18), 8452–8456. https://doi.org/10.1073/pnas.1000496107

Bostan, A. C., Dum, R. P., & Strick, P. L. (2013). Cerebellar networks with the cerebral cortex and basal ganglia. In *Trends in Cognitive Sciences* (Vol. 17, Issue 5, pp. 241–254). https://doi.org/10.1016/j.tics.2013.03.003

Bostan, A. C., & Strick, P. L. (2018). *The basal ganglia and the cerebellum: nodes in an integrated network*. https://doi.org/10.1038/s41583

Boyden, E. S., Katoh, A., Pyle, J. L., Chatila, T. A., Tsien, R. W., & Raymond, J. L. L. (2006). Selective Engagement of Plasticity Mechanisms for Motor Memory Storage. *Neuron*, *51*(6), 823–834. https://doi.org/10.1016/j.neuron.2006.08.026

Brecher, G. A. (1932). Die Entstehung und biologische Bedeutung der subjektiven Zeiteinheit, - des Momentes. *Zeitschrift Für Vergleichende Physiologie*, *18*(1), 204–243. https://doi.org/10.1007/BF00338160

Breska, A., & Ivry, R. B. (2016). Taxonomies of timing: Where does the cerebellum fit in? In *Current Opinion in Behavioral Sciences* (Vol. 8, pp. 282–288). Elsevier Ltd. https://doi.org/10.1016/j.cobeha.2016.02.034

Breska, A., & Ivry, R. B. (2021). The human cerebellum is essential for modulating perceptual sensitivity based on temporal expectations. *ELife*, *10*, 1–11. https://doi.org/10.7554/eLife.66743

Brochu, G., Maler, L., & Hawkes, R. (1990). Zebrin II: A polypeptide antigen expressed selectively by purkinje cells reveals compartments in rat and fish cerebellum. *Journal of Comparative Neurology*, *291*(4), 538–552. https://doi.org/10.1002/cne.902910405

Brodal, P. (2014). Pontine Nuclei. In *Encyclopedia of the Neurological Sciences* (pp. 938–940). Academic Press. https://doi.org/10.1016/B978-0-12-385157-4.01173-8

Brodmann, K. (1909). Vergleichende Lokalisationslehre der Grosshirnrinde in ihren Prinzipien dargestelle auf Grund des Zellenbaues. In *The Journal of Nervous and Mental Disease* (Vol. 44). https://archive.org/details/b28062449/page/22/mode/2up

Bryant, J. L., Boughter, J. D., Gong, S., Ledoux, M. S., & Heck, D. H. (2010). Cerebellar cortical output encodes temporal aspects of rhythmic licking movements and is necessary for normal licking frequency. *European Journal of Neuroscience*, *32*(1), 41–52. https://doi.org/10.1111/j.1460-9568.2010.07244.x

Buchanan, T. W., Driscoll, D., Mowrer, S. M., Sollers, J. J., Thayer, J. F., Kirschbaum, C., & Tranel, D. (2010). Medial prefrontal cortex damage affects physiological and psychological stress responses differently in men and women. *Psychoneuroendocrinology*, *35*(1), 56–66. https://doi.org/10.1016/j.psyneuen.2009.09.006

Buckner, R. L., Krienen, F. M., Castellanos, A., Diaz, J. C., & Thomas Yeo, B. T. (2011). The organization of the human cerebellum estimated by intrinsic functional connectivity. *Journal of Neurophysiology*, *106*(5), 2322–2345. https://doi.org/10.1152/jn.00339.2011

Buhusi, C. V., & Meck, W. H. (2009). Relative time sharing: New findings and an extension of the resource allocation model of temporal processing. *Philosophical Transactions of the Royal Society B: Biological Sciences*, *364*(1525), 1875–1885. https://doi.org/10.1098/rstb.2009.0022

Buhusi, C. V, & Meck, W. H. (2005). What makes us tick? Functional and neural mechanisms of interval timing. In *Nature Reviews Neuroscience* (Vol. 6, Issue 10, pp. 755–765). https://doi.org/10.1038/nrn1764

Burkhalter, A. (2008). Many Specialists for Suppressing Cortical Excitation. In *Frontiers in Neuroscience* (Vol. 2, Issue 2, pp. 155–167). Frontiers Media SA. https://doi.org/10.3389/neuro.01.026.2008

Buzsáki, G., & Draguhn, A. (2004). Neuronal Oscillations in Cortical Networks. *Science*, *304*(June), 1926–1929. http://science.sciencemag.org/

Cajal, S. R. Y. (1894). The Croonian lecture.—La fine structure des centres nerveux. *Proceedings of the Royal Society of London*, *55*(331–335), 444–468. https://doi.org/10.1098/rspl.1894.0063

Cardin, J. A., Carlén, M., Meletis, K., Knoblich, U., Zhang, F., Deisseroth, K., Tsai, L. H., & Moore, C. I. (2009). Driving fast-spiking cells induces gamma rhythm and controls sensory responses. *Nature*, *459*(7247), 663–667. https://doi.org/10.1038/nature08002

Carlén, M. (2017). What constitutes the prefrontal cortex? In *Science* (Vol. 358, Issue 6362, pp. 478–482). American Association for the Advancement of Science. https://doi.org/10.1126/science.aan8868

Carta, I., Chen, C. H., Schott, A. L., Dorizan, S., & Khodakhah, K. (2019). Cerebellar modulation of the reward circuitry and social behavior. *Science*, *363*(6424), eaav0581. https://doi.org/10.1126/science.aav0581

Casanova, M. F., Buxhoeveden, D., & Gomez, J. (2003). Disruption in the Inhibitory Architecture of the Cell Minicolumn: Implications for Autisim. In *Neuroscientist* (Vol. 9, Issue 6, pp. 496–507). https://doi.org/10.1177/1073858403253552

Casini, L., & Vidal, F. (2011). The SMAs: Neural substrate of the temporal accumulator? *Frontiers in Integrative*

Neuroscience, *5*(5). https://doi.org/10.3389/fnint.2011.00035

Catani, M., & Sandrone, S. (2015). Brain Renaissance. In *Brain Renaissance*. Oxford University Press. https://doi.org/10.1093/med/9780199383832.001.0001

Cauller, L. J., & Connors, B. W. (1994). Synaptic physiology of horizontal afferents to layer I in slices of rat SI neocortex. *Journal of Neuroscience*, *14*(2), 751–762. https://doi.org/10.1523/jneurosci.14-02-00751.1994

Cerminara, N. L., & Apps, R. (2011). Behavioural significance of cerebellar modules. *Cerebellum*, *10*(3), 484–494. https://doi.org/10.1007/s12311-010-0209-2

Cerminara, N. L., Lang, E. J., Sillitoe, R. V, & Apps, R. (2015). Redefining the cerebellar cortex as an assembly of non-uniform Purkinje cell microcircuits. In *Nature Reviews Neuroscience* (Vol. 16, Issue 2, pp. 79–93). NIH Public Access. https://doi.org/10.1038/nrn3886

Chabrol, Francois P., Blot, A., & Mrsic-Flogel, T. D. (2019). Cerebellar Contribution to Preparatory Activity in Motor Neocortex. *Neuron*, *103*(3), 506-519.e4. https://doi.org/10.1016/j.neuron.2019.05.022

Chabrol, François P, Arenz, A., Wiechert, M. T., Margrie, T. W., & Digregorio, D. A. (2015). Synaptic diversity enables temporal coding of coincident multisensory inputs in single neurons. *Nature Neuroscience*, *18*(5), 718–727. https://doi.org/10.1038/nn.3974

Chan-Palay, V. (1977). The Cerebellar Dentate Nucleus. In *Cerebellar Dentate Nucleus* (pp. 1–24). Springer Berlin Heidelberg. https://doi.org/10.1007/978-3-642-66498-4_1

Chapman, P. F., Steinmetz, J. E., Sears, L. L., & Thompson, R. F. (1990). Effects of lidocaine injection in the interpositus nucleus and red nucleus on conditioned behavioral and neuronal responses. *Brain Research*, *537*(1–2), 149–156. https://doi.org/10.1016/0006-8993(90)90351-B

Chaumont, J., Guyon, N., Valera, A., Dugué, G. P., Popa, D., Marcaggi, P., Gautheron, V., Reibel-Foisset, S., Dieudonné, S., Stephan, A., Barrot, M., Cassel, J.-C., Dupont, J.-L., Doussau, F., Poulain, B., Selimi, F., Léna, C., & Isope, P. (2013). Clusters of cerebellar Purkinje cells control their afferent climbing fiber discharge. *Proceedings of the National Academy of Sciences of the United States of America*, *110*(40), 16223–16228. https://doi.org/10.1073/pnas.1302310110

Chen, C. H., Fremont, R., Arteaga-Bracho, E. E., & Khodakhah, K. (2014). Short latency cerebellar modulation of the basal ganglia. *Nature Neuroscience*, *17*(12), 1767–1775. https://doi.org/10.1038/nn.3868

Chester, S. C., & Reznick, B. R. (1987). Ataxia after severe head injury: The pathological substrate. *Annals of Neurology*, *22*(1), 77–79. https://doi.org/10.1002/ana.410220117

Church, R. M., & Broadbent, H. A. (1990). Alternative representations of time, number, and rate. *Cognition*, *37*(1–2), 55–81. https://doi.org/10.1016/0010-0277(90)90018-F

Cicirata, F., Serapide, M. F., Parenti, R., Pantò, M. R., Zappalà, A., Nicotra, A., & Cicero, D. (2005). The basilar pontine nuclei and the nucleus reticularis tegmenti pontis subserve distinct cerebrocerebellar pathways. In *Progress in Brain Research* (Vol. 148, pp. 259–282). Elsevier. https://doi.org/10.1016/S0079-

6123(04)48021-2

Coffman, K. A., Dum, R. P., & Strick, P. L. (2011). Cerebellar vermis is a target of projections from the motor areas in the cerebral cortex. *Proceedings of the National Academy of Sciences of the United States of America*, *108*(38), 16068–16073. https://doi.org/10.1073/pnas.1107904108

Collins, D. P., Anastasiades, P. G., Marlin, J. J., & Carter, A. G. (2018). Reciprocal Circuits Linking the Prefrontal Cortex with Dorsal and Ventral Thalamic Nuclei. *Neuron*, *98*(2), 366-379.e4. https://doi.org/10.1016/j.neuron.2018.03.024

Colotla, V. A., & Bach-Y-Rita, P. (2002). Shepherd Ivory Franz: His contributions to neuropsychology and rehabilitation. *Cognitive, Affective and Behavioral Neuroscience*, *2*(2), 141–148. https://doi.org/10.3758/CABN.2.2.141

Constantinidis, C., Williams, G. V., & Goldman-Rakic, P. S. (2002). A role for inhibition in shaping the temporal flow of information in prefrontal cortex. *Nature Neuroscience*, *5*(2), 175–180. https://doi.org/10.1038/nn799

Cossart, R., Aronov, D., & Yuste, R. (2003). Attractor dynamics of network UP states in the neocortex. *Nature*, *423*(6937), 283–288. https://doi.org/10.1038/nature01614

Coull, Jennifer T., Cotti, J., & Vidal, F. (2016). Differential roles for parietal and frontal cortices in fixed versus evolving temporal expectations: Dissociating prior from posterior temporal probabilities with fMRI. *NeuroImage*, *141*, 40–51. https://doi.org/10.1016/j.neuroimage.2016.07.036

Coull, JT T., & Nobre, A. C. (2008). Dissociating explicit timing from temporal expectation with fMRI. In *Current Opinion in Neurobiology* (Vol. 18, Issue 2, pp. 137–144). https://doi.org/10.1016/j.conb.2008.07.011

Cowan, N. (1988). Evolving Conceptions of Memory Storage, Selective Attention, and Their Mutual Constraints Within the Human Information-Processing System. *Psychological Bulletin*, *104*(2), 163–191. https://doi.org/10.1037/0033-2909.104.2.163

Cravo, A. M., Rohenkohl, G., Wyart, V., & Nobre, A. C. (2013). Temporal expectation enhances contrast sensitivity by phase entrainment of low-frequency oscillations in visual cortex. *Journal of Neuroscience*, *33*(9), 4002–4010. https://doi.org/10.1523/JNEUROSCI.4675-12.2013

D'Angelo, E., Solinas, S., Mapelli, J., Gandolfi, D., Mapelli, L., & Prestori, F. (2013). The cerebellar Golgi cell and spatiotemporal organization of granular layer activity. In *Frontiers in Neural Circuits* (Vol. 0, Issue APR 2013, p. 93). Frontiers. https://doi.org/10.3389/fncir.2013.00093

Darmohray, D. M., Jacobs, J. R., Marques, H. G., & Carey, M. R. (2019). Spatial and Temporal Locomotor Learning in Mouse Cerebellum. *Neuron*, *102*(1), 217-231.e4. https://doi.org/10.1016/j.neuron.2019.01.038

de Solages, C., Szapiro, G., Brunel, N., Hakim, V., Isope, P., Buisseret, P., Rousseau, C., Barbour, B., & Léna, C. (2008). High-Frequency Organization and Synchrony of Activity in the Purkinje Cell Layer of the Cerebellum. *Neuron*, *58*(5), 775–788. https://doi.org/10.1016/j.neuron.2008.05.008

DeFelipe, J., & Fariñas, I. (1992). The pyramidal neuron of the cerebral cortex: Morphological and chemical characteristics of the synaptic inputs. In *Progress in Neurobiology* (Vol. 39, Issue 6, pp. 563–607). Prog Neurobiol. https://doi.org/10.1016/0301-0082(92)90015-7

Dehaene, S. (2003). The neural basis of the Weber-Fechner law: A logarithmic mental number line. In *Trends in Cognitive Sciences* (Vol. 7, Issue 4, pp. 145–147). https://doi.org/10.1016/S1364-6613(03)00055-X

Demirtas-Tatlidede, A., Freitas, C., Cromer, J. R., Safar, L., Ongur, D., Stone, W. S., Seidman, L. J., Schmahmann, J. D., & Pascual-Leone, A. (2010). Safety and proof of principle study of cerebellar vermal theta burst stimulation in refractory schizophrenia. *Schizophrenia Research*, *124*(1–3), 91–100. https://doi.org/10.1016/j.schres.2010.08.015

Denker, M., Yegenoglu, A., & Grün, S. (2018). Collaborative HPC-enabled workflows on the HBP Collaboratory using the Elephant framework. *Neuroinformatics 2018*, 19.

Diedrichsen, J., King, M., Hernandez-Castillo, C., Sereno, M., & Ivry, R. B. (2019). Universal Transform or Multiple Functionality? Understanding the Contribution of the Human Cerebellum across Task Domains. In *Neuron* (Vol. 102, Issue 5, pp. 918–928). https://doi.org/10.1016/j.neuron.2019.04.021

Dieudonné, S. (1998). Submillisecond kinetics and low efficacy of parallel fibre-Golgi cell synaptic currents in the rat cerebellum. *Journal of Physiology*, *510*(3), 845–866. https://doi.org/10.1111/j.1469-7793.1998.845bj.x

Donahue, C. J., Glasser, M. F., Preuss, T. M., Rilling, J. K., & Van Essen, D. C. (2018). Quantitative assessment of prefrontal cortex in humans relative to nonhuman primates. *Proceedings of the National Academy of Sciences of the United States of America*, *115*(22), E5183–E5192. https://doi.org/10.1073/pnas.1721653115

Donnelly, N. A., Paulsen, O., Robbins, T. W., & Dalley, J. W. (2015). Ramping single unit activity in the medial prefrontal cortex and ventral striatum reflects the onset of waiting but not imminent impulsive actions. *European Journal of Neuroscience*, *41*(12), 1524–1537. https://doi.org/10.1111/ejn.12895

Eccles, J. C., Llinás, R., & Sasaki, K. (1966). The excitatory synaptic action of climbing fibres on the Purkinje cells of the cerebellum. *The Journal of Physiology*, *182*(2), 268–296. https://doi.org/10.1113/jphysiol.1966.sp007824

Eccles, John C., Ito, M., & Szentágothai, J. (1967). The Cerebellum as a Neuronal Machine. In *The Cerebellum as a Neuronal Machine*. Springer Berlin Heidelberg. https://doi.org/10.1007/978-3-662-13147-3

Eling, P., & Finger, S. (2019). Franz joseph gall on the cerebellum as the organ for the reproductive drive. In *Frontiers in Neuroanatomy* (Vol. 13, p. 40). Frontiers. https://doi.org/10.3389/fnana.2019.00040

Elliott, M. A., Shi, Z., & Kelly, S. D. (2006). A moment to reflect upon perceptual synchrony. In *Journal of Cognitive Neuroscience* (Vol. 18, Issue 10, pp. 1663–1665). https://doi.org/10.1162/jocn.2006.18.10.1663

Elliott, M. A., Shi, Z., & Sürer, F. (2007). The effects of subthreshold synchrony on the perception of simultaneity. *Psychological Research*, *71*(6), 687–693. https://doi.org/10.1007/s00426-006-0057-3

Filho, R. V. T. (2020). Phineas gage's great legacy. *Dementia e Neuropsychologia*, *14*(4), 419–421. https://doi.org/10.1590/1980-57642020dn14-040013

Finger, S. (2004). Paul Broca (1824-1880). *Journal of Neurology*, *251*(6), 769–770. https://doi.org/10.1007/s00415-004-0456-6

Fluorens, P. (1824). *Recherches expérimentales sur les propriétés et les fonctions du système nerveux, dans les animaux vertébrés.* https://www.worldcat.org/title/recherches-experimentales-sur-les-proprietes-et-les-fonctions-du-systeme-nerveux-dans-les-animaux-vertebres/oclc/29167647

Franklin, B. J., & Paxinos, G. (2007). The mouse brain in stereotaxic coordinates. Third Edition. In *Academic Press*. https://doi.org/10.1016/B978-0-12-374247-6.50004-3

Freemon, F. R. (1994). Galen's ideas on neurological function. *Journal of the History of the Neurosciences*, *3*(4), 263–271. https://doi.org/10.1080/09647049409525619

Fries, P. (2005). A mechanism for cognitive dynamics: Neuronal communication through neuronal coherence. *Trends in Cognitive Sciences*, *9*(10), 474–480. https://doi.org/10.1016/j.tics.2005.08.011

Frith, C. D., & Frith, U. (1999). Interacting minds - A biological basis. In *Science* (Vol. 286, Issue 5445, pp. 1692–1695). Science. https://doi.org/10.1126/science.286.5445.1692

Fujita, H., Kodama, T., & du Lac, S. (2020). Modular output circuits of the fastigial nucleus mediate diverse motor and nonmotor functions of the cerebellar vermis. *ELife*, 1–36. https://doi.org/10.1101/2020.04.23.047100

Fuster, J. M. (2001). The Prefrontal Cortex—An Update: Time Is of the Essence. In *Neuron* (Vol. 30).

Fuster, J. M. (2002). Frontal lobe and cognitive development. In *Journal of Neurocytology* (Vol. 31, Issues 3-5 SPEC. ISS., pp. 373–385). J Neurocytol. https://doi.org/10.1023/A:1024190429920

Fuster, J. M. (2006). The cognit: A network model of cortical representation. *International Journal of Psychophysiology*, *60*(2), 125–132. https://doi.org/10.1016/j.ijpsycho.2005.12.015

Fuster, J. M. (2008). The Prefrontal Cortex. In *The Prefrontal Cortex*. https://doi.org/10.1016/B978-0-12-373644-4.X0001-1

Gao, Z., Davis, C., Thomas, A. M., Economo, M. N., Abrego, A. M., Svoboda, K., De Zeeuw, C. I., & Li, N. (2018). A cortico-cerebellar loop for motor planning. *Nature*, *563*(7729), 113–116. https://doi.org/10.1038/s41586-018-0633-x

Garcia, S., Guarino, D., Jaillet, F., Jennings, T., Pröpper, R., Rautenberg, P. L., Rodgers, C. C., Sobolev, A., Wachtler, T., Yger, P., & Davison, A. P. (2014). Neo: An object model for handling electrophysiology data in multiple formats. *Frontiers in Neuroinformatics*, *8*(FEB), 10. https://doi.org/10.3389/fninf.2014.00010

Geiser, E., Zaehle, T., Jancke, L., & Meyer, M. (2008). The neural correlate of speech rhythm as evidenced by metrical speech processing. *Journal of Cognitive Neuroscience*, *20*(3), 541–552. https://doi.org/10.1162/jocn.2008.20029

Gibbon, J. (1977). Scalar expectancy theory and Weber's law in animal timing. *Psychological Review*, *84*(3),

279–325. https://doi.org/10.1037/0033-295X.84.3.279

Gibbon, J., Church, R. M., & Meck, W. H. (1984). Scalar Timing in Memory. *Annals of the New York Academy of Sciences*, *423*(1), 52–77. https://doi.org/10.1111/j.1749-6632.1984.tb23417.x

Giersch, A., Lalanne, L., Corves, C., Seubert, J., Shi, Z., Foucher, J., & Elliott, M. A. (2009). Extended visual simultaneity thresholds in patients with schizophrenia. *Schizophrenia Bulletin*, *35*(4), 816–825. https://doi.org/10.1093/schbul/sbn016

Giersch, A., Lalanne, L., & Isope, P. (2016). Implicit Timing as the Missing Link between Neurobiological and Self Disorders in Schizophrenia? *Frontiers in Human Neuroscience*, *10*, 303. https://doi.org/10.3389/fnhum.2016.00303

Giersch, A., Lalanne, L., van Assche, M., & Elliott, M. A. (2013). On disturbed time continuity in schizophrenia: An elementary impairment in visual perception? *Frontiers in Psychology*, *4*(MAY), 1–10. https://doi.org/10.3389/fpsyg.2013.00281

Giersch, A., Poncelet, P. E., Capa, R. L., Martin, B., Duval, C. Z., Curzietti, M., Hoonacker, M., van Assche, M., & Lalanne, L. (2015). Disruption of information processing in schizophrenia: The time perspective. *Schizophrenia Research: Cognition*, *2*(2), 78–83. https://doi.org/10.1016/j.scog.2015.04.002

Giguere, M., & Goldman-Rakic, P. S. (1988). Mediodorsal nucleus: Areal, laminar, and tangential distribution of afferents and efferents in the frontal lobe of rhesus monkeys. *Journal of Comparative Neurology*, *277*(2), 195–213. https://doi.org/10.1002/cne.902770204

Gisiger, T., & Boukadoum, M. (2011). Mechanisms gating the flow of information in the cortex: What they might look like and what their uses may be. *Frontiers in Computational Neuroscience*, *5*, 1. https://doi.org/10.3389/fncom.2011.00001

Glickstein, M., Strata, P., & Voogd, J. (2009). Cerebellum: history. *Neuroscience*, *162*(3), 549–559. https://doi.org/10.1016/j.neuroscience.2009.02.054

Glickstein, Mitch. (2006). Golgi and Cajal: The neuron doctrine and the 100th anniversary of the 1906 Nobel Prize. In *Current Biology* (Vol. 16, Issue 5, pp. R147–R151). Elsevier. https://doi.org/10.1016/j.cub.2006.02.053

Goldman-Rakic, P. S., & Porrino, L. J. (1985). The primate mediodorsal (MD) nucleus and its projection to the frontal lobe. *Journal of Comparative Neurology*, *242*(4), 535–560. https://doi.org/10.1002/cne.902420406

Gooch, C. M., Wiener, M., Wencil, E. B., & Coslett, H. B. (2010). Interval timing disruptions in subjects with cerebellar lesions. *Neuropsychologia*, *48*(4), 1022–1031. https://doi.org/10.1016/j.neuropsychologia.2009.11.028

Gross, D., & Schäfer, G. (2011). Egas Moniz (1874-1955) and the “invention” of modern psychosurgery: A historical and ethical reanalysis under special consideration of Portuguese original sources. *Neurosurgical Focus*, *30*(2), E8. https://doi.org/10.3171/2010.10.FOCUS10214

Guell, X., D'Mello, A. M., Hubbard, N. A., Romeo, R. R., Gabrieli, J. D. E., Whitfield-Gabrieli, S., Schmahmann, J. D., & Anteraper, S. A. (2020). Functional Territories of Human Dentate Nucleus. *Cerebral Cortex*, *30*(4), 2401–2417. https://doi.org/10.1093/cercor/bhz247

Guell, X., Gabrieli, J. D. E., & Schmahmann, J. D. (2018). Embodied cognition and the cerebellum: Perspectives from the Dysmetria of Thought and the Universal Cerebellar Transform theories. *Cortex*, *100*, 140–148. https://doi.org/10.1016/j.cortex.2017.07.005

Guillery, R. W. (1995). Anatomical evidence concerning the role of the thalamus in corticocortical communication: a brief review. *Journal of Anatomy*, *187 (Pt 3*(Pt 3), 583–592. /pmc/articles/PMC1167461/?report=abstract

Guldin, W. O., Pritzel, M., & Markowitsch, H. J. (1981). Prefrontal cortex of the mouse defined as cortical projection area of the thalamic mediodorsal nucleus. *Brain, Behavior and Evolution*, *19*(3–4), 93–107. https://doi.org/10.1159/000121636

Guo, C., Rudolph, S., Neuwirth, M. E., & Regehr, W. G. (2021). Purkinje cell outputs selectively inhibit a subset of unipolar brush cells in the input layer of the cerebellar cortex. *ELife*, *10*. https://doi.org/10.7554/elife.68802

Gurnani, H., & Silver, R. A. (2021). Multidimensional population activity in an electrically coupled inhibitory circuit in the cerebellar cortex. *Neuron*, *109*(10), 1739-1753.e8. https://doi.org/10.1016/j.neuron.2021.03.027

Harris, C. R., Millman, K. J., van der Walt, S. J., Gommers, R., Virtanen, P., Cournapeau, D., Wieser, E., Taylor, J., Berg, S., Smith, N. J., Kern, R., Picus, M., Hoyer, S., van Kerkwijk, M. H., Brett, M., Haldane, A., del Río, J. F., Wiebe, M., Peterson, P., … Oliphant, T. E. (2020). Array programming with NumPy. In *Nature* (Vol. 585, Issue 7825, pp. 357–362). Nature Publishing Group. https://doi.org/10.1038/s41586-020-2649-2

Harvey, R. J., & Napper, R. M. A. (1991). Quantitatives studies on the mammalian cerebellum. In *Progress in Neurobiology* (Vol. 36, Issue 6, pp. 437–463). https://doi.org/10.1016/0301-0082(91)90012-P

Hawkes, R., & Leclerc, N. (1987). Antigenic map of the rat cerebellar cortex: The distribution of parasagittal bands as revealed by monoclonal anti-purkinje cell antibody mabQ113. *Journal of Comparative Neurology*, *256*(1), 29–41. https://doi.org/10.1002/cne.902560104

Heck, D. H., Thach, W. T., & Keating, J. G. (2007). On-beam synchrony in the cerebellum as the mechanism for the timing and coordination of movement. *Proceedings of the National Academy of Sciences of the United States of America*, *104*(18), 7658–7663. https://doi.org/10.1073/pnas.0609966104

Heffley, W., & Hull, C. (2019). Classical conditioning drives learned reward prediction signals in climbing fibers across the lateral cerebellum. *ELife*, *8*. https://doi.org/10.7554/elife.46764

Heffley, W., Song, E. Y., Xu, Z., Taylor, B. N., Hughes, M. A., McKinney, A., Joshua, M., & Hull, C. (2018). Coordinated cerebellar climbing fiber activity signals learned sensorimotor predictions. *Nature Neuroscience*, *21*(10), 1431–1441. https://doi.org/10.1038/s41593-018-0228-8

Herbst, S. K., & Obleser, J. (2017). Implicit variations of temporal predictability: Shaping the neural oscillatory

and behavioural response. *Neuropsychologia*, *101*, 141–152. https://doi.org/10.1016/j.neuropsychologia.2017.05.019

Herbst, S. K., & Obleser, J. (2019). Implicit temporal predictability enhances pitch discrimination sensitivity and biases the phase of delta oscillations in auditory cortex. *NeuroImage*, *203*. https://doi.org/10.1016/j.neuroimage.2019.116198

Herzfeld, D. J., Hall, N. J., Tringides, M., & Lisberger, S. G. (2020). Principles of operation of a cerebellar learning circuit. *ELife*, *9*. https://doi.org/10.7554/eLife.55217

Herzfeld, D. J., Kojima, Y., Soetedjo, R., & Shadmehr, R. (2018). Encoding of error and learning to correct that error by the Purkinje cells of the cerebellum. *Nature Neuroscience*, *21*(5), 736–743. https://doi.org/10.1038/s41593-018-0136-y

Heskje, J., Heslin, K., De Corte, B. J., Walsh, K. P., Kim, Y., Han, S., Carlson, E. S., & Parker, K. L. (2020). Cerebellar D1DR-expressing neurons modulate the frontal cortex during timing tasks. In *Neurobiology of Learning and Memory* (Vol. 170, p. 107067). Academic Press Inc. https://doi.org/10.1016/j.nlm.2019.107067

Holmes, G. (1917). The symptoms of acute cerebellar injuries due to gunshot injuries. *Brain*, *40*(4), 461–535. https://doi.org/10.1093/brain/40.4.461

Hoshi, E., Tremblay, L., Féger, J., Carras, P. L., & Strick, P. L. (2005). The cerebellum communicates with the basal ganglia. *Nature Neuroscience*, *8*(11), 1491–1493. https://doi.org/10.1038/nn1544

Hubel, D. H., Wiesel, T. N., & Stryker, M. P. (1977). Orientation columns in macaque monkey visual cortex demonstrated by the 2-deoxyglucose autoradiographic technique. *Nature*, *269*(5626), 328–330. https://doi.org/10.1038/269328a0

Hunter, J. D. (2007). Matplotlib: A 2D graphics environment. *Computing in Science and Engineering*, *9*(3), 90–95. https://doi.org/10.1109/MCSE.2007.55

Husson, Z., Rousseau, C. V., Broll, I., Zeilhofer, H. U., & Dieudonné, S. (2014). Differential GABAergic and glycinergic inputs of inhibitory interneurons and purkinje cells to principal cells of the cerebellar nuclei. *Journal of Neuroscience*, *34*(28), 9418–9431. https://doi.org/10.1523/JNEUROSCI.0401-14.2014

Ichinohe, N., Mori, F., & Shoumura, K. (2000). A di-synaptic projection from the lateral cerebellar nucleus to the laterodorsal part of the striatum via the central lateral nucleus of the thalamus in the rat. *Brain Research*, *880*(1–2), 191–197. https://doi.org/10.1016/S0006-8993(00)02744-X

Ishikawa, T., Shimuta, M., & Häuser, M. (2015). Multimodal sensory integration in single cerebellar granule cells in vivo. *ELife*, *4*(DECEMBER2015). https://doi.org/10.7554/eLife.12916

Isope, P., & Barbour, B. (2002). Properties of unitary granule cell→Purkinje cell synapses in adult rat cerebellar slices. *Journal of Neuroscience*, *22*(22), 9668–9678. https://doi.org/10.1523/jneurosci.22-22-09668.2002

Ito, M., Yoshida, M., & Obata, K. (1964). Monosynaptic inhibition of the intracerebellar nuclei induced from the cerebellar cortex. *Experientia*, *20*(10), 575–576. https://doi.org/10.1007/BF02150304

Ito, Masao. (1984). The Cerebellum and Neural Control. In *Science*. Raven Press. https://doi.org/10.1126/science.229.4713.547

Ito, Masao. (2008). Control of mental activities by internal models in the cerebellum. *Natue Reviews Neuroscience*, *Box 1*. www.nature.com/reviews/neuro

Ito, Masao, & Kano, M. (1982). Long-lasting depression of parallel fiber-Purkinje cell transmission induced by conjunctive stimulation of parallel fibers and climbing fibers in the cerebellar cortex. *Neuroscience Letters*, *33*(3), 253–258. https://doi.org/10.1016/0304-3940(82)90380-9

Jacobi, H., Faber, J., Timmann, D., & Klockgether, T. (2021). Update cerebellum and cognition. *Journal of Neurology*, *1*, 1–5. https://doi.org/10.1007/s00415-021-10486-w

Jacobsen, C. F., & Nissen, H. W. (1937). Studies of cerebral function in primates. IV. The effects of frontal lobe lesions on the delayed alternation habit in monkeys. *Journal of Comparative Psychology*, *23*(1), 101–112. https://doi.org/10.1037/h0056632

Jansen, J., & Brodal, A. (1940). Experimental studies on the intrinsic fibers of the cerebellum. II. The cortico-nuclear projection. *Journal of Comparative Neurology*, *73*(2), 267–321. https://doi.org/10.1002/cne.900730204

Janssen, P., & Shadlen, M. N. (2005). A representation of the hazard rate of elapsed time in macaque area LIP. *Nature Neuroscience*, *8*(2), 234–241. https://doi.org/10.1038/nn1386

Jarovi, J., Volle, J., Yu, X., Guan, L., & Takehara-Nishiuchi, K. (2018). Prefrontal theta oscillations promote selective encoding of behaviorally relevant events. *ENeuro*, *5*(6). https://doi.org/10.1523/ENEURO.0407-18.2018

Jayadev, S., & Bird, T. D. (2013). Hereditary ataxias: Overview. In *Genetics in Medicine* (Vol. 15, Issue 9, pp. 673–683). Nature Publishing Group. https://doi.org/10.1038/gim.2013.28

Joel, D., Weiner, I., & Feldon, J. (1997). Electrolytic lesions of the medial prefrontal cortex in rats disrupt performance on an analog of the Wisconsin Card Sorting Test, but do not disrupt latent inhibition: Implications for animal models of schizophrenia. *Behavioural Brain Research*, *85*(2), 187–201. https://doi.org/10.1016/S0166-4328(97)87583-3

Kamali, A., Kramer, L. A., Frye, R. E., Butler, I. J., & Hasan, K. M. (2010). Diffusion tensor tractography of the human brain cortico-ponto-cerebellar pathways: a quantitative preliminary study. *Journal of Magnetic Resonance Imaging : JMRI*, *32*(4), 809–817. https://doi.org/10.1002/jmri.22330

Kandel, E., Schwartz, J. H., Jessell, T. M., Siegelbaum, S. A., & Hudspeth, A. (2013). *Principles of Neural Science, 5th ed*. The McGraw-Hill Companies, Inc. https://doi.org/10.1128/AAC.03728-14

Kawaguchi, Y., & Kubota, Y. (1997). GABAergic cell subtypes and their synaptic connections in rat frontal cortex. *Cerebral Cortex*, *7*(6), 476–486. https://doi.org/10.1093/cercor/7.6.476

Kawai, R., Markman, T., Poddar, R., Ko, R., Fantana, A. L., Dhawale, A. K., Kampff, A. R., & Ölveczky, B. P. (2015). Motor Cortex Is Required for Learning but Not for Executing a Motor Skill. *Neuron*, *86*(3), 800–

812. https://doi.org/10.1016/j.neuron.2015.03.024

Kebschul, J. M., Richman, E. B., Ringach, N., Friedmann, D., Albarran, E., Kolluru, S. S., Jones, R. C., Allen, W. E., Wang, Y., Cho, S. W., Zhou, H., Ding, J. B., Chang, H. Y., Deisseroth, K., Quake, S. R., & Luo, L. (2020). Cerebellar nuclei evolved by repeatedly duplicating a conserved cell-type set. *Science*, *370*(6523). https://doi.org/10.1126/science.abd5059

Kelly, E., Meng, F., Fujita, H., Morgado, F., Kazemi, Y., Rice, L. C., Ren, C., Escamilla, C. O., Gibson, J. M., Sajadi, S., Pendry, R. J., Tan, T., Ellegood, J., Albert Basson, M., Blakely, R. D., Dindot, S. V., Golzio, C., Hahn, M. K., Katsanis, N., … Tsai, P. T. (2020). Regulation of autism-relevant behaviors by cerebellar–prefrontal cortical circuits. *Nature Neuroscience*. https://doi.org/10.1038/s41593-020-0665-z

Kelly, R. M., & Strick, P. L. (2003). Cerebellar loops with motor cortex and prefrontal cortex of a nonhuman primate. *Journal of Neuroscience*, *23*(23), 8432–8444. https://doi.org/10.1523/jneurosci.23-23-08432.2003

Kim, H., Ährlund-Richter, S., Wang, X., Deisseroth, K., & Carlén, M. (2016). Prefrontal Parvalbumin Neurons in Control of Attention. *Cell*, *164*(1–2), 208–218. https://doi.org/10.1016/j.cell.2015.11.038

Kim, J., Jung, A. H., Byun, J., Jo, S., & Jung, M. W. (2009). Inactivation of medial prefrontal cortex impairs time interval discrimination in rats. *Frontiers in Behavioral Neuroscience*, *3*(NOV), 38. https://doi.org/10.3389/neuro.08.038.2009

Klein, J. C., Rushworth, M. F. S., Behrens, T. E. J., Mackay, C. E., de Crespigny, A. J., D'Arceuil, H., & Johansen-Berg, H. (2010). Topography of connections between human prefrontal cortex and mediodorsal thalamus studied with diffusion tractography. *NeuroImage*, *51*(2), 555–564. https://doi.org/10.1016/j.neuroimage.2010.02.062

Koch, G., Oliveri, M., Torriero, S., & Caltagirone, C. (2003). Underestimation of time perception after repetitive transcranial magnetic stimulation. *Neurology*, *60*(11), 1844–1846. https://doi.org/10.1212/WNL.60.11.1844

Koekkoek, S. K. E., Hulscher, H. C., Dortland, B. R., Hensbroek, R. A., Elgersma, Y., Ruigrok, T. J. H., & De Zeeuw, C. I. (2003). Cerebellar LTD and learning-dependent timing of conditioned eyelid responses. *Science*, *301*(5640), 1736–1739. https://doi.org/10.1126/science.1088383

Koene, R. A., & Hasselmo, M. E. (2005). An integrate-and-fire model of prefrontal cortex neuronal activity during performance of goal-directed decision making. *Cerebral Cortex*, *15*(12), 1964–1981. https://doi.org/10.1093/cercor/bhi072

Konstantoudaki, X., Papoutsi, A., Chalkiadaki, K., Poirazi, P., & Sidiropoulou, K. (2014). Modulatory effects of inhibition on persistent activity in a cortical microcircuit model. *Frontiers in Neural Circuits*, *8*(JAN). https://doi.org/10.3389/fncir.2014.00007

Kopell, N. J., Gritton, H. J., Whittington, M. A., & Kramer, M. A. (2014). Beyond the connectome: The dynome. In *Neuron* (Vol. 83, Issue 6, pp. 1319–1328). NIH Public Access. https://doi.org/10.1016/j.neuron.2014.08.016

Korn, H., & Axelrad, H. (1980). Electrical inhibition of Purkinje cells in the cerebellum of the rat (field effect/parallel fibers/basket cells/neuronal synchronization). In *Neurobiology* (Vol. 77, Issue 10).

Kostadinov, D., Beau, M., Pozo, M. B., & Häusser, M. (2019). Predictive and reactive reward signals conveyed by climbing fiber inputs to cerebellar Purkinje cells. *Nature Neuroscience*, *22*(6), 950–962. https://doi.org/10.1038/s41593-019-0381-8

Kozareva, V., Martin, C., Osorno, T., Rudolph, S., Guo, C., Vanderburg, C., Nadaf, N., Regev, A., Regehr, W., & Macosko, E. (2020). A transcriptomic atlas of the mouse cerebellum reveals regional specializations and novel cell types. *BioRxiv*, 2020.03.04.976407. https://doi.org/10.1101/2020.03.04.976407

Krienen, F. M., & Buckner, R. L. (2009). Segregated fronto-cerebellar circuits revealed by intrinsic functional connectivity. *Cerebral Cortex*, *19*(10), 2485–2497. https://doi.org/10.1093/cercor/bhp135

Krimer, L. S., & Goldman-Rakic, P. S. (2001). Prefrontal microcircuits: Membrane properties and excitatory input of local, medium, and wide arbor interneurons. *Journal of Neuroscience*, *21*(11), 3788–3796. https://doi.org/10.1523/jneurosci.21-11-03788.2001

Kronland-Martinet, R., Morlet, J., & Grossmann, A. (1987). ANALYSIS OF SOUND PATTERNS THROUGH WAVELET TRANSFORMS. *International Journal of Pattern Recognition and Artificial Intelligence*, *01*(02), 273–302. https://doi.org/10.1142/s0218001487000205

Kuramoto, E., Pan, S., Furuta, T., Tanaka, Y. R., Iwai, H., Yamanaka, A., Ohno, S., Kaneko, T., Goto, T., & Hioki, H. (2017). Individual mediodorsal thalamic neurons project to multiple areas of the rat prefrontal cortex: A single neuron-tracing study using virus vectors. *Journal of Comparative Neurology*, *525*(1), 166–185. https://doi.org/10.1002/cne.24054

Laidi, C., Levenes, C., Suarez-Perez, A., Février, C., Durand, F., Bouaziz, N., & Januel, D. (2020). Cognitive Impact of Cerebellar Non-invasive Stimulation in a Patient With Schizophrenia. *Frontiers in Psychiatry*, *11*(March), 1–7. https://doi.org/10.3389/fpsyt.2020.00174

Lainé, J., & Axelrad, H. (2002). Extending the cerebellar Lugaro cell class. *Neuroscience*, *115*(2), 363–374. https://doi.org/10.1016/S0306-4522(02)00421-9

Lalanne, L., Van Assche, M., & Giersch, A. (2012). When predictive mechanisms go wrong: Disordered visual synchrony thresholds in schizophrenia. *Schizophrenia Bulletin*, *38*(3), 506–513. https://doi.org/10.1093/schbul/sbq107

Larry, N., Yarkoni, M., Lixenberg, A., & Joshua, M. (2019). Cerebellar climbing fibers encode expected reward size. *ELife*, *8*. https://doi.org/10.7554/eLife.46870

Larsell, O. (1937). The cerebellum: A review and interpretation. *Archives of Neurology And Psychiatry*, *38*(3), 580–607. https://doi.org/10.1001/archneurpsyc.1937.02260210146011

Laubach, M., Amarante, L. M., Swanson, T. K., & White, S. R. (2018). What, if anything, is rodent prefrontal cortex? *Eneuro*, *5*(5), ENEURO.0315-18.2018. https://doi.org/10.1523/ENEURO.0315-18.2018

Lee, B. C., Choi, J., & Martin, B. J. (2020). Roles of the prefrontal cortex in learning to time the onset of pre-

existing motor programs. *PLoS ONE*, *15*(11 November), e0241562. https://doi.org/10.1371/journal.pone.0241562

Leergaard, T. B. (2003). Clustered and laminar topographic patterns in rat cerebro-pontine pathways. In *Anatomy and Embryology* (Vol. 206, Issue 3, pp. 149–162). Springer Verlag. https://doi.org/10.1007/s00429-002-0272-7

Leergaard, T. B., & Bjaalie, J. G. (2007). Topography of the complete corticopontine projection: From experiments to principal Maps. *Frontiers in Neuroscience*, *1*(1), 211–223. https://doi.org/10.3389/neuro.01.1.1.016.2007

Leergaard, T. B., Lillehaug, S., De Schutter, E., Bower, J. M., & Bjaalie, J. G. (2006). Topographical organization of pathways from somatosensory cortex through the pontine nuclei to tactile regions of the rat cerebellar hemispheres. *European Journal of Neuroscience*, *24*(10), 2801–2812. https://doi.org/10.1111/j.1460-9568.2006.05150.x

Leiner, H. C., Leiner, A. L., & Dow, R. S. (1991). The human cerebro-cerebellar system: its computing, cognitive, and language skills. *Behavioural Brain Research*, *44*(2), 113–128. https://doi.org/10.1016/S0166-4328(05)80016-6

Lewis, B. L., & O'Donnell, P. (2000). Ventral tegmental area afferents to the prefrontal cortex maintain membrane potential "up" states in pyramidal neurons via D1 dopamine receptors. *Cerebral Cortex*, *10*(12), 1168–1175. https://doi.org/10.1093/cercor/10.12.1168

Lewis, P. A., & Miall, R. C. (2003a). Distinct systems for automatic and cognitively controlled time measurement: Evidence from neuroimaging. In *Current Opinion in Neurobiology* (Vol. 13, Issue 2, pp. 250–255). Elsevier Ltd. https://doi.org/10.1016/S0959-4388(03)00036-9

Lewis, P. A., & Miall, R. C. (2003b). Brain activation patterns during measurement of sub- and supra-second intervals. *Neuropsychologia*, *41*(12), 1583–1592. https://doi.org/10.1016/S0028-3932(03)00118-0

Lewis, P. A., & Miall, R. C. (2006). Remembering the time: a continuous clock. *Trends in Cognitive Sciences*, *10*(9), 401–406. https://doi.org/10.1016/j.tics.2006.07.006

Lim, L., Mi, D., Llorca, A., & Marín, O. (2018). Development and Functional Diversification of Cortical Interneurons. In *Neuron* (Vol. 100, Issue 2, pp. 294–313). Cell Press. https://doi.org/10.1016/j.neuron.2018.10.009

Limperopoulos, C., Bassan, H., Gauvreau, K., Robertson, R. L., Sullivan, N. R., Benson, C. B., Avery, L., Stewart, J., Soul, J. S., Ringer, S. A., Volpe, J. J., & Du Plessis, A. J. (2007). Does cerebellar injury in premature infants contribute to the high prevalence of long-term cognitive, learning, and behavioral disability in survivors? *Pediatrics*, *120*(3), 584–593. https://doi.org/10.1542/peds.2007-1041

Lisberger, S. G. (2021). The Rules of Cerebellar Learning: Around the Ito Hypothesis. In *Neuroscience* (Vol. 462, pp. 175–190). Elsevier Ltd. https://doi.org/10.1016/j.neuroscience.2020.08.026

Lisberger, S. G., & Pavelko, T. A. (1988). Brain stem neurons in modified pathways for motor learning in the primate vestibulo-ocular reflex. *Science*, *242*(4879), 771–773. https://doi.org/10.1126/science.3142040

Lisman, J. E., & Idiart, M. A. P. (1995). Storage of 7 ± 2 short-term memories in oscillatory subcycles. *Science*, *267*(5203), 1512–1515. https://doi.org/10.1126/science.7878473

Locke, T. M., Soden, M. E., Miller, S. M., Hunker, A., Knakal, C., Licholai, J. A., Dhillon, K. S., Keene, C. D., Zweifel, L. S., & Carlson, E. S. (2018). Dopamine D1 Receptor–Positive Neurons in the Lateral Nucleus of the Cerebellum Contribute to Cognitive Behavior. *Biological Psychiatry*, *84*(6), 401–412. https://doi.org/10.1016/j.biopsych.2018.01.019

Loewenstein, Y., Mahon, S., Chadderton, P., Kitamura, K., Sompolinsky, H., Yarom, Y., & Hausser, M. (2005). Bistability of cerebellar Purkinje cells modulated by sensory stimulation. *Nature Neuroscience*, *8*(2), 202–211. https://doi.org/10.1038/nn1393

Luce, R. D. (2008). Response Times: Their Role in Inferring Elementary Mental Organization. In *Response Times: Their Role in Inferring Elementary Mental Organization*. Oxford University Press. https://doi.org/10.1093/acprof:oso/9780195070019.001.0001

Luciani, L. (1891). *Il Cervelletto. Nuovi Studi di Fisiologia Normale e Patologica*. https://doi.org/10.2307/2175726

Lustig, C., Matell, M. S., & Meck, W. H. (2005). Not "just" a coincidence: Frontal-striatal interactions in working memory and interval timing. *Memory*, *13*(3–4), 441–448. https://doi.org/10.1080/09658210344000404

MacLeod, C. E., Zilles, K., Schleicher, A., Rilling, J. K., & Gibson, K. R. (2003). Expansion of the neocerebellum in Hominoidea. *Journal of Human Evolution*, *44*(4), 401–429. https://doi.org/10.1016/S0047-2484(03)00028-9

Maier, S. F., Amat, J., Baratta, M. V., Paul, E., & Watkins, L. R. (2006). Behavioral control, the medial prefrontal cortex, and resilience. *Dialogues in Clinical Neuroscience*, *8*(4), 397–406. https://doi.org/10.31887/dcns.2006.8.4/smaier

Mangels, J. A., Ivry, R. B., & Shimizu, N. (1998). Dissociable contributions of the prefrontal and neocerebellar cortex to time perception. *Cognitive Brain Research*, *7*(1), 15–39. https://doi.org/10.1016/S0926-6410(98)00005-6

Manni, E., & Petrosini, L. (1997). *Total cerebellar ablations Analysing the phenomena elicited by a total cerebel-lectomy, Luciani reports the presence of opisthotonos* (Vol. 20, Issue 3).

Markowitsch, H. J., & Pritzel, M. (1981). Prefrontal cortex of the guinea pig (Cavia porcellus) defined as cortical projection area of the thalamic mediodorsal nucleus. *Brain, Behavior and Evolution*, *18*(1–2), 80–95. https://doi.org/10.1159/000121778

Marr, D. (1969). A theory of cerebellar cortex. *The Journal of Physiology*, *202*(2), 437–470. https://doi.org/10.1113/jphysiol.1969.sp008820

Mason, P. H. (2015). Degeneracy: Demystifying and destigmatizing a core concept in systems biology. In *Complexity* (Vol. 20, Issue 3, pp. 12–21). John Wiley & Sons, Ltd. https://doi.org/10.1002/cplx.21534

Matano, S. (2001). Brief communication: Proportions of the ventral half of the cerebellar dentate nucleus in

humans and great apes. *American Journal of Physical Anthropology*, *114*(2), 163–165. https://doi.org/10.1002/1096-8644(200102)114:2<163::AID-AJPA1016>3.0.CO;2-F

Matell, M. S., & Meck, W. H. (2004). Cortico-striatal circuits and interval timing: Coincidence detection of oscillatory processes. In *Cognitive Brain Research* (Vol. 21, Issue 2, pp. 139–170). https://doi.org/10.1016/j.cogbrainres.2004.06.012

Matell, M. S., Meck, W. H., & Nicolelis, M. A. L. (2003). Interval timing and the encoding of signal duration by ensembles of cortical and striatal neurons. *Behavioral Neuroscience*, *117*(4), 760–773. https://doi.org/10.1037/0735-7044.117.4.760

Mathis, A., Mamidanna, P., Cury, K. M., Abe, T., Murthy, V. N., Mathis, M. W., & Bethge, M. (2018). DeepLabCut: markerless pose estimation of user-defined body parts with deep learning. *Nature Neuroscience*, *21*(9), 1281–1289. https://doi.org/10.1038/s41593-018-0209-y

Mauk, M. D., & Buonomano, D. V. (2004). The neural basis of temporal processing. In *Annual Review of Neuroscience* (Vol. 27, pp. 307–340). https://doi.org/10.1146/annurev.neuro.27.070203.144247

McCormick, D. A., Connors, B. W., Lighthall, J. W., & Prince, D. A. (1985). Comparative electrophysiology of pyramidal and sparsely spiny stellate neurons of the neocortex. *Journal of Neurophysiology*, *54*(4), 782–806. https://doi.org/10.1152/jn.1985.54.4.782

McCormick, D. A., & Thompson, R. F. (1984). Cerebellum: Essential involvement in the classically conditioned eyelid response. *Science*, *223*(4633), 296–299. https://doi.org/10.1126/science.6701513

McDevitt, C. J., Ebner, T. J., & Bloedel, J. R. (1987). Relationships between simultaneously recorded Purkinje cells and nuclear neurons. *Brain Research*, *425*(1), 1–13. https://doi.org/10.1016/0006-8993(87)90477-X

McKinney, W. (2010). Data Structures for Statistical Computing in Python. *Proceedings of the 9th Python in Science Conference*, 56–61. https://doi.org/10.25080/majora-92bf1922-00a

Menegas, W., Bergan, J. F., Ogawa, S. K., Isogai, Y., Venkataraju, K. U., Osten, P., Uchida, N., & Watabe-Uchida, M. (2015). Dopamine neurons projecting to the posterior striatum form an anatomically distinct subclass. *ELife*, *4*(AUGUST2015). https://doi.org/10.7554/eLife.10032

Middleton, F. A., & Strick, P. L. (2001). Cerebellar projections to the prefrontal cortex of the primate. *Journal of Neuroscience*, *21*(2), 700–712. https://doi.org/10.1523/jneurosci.21-02-00700.2001

Miles, F. A., & Eighmy, B. B. (1980). Long-term adaptive changes in primate vestibuloocular reflex. I. Behavioral observations. *Journal of Neurophysiology*, *43*(5), 1406–1425. https://doi.org/10.1152/jn.1980.43.5.1406

Miles, F. A., & Lisberger, S. G. (1981). Plasticity in the vestibulo-ocular reflex: a new hypothesis. In *Annual review of neuroscience* (Vol. 4, pp. 273–299). Annu Rev Neurosci. https://doi.org/10.1146/annurev.ne.04.030181.001421

Miller, E. K. (2000). The prefontral cortex and cognitive control. *Nature Reviews Neuroscience*, *1*(1), 59–65. https://doi.org/10.1038/35036228

Miller, G. A. (1956). The magical number seven, plus or minus two: some limits on our capacity for processing

information. *Psychological Review*, *63*(2), 81–97. https://doi.org/10.1037/h0043158

Mitchell, A. S. (2015). The mediodorsal thalamus as a higher order thalamic relay nucleus important for learning and decision-making. In *Neuroscience and Biobehavioral Reviews* (Vol. 54, pp. 76–88). Elsevier Ltd. https://doi.org/10.1016/j.neubiorev.2015.03.001

Mitchell, B. D., & Cauller, L. J. (2001). Corticocortical and thalamocortical projections to layer I of the frontal neocortex in rats. *Brain Research*, *921*(1–2), 68–77. https://doi.org/10.1016/S0006-8993(01)03084-0

Mitchell, S. J., & Silver, R. A. (2003). Shunting inhibition modulates neuronal gain during synaptic excitation. *Neuron*, *38*(3), 433–445. https://doi.org/10.1016/S0896-6273(03)00200-9

Moberget, T., Gullesen, E. H., Andersson, S., Ivry, R. B., & Endestad, T. (2014). Generalized role for the cerebellum in encoding internal models: Evidence from semantic processing. *Journal of Neuroscience*, *34*(8), 2871–2878. https://doi.org/10.1523/JNEUROSCI.2264-13.2014

Moberget, T., & Ivry, R. B. (2016). Cerebellar contributions to motor control and language comprehension: Searching for common computational principles. *Annals of the New York Academy of Sciences*, *1369*(1), 154–171. https://doi.org/10.1111/nyas.13094

Mogensen, J., & Holm, S. (1994). The prefrontal cortex and variants of sequential behaviour: indications of functional differentiation between subdivisions of the rat's prefrontal cortex. *Behavioural Brain Research*, *63*(1), 89–100. https://doi.org/10.1016/0166-4328(94)90054-X

Morecraft, R. J., Ge, J., Stilwell-Morecraft, K. S., Rotella, D. L., Pizzimenti, M. A., & Darling, W. G. (2018). New Corticopontine Connections in the Primate Brain: Contralateral Projections From the Arm/Hand Area of the Precentral Motor Region. *Frontiers in Neuroanatomy*, *12*. https://doi.org/10.3389/fnana.2018.00068

Mountcastle, V. B. (1957). Modality and topographic properties of single neurons of cat's somatic sensory cortex. *Journal of Neurophysiology*, *20*(4), 408–434. https://doi.org/10.1152/jn.1957.20.4.408

Mountcastle, Vernon B. (1997). The columnar organization of the neocortex. In *Brain* (Vol. 120, Issue 4, pp. 701–722). https://doi.org/10.1093/brain/120.4.701

Mugnaini, E., Sekerková, G., & Martina, M. (2011). The unipolar brush cell: A remarkable neuron finally receiving deserved attention. In *Brain Research Reviews* (Vol. 66, Issues 1–2, pp. 220–245). NIH Public Access. https://doi.org/10.1016/j.brainresrev.2010.10.001

Nácher, V., Ledberg, A., Deco, G., & Romo, R. (2013). Coherent delta-band oscillations between cortical areas correlate with decision making. *Proceedings of the National Academy of Sciences of the United States of America*, *110*(37), 15085–15090. https://doi.org/10.1073/pnas.1314681110

Nagai, Y., Critchley, H. D., Featherstone, E., Fenwick, P. B. C., Trimble, M. R., & Dolan, R. J. (2004). Brain activity relating to the contingent negative variation: An fMRI investigation. *NeuroImage*, *21*(4), 1232–1241. https://doi.org/10.1016/j.neuroimage.2003.10.036

Najafi, F., & Medina, J. F. (2020). Bidirectional short-term plasticity during single-trial learning of cerebellar-driven eyelid movements in mice. *Neurobiology of Learning and Memory*, *170*.

https://doi.org/10.1016/j.nlm.2019.107097

Napper, R. M. A., & Harvey, R. J. (1988). Number of parallel fiber synapses on an individual Purkinje cell in the cerebellum of the rat. *Journal of Comparative Neurology*, *274*(2), 168–177. https://doi.org/10.1002/cne.902740204

Narayanan, N. S. (2016). Ramping activity is a cortical mechanism of temporal control of action. In *Current Opinion in Behavioral Sciences* (Vol. 8, pp. 226–230). https://doi.org/10.1016/j.cobeha.2016.02.017

Narayanan, R. T., Egger, R., de Kock, C. P. J., & Oberlaender, M. (2016). Neuronal Cell Types in the Neocortex. In *Axons and Brain Architecture* (pp. 183–202). Elsevier. https://doi.org/10.1016/b978-0-12-801393-9.00009-8

Nieuwenhuys, R., ten Donkelaar, H. J., & Nicholson, C. (1998). The Central Nervous System of Vertebrates. In *The Central Nervous System of Vertebrates*. Springer Berlin Heidelberg. https://doi.org/10.1007/978-3-642-18262-4

Niki, C., Kumada, T., Maruyama, T., Tamura, M., & Muragaki, Y. (2019). Role of frontal functions in executing routine sequential tasks. *Frontiers in Psychology*, *10*(FEB), 169. https://doi.org/10.3389/fpsyg.2019.00169

O'Reilly, J. X., Mesulam, M. M., & Nobre, A. C. (2008). The cerebellum predicts the timing of perceptual events. *Journal of Neuroscience*, *28*(9), 2252–2260. https://doi.org/10.1523/JNEUROSCI.2742-07.2008

Ogawa, T. (1935). Beiträge zur vergleichende Anatomie des Zentralnervensystems der Wassersaugetiere: Ober die Kleinhirnkerne der Pinnepedien und Zetazeen. *Arb Anat Inst Sendai*, *17*, 63–136. https://scholar.google.com/scholar_lookup?title=Beiträge zur vergleichende Anatomie des Zentralnervensystems der Wassersäugetiere&author=T. Ogawa&journal=Ueber die Kleinhirnkerne der Pinnipedien und Cetaceen. Arb Anat Inst Sendai&volume=17&pages=63-136&pu

Ohmae, S., & Medina, J. F. (2015). Climbing fibers encode a temporal-difference prediction error during cerebellar learning in mice. *Nature Neuroscience*, *18*(12), 1798–1803. https://doi.org/10.1038/nn.4167

Ohmae, S., Uematsu, A., & Tanaka, M. (2013). Temporally specific sensory signals for the detection of stimulus omission in the primate deep cerebellar nuclei. *Journal of Neuroscience*, *33*(39), 15432–15441. https://doi.org/10.1523/JNEUROSCI.1698-13.2013

Onoda, K., Takahashi, E., & Sakata, S. (2003). Event-related potentials in the frontal cortex, hippocampus, and cerebellum during a temporal discrimination task in rats. *Cognitive Brain Research*, *17*(2), 380–387. https://doi.org/10.1016/S0926-6410(03)00139-3

Opris, I., & Casanova, M. F. (2014). Prefrontal cortical minicolumn: From executive control to disrupted cognitive processing. In *Brain* (Vol. 137, Issue 7, pp. 1863–1875). https://doi.org/10.1093/brain/awt359

Opris, I., Fuqua, J. L., Huettl, P. F., Gerhardt, G. A., Berger, T. W., Hampson, R. E., & Deadwyler, S. A. (2012). Closing the loop in primate prefrontal cortex: Inter-laminar processing. *Frontiers in Neural Circuits*, *OCTOBER 2012*, 1–42. https://doi.org/10.3389/fncir.2012.00088

Opris, I., Hampson, R. E., Gerhardt, G. A., Berger, T. W., & Deadwyler, S. A. (2012). Columnar processing in primate pFC: Evidence for executive control microcircuits. *Journal of Cognitive Neuroscience*, *24*(12), 2337–2347. https://doi.org/10.1162/jocn_a_00307

Oscarsson, O. (1979). Functional units of the cerebellum; sagittal zones and microzones. *Trends Neurosci.*, *2*, 143–145.

Özcan, O. O., Wang, X., Binda, F., Dorgans, K., de Zeeuw, C. I., Gao, Z., Aertsen, A., Kumar, A., & Isope, P. (2020). Differential coding strategies in glutamatergic and GABAergic neurons in the medial cerebellar nucleus. *Journal of Neuroscience*, *40*(1), 159–170. https://doi.org/10.1523/JNEUROSCI.0806-19.2019

Palay, S. L., & Chan-Palay, V. (1974). Cerebellar Cortex. In *Cerebellar Cortex*. Springer Berlin Heidelberg. https://doi.org/10.1007/978-3-642-65581-4

Palesi, F., De Rinaldis, A., Castellazzi, G., Calamante, F., Muhlert, N., Chard, D., Tournier, J. D., Magenes, G., D'Angelo, E., & Wheeler-Kingshott, C. A. M. G. (2017). Contralateral cortico-ponto-cerebellar pathways reconstruction in humans in vivo: Implications for reciprocal cerebro-cerebellar structural connectivity in motor and non-motor areas. *Scientific Reports*, *7*(1), 12841. https://doi.org/10.1038/s41598-017-13079-8

Parker, K. L. (2016). Timing tasks synchronize cerebellar and frontal ramping activity and theta oscillations: Implications for cerebellar stimulation in diseases of impaired cognition. *Frontiers in Psychiatry*, *6*(JAN). https://doi.org/10.3389/fpsyt.2015.00190

Parker, K. L., Chen, K. H., Kingyon, J. R., Cavanagh, J. F., & Narayanan, N. S. (2014). D1-dependent 4 Hz oscillations and ramping activity in rodent medial frontal cortex during interval timing. *Journal of Neuroscience*, *34*(50), 16774–166783. https://doi.org/10.1523/JNEUROSCI.2772-14.2014

Parker, K. L., Kim, Y. C., Kelley, R. M., Nessler, A. J., Chen, K.-H., Muller-Ewald, V. A., Andreasen, N. C., & Narayanan, N. S. (2017). Delta-frequency stimulation of cerebellar projections can compensate for schizophrenia-related medial frontal dysfunction. *Molecular Psychiatry*, *22*(5), 647–655. https://doi.org/10.1038/mp.2017.50

Paz-Alonso, P. M., Bunge, S. A., & Ghetti, S. (2014). *Emergence of Higher Cognitive Functions: Reorganization of Large-Scale Brain Networks During Childhood And Adolescence of a single chapter of a title in Oxford Handbooks Online for personal use (for details see Privacy Policy and Legal Notice) Emergence o*. https://doi.org/10.1093/oxfordhb/9780199935291.013.003

Pedregosa, F. \emphet al., Pedregosa, F., Weiss, R., Brucher, M., Pedregosa, F. et al., Pedregosa, F., Varoquaux, G., Gramfort, A., Michel, V., Thirion, B., Grisel, O., Blondel, M., Prettenhofer, P., Weiss, R., Dubourg, V., Vanderplas, J., Passos, A., Cournapeau, D., Brucher, M., … Duchesnay, E. (2011). Scikit-learn: Machine Learning in Python. *Journal of Machine Learning Research*, *12*(85), 2825–2830. http://jmlr.org/papers/v12/pedregosa11a.html

Perrett, S. P., Ruiz, B. P., & Mauk, M. D. (1993). Cerebellar cortex lesions disrupt learning-dependent timing of conditioned eyelid responses. *Journal of Neuroscience*, *13*(4), 1708–1718.

https://doi.org/10.1523/jneurosci.13-04-01708.1993

Person, A. L., & Raman, I. M. (2012). Purkinje neuron synchrony elicits time-locked spiking in the cerebellar nuclei. *Nature*, *481*(7382), 502–505. https://doi.org/10.1038/nature10732

Petter, E. A., Lusk, N. A., Hesslow, G., & Meck, W. H. (2016). Interactive roles of the cerebellum and striatum in sub-second and supra-second timing: Support for an initiation, continuation, adjustment, and termination (ICAT) model of temporal processing. In *Neuroscience and Biobehavioral Reviews* (Vol. 71, pp. 739–755). Elsevier Ltd. https://doi.org/10.1016/j.neubiorev.2016.10.015

Pichitpornchai, C., Rawson, J. A., & Rees, S. (1994). Morphology of parallel fibres in the cerebellar cortex of the rat: An experimental light and electron microscopic study with biocytin. *Journal of Comparative Neurology*, *342*(2), 206–220. https://doi.org/10.1002/cne.903420205

Pierce, K., & Courchesne, E. (2001). Evidence for a cerebellar role in reduced exploration and stereotyped behavior in autism. *Biological Psychiatry*, *49*(8), 655–664. https://doi.org/10.1016/S0006-3223(00)01008-8

Piras, F., & Coull, J. T. (2011). Implicit, predictive timing draws upon the same scalar representation of time as explicit timing. *PLoS ONE*, *6*(3), e18203. https://doi.org/10.1371/journal.pone.0018203

Pisano, T. J., Dhanerawala, Z. M., Kislin, M., Bakshinskaya, D., Engel, E. A., Lee, J., de Oude, N. L., Hansen, E. J., Venkataraju, K. U., Hoebeek, F. E., Richardson, B. D., Verpeut, J. L., Boele, H.-J., & Wang, S. (2021). Homologous organization of cerebellar pathways to sensory, motor, and associative forebrain. *Cell Reports*, *36*(12), 109721. https://doi.org/10.2139/ssrn.3810000

Preul, M. C., & Dagi, T. F. (2017). London 1935: The frontal lobe, insanity, and a brain surgery. In *Neurosurgical Focus* (Vol. 43, Issue 3). https://doi.org/10.3171/2017.6.FOCUS17429

Preuss, T. M. (1995). Do rats have prefrontal cortex? The Rose-Woolsey-Akert program reconsidered. *Journal of Cognitive Neuroscience*, *7*(1), 1–24. https://doi.org/10.1162/jocn.1995.7.1.1

Radnikow, G., & Feldmeyer, D. (2018). Layer- and cell type-specific modulation of excitatory neuronal activity in the neocortex. In *Frontiers in Neuroanatomy* (Vol. 12, p. 1). Frontiers. https://doi.org/10.3389/fnana.2018.00001

Ragozzino, M. E., Detrick, S., & Kesner, R. P. (1999). Involvement of the prelimbic-infralimbic areas of the rodent prefrontal cortex in behavioral flexibility for place and response learning. *Journal of Neuroscience*, *19*(11), 4585–4594. https://doi.org/10.1523/jneurosci.19-11-04585.1999

Rakic, P. (1988). Specification of cerebral cortical areas. *Science*, *241*(4862), 170–176. https://doi.org/10.1126/science.3291116

Rakic, P. (1995). Radial versus tangential migration of neuronal clones in the developing cerebral cortex. In *Proceedings of the National Academy of Sciences of the United States of America* (Vol. 92, Issue 25, pp. 11323–11327). https://doi.org/10.1073/pnas.92.25.11323

Rakic, P. (2008). Confusing cortical columns. In *Proceedings of the National Academy of Sciences of the United*

States of America (Vol. 105, Issue 34, pp. 12099–12100). https://doi.org/10.1073/pnas.0807271105

Raman, I. M., & Bean, B. P. (1999a). Ionic currents underlying spontaneous action potentials in isolated cerebellar purkinje neurons. *Journal of Neuroscience*, *19*(5), 1663–1674. https://doi.org/10.1523/jneurosci.19-05-01663.1999

Raman, I. M., & Bean, B. P. (1999b). Properties of sodium currents and action potential firing in isolated cerebellar Purkinje neurons. *Annals of the New York Academy of Sciences*, *868*(1), 93–96. https://doi.org/10.1111/j.1749-6632.1999.tb11279.x

Raman, I. M., Gustafson, A. E., & Padgett, D. (2000). Ionic currents and spontaneous firing in neurons isolated from the cerebellar nuclei. *Journal of Neuroscience*, *20*(24), 9004–9016. https://doi.org/10.1523/jneurosci.20-24-09004.2000

Ramnani, N. (2006). The primate cortico-cerebellar system: Anatomy and function. *Nature Reviews Neuroscience*, *7*(7), 511–522. https://doi.org/10.1038/nrn1953

Ramnani, N., Behrens, T. E. J., Johansen-Berg, H., Richter, M. C., Pinsk, M. A., Andersson, J. L. R., Rudebeck, P., Ciccarelli, O., Richter, W., Thompson, A. J., Gross, C. G., Robson, M. D., Kastner, S., & Matthews, P. M. (2006). The evolution of prefrontal inputs to the cortico-pontine system: Diffusion imaging evidence from macaque monkeys and humans. *Cerebral Cortex*, *16*(6), 811–818. https://doi.org/10.1093/cercor/bhj024

Rao, S. G., Williams, G. V., & Goldman-Rakic, P. S. (1999). Isodirectional tuning of adjacent interneurons and pyramidal cells during working memory: Evidence for microcolumnar organization in PFC. *Journal of Neurophysiology*, *81*(4), 1903–1916. https://doi.org/10.1152/jn.1999.81.4.1903

Rao, S. G., Williams, G. V., & Goldman-Rakic, P. S. (2000). Destruction and creation of spatial tuning by disinhibition: GABA(A) blockade of prefrontal cortical neurons engaged by working memory. *Journal of Neuroscience*, *20*(1), 485–494. https://doi.org/10.1523/jneurosci.20-01-00485.2000

Raymond, J. L., & Medina, J. F. (2018). Computational Principles of Supervised Learning in the Cerebellum. *Annual Review of Neuroscience*, *41*(1), 233–253. https://doi.org/10.1146/annurev-neuro-080317-061948

Reinert, S., Hübener, M., Bonhoeffer, T., & Goltstein, P. M. (2021). Mouse prefrontal cortex represents learned rules for categorization. *Nature*, *593*(7859), 411–417. https://doi.org/10.1038/s41586-021-03452-z

Reppert, S. M., & Weaver, D. R. (2002). Coordination of circadian timing in mammals. In *Nature* (Vol. 418, Issue 6901, pp. 935–941). Nature. https://doi.org/10.1038/nature00965

Rilling, J. K. (2006). Human and NonHuman primate brains: Are they allometrically scaled versions of the same design? *Evolutionary Anthropology*, *15*(2), 65–77. https://doi.org/10.1002/evan.20095

Rolando, L. (1809). Saggio Sopra la Vera Struttura Del Cervello Dell'uomo e Degli Animali Sopra le Funzioni del Sistema Nervoso. *(Sassari, Stamperia Di S. S. R. M. Privilegiata)*. https://www.amazon.it/struttura-cervello-delluomo-animali-funzioni/dp/882711517X

Roš, H., Sachdev, R. N. S., Yu, Y., Šestan, N., & McCormick, D. A. (2009). Neocortical networks entrain neuronal

circuits in cerebellar cortex. *Journal of Neuroscience*, *29*(33), 10309–10320. https://doi.org/10.1523/JNEUROSCI.2327-09.2009

Rose, J. E., & Woosley, C. N. (1948). The orbitofrontal cortex and its connections with the mediodorsal nucleus in rabbit, sheep and cat. *Research Publications - Association for Research in Nervous and Mental Disease*, *27 1 vol.)*, 210–232. https://europepmc.org/article/med/18106857

Roux, S. G., Cenier, T., Garcia, S., Litaudon, P., & Buonviso, N. (2007). A wavelet-based method for local phase extraction from a multi-frequency oscillatory signal. *Journal of Neuroscience Methods*, *160*(1), 135–143. https://doi.org/10.1016/j.jneumeth.2006.09.001

Rowland, N. C., & Jaeger, D. (2005). Coding of tactile response properties in the rat deep cerebellar nuclei. *Journal of Neurophysiology*, *94*(2), 1236–1251. https://doi.org/10.1152/jn.00285.2005

Rudy, B., Fishell, G., Lee, S. H., & Hjerling-Leffler, J. (2011). Three groups of interneurons account for nearly 100% of neocortical GABAergic neurons. *Developmental Neurobiology*, *71*(1), 45–61. https://doi.org/10.1002/dneu.20853

Sacchetti, B., Scelfo, B., & Strata, P. (2009). Cerebellum and emotional behavior. In *Neuroscience* (Vol. 162, Issue 3, pp. 756–762). Neuroscience. https://doi.org/10.1016/j.neuroscience.2009.01.064

Sakamoto, T., & Endo, S. (2010). Amygdala, deep cerebellar nuclei and red nucleus contribute to delay eyeblink conditioning in C57BL/6 mice. *European Journal of Neuroscience*, *32*(9), 1537–1551. https://doi.org/10.1111/j.1460-9568.2010.07406.x

Sanchez-Vives, M. V., & McCormick, D. A. (2000). Cellular and network mechanisms of rhytmic recurrent activity in neocortex. *Nature Neuroscience*, *3*(10), 1027–1034. https://doi.org/10.1038/79848

Sawaguchi, T., Matsumura, M., & Kubota, K. (1988). Delayed response deficit in monkeys by locally disturbed prefrontal neuronal activity by bicuculline. *Behavioural Brain Research*, *31*(2), 193–198. https://doi.org/10.1016/0166-4328(88)90023-X

Sawilowsky, S. S. (2009). New Effect Size Rules of Thumb. *Journal of Modern Applied Statistical Methods*, *8*(2), 597–599. https://doi.org/10.22237/jmasm/1257035100

Schmahmann, J. D. (2000). The role of the cerebellum in affect and psychosis. *Journal of Neurolinguistics*, *13*(2–3), 189–214. https://doi.org/10.1016/S0911-6044(00)00011-7

Schmahmann, J. D. (2004). Disorders of the cerebellum: Ataxia, dysmetria of thought, and the cerebellar cognitive affective syndrome. In *Journal of Neuropsychiatry and Clinical Neurosciences* (Vol. 16, Issue 3, pp. 367–378). https://doi.org/10.1176/jnp.16.3.367

Schmahmann, J. D., Guell, X., Stoodley, C. J., & Halko, M. A. (2019). The Theory and Neuroscience of Cerebellar Cognition. *Annual Review of Neuroscience*, *42*(1), 337–364. https://doi.org/10.1146/annurev-neuro-070918-050258

Schmahmann, J. D., & Pandya, D. N. (1995). Prefrontal cortex projections to the basilar pons in rhesus monkey: implications for the cerebellar contribution to higher function. *Neuroscience Letters*, *199*(3), 175–178.

https://doi.org/10.1016/0304-3940(95)12056-A

Schmahmann, J. D., & Sherman, J. C. (1998). The cerebellar cognitive affective syndrome. *Brain*, *121*(4), 561–579. https://doi.org/10.1093/brain/121.4.561

Schoenemann, P. T., Sheehan, M. J., & Glotzer, L. D. (2005). Prefrontal white matter volume is disproportionately larger in humans than in other primates. *Nature Neuroscience*, *8*(2), 242–252. https://doi.org/10.1038/nn1394

Schonewille, M., Belmeguenai, A., Koekkoek, S. K., Houtman, S. H., Boele, H. J., van Beugen, B. J., Gao, Z., Badura, A., Ohtsuki, G., Amerika, W. E., Hosy, E., Hoebeek, F. E., Elgersma, Y., Hansel, C., & De Zeeuw, C. I. (2010). Purkinje cell-specific knockout of the protein phosphatase PP2B impairs potentiation and cerebellar motor learning. *Neuron*, *67*(4), 618–628. https://doi.org/10.1016/j.neuron.2010.07.009

Schüz, a, & Braitenberg, V. (2001). Cerebral Cortex: Organization and Function. In *International Encyclopedia of the Social & Behavioral Sciences* (pp. 1634–1640). https://doi.org/10.1016/b0-08-043076-7/03443-4

Sengul, G., & Watson, C. (2015). Ascending and Descending Pathways in the Spinal Cord. In *The Rat Nervous System: Fourth Edition* (pp. 115–130). Elsevier Inc. https://doi.org/10.1016/B978-0-12-374245-2.00008-5

Sereno, M. I., Diedrichsen, J. rn, Tachrount, M., Testa-Silva, G., D Arceuil, H., & De Zeeuw, C. (2020). The human cerebellum has almost 80% of the surface area of the neocortex. *Proceedings of the National Academy of Sciences of the United States of America*, *117*(32), 19538–19543. https://doi.org/10.1073/pnas.2002896117

Shadmehr, R. (2020). Population coding in the cerebellum: A machine learning perspective. In *Journal of Neurophysiology* (Vol. 124, Issue 6, pp. 2022–2051). American Physiological Society Bethesda, MD. https://doi.org/10.1152/jn.00449.2020

Shambes, G. M., Gibson, J. M., & Welker, W. (1978). Fractured somatotopy in granule cell tactile areas of rat cerebellar hemispheres revealed by micromapping. *Brain, Behavior and Evolution*, *15*(2), 94–140. https://doi.org/10.1159/000123774

Shaw, P., Kabani, N. J., Lerch, J. P., Eckstrand, K., Lenroot, R., Gogtay, N., Greenstein, D., Clasen, L., Evans, A., Rapoport, J. L., Giedd, J. N., & Wise, S. P. (2008). Neurodevelopmental trajectories of the human cerebral cortex. *Journal of Neuroscience*, *28*(14), 3586–3594. https://doi.org/10.1523/JNEUROSCI.5309-07.2008

Shergill, S. S., Samson, G., Bays, P. M., Frith, C. D., & Wolpert, D. M. (2005). Evidence for sensory prediction deficits in schizophrenia. *American Journal of Psychiatry*, *162*(12), 2384–2386. https://doi.org/10.1176/appi.ajp.162.12.2384

Sherman, S. M., & Guillery, R. W. (2011). Distinct functions for direct and transthalamic corticocortical connections. *Journal of Neurophysiology*, *106*(3), 1068–1077. https://doi.org/10.1152/jn.00429.2011

Shipp, S. (2007). Structure and function of the cerebral cortex. In *Current Biology* (Vol. 17, Issue 12). https://doi.org/10.1016/j.cub.2007.03.044

Shipp, S., Adams, R. A., & Friston, K. J. (2013). Reflections on agranular architecture: Predictive coding in the

motor cortex. In *Trends in Neurosciences* (Vol. 36, Issue 12, pp. 706–716). https://doi.org/10.1016/j.tins.2013.09.004

Shone, G., Raphael, Y., & Miller, J. M. (1991). Hereditary deafness occurring in cd/1 mice. *Hearing Research*, *57*(1), 153–156. https://doi.org/10.1016/0378-5955(91)90084-M

Sillitoe, R. V., Lackey, E. P., & Heck, D. H. (2018). Recent advances in understanding the mechanisms of cerebellar granule cell development and function and their contribution to behavior. In *F1000Research* (Vol. 7). Faculty of 1000 Ltd. https://doi.org/10.12688/f1000research.15021.1

Simat, M., Parpan, F., & Fritsch, J. M. (2007). Heterogeneity of glycinergic and gabaergic interneurons in the granule cell layer of mouse cerebellum. *Journal of Comparative Neurology*, *500*(1), 71–83. https://doi.org/10.1002/cne.21142

Snow, W. M., Stoesz, B. M., & Anderson, J. E. (2014). The cerebellum in emotional processing: Evidence from human and non-human animals. In *AIMS Neuroscience* (Vol. 1, Issue 1, pp. 96–119). AIMS Press. https://doi.org/10.3934/Neuroscience.2014.1.96

Sokolov, A. A., Miall, R. C., & Ivry, R. B. (2017). The Cerebellum: Adaptive Prediction for Movement and Cognition. In *Trends in Cognitive Sciences* (Vol. 21, Issue 5, pp. 313–332). Elsevier Ltd. https://doi.org/10.1016/j.tics.2017.02.005

Spencer, R. M. C., Zelaznik, H. N., Diedrichsen, J., & Ivry, R. B. (2003). Disrupted timing of discontinuous but not continuous movements by cerebellar lesions. *Science*, *300*(5624), 1437–1439. https://doi.org/10.1126/science.1083661

Stoodley, C. J. (2016). The Cerebellum and Neurodevelopmental Disorders. In *Cerebellum* (Vol. 15, Issue 1, pp. 34–37). Springer New York LLC. https://doi.org/10.1007/s12311-015-0715-3

Stoodley, C. J., D'Mello, A. M., Ellegood, J., Jakkamsetti, V., Liu, P., Nebel, M. B., Gibson, J. M., Kelly, E., Meng, F., Cano, C. A., Pascual, J. M., Mostofsky, S. H., Lerch, J. P., & Tsai, P. T. (2017). Altered cerebellar connectivity in autism and cerebellar-mediated rescue of autism-related behaviors in mice. *Nature Neuroscience*, *20*(12), 1744–1751. https://doi.org/10.1038/s41593-017-0004-1

Stoodley, C. J., & Schmahmann, J. D. (2009). Functional topography in the human cerebellum: A meta-analysis of neuroimaging studies. *NeuroImage*, *44*(2), 489–501. https://doi.org/10.1016/j.neuroimage.2008.08.039

Strakowski, S. M., DelBello, M. P., & Adler, C. M. (2005). The functional neuroanatomy of bipolar disorder: A review of neuroimaging findings. In *Molecular Psychiatry* (Vol. 10, Issue 1, pp. 105–116). Mol Psychiatry. https://doi.org/10.1038/sj.mp.4001585

Strick, P. L., Dum, R. P., & Fiez, J. A. (2009). Cerebellum and Nonmotor Function. *Annual Review of Neuroscience*, *32*(1), 413–434. https://doi.org/10.1146/annurev.neuro.31.060407.125606

Sugihara, I., Fujita, H., Na, J., Quy, P. N., Li, B. Y., & Ikeda, D. (2009). Projection of reconstructed single Purkinje cell axons in relation to the cortical and nuclear aldolase C compartments of the rat cerebellum. *Journal of Comparative Neurology*, *512*(2), 282–304. https://doi.org/10.1002/cne.21889

Sultan, F, & Braitenberg, V. (1993). Shapes and sizes of different mammalian cerebella. A study in quantitative comparative neuroanatomy. *Journal Fur Hirnforschung*, *34*(1), 79–92.

Sultan, Fahad, Augath, M., Hamodeh, S., Murayama, Y., Oeltermann, A., Rauch, A., & Thier, P. (2012). Unravelling cerebellar pathways with high temporal precision targeting motor and extensive sensory and parietal networks. *Nature Communications*, *3*(1), 1–10. https://doi.org/10.1038/ncomms1912

Sultan, Fahad, & Bower, J. M. (1998). Quantitative golgi study of the rat cerebellar molecular layer interneurons using principal component analysis. *Journal of Comparative Neurology*, *393*(3), 353–373. https://doi.org/10.1002/(SICI)1096-9861(19980413)393:3<353::AID-CNE7>3.0.CO;2-0

Sultan, K. T., & Shi, S. H. (2018). Generation of diverse cortical inhibitory interneurons. In *Wiley Interdisciplinary Reviews: Developmental Biology* (Vol. 7, Issue 2). NIH Public Access. https://doi.org/10.1002/wdev.306

Sutton, A. C., O'Connor, K. A., Pilitsis, J. G., & Shin, D. S. (2015). Stimulation of the subthalamic nucleus engages the cerebellum for motor function in parkinsonian rats. *Brain Structure and Function*, *220*(6), 3595–3609. https://doi.org/10.1007/s00429-014-0876-8

Suvrathan, A., Payne, H. L., & Raymond, J. L. (2016). Timing Rules for Synaptic Plasticity Matched to Behavioral Function. *Neuron*, *92*(5), 959–967. https://doi.org/10.1016/j.neuron.2016.10.022

Szapiro, G., & Barbour, B. (2007). Multiple climbing fibers signal to molecular layer interneurons exclusively via glutamate spillover. *Nature Neuroscience*, *10*(6), 735–742. https://doi.org/10.1038/nn1907

Szczepanski, S. M., & Knight, R. T. (2014). Insights into Human Behavior from Lesions to the Prefrontal Cortex. In *Neuron* (Vol. 83, Issue 5, pp. 1002–1018). Cell Press. https://doi.org/10.1016/j.neuron.2014.08.011

Szentágothai, J., & Rajkovits, K. (1959). Über den Ursprung der Kletterfasern des Kleinhirns. *Zeitschrift Für Anatomie Und Entwicklungsgeschichte*, *121*(2), 130–141. https://doi.org/10.1007/BF00525203

Takeuchi, D., Hirabayashi, T., Tamura, K., & Miyashita, Y. (2011). Reversal of interlaminar signal between sensory and memory processing in monkey temporal cortex. *Science*, *331*(6023), 1443–1447. https://doi.org/10.1126/science.1199967

Tallot, L., & Doyère, V. (2020). Neural encoding of time in the animal brain. In *Neuroscience and Biobehavioral Reviews* (Vol. 115, pp. 146–163). Elsevier Ltd. https://doi.org/10.1016/j.neubiorev.2019.12.033

Tallot, L., Graupner, M., Diaz-Mataix, L., & Doyère, V. (2020). Beyond freezing: Temporal expectancy of an aversive event engages the amygdalo-prefronto-dorsostriatal network. *Cerebral Cortex*, *30*(10), 5257–5269. https://doi.org/10.1093/cercor/bhaa100

Tasic, B., Yao, Z., Graybuck, L. T., Smith, K. A., Nguyen, T. N., Bertagnolli, D., Goldy, J., Garren, E., Economo, M. N., Viswanathan, S., Penn, O., Bakken, T., Menon, V., Miller, J., Fong, O., Hirokawa, K. E., Lathia, K., Rimorin, C., Tieu, M., … Zeng, H. (2018). Shared and distinct transcriptomic cell types across neocortical areas. *Nature*, *563*(7729), 72–78. https://doi.org/10.1038/s41586-018-0654-5

Teki, S., Grube, M., Kumar, S., & Griffiths, T. D. (2011). Distinct neural substrates of duration-based and beat-

based auditory timing. *Journal of Neuroscience*, *31*(10), 3805–3812. https://doi.org/10.1523/JNEUROSCI.5561-10.2011

Teune, T. M., Burg, J. V. A. N. D. E. R., Zeeuw, C. I. D. E., & Voogd, J. (1998). Single Purkinje Cell Can Innervate Multiple Classes of Projection Neurons in the Cerebellar Nuclei of the Rat: A Light Microscopic and Ultrastructural Triple-Tracer Study in the Rat. *Journal of Comparative Neurology*, *178*(April 1997), 164–178.

Thach, W. T. (1968). Discharge of Purkinje and cerebellar nuclear neurons during rapidly alternating arm movements in the monkey. *Journal of Neurophysiology*, *31*(5), 785–797. https://doi.org/10.1152/jn.1968.31.5.785

Thoma, P., Bellebaum, C., Koch, B., Schwarz, M., & Daum, I. (2008). The cerebellum is involved in reward-based reversal learning. *Cerebellum*, *7*(3), 433–443. https://doi.org/10.1007/s12311-008-0046-8

Thomson, A. M. (2010). Neocortical layer 6, a review. In *Frontiers in Neuroanatomy* (Vol. 0, Issue MARCH, p. 13). Frontiers. https://doi.org/10.3389/fnana.2010.00013

Thomson, A. M., & Lamy, C. (2007). Functional Maps of Neocortical Local Circuitry. In *Frontiers in Neuroscience* (Vol. 1, Issue 1, pp. 19–42). Frontiers. https://doi.org/10.3389/neuro.01.1.1.002.2007

Thomson, A. M., West, D. C., Wang, Y., & Bannister, A. P. (2002). Synaptic connections and small circuits involving excitatory and inhibitory neurons in layers 2-5 of adult rat and cat neocortex: Triple intracellular recordings and biocytin labelling in vitro. *Cerebral Cortex*, *12*(9), 936–953. https://doi.org/10.1093/cercor/12.9.936

Thürling, M., Kahl, F., Maderwald, S., Stefanescu, R. M., Schlamann, M., Boele, H. J., De Zeeuw, C. I., Diedrichsen, J., Ladd, M. E., Koekkoek, S. K. E., & Timmann, D. (2015). Cerebellar cortex and cerebellar nuclei are concomitantly activated during eyeblink conditioning: A 7T fMRI study in humans. *Journal of Neuroscience*, *35*(3), 1228–1239. https://doi.org/10.1523/JNEUROSCI.2492-14.2015

Tiemeier, H., Lenroot, R. K., Greenstein, D. K., Tran, L., Pierson, R., & Giedd, J. N. (2010). Cerebellum development during childhood and adolescence: A longitudinal morphometric MRI study. *NeuroImage*, *49*(1), 63–70. https://doi.org/10.1016/j.neuroimage.2009.08.016

Tomassini, A., Ruge, D., Galea, J. M., Penny, W., & Bestmann, S. (2016). The role of dopamine in temporal uncertainty. *Journal of Cognitive Neuroscience*, *28*(1), 96–110. https://doi.org/10.1162/jocn_a_00880

Tomlinson, S. P., Davis, N. J., Morgan, H. M., & Bracewell, R. M. (2014). Cerebellar contributions to verbal working memory. *Cerebellum*, *13*(3), 354–361. https://doi.org/10.1007/s12311-013-0542-3

Totah, N. K. B., Jackson, M. E., & Moghaddam, B. (2013a). Preparatory attention relies on dynamic interactions between prelimbic cortex and anterior cingulate cortex. *Cerebral Cortex*, *23*(3), 729–738. https://doi.org/10.1093/cercor/bhs057

Totah, N. K. B., Jackson, M. E., & Moghaddam, B. (2013b). Preparatory attention relies on dynamic interactions between prelimbic cortex and anterior cingulate cortex. *Cerebral Cortex*, *23*(3), 729–738. https://doi.org/10.1093/cercor/bhs057

Triviño, M., Arnedo, M., Lupiáñez, J., Chirivella, J., & Correa, Á. (2011). Rhythms can overcome temporal orienting deficit after right frontal damage. *Neuropsychologia*, *49*(14), 3917–3930. https://doi.org/10.1016/j.neuropsychologia.2011.10.009

Tzschentke, T. M. (2000). The medial prefrontal cortex as a part of the brain reward system. In *Amino Acids* (Vol. 19, Issue 1, pp. 211–219). Amino Acids. https://doi.org/10.1007/s007260070051

Uusisaari, M., & de Schutter, E. (2011). The mysterious microcircuitry of the cerebellar nuclei. *Journal of Physiology*, *589*(14), 3441–3457. https://doi.org/10.1113/jphysiol.2010.201582

Uusisaari, M., & Knöpfel, T. (2011). Functional classification of neurons in the mouse lateral Cerebellar Nuclei. *Cerebellum*, *10*(4), 637–646. https://doi.org/10.1007/s12311-010-0240-3

Uusisaari, M., Obata, K., & Knöpfel, T. (2007). Morphological and electrophysiological properties of GABAergic and non-GABAergic cells in the deep cerebellar nuclei. *Journal of Neurophysiology*, *97*(1), 901–911. https://doi.org/10.1152/jn.00974.2006

Uusisaari, M. Y., & Knöpfel, T. (2012). Diversity of neuronal elements and circuitry in the cerebellar nuclei. *Cerebellum*, *11*(2), 420–421. https://doi.org/10.1007/s12311-011-0350-6

Vallat, R. (2018). Pingouin: statistics in Python. *Journal of Open Source Software*, *3*(31), 1026. https://doi.org/10.21105/joss.01026

Vallesi, A., Shallice, T., & Walsh, V. (2007). Role of the prefrontal cortex in the foreperiod effect: TMS evidence for dual mechanisms in temporal preparation. *Cerebral Cortex*, *17*(2), 466–474. https://doi.org/10.1093/cercor/bhj163

van Beugen, B. J., Gao, Z., Boele, H. J., Hoebeek, F., & De Zeeuw, C. I. (2013). High frequency burst firing of granule cells ensures transmission at the parallel fiber to purkinje cell synapse at the cost of temporal coding. *Frontiers in Neural Circuits*, *0*(APR 2013), 95. https://doi.org/10.3389/fncir.2013.00095

Van De Werd, H. J. J. M., Rajkowska, G., Evers, P., & Uylings, H. B. M. (2010). Cytoarchitectonic and chemoarchitectonic characterization of the prefrontal cortical areas in the mouse. *Brain Structure and Function*, *214*(4), 339–353. https://doi.org/10.1007/s00429-010-0247-z

van Rijn, H., Gu, B. M., & Meck, W. H. (2014). Dedicated clock/timing-circuit theories of time perception and timed performance. *Advances in Experimental Medicine and Biology*, *829*, 75–99. https://doi.org/10.1007/978-1-4939-1782-2_5

van Rijn, H., Kononowicz, T. W., Meck, W. H., Ng, K. K., & Penney, T. B. (2011). Contingent negative variation and its relation to time estimation: A theoretical evaluation. *Frontiers in Integrative Neuroscience*, *0*(DECEMBER), 91. https://doi.org/10.3389/fnint.2011.00091

vanVugt, M. K., Simen, P., Nystrom, L. E., Holmes, P., & Cohen, J. D. (2012). EEG oscillations reveal neural correlates of evidence accumulation. *Frontiers in Neuroscience*, *6*(JULY), 1–13. https://doi.org/10.3389/fnins.2012.00106

Vervaeke, K., LÖrincz, A., Gleeson, P., Farinella, M., Nusser, Z., & Silver, R. A. (2010). Rapid Desynchronization

of an Electrically Coupled Interneuron Network with Sparse Excitatory Synaptic Input. *Neuron*, *67*(3), 435–451. https://doi.org/10.1016/j.neuron.2010.06.028

Virtanen, P., Gommers, R., Oliphant, T. E., Haberland, M., Reddy, T., Cournapeau, D., Burovski, E., Peterson, P., Weckesser, W., Bright, J., van der Walt, S. J., Brett, M., Wilson, J., Millman, K. J., Mayorov, N., Nelson, A. R. J., Jones, E., Kern, R., Larson, E., … Vázquez-Baeza, Y. (2020). SciPy 1.0: fundamental algorithms for scientific computing in Python. *Nature Methods*, *17*(3), 261–272. https://doi.org/10.1038/s41592-019-0686-2

Vogt, B. A. (2016). Midcingulate cortex: Structure, connections, homologies, functions and diseases. *Journal of Chemical Neuroanatomy*, *74*, 28–46. https://doi.org/10.1016/j.jchemneu.2016.01.010

Voogd, J. (1967). Comparative aspects of the structure and fibre connexions of the mammalian cerebellum. *Prog Brain Res*, *25*, 94–134.

Voogd, Jan. (1969). The importance of fiber connections in the comparative anatomy of the mammalian cerebellum. *In: Llinas R, Editor. Neu- Robiology of Cerebellar Evolution and Development AMA-ERF Institute for Biomedical Research Chicago*, 493–514.

Voogd, Jan, Pardoe, J., Ruigrok, T. J. H., & Apps, R. (2003). The distribution of climbing and mossy fiber collateral branches from the copula pyramidis and the paramedian lobule: Congruence of climbing fiber cortical zones and the pattern of zebrin banding within the rat cerebellum. *Journal of Neuroscience*, *23*(11), 4645–4656. https://doi.org/10.1523/jneurosci.23-11-04645.2003

Voogd, Jan, & Ruigrok, T. J. H. (2012). Cerebellum and Precerebellar Nuclei. In *The Human Nervous System* (pp. 471–545). Elsevier Inc. https://doi.org/10.1016/B978-0-12-374236-0.10015-X

Wagner, M. J., Kim, T. H., Savall, J., Schnitzer, M. J., & Luo, L. (2017). Cerebellar granule cells encode the expectation of reward. *Nature*, *544*(7648), 96–100. https://doi.org/10.1038/nature21726

Wagner, M. J., & Luo, L. (2020). Neocortex–Cerebellum Circuits for Cognitive Processing. In *Trends in Neurosciences* (Vol. 43, Issue 1, pp. 42–54). https://doi.org/10.1016/j.tins.2019.11.002

Walter, W. G., Cooper, R., Aldridge, V. J., McCallum, W. C., & Winter, A. L. (1964). Contingent negative variation : An electric sign of sensori-motor association and expectancy in the human brain. *Nature*, *203*(4943), 380–384. https://doi.org/10.1038/203380a0

Ward, R. D., Kellendonk, C., Kandel, E. R., & Balsam, P. D. (2012). Timing as a window on cognition in schizophrenia. In *Neuropharmacology* (Vol. 62, Issue 3, pp. 1175–1181). NIH Public Access. https://doi.org/10.1016/j.neuropharm.2011.04.014

Watabe-Uchida, M., Eshel, N., & Uchida, N. (2017). Neural Circuitry of Reward Prediction Error. *Annual Review of Neuroscience*, *40*, 373–394. https://doi.org/10.1146/annurev-neuro-072116-031109

Watabe-Uchida, M., Zhu, L., Ogawa, S. K., Vamanrao, A., & Uchida, N. (2012). Whole-Brain Mapping of Direct Inputs to Midbrain Dopamine Neurons. *Neuron*, *74*(5), 858–873. https://doi.org/10.1016/j.neuron.2012.03.017

Watson, T. C., Becker, N., Apps, R., & Jones, M. W. (2014). Back to front: cerebellar connections and interactions with the prefrontal cortex. *Frontiers in Systems Neuroscience*, *8*. https://doi.org/10.3389/fnsys.2014.00004

Watson, T. C., Jones, M. W., & Apps, R. (2009). Electrophysiological mapping of novel prefrontal - Cerebellar pathways. *Frontiers in Integrative Neuroscience*, *3*(AUG), 18. https://doi.org/10.3389/neuro.07.018.2009

Welch, P. (1967). The use of fast Fourier transform for the estimation of power spectra: A method based on time averaging over short, modified periodograms. *IEEE Transactions on Audio and Electroacoustics*, *15*(2), 70–73.

Whitford, T. J., Mathalon, D. H., Shenton, M. E., Roach, B. J., Bammer, R., Adcock, R. A., Bouix, S., Kubicki, M., De Siebenthal, J., Rausch, A. C., Schneiderman, J. S., & Ford, J. M. (2011). Electrophysiological and diffusion tensor imaging evidence of delayed corollary discharges in patients with schizophrenia. *Psychological Medicine*, *41*(5), 959–969. https://doi.org/10.1017/S0033291710001376

Wiesendanger, R., & Wiesendanger, M. (1982). The corticopontine system in the rat. I. Mapping of corticopontine neurons. *Journal of Comparative Neurology*, *208*(3), 215–226. https://doi.org/10.1002/cne.902080302

Williams, S. M., Goldman-Rakic, P. S., & Leranth, C. (1992). The synaptology of parvalbumin-immunoreactive neurons in the primate prefrontal cortex. *Journal of Comparative Neurology*, *320*(3), 353–369. https://doi.org/10.1002/cne.903200307

Wilson, C. J., & Groves, P. M. (1981). Spontaneous firing patterns of identified spiny neurons in the rat neostriatum. *Brain Research*, *220*(1), 67–80. https://doi.org/10.1016/0006-8993(81)90211-0

Wiltse, L. L., & Pait, T. G. (1998). Historical perspective herophilus of Alexandria (325-255 B. C.): The father of anatomy. *Spine*, *23*(17), 1904–1914. https://doi.org/10.1097/00007632-199809010-00022

Winkler, I., & Czigler, I. (2012). Evidence from auditory and visual event-related potential (ERP) studies of deviance detection (MMN and vMMN) linking predictive coding theories and perceptual object representations. In *International Journal of Psychophysiology* (Vol. 83, Issue 2, pp. 132–143). https://doi.org/10.1016/j.ijpsycho.2011.10.001

Wise, A. K., Cerminara, N. L., Marple-Horvat, D. E., & Apps, R. (2010). Mechanisms of synchronous activity in cerebellar Purkinje cells. *Journal of Physiology*, *588*(13), 2373–2390. https://doi.org/10.1113/jphysiol.2010.189704

Wise, S. P. (2008). Forward frontal fields: phylogeny and fundamental function. *Trends in Neurosciences*, *31*(12), 599–608. https://doi.org/10.1016/j.tins.2008.08.008

Witter, L., Canto, C. B., Hoogland, T. M., de Gruijl, J. R., & De Zeeuw, C. I. (2013). Strength and timing of motor responses mediated by rebound firing in the cerebellar nuclei after Purkinje cell activation. *Frontiers in Neural Circuits*, *7*(AUG), 133. https://doi.org/10.3389/fncir.2013.00133

Witter, L., Rudolph, S., Pressler, R. T., Lahlaf, S. I., & Regehr, W. G. (2016). Purkinje Cell Collaterals Enable Output Signals from the Cerebellar Cortex to Feed Back to Purkinje Cells and Interneurons. *Neuron*,

91(2), 312–319. https://doi.org/10.1016/j.neuron.2016.05.037

Wolpert, D M, & Kawato, M. (1998). Multiple paired forward and inverse models for motor control. *Neural Networks*, *11*(7–8), 1317–1329. https://doi.org/10.1016/S0893-6080(98)00066-5

Wolpert, Daniel M., Miall, R. C., & Kawato, M. (1998). Internal models in the cerebellum. In *Trends in Cognitive Sciences* (Vol. 2, Issue 9, pp. 338–347). https://doi.org/10.1016/S1364-6613(98)01221-2

Wu, H. S., Sugihara, I., & Shinoda, Y. (1999). Projection patterns of single mossy fibers originating from the lateral reticular nucleus in the rat cerebellar cortex and nuclei. *Journal of Comparative Neurology*, *411*(1), 97–118. https://doi.org/10.1002/(SICI)1096-9861(19990816)411:1<97::AID-CNE8>3.0.CO;2-O

Xiao, D., Zikopoulos, B., & Barbas, H. (2009). Laminar and modular organization of prefrontal projections to multiple thalamic nuclei. *Neuroscience*, *161*(4), 1067–1081. https://doi.org/10.1016/j.neuroscience.2009.04.034

Xu, M., Zhang, S. Y., Dan, Y., & Poo, M. M. (2014). Representation of interval timing by temporally scalable firing patterns in rat prefrontal cortex. *Proceedings of the National Academy of Sciences of the United States of America*, *111*(1), 480–485. https://doi.org/10.1073/pnas.1321314111

Zelaznik, H. N., Spencer, R. M. C., & Ivry, R. B. (2002). Dissociation of explicit and implicit timing in repetitive tapping and drawing movements. *Journal of Experimental Psychology: Human Perception and Performance*, *28*(3), 575–588. https://doi.org/10.1037/0096-1523.28.3.575

Zemanick, M. C., Strick, P. L., & Dix, R. D. (1991). Direction of transneuronal transport of herpes simplex virus 1 in the primate motor system is strain-dependent. *Proceedings of the National Academy of Sciences of the United States of America*, *88*(18), 8048–8051. https://doi.org/10.1073/pnas.88.18.8048

Zhang, X., Baer, A. G., Price, J. M., Jones, P. C., Garcia, B. J., Romero, J., Cliff, A. M., Mi, W., Brown, J. B., Jacobson, D. A., Lydic, R., & Baghdoyan, H. A. (2020). Neurotransmitter networks in mouse prefrontal cortex are reconfigured by isoflurane anesthesia. *Journal of Neurophysiology*, *123*(6), 2285–2296. https://doi.org/10.1152/jn.00092.2020

Zhang, Z., Cai, D. C., Wang, Z., Zeljic, K., Wang, Z., & Wang, Y. (2019). Isoflurane-induced burst suppression increases intrinsic functional connectivity of the monkey brain. *Frontiers in Neuroscience*, *13*(APR). https://doi.org/10.3389/fnins.2019.00296

Supplementary Figures

STEADY PROTOCOL

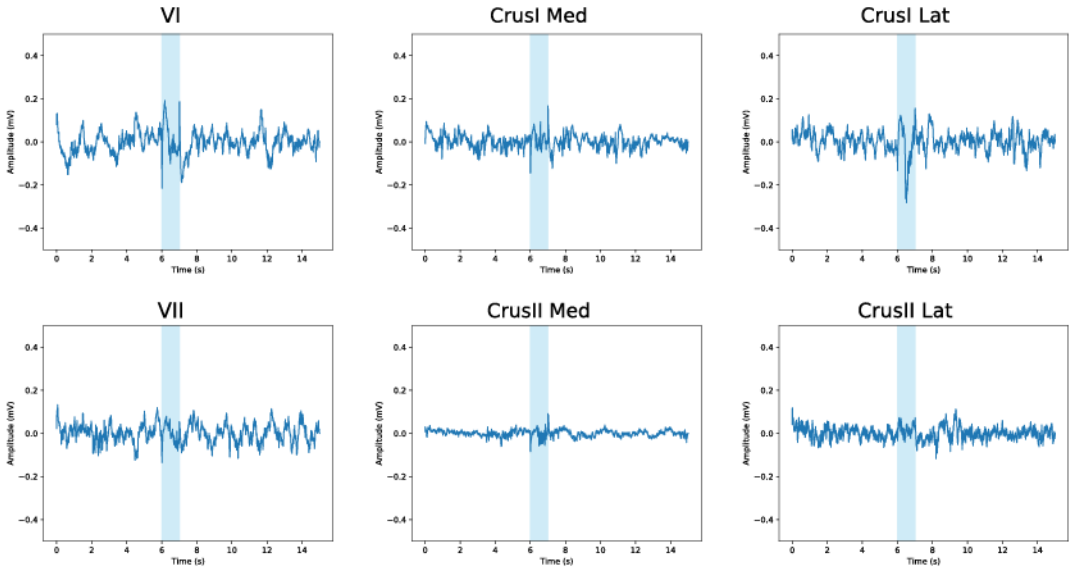

PULSES PROTOCOL

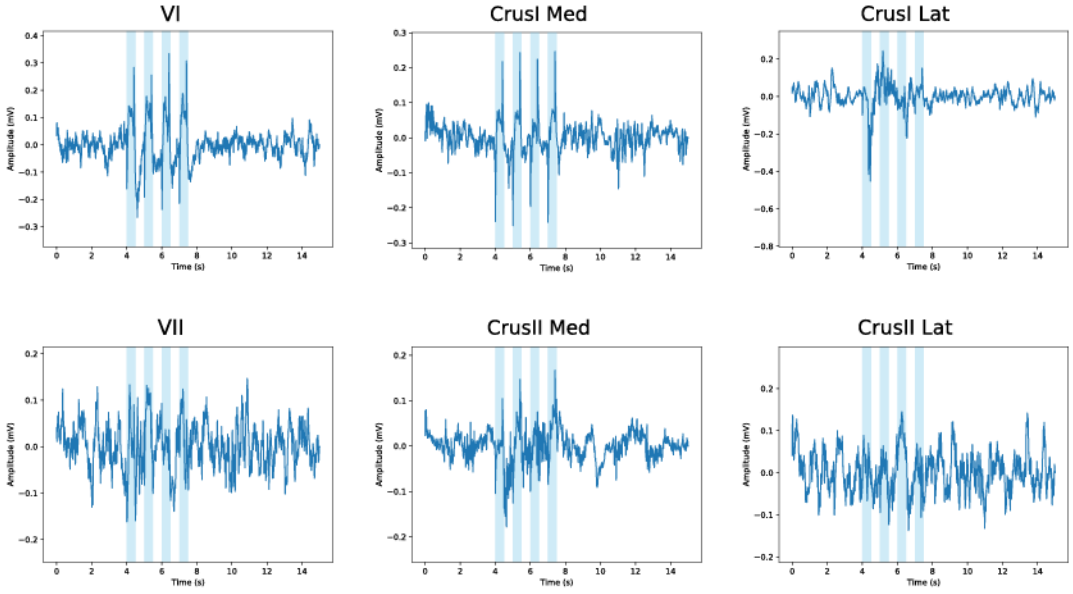

Supp.Fig.1 Mapping of cerebello-prefrontal functional connections

Uncropped plots from Fig.25. (Steady protocol) and the relative plots for the second protocol (pulses protocol) used. Vertical blue bands: time and duration of thephotostimulation. Stimulation artefacts are visible in some of the figures.

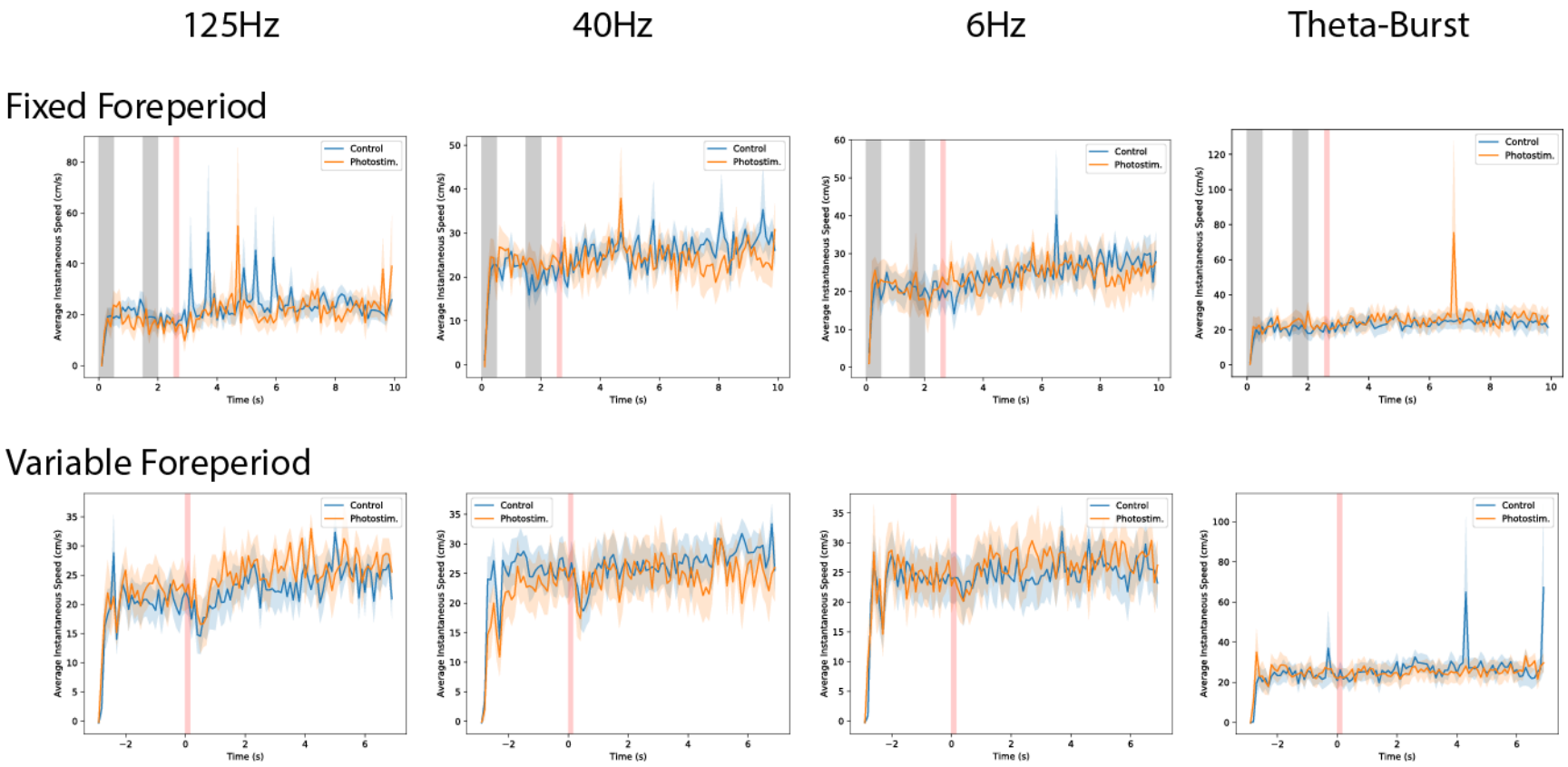

Supp.Fig.2 Speed of the mouse by protocol of stimulation

Time course of the speed separated by stimulation sessions (in Fig.26Ai-Bi the speed is obtained by merging the various protocols of stimulation). The control in this case is the respective internal control (first 30 trials of each session). The variable foreperiod traces are aligned to the reward.

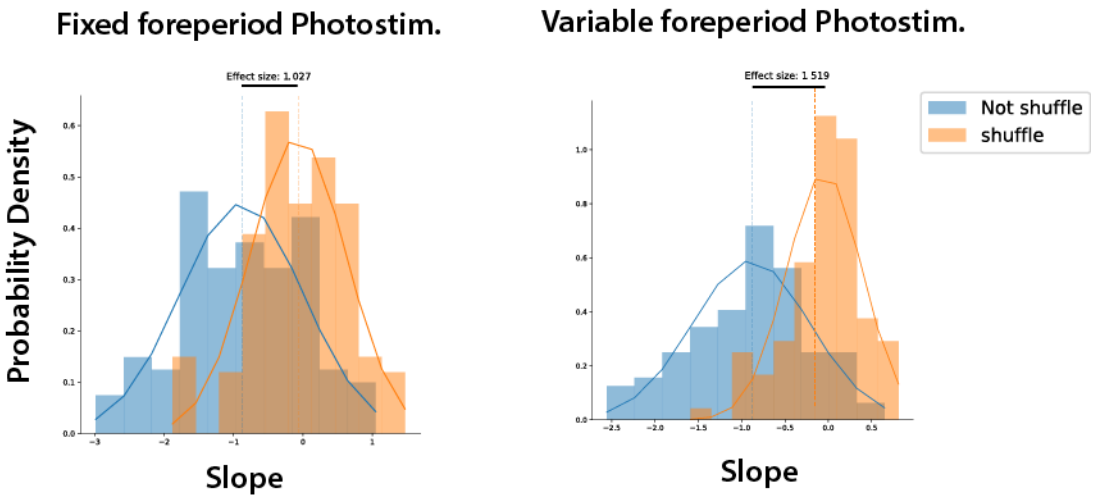

Supp.Fig.3 Mice slowdown in anticipation of the reward even with photo-stimulation

Same analysis as Fig.27A but performed on photostimulation sessions for fixed (left) and variable (right) foreperiod.

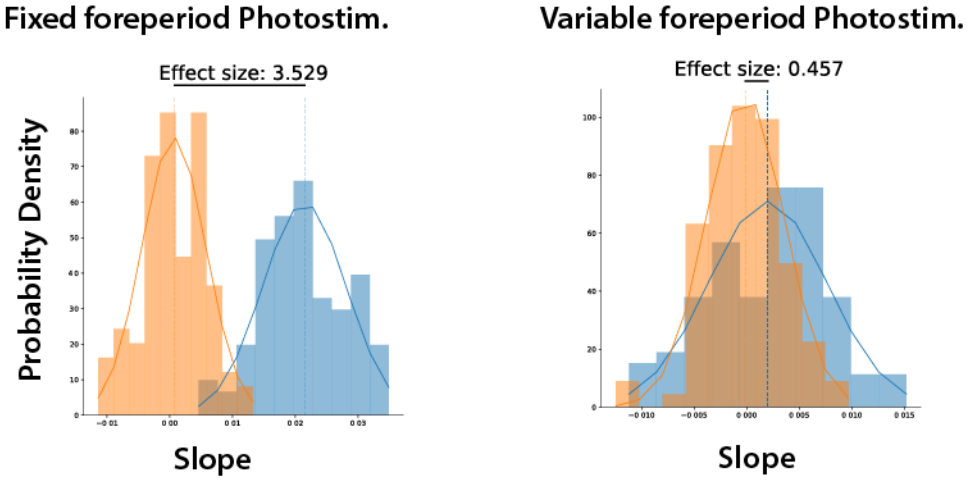

Supp.Fig.4 Anticipatory licking behaviour of Photostimulation sessions

Same analysis as Fig.28C but performed on photostimulation sessions for fixed (left) and variable (right) foreperiod.

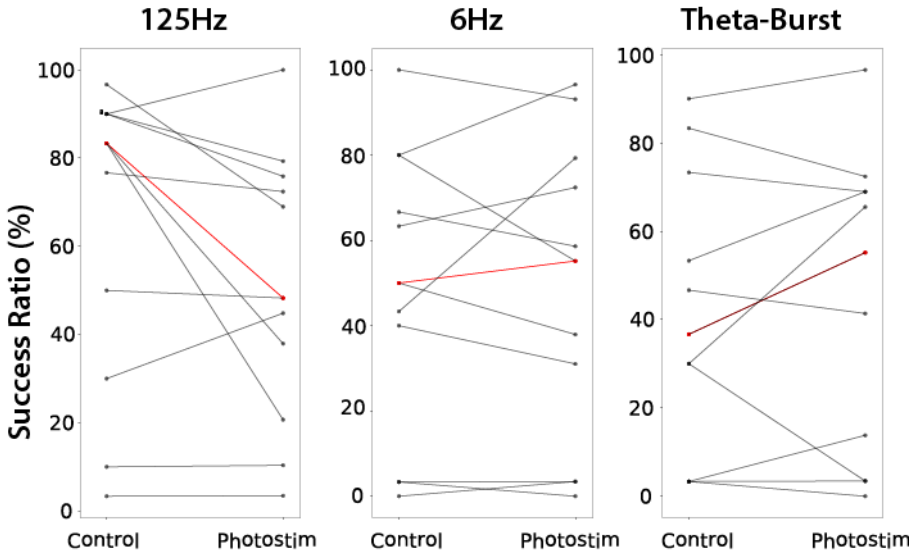

Supp.Fig.5 Success ratio for sessions with variable foreperiod

Same analysis as Fig.30B but performed on sessions with variable foreperiod. The plot with the protocol of 40Hz is already shown in Fig.30Aii

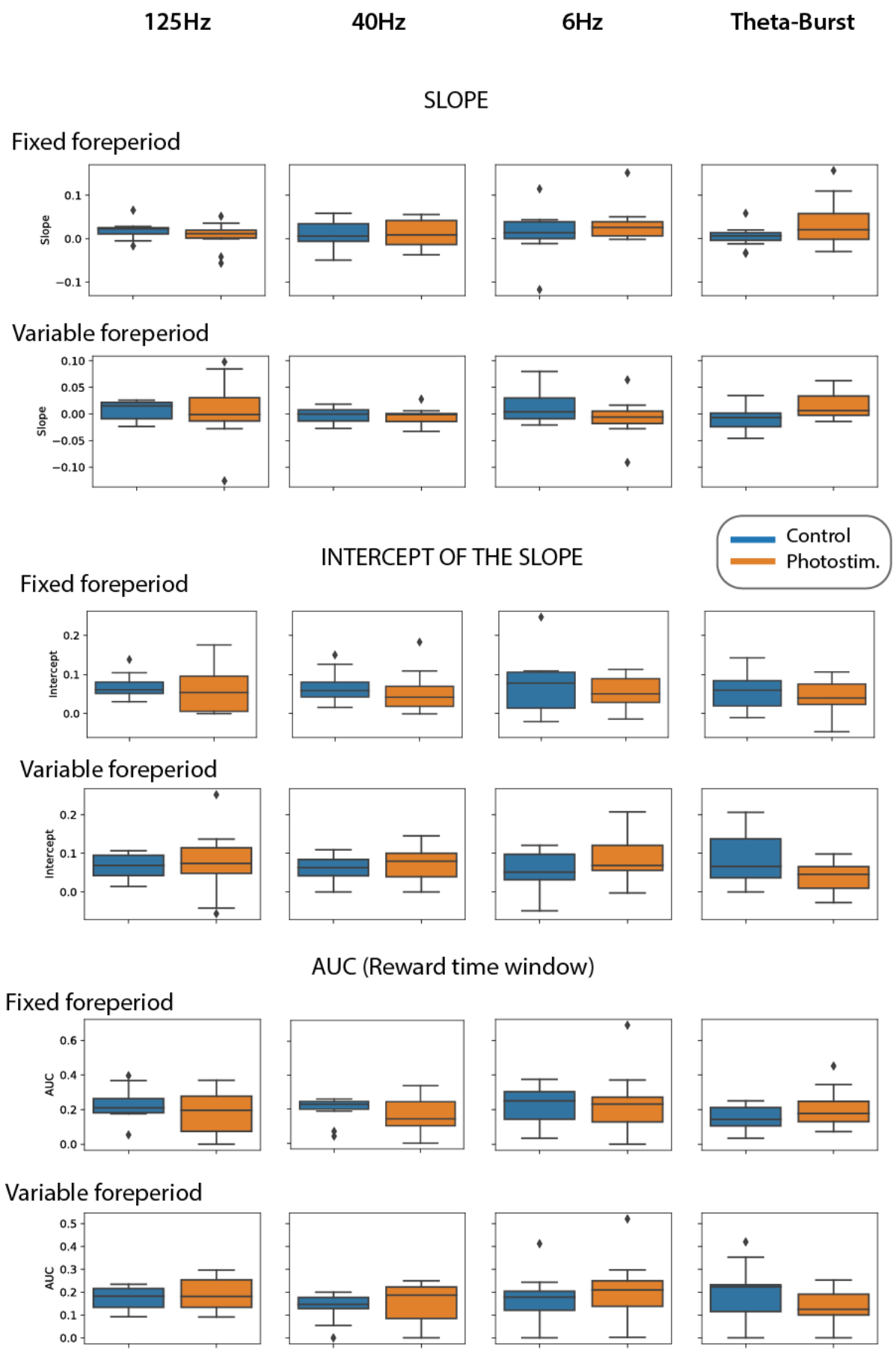

Supp.Fig.6 Analysis of the anticipatory licking behavior by protocol
Plots from all sessions for the analysis as Fig.32.

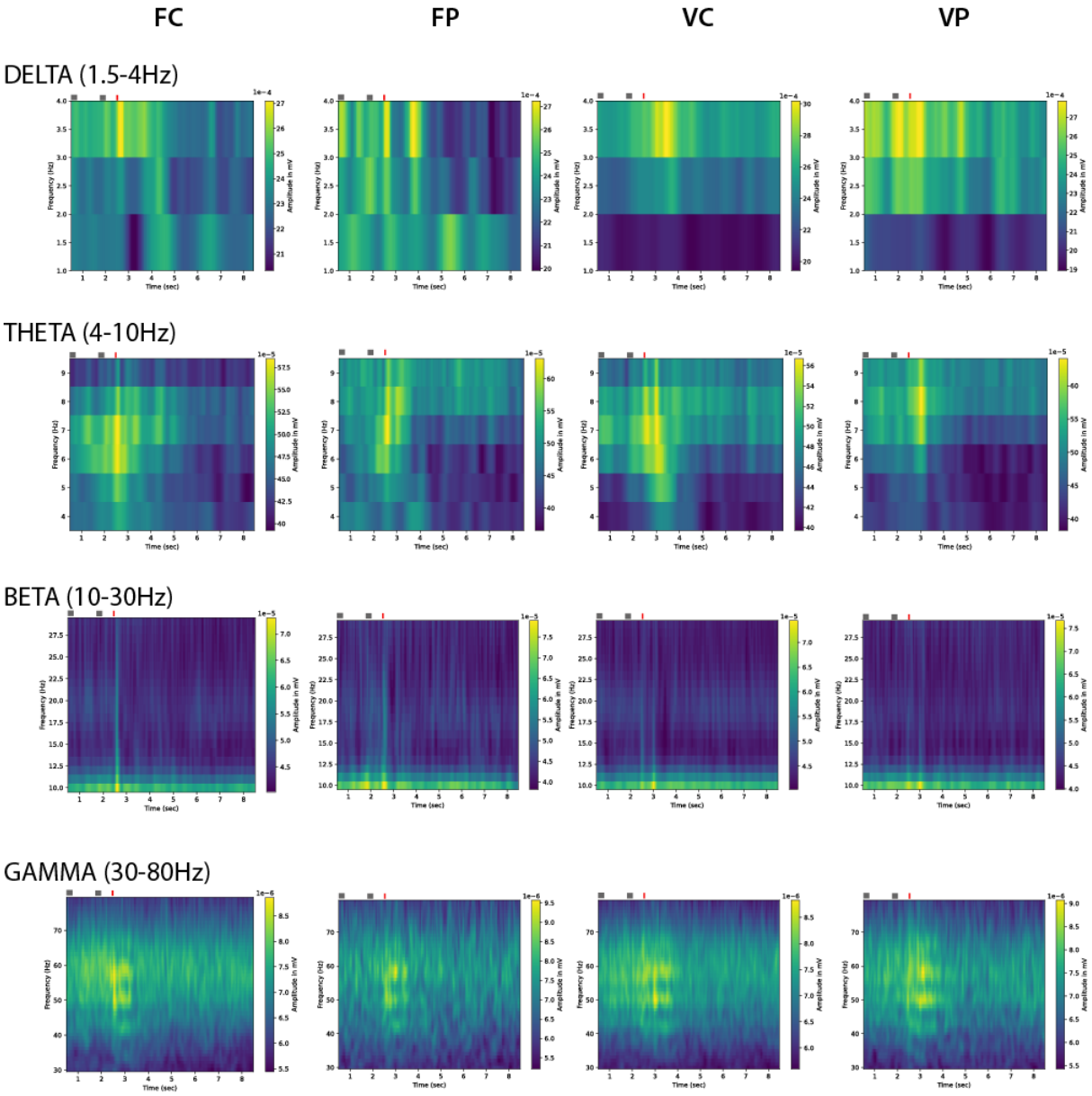

Supp.Fig.7 Time-Frequecy plots by frequency band and experimental ocndition

Average time-frequency plots of all mice as in Fig.33A. Colorcoded is represented the average amplitude by frequency bin (specific scale given for each plot). Grey and red bars on top of each plot represent time and duration of two visual cues and reward, respectively.

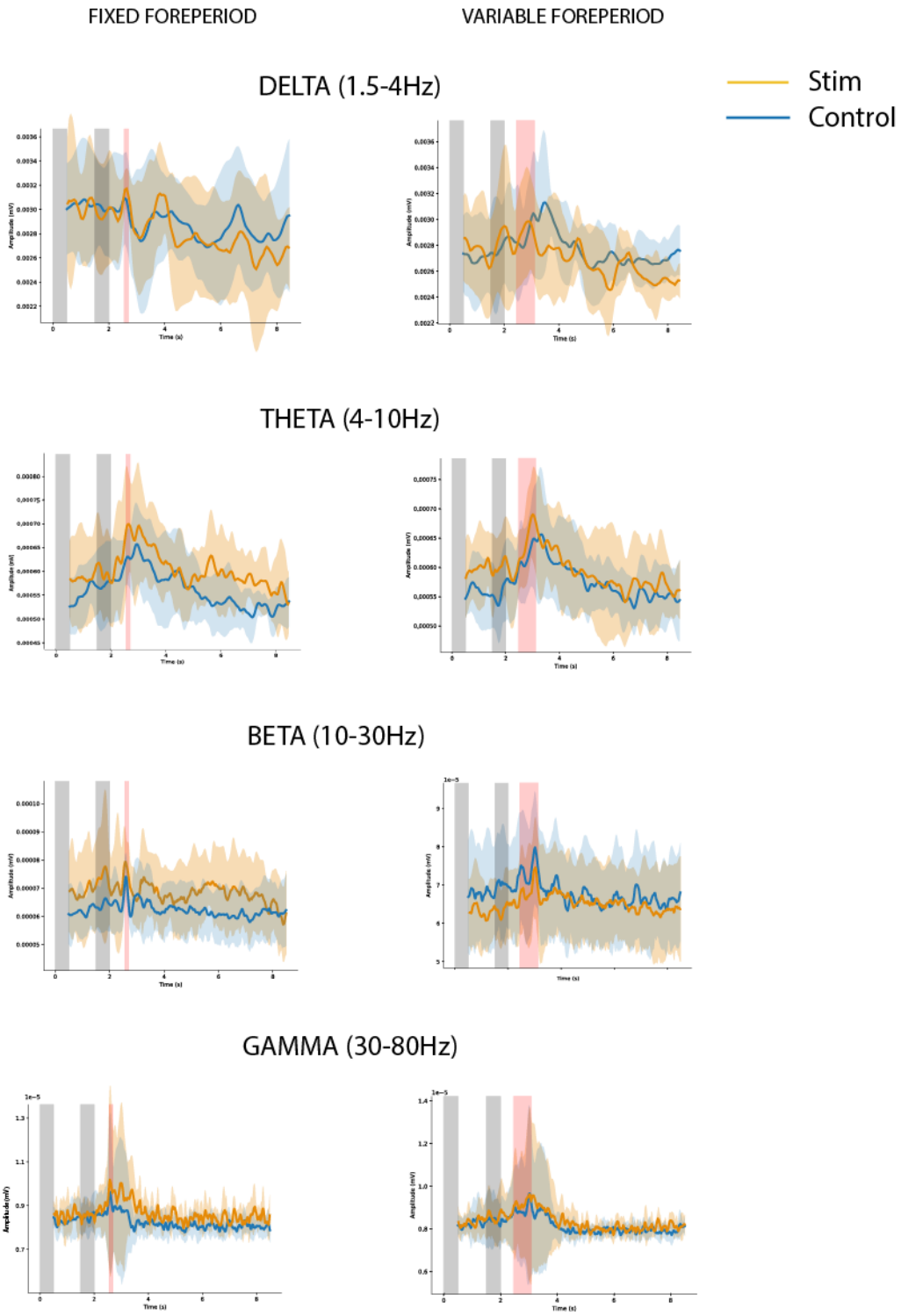

Supp.Fig.8 Ridge of the amplitude by frequency band

Average ridge of the amplitue of all mice as in Fig.33B, divided by frequency band and by experimental condition. Grey and red vertical bars: time and duration of two visual cues and reward, respectively. Please note that the reward band in the variable foreperiod condition spans all the possible moments of presence of the reward, due to the variability of it delivery.

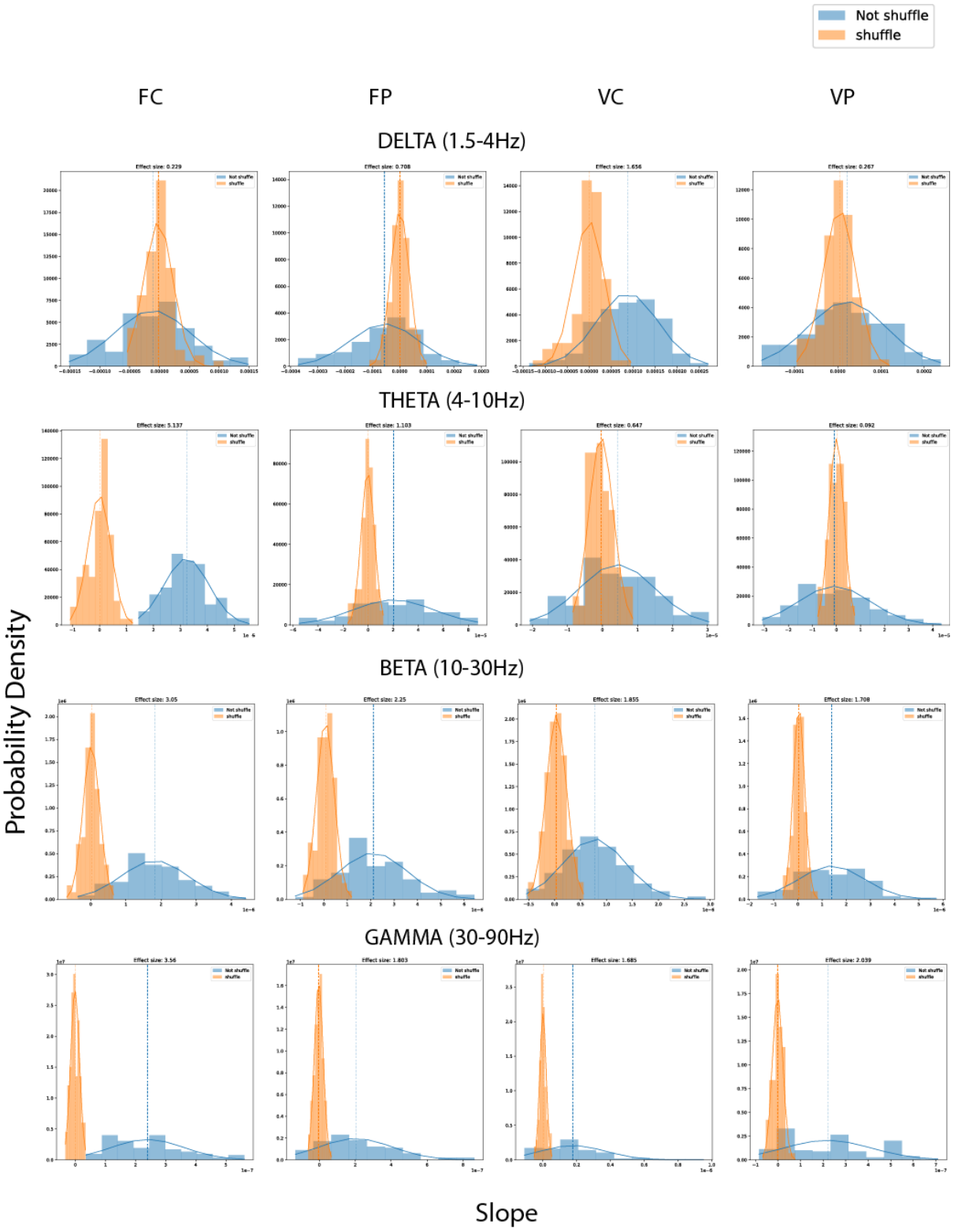

Supp.Fig.9 Slope of the ridge of the amplitude by frequency band compared to shuffled distribution
Average ridge of the amplitue of all mice compared to an equally bootstrapped shuffled distribution as in Fig.33C-D, divided by frequency band and by experimental condition. Continuous line: gaussian fit of the corresponding distribution. Dotted line: mean of the corresponding distribution.

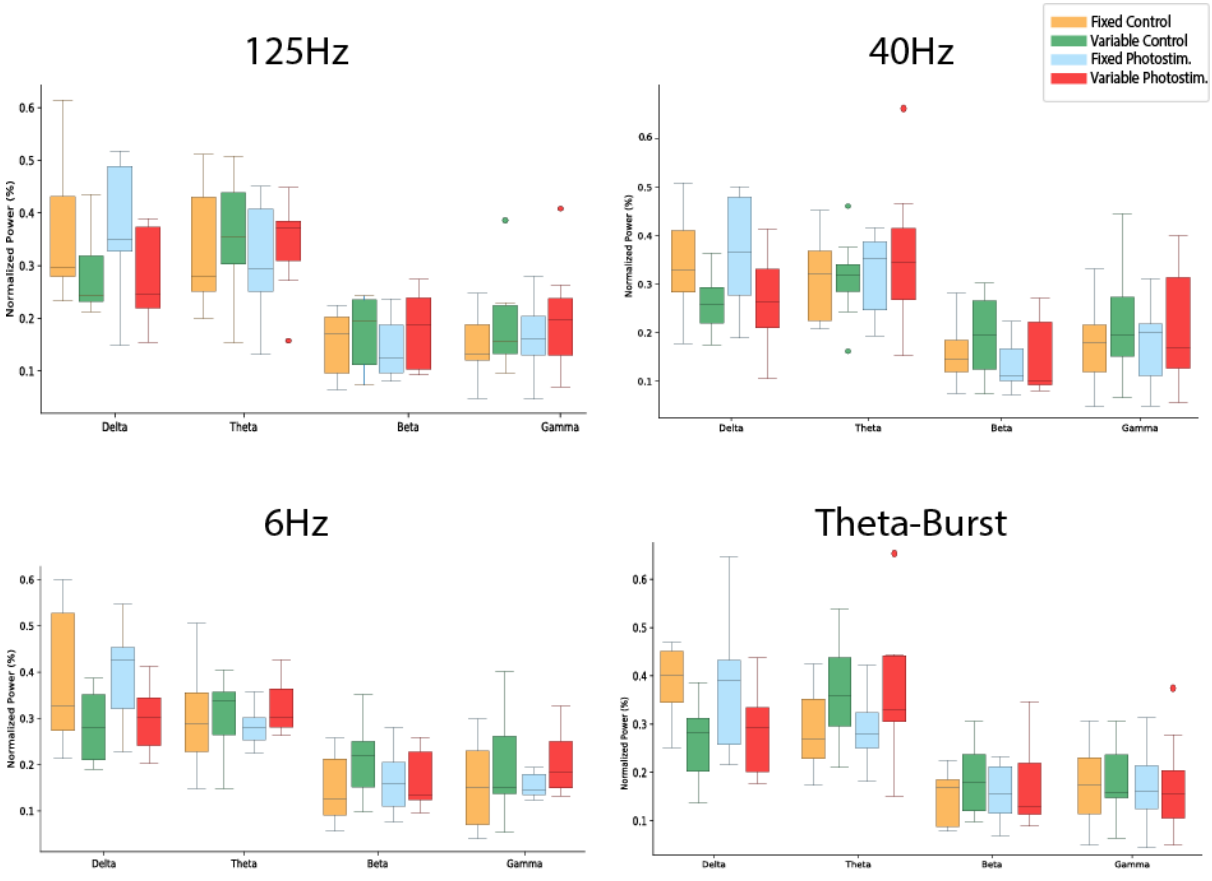

Supp.Fig.10 Fraction of total power by frequency band

Fraction of the total normalized power of all mice by the four experimental conditions. The four plots are the four protocols of stimulation used (Fig.34A is the merged data of these four plots).

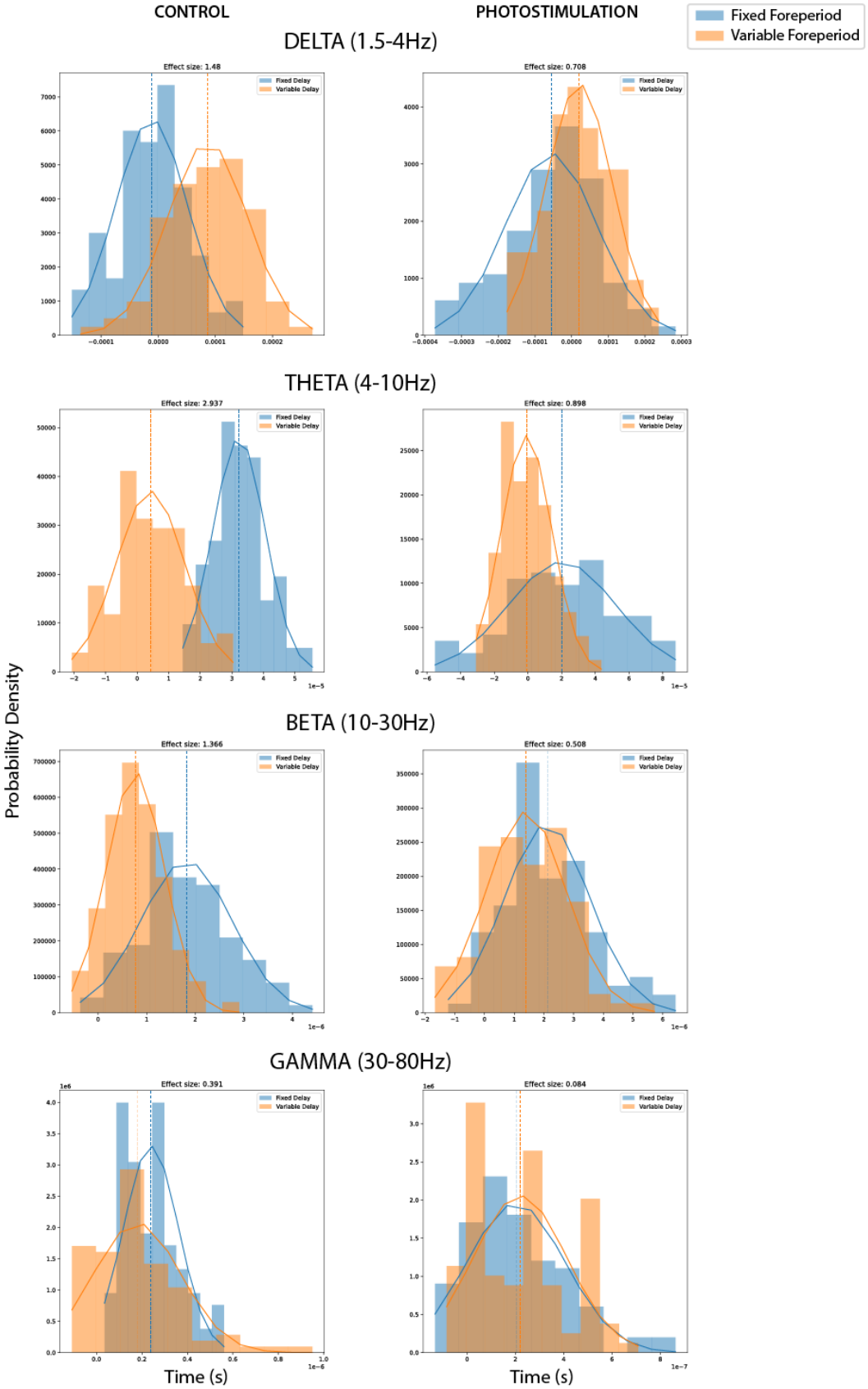

Supp.Fig.11 Slope of the ridge of the average amplitude by frequency band
Bootstrapped distribution of the slope values of the ridge of the amplitude. Comparison of Fixed (blue) and variable (orange) foreperiods for the various frequency bands in both control (left column) and photostimulation (right column) conditions. Continuous line: gaussian fit of the corresponding distribution. Dotted line: mean of the corresponding distribution.

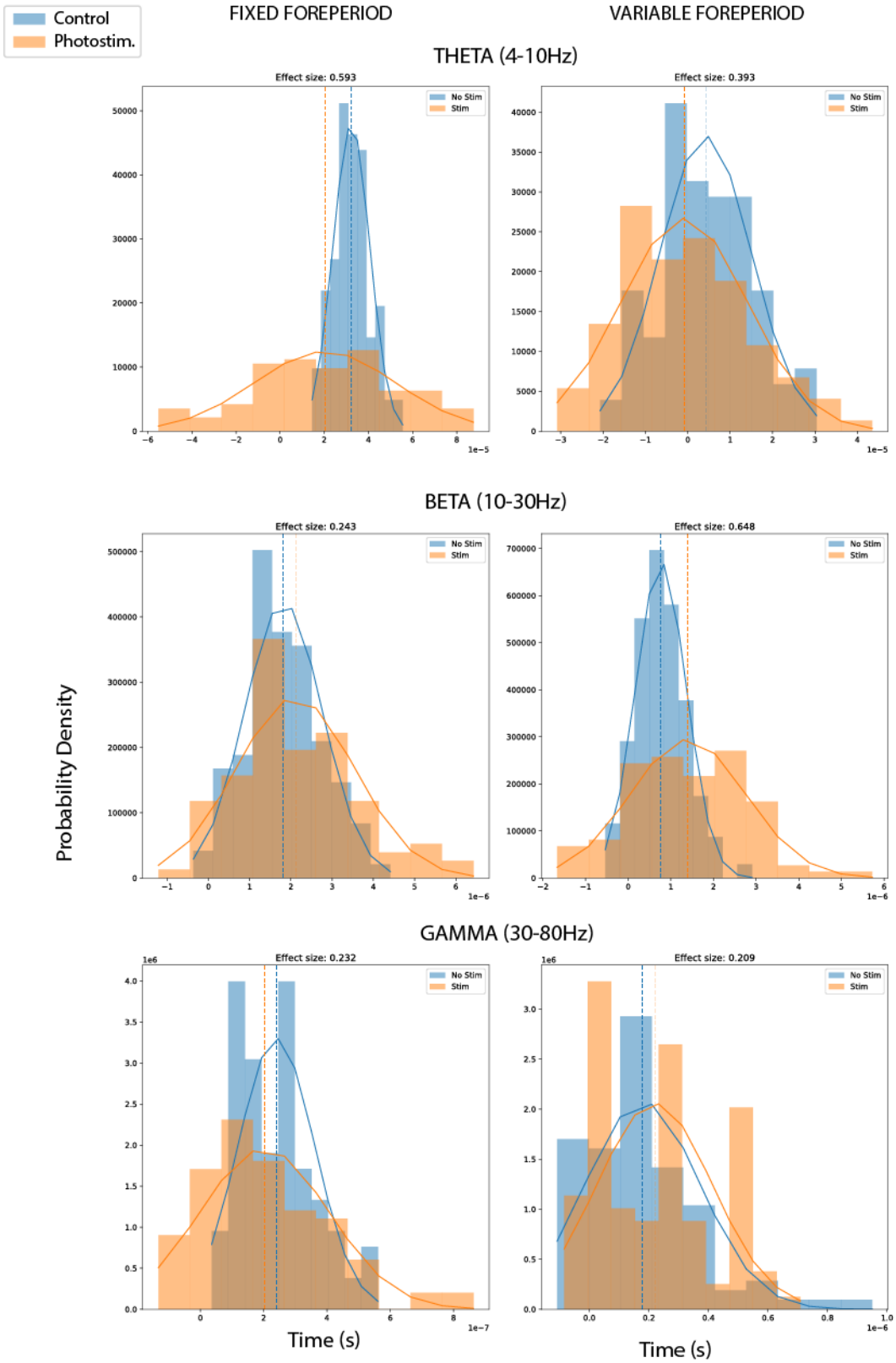

Supp.Fig.12 Slope of the ridge of the average amplitude by frequency band
Bootstrapped distribution of the slope values of the ridge of the amplitude. Comparison of control (blue) and photostimulation (orange) conditions for the various frequency bands in both fixed (left column) and variable (right column) foreperiods. Continuous line: gaussian fit of the corresponding distribution. Dotted line: mean of the corresponding distribution.

Résumé étendu en français

Le temps implicite dans la boucle cérébello-préfrontale.

Une nouvelle approche chez la souris

1. Introduction

Le cervelet est impliqué dans la coordination motrice et l'enchaînement temporel de nos actions. Il reçoit des informations sensorimotrices de la périphérie, du système vestibulaire et du cortex cérébral. Lorsqu'un plan moteur est généré dans le cortex, une copie de celui-ci est toujours envoyée au cervelet en tant que copie efférente. Grâce à cela, le cervelet peut détecter les erreurs de mouvements et les corriger à l'échelle de la milliseconde.

Le cervelet joue également un rôle central dans la cognition et la pensée abstraite. Sa connexion réciproque avec le cortex préfrontal (PFC), relayée par le thalamus, est particulièrement importante à cet égard. Des altérations de cette voie cérébello-thalamo-préfrontale sont impliquées dans de multiples maladies neuropsychiatriques telles que les troubles du spectre autistique et la schizophrénie.

Anne Giersch et ses collègues ont consacré leurs recherches à l'étude des altérations de la perception du temps chez les patients schizophrènes. Ils ont pu identifier des altérations subtiles de la perception implicite du temps (avec des intervalles de temps aussi petits que 8ms) chez les patients par rapport aux témoins sains (Giersch et al., 2015 ; Lalanne et al., 2012). Nancy Andreasen a suggéré un rôle possible du cervelet et du PFC dans l'intégration temporelle implicite et l'altération de ce réseau dans la schizophrénie. Ainsi, elle propose que certains symptômes de la schizophrénie s'apparentent à une " dysmétrie cognitive " (Andreasen, 1999).

Notre projet vise à développer un paradigme comportemental pour étudier l'intégration temporelle implicite dans le cortex préfrontal et le cervelet de la souris en stimulant par optogénétique le cervelet pour perturber la boucle cérébello-thalamique-préfrontale et en enregistrant l'activité neuronale dans le PFC.

Ce que nous définissons comme implicite est l'élaboration inconsciente du temps. Ceci est réalisable lorsque le temps n'est pas un paramètre clé de la tâche comportementale mais une propriété émergente de celle-ci.

2. Matériels et méthodes

11 souris adultes des deux sexes ont été utilisées. Les cellules de Purkinje expriment la Channelrhodopsin 2. Ces cellules constituent la seule sortie du cortex cérébelleux. Ainsi, nous avons pu activer de manière optogénétique les CrusI droits dans les hémisphères cérébelleux à l'aide d'une fibre optique implantée à la surface du cervelet. Nous avons également implanté une série d'électrodes dans l'aire prélimbique (PrL) gauche du cortex préfrontal. De

cette façon, nous avons pu enregistrer l'activité électrophysiologique du réseau ainsi que la décharge de neurones individuels dans la PrL.

Nous avons utilisé quatre protocoles de stimulation optogénétique différents du cervelet pour étudier un effet possible de la fréquence de stimulation sur le réseau. Les quatre protocoles de stimulation diffèrent par la fréquence des impulsions lumineuses : 125Hz, 40Hz, 6Hz et Theta-Burst (bursts de 100Hz imbriqués dans une oscillation plus lente de 5Hz). Finalement, en raison de la faible taille de l'échantillon, les analyses ont été effectuées en fusionnant les enregistrements obtenus avec tous les protocoles de stimulation. L'objectif étant de déterminer si la boucle cérébello-préfrontale est impliquée dans le traitement du timing implicite, cette couche plus superficielle est suffisante dans un premier temps.

La tâche comportementale est une adaptation du paradigme de la période antérieure variable.

Les souris avaient la tête fixée et se trouvaient sur une roue. Deux signaux visuels étaient joués en séquence (à 1s d'intervalle), puis une récompense était délivrée après un délai fixe de 500 ms (période antérieure fixe) ou un délai variable choisi aléatoirement entre 400 et 900 ms (période antérieure variable). Cette tâche a été développée afin de sonder la perception implicite du temps, les souris sont invitées à lécher une goutte d'eau après un délai spécifique et modifiable. De cette façon, nous pouvons étudier l'intégration temporelle par le biais de changements dans le comportement de léchage, qu'il soit augmenté en prévision de la récompense (comportement anticipatif) ou supprimé jusqu'au moment précis de la récompense (diminution du temps de réaction). Comme la récompense n'était pas conditionnée à la réalisation de la tâche, les souris n'ont pas eu besoin d'apprendre les délais, mais l'aspect temporel est devenu une propriété implicite et émergente de la tâche.

La prédiction temporelle peut être caractérisée par un changement progressif de l'activité des neurones, qui peuvent augmenter ou diminuer leur activité de manière constante sur des périodes de temps pertinentes sur le plan comportemental. Cette activité est également appelée anticipation. En outre, nous surveillons une éventuelle anticipation dans le comportement de léchage lui-même.

Le cortex cérébelleux (CrusI) a été stimulé entre le deuxième indice et la libération de la récompense, un moment où l'anticipation est supposée être la plus forte. Cette configuration permet d'enregistrer la signature comportementale et électrophysiologique de l'activité d'anticipation, les effets possibles dus à l'altération du réseau cérébelleux-thalamique-préfrontal, et les différences possibles dues à la nature variable ou fixe de la période d'anticipation dans la tâche.

Les souris ont eu en moyenne 11 jours consécutifs d'entraînement (avec période antérieure variable mais sans photostimulation). Une fois considérées comme prêtes, elles ont été soumises à deux jours d'expérimentation au cours desquels leur CrusI droit a été stimulé par

optogénétique à quatre fréquences différentes. Le premier jour était avec une période antérieure variable, tandis que le deuxième jour était avec une période antérieure fixe.

3. Résultats

3.1. Comportement

Pour confirmer que la stimulation du cortex cérébelleux n'a pas d'implications motrices directes, nous avons d'abord analysé la vitesse de course des souris au cours des différentes sessions. La vitesse instantanée a été comparée entre les sessions de contrôle et de photostimulation. Aucune différence n'a été trouvée dans les quatre protocoles de stimulation, ni avec la fixation d'une période antérieure variable, ce qui suggère qu'il n'y a pas d'altération motrice majeure due à la photostimulation.

Pour quantifier les changements dans le comportement de léchage, nous avons utilisé des mesures qui prennent en compte différents aspects de l'évolution temporelle, notamment : les changements dans l'anticipation (si elle est présente) et la performance dans la tâche (si la souris effectue la tâche ou non et, si elle le fait, quelle attention elle y porte). Pour ces raisons, nous avons effectué deux analyses distinctes sur les données de léchage.

Nous considérons quatre conditions expérimentales : 1) contrôle interne de la condition de période antérieure fixe, appelé contrôle fixe (FC) ; 2) photostimulation pendant la période antérieure fixe (indépendamment du protocole de stimulation utilisé), appelée photostimulation fixe (FP) ; 3) contrôle interne de la condition de période antérieure variable, appelé contrôle variable (VC) ; 4) photostimulation pendant la période antérieure variable (indépendamment du protocole de stimulation utilisé), appelée photostimulation variable (VP).

Tout d'abord, nous avons quantifié la performance globale de la tâche en calculant le taux de réussite pour chaque souris. La stimulation optogénétique a réduit significativement le taux de réussite dans les deux conditions de période antérieure. Aucune différence n'a été trouvée entre les deux conditions de contrôle, mais la PF était significativement plus faible par rapport à la VP. Ceci indique probablement un effet de la période antérieure sur les niveaux d'attention dans lesquels le cervelet est également impliqué.

Pour la deuxième analyse effectuée sur les données de léchage, la pente du taux de léchage pendant la période antérieure a été calculée à partir de l'histogramme temporel des léchages d'une session entière pour chaque souris. Ces valeurs ont été bootstrapées 100 fois et comparées d'abord avec une distribution également bootstrapée de valeurs mélangées (obtenues en mélangeant dans le temps les comptes de léchage (bins) des histogrammes temporels de la période antérieure) pour déterminer si les souris ont montré un comportement de léchage anticipé. Dans les deux conditions de la période antérieure, FC et VC, les souris ont effectivement montré une augmentation du taux de léchage en anticipation de la récompense. Ces distributions bootstrappées ont ensuite été comparées entre FC et VC,

et il en résulte que les souris peuvent anticiper davantage une récompense avec une période antérieure fixe (FC avait une pente plus élevée que VC). Ce phénomène est décrit dans la littérature comme "l'effet de la période préalable".

3.2. Electrophysiologie

L'activité du réseau a été analysée par le biais du potentiel de champ local (LFP). L'amplitude du signal par bande de fréquence a été calculée au moyen d'une convolution complexe d'ondelettes de Morlet. Ensuite, la crête de cette amplitude a été extraite et bootstrapée (comme dans l'analyse précédente). Deux bandes de fréquences ont été particulièrement intéressantes : delta (1,5-4Hz) et thêta (4-10Hz). La bande delta montre une activité de rampe verrouillée avec la récompense uniquement pendant la VC, tandis que pendant la période antérieure fixe et la VP, la crête est plate. A l'opposé, la bande thêta montre une activité de rampe uniquement pendant la période antérieure fixe. Il est intéressant de noter que la stimulation n'affecte ces deux oscillations que lorsqu'il y a une rampe, mais qu'elle les affecte différemment. Dans le cas de la bande delta, le ramping est aboli par la photostimulation. Dans le cas de l'oscillation thêta, la photostimulation n'affecte pas la tendance centrale des données (la moyenne de la FP reste une oscillation) mais elle augmente la variance de l'ensemble des données.

Sur les enregistrements multi-unités, la décharge des neurones a d'abord été étudiée en identifiant les unités individuelles par le tri des pointes. Un total de 327 unités a été isolé. En utilisant deux paramètres de la forme d'onde moyenne (l'amplitude de pic à creux et la largeur de la demi-amplitude), un regroupement a été effectué pour identifier les cellules pyramidales putatives (n=306) et les interneurones putatifs (n=21) (voir Barthó et al., 2004). En raison du faible nombre d'interneurones, les analyses ont été effectuées uniquement sur les cellules pyramidales putatives.

Une analyse en composantes principales (ACP) suivie d'un regroupement hiérarchique a été effectuée sur des caractéristiques sélectionnées des unités isolées. Cela nous a permis de regrouper les unités en fonction de leur comportement pendant la tâche. Pour quantifier les changements dans le réseau, deux paramètres ont été extraits de chaque groupe : le taux de tir moyen (du début de l'essai à la récompense) et la pente de la période antérieure. Dans les quatre conditions expérimentales, il existe des unités clairement entraînées par la tâche comportementale.

4. Conclusions

Au cours de mon doctorat, j'ai pu mettre en place une tâche comportementale pour étudier le rôle du réseau cérébello-préfrontal dans le traitement implicite du temps et développer les chirurgies et les techniques d'entraînement nécessaires. Cette tâche s'est avérée efficace en nous permettant d'étudier l'anticipation d'une récompense par le biais de données comportementales et électrophysiologiques.

Les données comportementales ont montré des effets clairs de la période antérieure sur le comportement des souris, confirmant l'effet de la période antérieure.

Les données électrophysiologiques montrent une possible spécialisation des bandes de fréquences dans différentes tâches, et peuvent mettre en évidence un rôle proéminent du delta dans la prédiction d'un événement variable, alors que le thêta semble plus impliqué dans la mise en mémoire d'un intervalle de temps fiable.

Le cortex préfrontal est une structure en couches avec un haut degré de réseaux récurrents entre les couches de la même colonne fonctionnelle et de colonnes différentes. De plus, nous enregistrons à partir de la couche V qui est la sortie principale de la PrL vers des structures sous-corticales (Opris & Casanova, 2014) tout en étant impliquée dans ces réseaux récursifs locaux.

Ce que nous pouvons constater à partir de nos analyses est que le réseau dans son ensemble est effectivement dirigé par la tâche avec des différences, également dans ce cas, dues aux différentes conditions de timing.

Summary Figure of the main results

		Fixed vs Variable		Control vs Photostim.	
		Control	Photostim.	Fixed	Variable
Behavior	Deceleration	FC > VC	FP = VP	FC = FP	VC = VP
	Anticipatory Licking	FC > VC	FP > VP	FC < FP	VC = VP*
	Success Ratio	FC = VC	FP < VP	FC > FP	VC > VP
	Number of licks Before the reward	FC > VC	FP = VP	FC > FP	VC = VP
	Number of licks after the reward	FC = VC	FP = VP	FC > FP	VC > VP
Ridge Amplitude	Delta (1.5-4Hz)	FC < VC	FP = VP	FC = FP	VC > VP
	Theta (4-10Hz)	FC > VC	FP > VP	FC = FP	VC ≠ VP**

* Theta-Burst: VC < VP

** Same mean but variance increased by VP

FC = Fixed Foreperiod Control
FP = Fixed Foreperiod Photostim.
VC = Variable Foreperiod Control
VP = Variable Foreperiod Photostim.

Université de Strasbourg

École Doctorale des Sciences de la Vie et de la Santé STRASBOURG

Federica LARENO FACCINI

Implicit time in the cerebello-prefrontal network. A novel approach in mice

Résumé en français

Un nombre croissant de publications montre une implication du cervelet dans la gestion des prédictions temporelles et des attentes des événements moteurs et cognitifs. D'autre part, le cortex préfrontal médian (CPM) est largement considéré comme la zone où se fait l'intégration entre les modèles internes et la cognition. De plus, le mPFC est impliqué dans la plupart des modèles de perception du temps, ce qui en fait un candidat idéal pour gérer les comportements prédictifs. Les expériences de traçage et la tâche de chronométrage par intervalles ont mis en évidence une connexion entre ces deux zones.

Nous avons donc développé un modèle pour étudier le rôle du cervelet dans le développement et la mise à jour des prédictions temporelles implicites dans le mPFC des souris. Nous avons enregistré l'activité extracellulaire dans le mPFC (en particulier dans l'aire prélimbique gauche, PrL) pendant que les souris, la tête fixée, effectuaient la tâche suivante, de période antérieure variable : deux indices sont présentés dans une séquence suivie d'une récompense délivrée à un moment fixe ou variable (choisi au hasard entre deux délais possibles). En même temps, nous photoactivons des cellules de Purkinje cérébelleuses de souris L7-Channelrhdopsin2 à des fréquences spécifiques, au-dessus du Crus I controlatéral. Le but de la stimulation optogénétique est d'interférer avec la décharge neuronale dans le mPFC.

Nous confirmons l'effet de la période antérieure, déjà décrit dans la littérature, pour lequel les réponses sont plus rapides et plus précises lorsque l'intervalle entre un indice et un signal de départ/récompense (période antérieure) est constant. Il est intéressant de noter que nous rapportons un comportement différent de deux oscillations préfrontales importantes : delta (1,5-4Hz) et thêta (4-10Hz). Elles présentent un comportement de rampe uniquement lorsque la période antérieure est variable et fixe, respectivement. De plus, la photostimulation cérébelleuse n'affecte ces oscillations que si elles présentent un comportement de rampe. Ceci est probablement représentatif des différents substrats neuronaux recrutés par les deux conditions de période antérieure.

Résumé en anglais

A growing body of literature is showing an involvement of the cerebellum in managing time predictions and expectations of motor and cognitive events. On the other hand the medial prefrontal cortex (mPFC) is widely considered the area where there is the integration between internal models and cognition. Moreover, mPFC is involved in most of the models for time perception, making it an ideal candidate for handling predictive behaviors. Both tracing experiments and interval timing task highlighted a connection between these two areas.

We thus developed a model to investigate the role of the cerebellum in the creation and update of implicit temporal predictions in mPFC of mice. We recorded the extracellular activity in the mPFC (specifically left prelimbic area, PrL) while the head-restrained mice perform the following variable foreperiod task: two cues are presented in a sequence followed by a reward delivered at either a fixed or a variable time point (randomly chosen between two possible delays). At the same time, we photoactivate cerebellar Purkinje cells of L7-Channelrhdopsin2 mice at specific frequencies, above contralateral Crus I. The aim of the optogenetic stimulation is to interfere with neuronal discharge in the mPFC.

We confirm the foreperiod effect, already described in the literature, for which responses are faster and more accurate when an interval between a cue and a go signal/reward (foreperiod) is constant. Interestingly we report different behavior of two important prefrontal oscillations: delta (1.5-4Hz) and theta (4-10Hz). They show ramping behavior only when the foreperiod is variable and fixed, respectively. Moreover, cerebellar photostimulation affects these oscillations only if they are ramping. This is probably representative of different neural substrates recruited by the two foreperiod conditions.